Molecular and cellular studies examining the biological significance of different isoforms of the receptor tyrosine kinase, c-Kit

Antony Charles Cambareri
B. Sc. (Hons)

Institute of Medical and Veterinary Science

Department of Medicine
University of Adelaide
South Australia

A thesis submitted to the University of Adelaide
in candidature for the degree of Doctor of Philosophy
October 2004

Declaration

This thesis contains no material that has been accepted for the award of any other degree or diploma in any other university. To the best of my knowledge and belief, this thesis contains no material previously published or written by another person, except where due reference has been made in the text.

I give consent to this copy of my thesis, when deposited in the University Library, being available for loan and photocopying.

Antony C Cámbareri

6/10/04

Acknowledgments

I would like to sincerely thank my supervisors, Professor Leonie Ashman and Professor Bik To. I thank them both for their encouragement, persistence and support over the period of this work.

Special thanks to Steve Fitter, who was pivotal in "retraining" me in the art of science upon my return to the lab from "the dark side". He is both a great friend and a legendary molecular biologist (it is true that it will work if you add a microlitre!). I also thank Andrew Zannettino for spending the time to critique drafts of this thesis, and for valuable input to experimental design.

I acknowledge the valuable technical assistance of Ly Nguyen and Peter Konstantopolous from the Leukaemia Haemopoiesis Laboratory. Thanks also to Sue Branford and Rebecca Lawrence for their assistance with Quantitative PCR. Thankyou to Alan Bishop and Sandy MacIntyre, who provided valued assistance in the operation of the flow cytometers and sorters, Dr Jo Woodcock for assistance with saturation binding assays and Paul Sincock, who was a valuable resource in educating me in the finer points of confocal microscopy. I also thanks all members of the previous Leukaemia Haemopoiesis Laboratory headed by Leonie Ashman, as well as current members of the Mathew Roberts Laboratory headed by Andrew Zannettino and Stan Gronthos, for their support and assistance, and making work an enjoyable place to be!

Finally, I thank my family. My parents made many sacrifices to equip me with the skills and education to achieve this, and I am forever indebted to them for this. My

darling wife, Bron, has provided the most crucial support throughout this study. Her patience, encouragement and faith have never wavered and are the driving force behind any success I achieve. Thanks also to my daughter, Tiana. She is too young to realise this yet, but has been a model child with a beautiful nature. This allowed me the time to devote more efforts than would normally be possible in family time toward completion of this thesis.

Errata Insert –

Abstract: page xiii, 1st Para – additional sentence:
The c-Kit isoforms analysed throughout this thesis arise by differential splicing at 1 site in the c-Kit gene resulting in the insertion/deletion of 12bp encoding the amino acids GNNK. These are referred to as GNNK+ and GNNK- throughout the thesis.

Chapter 1, Section 1.1.2, p5, para 2:
Replace "epinephrin: with "ephrin"

Chapter 3, Table Legend, Table 3.3:
Add "A, B, C represent separate pools of NIH3T3 infectants with different levels of surface expression c-Kit."

Chapter 3, Section 3.2, p97, last sentence:
Change to "The findings of that study are discussed in this section."

Chapter 3, Figure 3.9
Replace "12-s+ PMAPK" with "GNNK-" and "12+s+ PMAPK" with "GNNK+"
Replace "0", "15" and "30" with "0 min", "15 min", and "30 min" respectively

Chapter 4, Introduction, p118, Para 2 after 1st sentence:
Insert "Previous studies by Ferrao et al. (Ferrao et al., 1997) had demonstrated that stimulation of MIHC expressing c-Kit could differentiate in response to exogenous SCF."

Chapter 4, Introduction, p119, Para 1 after 1st sentence:
Insert at end "and is activated by SCF stimulation (Liang et al., 2002*; Ueda et al., 2002**)."

Chapter 4, Section 4.1.5, p125, Para 1, last sentence:
Replace "AMV" with "Myeloproliferative Sarcoma Virus (MPSV)"

Chapter 5, Section 5.4.2, last sentence, p168:
Add "To confirm this, nuclear run on assays or Actinomycin D experiments to assess mRNA stability are required."

Chapter 5, Section 5.5, 1st para, 2nd sentence on p173:
Replace sentence with "It has often been noted that c-Kit is down-modulated in mobilisation of CD34 cells, however this did not appear to be at the level of mRNA transcription or stability, although experimentation such as nuclear run on assays is required to confirm this."

* Liang, X., Wisniewski, D., Strife, A., Shivakrupa, Clarkson, B. and Resh, M.D. (2002). Phosphatidylinositol 3-kinase and Src family kinases are required for phosphorylation and membrane recruitment of Dok-1 in c-Kit signaling. *J Biol Chem* **277** (16), 13732-8

** Ueda, S., Mizuki, M. Ikeda, H., Tsujimura, T. Matsumura, I., Nakano, K., Daino, H., Honda, Z.Z., Sonoyama, J., Shibayama, H., Sugahara, H., Machii, T., and Kanakura, Y. (2002) Critical roles of c-Kit tyrosine residues 567 and 719 in stem cell factor –induced chemotaxis: contribution of src family kinase and PI3-kinase on calcium mobilization and cell migration. *Blood* **99**(9), 3342-9

Abbreviations

6FAM	6-Carboxyfluorescein
α-MEM	Alpha modification of minimum essential medium
ATP	Adenosine triphosphate
BM MNCs	Bone marrow mononuclear cells
bp	Base pair(s)
BSA	Bovine serum albumin
CD	Cluster of differentiation
CD117	c-Kit
cDNA	Complimentary DNA
CFU	Colony Forming Unit
Chi c-Kit	Chimaeric human/mouse c-Kit
c-Kit	CD117, Stem Cell Factor Receptor
COOH	Carboxy (terminus)
CSF	Colony stimulating factor
DEPC	Diethylpyrocarbonate
DMEM	Dulbecco's modified eagles medium
DMSO	Dimethyl sulphoxide
DNA	Deoxyribonucleic acid
ECF	Enhanced Chemifluorescence
EGF	Epidermal Growth Factor
EGFR	Epidermal Growth Factor Receptor
ELISA	Enzyme-linked immunosorbent assays
FACS	Fluorescence activated cell sorting

FCS	Foetal calf serum
FITC	Fluorescein isothiocyanate
G-CSF	Granulocyte-CSF
GIST	Gastrointestinal Stromal cell Tumour
GM-CSF	Granulocyte/macrophage-CSF
HBSS	Hank's balanced salt solution
ICC	Interstitial Cells of Cajal
Ig	Immunoglobulin
IgG_1, IgG_{2a}, IgG_{2b}	Immunoglobulin gamma-1, gamma-2a and gamma-2b isotype
Ig M	Immunoglobulin M
IMDM	Iscove's modified Dulbecco's medium
IMVS	Institute of Medical and Veterinary Science
IU	International units
JM	Juxtamembrane
kD	Kilodalton
LPS	Lipopolysaccaride
Mab	Monoclonal antibody
MAPK/ERK kinase	Mitogen-activated protein kinase/extracellular signal-regulated
MCS	Multiple cloning site
M-CSF	Macrophage colony-stimulating factor
MFI	Mean fluorescence intensity
MIHC	Myb Immortalised Haemopoietic Cells
mRNA	Messenger RNA
NH2	Amino (terminus)

NP-40	Nonidet P40
PB MNCs	Peripheral blood mononuclear cells
PBS	Phosphate-buffered saline
PBS/BSA/Az	PBS + 0.1% w/v BSA + 0.1% w/v Sodium Azide
PCR	Polymerase chain reaction
PDGF	Platelet Derived Growth Factor
PDGFR	Platelet Derived Growth Factor Receptor
PE	Phycoerythrin
PH	Pleckstrin Homology
PI3-K	Phosphatidyl Inositol-3 Kinase
PTB	Phosphotyrosine Binding
PTP	Protein Tyrosine Phosphatase
PVDF	Poly Vinyl Di Fluoride
RNA	Ribonucleic acid
RPMI-1640	Rosewell Park Memorial Institute Medium 1640
RTK	Receptor Tyrosine Kinase
RT-PCR	Reverse transcription- polymerase chain reaction
SCF	Stem Cell Factor, Kit Ligand, Mast Cell Growth Factor, Steel
Factor	
SCLC	Small cell Lung Carcinoma
SEM	Standard error of mean
SH2	Src Homology 2
SH3	Src Homology 3
TEMED	N, N, N' N'-tetramethyl-ethylenediamine
TM	Transmembrane

Ub	Ubiquitin
UV	Ultra violet
v/v	Volume per volume
w/v	Weight per volume

Contents

Abstract

c-Kit is a member of the Receptor Tyrosine Kinase Type III family and has four naturally occurring isoforms. The work presented in Chapter 3 utilised full-length human or murine c-Kit cDNA expressed in murine cells. Over-expression of normal c-Kit was capable of contributing to oncogenic transformation. The analysis of human c-Kit isoforms demonstrated dissociation of various indicators of transformation (anchorage independence, loss of contact inhibition, tumourigenicity) in the NIH3T3 cell model.

Biochemical analysis of the c-Kit signalling revealed qualitative and quantitative differences between the GNNK+ and GNNK- c-Kit isoforms. The GNNK- isoform was hyperphosphorylated more extensively and rapidly, and was also more efficiently ubiquitinated and degraded than the GNNK+ counterpart. PI3-K was recruited and activated equally by both isoforms. Phosphorylation of MAPK paralleled that of the c-Kit isoform's phosphorylation.

In Chapter 4, a new model was developed using a chimaeric human extracellular c-Kit/murine transmembrane + intracellular c-Kit. This new molecule, in conjunction with a murine Myb Immortalised Haemopoietic Cell (MIHC) line was used to investigate a number of biological outcomes stimulated by SCF simultaneously. A MIHC line lacking Lyn was also analysed.

Chimaeric c-Kit displayed the same signalling characteristics exhibited by its' full-length human counterpart. The model showed that the GNNK- isoform was superior

in its survival stimulus to GNNK+, but both were equivalent in promoting proliferation. The absence of Lyn reduced the ability of both isoforms to promote survival.

The aim of work in Chapter 5 was to elucidate the expression patterns of the c-Kit isoforms in subsets of normal human haemopoietic cells. Methodology was developed to detect GNNK+/- c-Kit mRNA from rare subsets of cells from bone marrow. As c-Kit is known to be down-modulated in mobilised peripheral blood stem cells, mobilised CD34+ cells were also investigated. In all haemopoietic cells analysed, there was no significant difference in expression patterns of the c-Kit isoforms, with all samples expressing approximately 90% of total c-Kit transcripts as the GNNK- isoform. c-Kit downmodulation observed in mobilisation of CD34+ cells was not influenced at the level of transcription, but at the protein level.

1 Introduction

1.1. c-Kit - a member of the Growth Factor Receptor Tyrosine Kinase Family

1.1.1. The Growth Factor Receptor Tyrosine Kinases

Receptor Tyrosine Kinases (RTKs) are a large family of growth factor receptors (Blume-Jensen et al., 2001). All growth factor receptors in this family possess a glycosylated extracellular ligand binding domain, a hydrophobic transmembrane domain, and a cytoplasmic domain that contains a tyrosine kinase catalytic domain. Based on sequence and structural similarities, there are now twenty classes (or types) of receptor tyrosine kinases (reviewed in (Blume-Jensen et al., 2001; Hanks et al., 1988; Heldin, 1995; Schlessinger, 2000; Ullrich et al., 1990; Yarden et al., 1988).

The extracellular domain of each RTK enables specific ligand binding and there is minimal sequence conservation in this domain between classes. The transmembrane domain is highly hydrophobic and of conserved length but not conserved sequence (even within a class of RTK). The juxtamembrane region is approximately 50 amino acids and is usually conserved within a class of RTK (Ullrich et al., 1990). The tyrosine kinase domain is highly conserved in all RTKs (Yarden et al., 1988). The carboxy terminal tail is most divergent, being highly variable in length and sequence (Yarden et al., 1988).

Figure 1.1 has been reproduced from Blume-Jensen and Hunter, 2001, to illustrate the structural variation between RTK classes. It is clear from this figure that the different classes of RTKs have employed highly variant structures to engage their ligand, yet

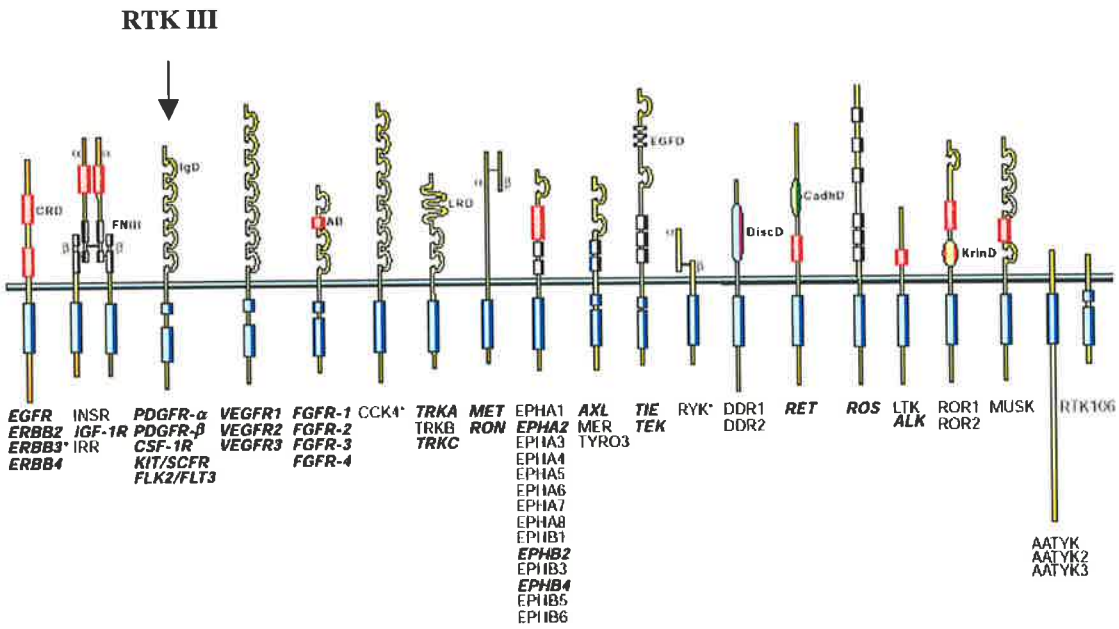

Figure 1.1

Receptor Tyrosine Kinase family

Adapted from Blume-Jensen and Hunter, 2001

still possess the same overall organisation and function. These structures are all required to engage with a ligand, transmitting a signal, via the intracellular tyrosine kinase domains, to initiate a signalling cascade. The different classes also employ a variety of mechanisms for regulation of the signalling response. Summarised below are some notable differences between the first few classes of RTKs

RTK type I includes the epidermal growth factor receptor (EGFR encoded by *c-erbB1*) and its close relatives HER-2/neu, HER-3 and HER-4 (encoded by *c-erbB2*, *3* and *4*, respectively). RTK type I receptors possess two cysteine-rich repeat sequences within the extracellular domain (Blume-Jensen et al., 2001)

In contrast, the RTK type II receptors, which include the insulin and insulin-like growth factor receptors, function as heterotetrameric structures involving two α and two β subunits. The α subunits bind the ligand and are disulphide-linked to the β subunits, which traverse the membrane and possess the tyrosine kinase domains. A cysteine-rich repeat sequence is found on each α subunit.

RTK type III includes the CSF-1R (encoded by *c-fms*), α and β PDGFR, flt3/flk2 and c-Kit. The human c-Kit cDNA sequence predicts that the protein possesses a 23 amino acid (aa) signal peptide, 497 aa extracellular domain, 23 aa transmembrane domain and 433 aa intracellular domain (Yarden et al., 1987a).

RTK IIIs do not have a cysteine-rich repeat sequence but instead possess 10 distinctively positioned cysteine residues which contribute to the formation of five immunoglobulin (Ig)-like domains within the extracellular region (Blume-Jensen et

al., 2001). RTK IIIs also differ in their intracellular region compared to other classes. The protein tyrosine kinase catalytic domain is interrupted by a poorly conserved, non-catalytic hydrophilic insertion sequence of varying length (70-100 residues) (77 aa for c-Kit). This region has been referred to as the kinase insert (KI) or interkinase domain (Blume-Jensen et al., 2001).

RTK type IV is structurally similar to RTK III also containing a KI domain, but only possesses two to three Ig-like loops in its extracellular domain. Fibroblast growth factor receptors (FGFR) are examples of this group.

Another subclass that also resembles RTK III but has 7 Ig-like loops in the extracellular domain includes flk1, flt1 and flt4, and members of the vascular endothelial growth factor (VEGF) receptor family. Additional RTK families also exist and new members are constantly being discovered (reviewed (Blume-Jensen et al., 2001; Heldin, 1995; Lemmon et al., 1994).

1.1.2. Signalling through RTKs

When ligand binds to the extracellular domain of the RTK, cross-linking of receptors by ligand and/or conformational changes occur, resulting in dimerisation (Ullrich et al., 1990). Dimerisation enables the cytoplasmic portions of the receptor subunits to come into close proximity in a stabilised fashion. Dimerisation initiates autophosphorylation of the receptors on tyrosine residues (Schlessinger et al., 1992) as well as catalytic activation (Schlessinger et al., 1995). In addition, dimerisation facilitates transphosphorylation of a Tyrosine in the activation loop of the kinase catalytic domain which leads to increased activity and the phosphorylation of other

tyrosine residues on the receptor, creating high-affinity binding sites for downstream components of the receptor's signalling pathways (Heldin, 1995; Hubbard et al., 2000).

Studies on crystallised insulin receptor, fibroblast growth factor receptor 1 and vascular endothelial growth factor receptor 2 have shed much light on the mechanisms of catalytic activation. Figure 1.2 illustrates the postulated mechanism. In the resting receptor, the activation loop of the catalytic domain blocks access of ATP and substrate (Hubbard et al., 2000; Mohammadi et al., 1998). The loop is quite mobile and is in equilibrium with the 'active state' allowing access of ATP and substrate (Blume-Jensen et al., 2001; Hubbard et al., 2000; Mohammadi et al., 1998; Schlessinger et al., 2000). Ligand induced dimerisation stabilises the "active state" long enough to facilitate transphosphorylation of the Tyrosine residue in the activation loop. Dimerisation alone is inadequate, indicating that other ligand induced conformation changes are necessary for this to happen (reviewed (Blume-Jensen et al., 2001; Huse et al., 2002)). However, recent analysis of the crystal structure of the active conformation of c-Kit cytoplasmic domains has revealed that the Y823 in the activation loop of the kinase domain is the last tyrosine to be phosphorylated in the trans-phosphorylation steps involved in c-Kit activation (Mol et al., 2003), and perhaps not required for activation of the kinase, unlike most other kinases. The first tyrosines to be phosphorylated were Y568 and Y570 in the juxtamembrane region. Mutations clustered near these residues confer constitutive activation of c-Kit, disregulating the receptor leading to cancerous lesions including GIST (Hirota et al., 1998; Nishida et al., 1998). This analysis also suggests that the activation loop is very close to an active configuration in the normal, monomeric, unphosphorylated c-Kit

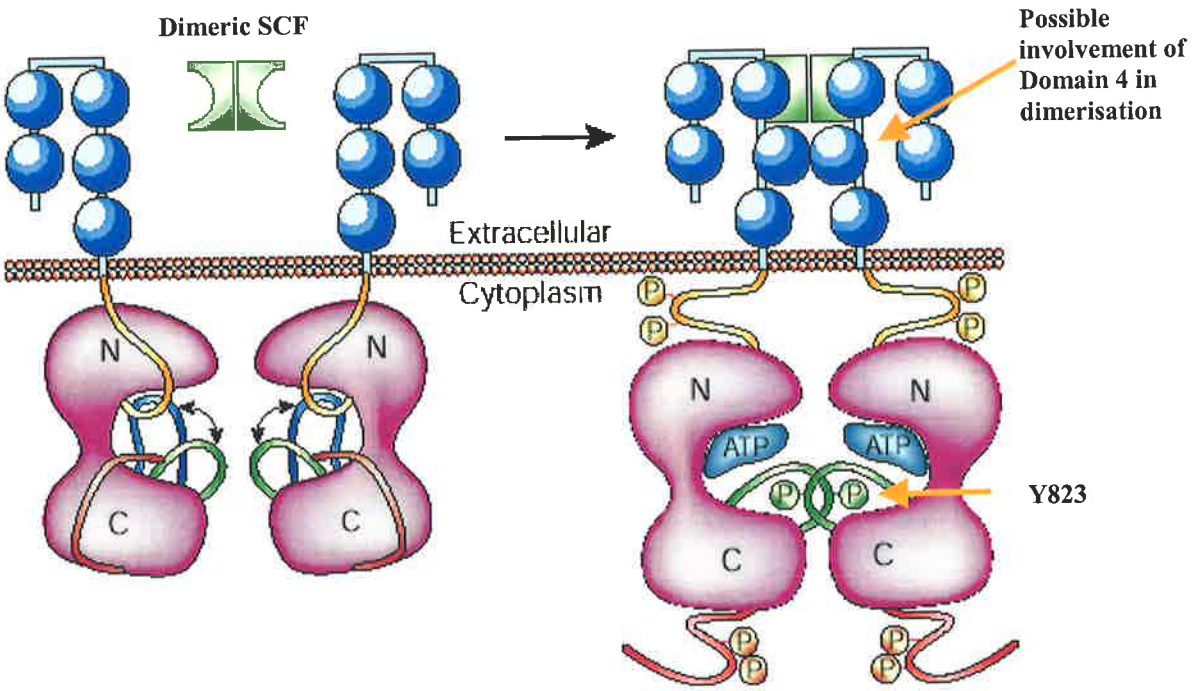

Figure 1.2

RTK Activation Mechanism

Left:
RTK kinase activity is tightly repressed in the resting state. The activation and catalytic loops of the kinase domain exist in an equilibrium between substrate "precluding" (blue) and substrate "accessible" (green). In addition, the Juxtamembrane region (orange) and c-terminal (red) may interfere with the N-terminal kinase lobe (N) and or substrate access.

Right:
Ligand induced receptor dimerisation and tyrosine autophosphorylation result in relief of the inhibitory constraints exerted by the activation loop, juxtamembrane domain and c-terminal tail.

Adapted from Blume-Jensen and Hunter, 2001

receptor, and suggests that the limiting factor may, in fact, be dimerisation (Mol et al., 2003). Of note, it was demonstrated that small molecule inhibitors for c-Kit such as STI-571 cannot fit into the catalytic domain of the receptor when in the active state, providing a mechanism for constitutively active c-Kit mutants to be highly resistant to the drug (Mol et al., 2004; Mol et al., 2003).

In addition to this, the juxtamembrane domain has also been reported to have autoinhibitory functions (Blume-Jensen et al., 2001). In the epinephrin receptor EphB2, analysis of the crystal structure of an unphosphorylated, autoinhibited receptor (juxtamembrane and kinase domain only) revealed that the juxtamembrane region adopts a conformation that distorts the kinase domain, blocking the activation segment of the kinase domain from adopting an active conformation. Phosphorylation of tyrosines within the juxtamembrane region were postulated to disturb this association with the kinase domain, releasing the kinase domain to adopt an active conformation, and also presenting phosphotyrosine sites for interaction with SH2 domain containing proteins that interact with the receptor (Wybenga-Groot et al., 2001).

The carboxy tail may also act, in some cases, to obstruct the catalytic site, and can be a target for phosphorylation/docking of Src homology 2 (SH2) and protein tyrosine binding (PTB) containing proteins (downstream signalling effectors) (Blume-Jensen et al., 2001).

1.1.3. c-Kit in Cancer

c-Kit, as well as being a crucial component of haemopoietic stem cell development, plays a critical role in mast cell and interstitial cells of Cajal (ICC) development and function. This is demonstrated by the depletion of these cell types where "loss of function" mutants of c-Kit are present (Fox et al., 2002; Hirota et al., 2000; Kitamura et al., 2001). In contrast, c-Kit "gain of function" mutations often result in oncogenesis in these cell lineages . The locations of these mutations lead to constitutive activation, but by different means.

Gain of function mutations in the cytoplasmic juxtamembrane region of c-Kit achieve activation by constitutive dimerisation (Kitamura et al., 2001) and de-repression of the kinase catalytic site (Chan et al., 2003). Such mutations are linked to GISTs and some mastocytosis cases (Casteran et al., 2003; Heinrich et al., 2002; Hirota et al., 2000; Yasuoka et al., 2003), as well as myogenic and neurogenic tumours (Yasuoka et al., 2003). As discussed in section 1.1.2 above, inactive c-Kit kinase domains are very close to their active conformation, and proximity of a binding partner (for dimerisation) is postulated to be the limiting step in the activation process, with dimerisation facilitated by the binding of SCF in normal c-Kit (Mol et al., 2003). The juxtamembrane region is also responsible for autoinhibition of c-Kit. It interacts with the ATP binding lobe of the kinase domain as demonstrated using peptides of the juxtamembrane domain. These peptides have been validated and shown to fold appropriately, mimicking the juxtamembrane domain structure of full length c-Kit. Mutations of these peptides corresponding to known juxtamembrane gain of function

mutations of c-Kit disrupted the structure of the domain and interfered with its association with the kinase domain (Chan et al., 2003).

Mutations in the kinase domain are often dimerisation independent in maintaining an active conformation of the catalytic domain (Kitamura et al., 2001). Mutation of Aspartate 816 in c-Kit's kinase domain leads to constitutive activation of c-Kit and mastocytosis (Casteran et al., 2003; Longley et al., 1999). This mutation has also been identified in a subset of patients with Chronic Myeloid Leukaemia (Pardanani et al., 2003), in germinal cell tumours and seminomas (Sakuma et al., 2003), as well as testicular germ cell tumours (Looijenga et al., 2003; Sakuma et al., 2003).

c-Kit has been implicated in other lesions including Small-Cell Lung Carcinoma (SCLC). Recent findings suggest that whilst c-Kit was detectable on 40% of cases studied, very few of these expressed activating mutations, and the presence or absence of c-Kit had little impact on patient survival (Boldrini et al., 2004). Another retrospective SCLC study showed that lack of c-Kit expression was associated with shorter median survival (Rohr et al., 2004).

A subset of angiosarcomas have also been demonstrated to express c-Kit, but in all of these cases, the c-Kit was not mutated and the abnormal expression was attributed to reversion of the affected cells to a phenotype of foetal endothelial cells that normally express c-Kit (Miettinen et al., 2000). A truncated form of c-Kit (containing the kinase domain through to the carboxy terminus) has also been identified in a subset of prostatic cancers, and in this subset, there is evidence of elevated Src family kinase activity (Paronetto et al., 2004).

1.2. HISTORY of c-Kit

1.2.1. - The discovery of the c-Kit proto-oncogene

Infectious filtrate obtained from a primary feline fibrosarcoma was shown by Besmer *et al* (Besmer et al., 1986) to transform feline embryo fibroblasts and mink cells. A feline leukaemia virus (FeLV) belonging to the Hardy-Zuckerman 4 strain (HZ4-FeSV) was identified as the transforming infectious agent. The transformed mink cells were unable to produce infectious HZ4-FeSV, but the retrovirus could be rescued by superinfection with a helper virus (the amphotropic murine leukaemia virus (MuLV). Therefore the HZ4-FeSV was replication-defective, suggesting that this transforming retrovirus may be harbouring an oncogene which was disrupting viral-replication. Analysis of the HZ4-FeSV provirus, obtained from mink infected cells, revealed a non-viral sequence specific to the HZ4-FeSV, which was designated v-Kit. Protein analysis using antisera specific for the gag protein, p27, of FeSV, immunoprecipitated an 80 kD protein, p80, suggesting that the gag and v-Kit products form a fusion protein. The structure of the HZ4-FeSV provirus was shown to contain a v-Kit insert of 1.1 KB in size, encoding a protein of 370 amino acids. In order to determine whether it was derived from a cellular gene, v-Kit sequence was used to probe cat, human and mouse DNA, and homologous sequences were found to be present in all species, the transcript ranging from 5 - 5.5 kb (Qiu et al., 1988; Yarden et al., 1987a).

Cloning of the cellular counter-part of v-Kit from both mouse and human cDNA libraries, obtained from brain and placenta respectively, revealed that structural differences existed between the v-Kit and c-Kit gene products. v-Kit had been truncated at both the NH2 and COOH termini during transduction. This results in a

product which lacks the entire extracellular domain, the transmembrane domain, the first 17 amino acid residues of the intracellular domain, as well as the COOH-terminal 49-50 amino acid residues which were replaced with 5 unrelated amino acids. Other differences also existed between murine c-Kit and v-Kit involving 20 amino acids (Qiu et al., 1988; Yarden et al., 1987a). All but three of these differences have been attributed to divergence between the species (Herbst et al., 1995a). The remaining three alterations have been shown to contribute to the oncogenicity of v-Kit.

Human c-Kit cDNA encodes a 976 amino acid polypeptide with a molecular weight of 145 kD (fully glycosylated; immature form = 125 kD) (Yarden et al., 1987a) and was therefore designated, p145c-Kit. p145c-Kit (throughout this thesis it will be referred to as c-Kit) shares major structural features with the macrophage colony-stimulating factor-1 receptor (CSF-1R), α and β platelet derived growth factor receptors (PDGFR) (Qiu et al., 1988; Yarden et al., 1987a) and flt3/flk2 receptor (Matthews et al., 1991; Rosnet et al., 1991) which are all growth factor receptors belonging to the receptor tyrosine kinase type III (RTK III) family. This family shares sequence homology within their catalytic kinase domain with c-Src. Despite their structural similarities, the non-catalytic sequences of the three proteins (ie CSF-1R, PDGFR and c-Kit) display sequence heterogeneity that is highest in the ligand binding domain and the kinase insert. These regions define the functional specificity of each receptor. Figure 1.3 shows a schematic representation of c-Kit.

Concurrent with the discovery of c-Kit gene in human species, the human c-Kit protein was identified in 1985 by Gadd and Ashman (Gadd et al., 1985). The protein was identified originally as an Acute Myeloid Leukaemia associated surface antigen

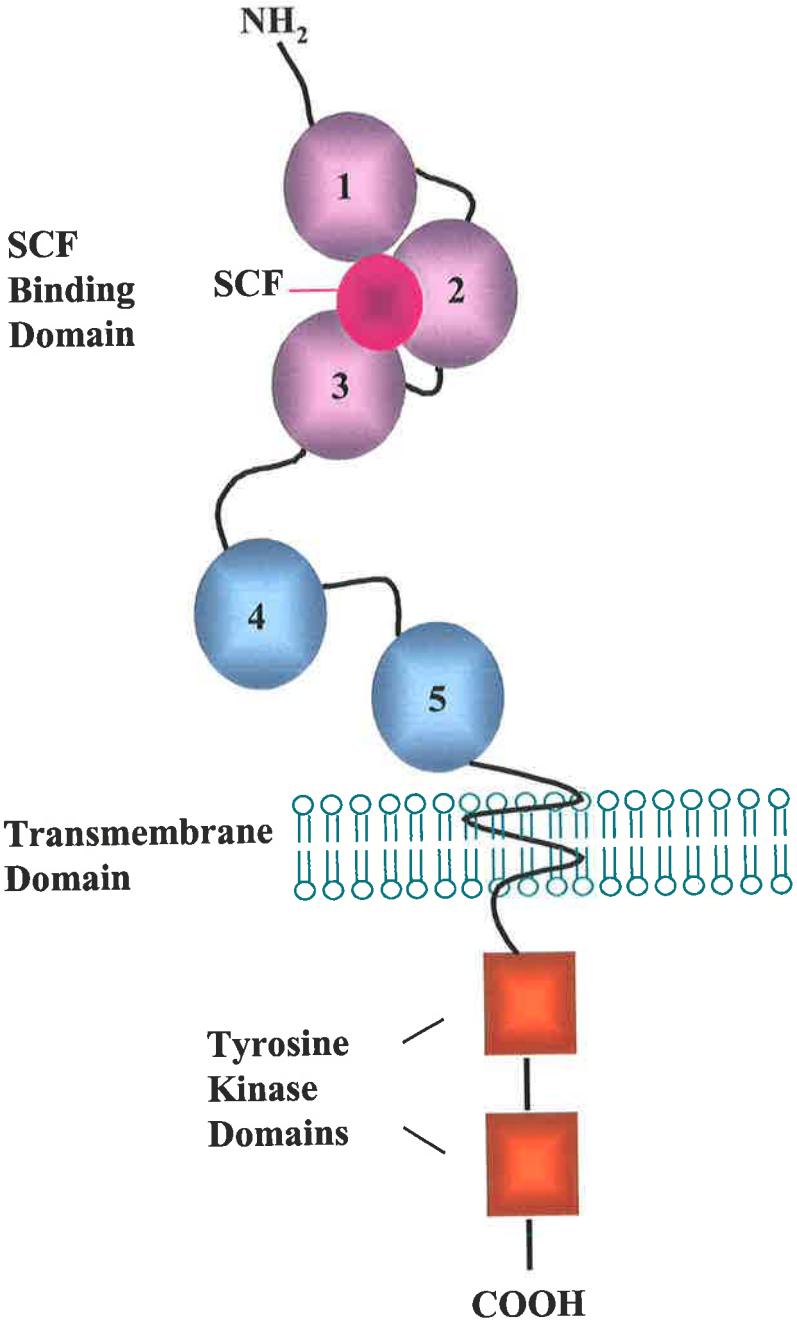

Figure 1.3

Schematic representation of c-Kit receptor

by Monoclonal Antibody (Mab) YB5.B8. Patients with blast cells expressing high levels of this surface antigen demonstrated very poor prognosis (Ashman et al., 1988). The protein was later identified as c-Kit (Ashman et al., 1991; Lerner et al., 1991).

1.2.2. *Association of c-Kit with the W locus*

Using somatic cell hybrid and in situ hybridisation techniques, c-Kit was mapped to the human long arm of chromosome 4 between 4q11-q21 and murine c-Kit to mouse chromosome 5 (Yarden et al., 1987a). The location of murine c-Kit on chromosome 5 led to the hypothesis that c-Kit may be linked to the W locus also found on this chromosome. Mutant mice carrying defects at the W loci (W19H and W44) were analysed for alterations in c-Kit and, in the case of W44, a rearrangement confined to the c-Kit gene was found linking c-Kit to the W locus (Chabot et al., 1988; Geissler et al., 1988). The existence of spontaneous W mutant mice provided an insight into the function of c-Kit. Many W mutant mice have been described thus far and display defects in gametogenesis (affecting fertility), melanogenesis (resulting in lack of hair pigmentation or "white-spotting"), defects in haemopoiesis (resulting in macrocytic anaemia and mast cell deficiencies) (reviewed (Kitamura et al., 1978; Russell, 1979; Sarvella et al., 1956)). DNA and protein analysis of c-Kit from mast cells obtained from various W mutant mice have revealed structural alterations within the c-Kit gene which range from genomic rearrangements and partial deletions to single point mutations (Geissler et al., 1988; Nocka et al., 1990b; Reith et al., 1990). Kinase activity associated with the c-Kit gene product was also affected in mast cells obtained from W mutant mice (Nocka et al., 1989; Reith et al., 1990). Demonstration that c-Kit was expressed by the lineages affected in the W mutant mice, such as foetal and adult erythropoietic tissues, mast cells and neural-crest-derived melanocytes

(Nocka et al., 1989), as well as the data described above provided sufficient evidence that the c-Kit gene and the murine white spotting locus (W) were allelic (Keshet et al., 1991; Lammie et al., 1994; Manova et al., 1991; Nocka et al., 1989; Ogawa et al., 1991; Ratajczak et al., 1992).

Mutations at the W locus represented the first examples of germ-line mutations in a mammalian proto-oncogene (Chabot et al., 1988). The W mutant mice vary in the severity of their defects which parallels with the severity of the mutation within c-Kit and whether the mice were homozygous or heterozygous for the c-Kit alleles. For the original W mutation, mice carrying one W allele (W/+) have a relatively mild phenotype displaying a ventral white spot, pigment free feet and tail tip, but their blood parameters and fertility are normal. Mice carrying both W alleles (W/W) die neonatally or in utero of severe macrocytic anaemia.

Many of the W mutations involve conserved amino acids within the tyrosine kinase domain of c-Kit resulting in the disruption of the biochemical activity of the receptor (see table 1.1 adapted from Bernstein *et al*, 1991 (Bernstein et al., 1991)). Mutations that abolish kinase activity due to deletion (W and W19H) (Chabot et al., 1988; Hayashi et al., 1991) or point mutation (W37 and W42) that result in loss-of-function or "null" mutations (Nocka et al., 1990b; Reith et al., 1990) were lethal in the homozygous state. In contrast, mutations which have residual kinase activity (Wv and W41) were viable as homozygotes (Nocka et al., 1990b; Reith et al., 1990). Certain mutations that cause severe effects in the heterozygous state exhibit strong "dominant negative" effects (Herskowitz, 1987). For example Wv, W41, and W42, which comprise mutations at distinct sites in the region encoding the kinase domain of the

W Mutation	Phenotype		c-Kit Kinase Activity	Molecular Lesion
	Heterozygote	Homozygote		
W^v	White spot, mild anaemia	White, anaemia, sterile	Low	Thr^{660} to Met
W^{41}	White spot, mild anaemia	Mostly white, anaemic, fertile	Good	Val^{831} to Met
W^{44}	White spot	Mostly white, reduced fertility	Low	Insertion in non-coding region
W^{57}	White spot	White patches, mildly anaemic, fertile	Low	Regulatory
W^{37}	Mostly white	Late lethal	Nil	Glu^{582} to Lys
W42	White, anaemic, reduced fertility	Late lethal	Nil	Asp790 to Asn
W	White spot	Late lethal	Nil	Small deletion
19H	White spot	Early lethal	Nil	Large deletion

Table 1.1

Summary of W mutants

Adapted from Bernstein et al, 1991

c-Kit gene, result in the production of impaired receptors with reduced or no intrinsic kinase activity but are nevertheless expressed on the cell surface (Reith et al., 1990). In heterozygotes, dimerisation between wild type and mutant c-Kit can occur. The mutant receptor therefore impairs the function of the wild type receptor by preventing transduction of the normal ligand-induced signal, in most cases preventing transphosphorylation of the wild type receptor within the dimer complex. Those mutations that result in lack of (W) or reduced levels (W37) of protein being expressed at the surface have less severe defects in heterozygotes (Nocka et al., 1990b). Typically this results in a 50% reduction in the number of functional receptors expressed at the surface in heterozygotes.

There are several aspects of the function of c-Kit that might be affected by W mutations, including ligand binding, tyrosine kinase activity, receptor autophosphorylation, association of c-Kit with certain downstream signalling molecules, ligand induced internalisation, and receptor downregulation. The different c-Kit mutations were shown to differentially affect coat colour, anaemia, mast cell deficiency and fertility with different severities, demonstrating the different biochemical events influenced by the activation of c-Kit. The level of receptor expression has also been shown to be of importance in determining the biological outcome of a cell (ie. Does the cell differentiate or proliferate in response to ligand?) and this may also explain the phenotypes seen in those mice with reduced levels of functional protein in the heterozygous state (eg W/+ mice).

In humans a similar phenotype to that displayed by W mutant mice is also seen in patients with the autosomal dominant genetic disorder of piebaldism. The phenotype

of these patients is characterised by patches of hair and skin which lack pigmentation due to the absence of melanocytes in these areas. In contrast to the mutant mice, fertility and anaemia do not appear to be associated with the piebald trait (Fleischman et al., 1991; Giebel et al., 1991; Ward et al., 1995). The defect seen in these patients is also due to deletions or point mutations located within the c-Kit gene on the long arm of chromosome 4, demonstrating piebaldism as the human condition equivalent to the dominant white spotting of the mouse (Ezoe et al., 1995; Fleischman et al., 1991; Giebel et al., 1991).

1.3. The ligand to c-Kit: The Link between W and Sl mutant mice

Around the same time as the discovery of c-Kit, the c-Kit ligand was identified in several laboratories in murine, rat and human systems. It has several names including Mast Cell Growth Factor (MGF) (Anderson et al., 1990; Williams et al., 1990), Steel Factor (SLF) (Williams et al., 1992), Kit Ligand (KL) (Flanagan et al., 1990; Huang et al., 1990; Nocka et al., 1990a) and Stem Cell Factor (SCF) (Zsebo et al., 1990). Throughout this thesis, the c-Kit ligand will be referred to as SCF.

SCF is a 248 amino acid transmembrane protein with a 36 amino acid cytoplasmic domain, 23 amino acid transmembrane domain and 189 amino acid extracellular domain (Ashman, 1999a; Broudy, 1997; Flanagan et al., 1990). Alternate splicing generates two mRNA species that include or exclude exon 6. The protein products, SCF^{220} and SCF^{248} are both membrane associated but SCF^{248} has an additional 28 amino acids (encoded by exon 6) in the extracellular juxtamembrane region (Ashman, 1999a; Broudy, 1997; Flanagan et al., 1990). See Figure 1.4 for a schematic representation of SCF isoforms.

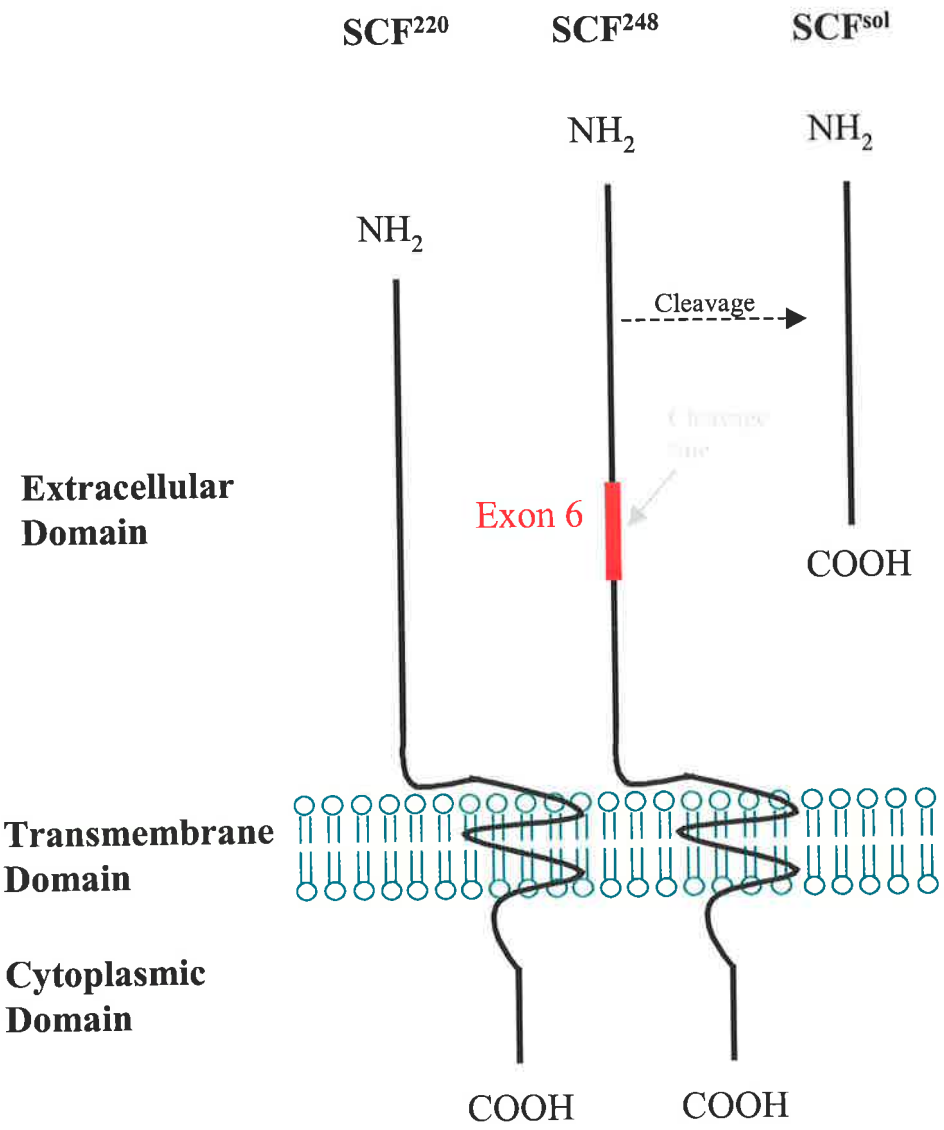

Figure 1.4

Schematic representation SCF showing structure of 2 isoforms and soluble SCF cleavage product

Williams *et al* (Williams et al., 1990) identified a soluble form of SCF in murine stromal cell culture supernatants. This form is produced by proteolytic cleavage of the longer isoform of SCF. This is due to the presence, in exon 6, of sequence encoding a serine protease cleavage site at amino acid 165 (Longley et al., 1997). There is also a chymase cleavage site at position 159 (also within exon 6 coding region) which is targeted by mast cell derived chymotrypsin like protease, producing a slightly smaller soluble SCF. Murine SCF has an extra cleavage site encoded in exon 7, leading to the formation of soluble SCF irrespective of which isoform is produced. Soluble and transmembrane SCF are both biologically active (Anderson et al., 1990).

Soluble SCF exists as both a non-covalent homodimer and a monomer (which is predominant) (Hsu et al., 1997). Zhang *et al* (Zhang et al., 2000) confirmed the dimeric structure by ascertaining the crystal structure of the soluble dimer. Dimerisation of SCF appears critical for biological activity – dimerisation defective SCF has very low activity (Hsu et al., 1997). However, confusion exists as artificially dimerised (disulphide bridged) SCF demonstrated higher activity than monomeric SCF in one study (Hsu et al., 1997) and no activity in another (Zhang et al., 2000). Membrane bound SCF is predominantly dimerised (Tajima et al., 1998). Deletion of the cytoplasmic domain affected dimerisation only slightly, but replacement with irrelevant amino acids decreased dimerisation substantially (Tajima et al., 1998). This suggests that subtle conformation changes of SCF effect its ability to dimerise, and the variation in activity of different SCF dimers (mutant/artificial) may reflect changes in conformation of the SCF dimer itself and its ability, therefore, to interact productively with its receptor, c-Kit.

Interestingly, Steel (Sl) mice, which have defects associated with the Sl locus localised on murine chromosome 10 (Sarvella et al., 1956), displayed a similar phenotype to the W mutant mice. Early experiments involving the analysis of the defects within the haemopoietic compartment revealed that the W mutant mice had a defect that was intrinsic to their stem cells now attributed to mutations within c-Kit. In contrast, the Sl mutant mice had a defect within the microenvironment required to support growth of primitive stem cells (Russell, 1979). These conclusions were drawn from transplantation experiments in which the injection of normal (+/+) bone marrow, as a source of stem cells, into unirradiated W/Wv mice resulted in the cure of their macrocytic anaemia and the production of spleen colony forming cells (CFU-S) (McCulloch et al., 1964; Russell, 1979; Russell et al., 1968) and mast cells (Kitamura et al., 1978). The injection of +/+ bone marrow cells into Sl/Sl^d mice could not cure their anaemia or produce CFU-S, suggesting that the stem cells within these mice were normal and that the microenvironment supporting the stem cells was impaired. As SCF mapped to chromosome 10 (Copeland et al., 1990; Zsebo et al., 1990), SCF was eventually shown to be allelic with the Sl locus.

Sl^d (Steel – Dickie) mice demonstrated the importance of the transmembrane region of SCF. The Sl^d mutation deletes the transmembrane and cytoplasmic domains, producing only soluble SCF which is fully capable of stimulating proliferation (Flanagan et al., 1991). These mice still have defects in haemopoietic cell development, melanocytes and germ cells, although less severe, highlighting the role of transmembrane SCF in these systems.

The Sl^{17H} mutant (Tajima et al., 1998) has a mutated cytoplasmic domain. It has the cytoplasmic domain substituted with 27 irrelevant amino acids and is surface expressed, but displays altered stability and dimerisation properties (Tajima et al., 1998). Mice expressing this mutant have decreased peritoneal mast cells, white spotting and males are sterile. Tajima *et al* (Tajima et al., 1998) also showed that the transmembrane form of SCF was important in adhesion of cells to bone marrow stroma and homing of transplanted haemopoietic cells to the spleen (shown in irradiated Sl^{17H} mice).

1.4. Biochemical analysis of c-Kit - Ligand Binding Domain

c-Kit has been demonstrated to show some cross species reactivity for the ligand, Stem Cell Factor. Murine or rat SCF is able to bind to both murine and human c-Kit, whereas the binding of human SCF to murine c-Kit is almost non-existent (Lev et al., 1993; Martin et al., 1990). This property has been exploited in experiments performed in this thesis.

The extracellular region of c-Kit consists of five distinct Ig-like domains. In order to determine the ligand binding domain of c-Kit, Lev *et al* (Lev et al., 1993) exploited its species specificity by producing chimaeric c-Kit consisting of murine and human c-Kit domains. Using the mouse receptor as the backbone and substituting human domains into it, the binding site of human SCF was localised. As well as the chimaeric receptor model, epitope mapping, using a number of Mab to the extracellular domain of c-Kit, combined with analysis of their abilities to block ligand binding, was used to localise the SCF binding site. Soluble ectodomains of c-Kit

were also employed to determine the minimal requirements of the extracellular domain for ligand binding (Blechman et al., 1993a; Blechman et al., 1993b) .

The ligand binding domain was confined to the three N-terminal Ig-like domains, with the second domain conferring high-affinity binding of human SCF (Lev et al., 1993). Domains I and III assisted domain II in its binding of ligand and a soluble protein possessing only the first two domains showed reduced affinity of SCF binding compared to one comprised of all three domains. High-affinity binding, involving the three N-terminal domains, may be attributed to domain III folding over the binding cleft in domain II and thereby inhibiting ligand dissociation. The ability of non-contiguous domains to stabilise ligand binding is also seen with the EGFR and insulin receptors (Schumacher et al., 1991) . Ligand competitive c-Kit Mabs (K44 and K57; (Blechman et al., 1993a)) were also found to bind to domain II, confirming that this domain contains the binding site for human SCF. Similarly the binding of PDGF-AA to αPDGFR was to the second domain of PDGFRα (Heidaran et al., 1992). Matous *et al* (Matous et al., 1996) confirmed SCF binding mapped to three distinct regions of SCF. This was later confirmed by the crystal structure of SCF showing three non-contiguous regions being juxtaposed on the surface of SCF (Jiang et al., 2000).

Similar studies were performed to determine the ligand binding site of rodent SCF to the murine c-Kit, using the human receptor as the backbone and substituting in murine c-Kit domains. The SCF binding site of the murine receptor lies mainly in domain III with some contribution from domain II. Therefore the binding domains of human and rodent SCF appear to be distinct but overlapping.

1.5. Ligand Induced Receptor Dimerisation

Ligand binding to the extracellular domain of RTK has been shown to trigger an intermolecular mechanism involving oligomerisation of the receptor molecules, resulting in the activation of their intrinsic protein tyrosine kinase and autophosphorylation (Bishayee et al., 1989; Honegger et al., 1990; Li et al., 1991; Yarden et al., 1987b) and reviewed in (Heldin, 1995; Ullrich et al., 1990). The mechanism of ligand induced dimerisation is still under investigation and many models have been proposed. For the EGFR, where the ligand is a monomer, it has been proposed that ligand binding induces conformational changes within the ligand bound receptors bringing them together to form a dimeric complex (Greenfield et al., 1989) . However, it has been demonstrated that EGF is multivalent and can simultaneously bind by distinct sites to two EGFR molecules (Lemmon et al., 1994) .

The ligands of the type III RTK, including SCF, exist as dimers, and it is still controversial whether the dimeric ligand brings about dimerisation of neighbouring receptors as a result of each ligand subunit binding a single receptor or whether the ligand binds to one receptor and then induces conformational changes leading to receptor dimerisation. Dimerisation of growth factor receptors enhances ligand binding affinity, activates protein tyrosine kinase activity and autophosphorylation of the receptor (Ben-Levy et al., 1992; Bishayee et al., 1989; Boni-Schnetzler et al., 1987; Heldin et al., 1989; Lemmon et al., 1994; Schlessinger, 1995; Spivak-Kroizman et al., 1992; Vassbotn et al., 1993; Williams, 1989; Yarden et al., 1987b) .

In the case of c-Kit, Blume-Jensen *et al*, (Blume-Jensen et al., 1991) demonstrated that the dimeric SCF molecule was responsible for inducing dimerisation of

neighbouring receptors. This was concluded from results demonstrating that, at excess concentrations, SCF binds monovalently resulting in a decrease in dimeric c-Kit. Similar findings were made with the PDGFR (Heldin et al., 1989). However, Lev *et al* (Lev et al., 1992b; Lev et al., 1992c) provided evidence that this model of ligand induced dimerisation may not be correct. This study failed to demonstrate inhibition of c-Kit dimer formation in the presence of excess ligand. Furthermore incubating purified human (deletion mutant lacking COOH-terminal 42 aa) and murine c-Kit in the presence of human SCF (which is species-selective) was able to induce cross-species receptor heterodimerisation (Lev et al., 1992b). These results implied that monovalent binding of human SCF was sufficient to induce c-Kit dimerisation and activate the receptor complex.

A putative dimerisation site of c-Kit has been localised to domain IV of the extracellular domain using deletion mutants and a Mab capable of inhibiting dimerisation (Blechman et al., 1995) . These data show that the extracellular domain of c-Kit is sufficient to induce dimerisation which is in contrast with the EGFR (Gunther et al., 1990) and the HER-2/neu receptor (Weiner et al., 1989). In the latter case dimerisation is attributed to the transmembrane domain (although the extracellular domain stabilises dimerisation) as an oncogenic form of the HER-2/neu receptor which has a single point mutation Val664 - Glu664 within this domain is constitutively dimeric and has tyrosine kinase activity (Bargmann et al., 1988; Qian et al., 1995; Weiner et al., 1989). The localisation of c-Kit dimerisation site to domain IV coincides with several activating mutations within this domain of the CSF-1 receptor, which result in receptor dimerisation (Carlberg et al., 1994; van Daalen Wetters et al., 1992) .

1.6. Ligand Induced Receptor Signalling

Signal transduction is a complex cascade of phosphorylation/dephosphorylation events on proteins and lipids, imparting incredibly fined tuned biological responses by the cell to external stimuli. For RTKs, dimerisation is the triggering event, leading to stabilisation of the kinase domain in the active state, which in turn, leads to trans and autophosphorylation of multiple target sites.

The signal transduction machinery of the cell has been described as a modular system (Pawson, 1995; Pawson, 2002). There are a series of modular domains present in all molecules involved in signal transduction, and the combinations of these modules, together with surrounding sequences, dictate the specificity and function of each component in the transduction pathways. Brief summaries of some of the most common consensus sequences or domains follow:

1.6.1. SH2

The first domains identified were found within Src kinase and were called Src Homology 2 (SH2) and Src Homology 3 (SH3) domains (Pawson, 1995). Proteins containing SH2 domains are involved in control of biochemical pathways, tyrosine phosphorylation/dephosphorylation, protein trafficking and cytoskeletal protein arrangement/function (Pawson, 1995). SH2 domains are approximately 100 amino acids in length and recognise specific phosphopeptides (Pawson et al., 1993). SH2 domains binding to optimal phosphopeptides do so with high affinity (Kd 10-100nM), and, in contrast, have no affinity at all for the same sequence when unphosphorylated. This wide disparity in affinity between phosphorylated and unphosphorylated

substrate creates a virtual "switch" mechanism for the association/activation of an SH2 containing protein with its upstream target.

Surrounding sequences impart additional specificity and contribute to the affinity over and above that imparted by the core recognition consensus sequence, and these surrounding sequences vary between proteins. This provides a means to impart the unique substrate specificity of each protein using such domains. Binding of SH2 containing proteins to, as an example, an RTK, will have consequences for the protein including phosphorylation (eg PLC-γ1 (Pawson et al., 1993)), or translocation to the membrane and activation of enzymic activity (eg. PI3-K (Pawson et al., 1993)).

1.6.2. SH3

SH3 domains are also found in many proteins involved in tyrosine kinase signalling, as well as proteins with involvement in cytoskeletal arrangement. SH3 domains are approximately 50 amino acids in length and recognise a consensus sequence X-P-X-X-P (Pawson, 1995; Smithgall, 1995). The affinity of SH3 domains for the proline rich target (Kd 5-100μM) is much lower than that of SH2 domains for their phosphorylated substrates (10-100nM) (Pawson, 1995). This domain has no reliance on phosphorylation for binding, but is more involved in protein-protein interactions, playing a role in holding proteins together in appropriate subcellular localisations (scaffolding function) (Pawson, 1995; Pawson et al., 1993; Smithgall, 1995).

Surrounding sequences again influence specificity of the domain for its target, and lower affinity for its substrate makes the domain more sensitive to conformational

changes within the interacting proteins. Some SH3 binding domains have conserved sequences for proline directed kinases such as MAP kinase (Pawson, 1995).

1.6.3. PH

Pleckstrin Homology (PH) domains have been found in many proteins including kinases, kinase substrates and cytoskeletal proteins (Pawson, 1995). It was unclear for some time as to what the true nature of the target "ligand" for a PH domain is. Phospholipids were implicated (Harlan et al., 1994), although X-Ray crystallography studies by Ferguson *et al* (Ferguson et al., 1994) and Timm *et al* (Timm et al., 1994) suggested this was not possible, as their was not a suitable hydrophobic cavity available to adequately accommodate the large lipid side chains. More recently, associations with phosphoinositides have been demonstrated (Vanhaesebroeck et al., 2000) and PH domains appear to play roles in phospholipid (eg PI3-K (Martin, 1998)), G protein coupled receptor signals and some PKC isoforms signalling processes (Lemmon et al., 1998; Pawson, 1995). The PH domain of human PKB/Akt (β isoform) has high specificity for the PI3K 2nd messengers PtIns(3,4,5)P3 and PtIns(3,4)P(2). The PH domain is responsible for the recruitment of PKB/Akt to the plasma membrane for its activation and contribution to the PI3-K signalling cascade (Milburn et al., 2003). Binding of the PH domain to the PtIns messengers also induces a conformational change in PKB/Akt, which converts it into a substrate for activation by phopho-inositide dependent kinase 1 (PDK1). This conformational change of PKB/Akt in response to its PH domain engagement of PtIns is unique for PH domains studied by crystallography (Milburn et al., 2003). The PKB/Akt PH domain demonstrated intrinsic flexibility in the 3 variable loops (present in all PH domains) responsible for association with PtIns moieties (Auguin et al., 2004). All

PH domain containing proteins are cytoplasmic and recruitable to the plasma membrane and the PH domain is believed to be responsible for this localisation (Pawson, 1995).

1.6.4. PTB

Phosphotyrosine binding (PTB) domains bind phosphorylated tyrosines in the context of a consensus target sequence of N-P-X-pY (Pawson, 1995) in an analogous fashion to the SH2 domains. More recently, however, non N-P-X-pY target sequences have been identified, broadening the specificity range of the PTB domain. Whilst the consensus recognition sequence is less stringent than for other modules (SH2, SH3, PH domains), the secondary and tertiary structural arrangements of this module are well conserved whilst generating a broad range of ligand specificities (Yan et al., 2002).

1.6.5. Modular Generation of Diversity

The four domain/module types described above are all defined on the basis of consensus recognition sites or structure. Surrounding sequences always contribute to fine tuning of the specificity/affinity of the module/domain for its target sequence/protein. These limited numbers of consensus regions have been used in the generation of the incredibly complex and interwoven signalling cascades of the cell. Diversity has been imparted by both the variation of local surrounding sequences of a protein, as well as the arrangement of multiple modules/domains within a protein. The combinations serve to fine tune interactions in each signalling cascade to the level necessary to adequately control responses to the many stimuli encountered by the cell

and elicit the appropriate range of responses using very limited numbers of basic molecular interactions

1.7. Signalling through c-Kit

As discussed in the preceding sections, dimerisation is a prerequisite for the activation of wild type RTKs and the subsequent recruitment of cytoplasmic molecules involved in signal transduction results in a cellular response. Following dimerisation, the receptors become phosphorylated on selected tyrosine residues within the cytoplasmic domain. This process is achieved by one receptor trans-phosphosphorylating the other within the dimer (reviewed in (Heldin, 1995; Ullrich et al., 1990). The PDGFRβ phosphotyrosines have been mapped and the receptor contains 9 phosphorylated tyrosine residues (Claesson-Welsh, 1994). Of these, only one is in the tyrosine kinase domain. This residue is conserved between RTKs (Y857 of the human PDGFRβ (Claesson-Welsh, 1994); Y807, Y809 of the murine and human CSF-1R, respectively (reviewed in (van der Geer et al., 1993); Y821, Y823 in murine and human c-Kit, respectively (Serve et al., 1995). Specifically, Y823 of human c-Kit is located in the activation loop of the kinase domain (Mol et al., 2003)). Substitution of Y821 in murine c-Kit by a phenylalanine residue impaired, but did not abolish, SCF-induced proliferation and survival of bone marrow derived mast cells (BMMC). The downstream events affected by this mutation at present are unclear but were independent of PI3-K, p21ras and mitogen-activated protein kinase (MAPK) activation and did not affect induction of the early response gene *c-fos* and *c-jun* (Serve et al., 1995). Similar mutations of the homologous residues in the CSF-1R and PDGFRβ impair mitogenic signalling (reviewed in (Claesson-Welsh, 1994; van der Geer et al., 1993). In a recent study by Ueda *et al* (Ueda et al., 2002), 22 individual

cytoplasmic tyrosine mutations of murine c-Kit were generated to identify key tyrosines responsible for Ca^{++} mobilisation and migration in BaF3 cells. Y567, Y569 (juxtamembrane region) and Y719 (interkinase PI3K binding site) all affected these cellular responses. Y567F reduced Lyn, p38 MAPK and Erk1/2 activation whereas Y719K abolished PI3-K recruitment to c-Kit. The contributions of these 2 pathways to cell migration and Ca^{++} mobilisation were synergistic. Y900 has been demonstrated to be a substrate for Src family kinases recruited to Y568 and Y570. This tyrosine is also located in the kinase domain, and is responsible for the recruitment of Crkll (Lennartsson et al., 2003). Figure 1.5, adapted from Scheijen and Griffin, 2002 (Scheijen et al., 2002), summarises some of the key interactions known with c-Kit which are further elucidated in the following sections.

1.7.1. PI3-Kinase

Many groups have shown that the SCF-induced phosphorylation of c-Kit results in the binding of the p85 subunit of PI3-K in a number of different cell types (Blume-Jensen et al., 1994; Lev et al., 1991; Lev et al., 1992a; Reith et al., 1991; Rottapel et al., 1991; Serve et al., 1994; Shearman et al., 1993). PI3-K is a heterodimer composed of an 85 kD SH2-containing regulatory and a 110 kD catalytic subunit; binding of p85 to phosphorylated tyrosine activates PI3-K activity. Using mutants lacking part of the c-Kit interkinase domain Lev *et al* (Lev et al., 1992a) localised this as the binding region for p85 and Y719 of murine c-Kit was shown to be the critical tyrosine residue involved (Serve et al., 1994). The corresponding residue in the human receptor is Y721 (Shearman et al., 1993). The phosphorylated tyrosine residues associated with the binding of p85 to the human βPDGFR (Y740 and Y751) (Claesson-Welsh, 1994) and CSF-1R (Y721) (Reedijk et al., 1992) were determined from mutagenesis and

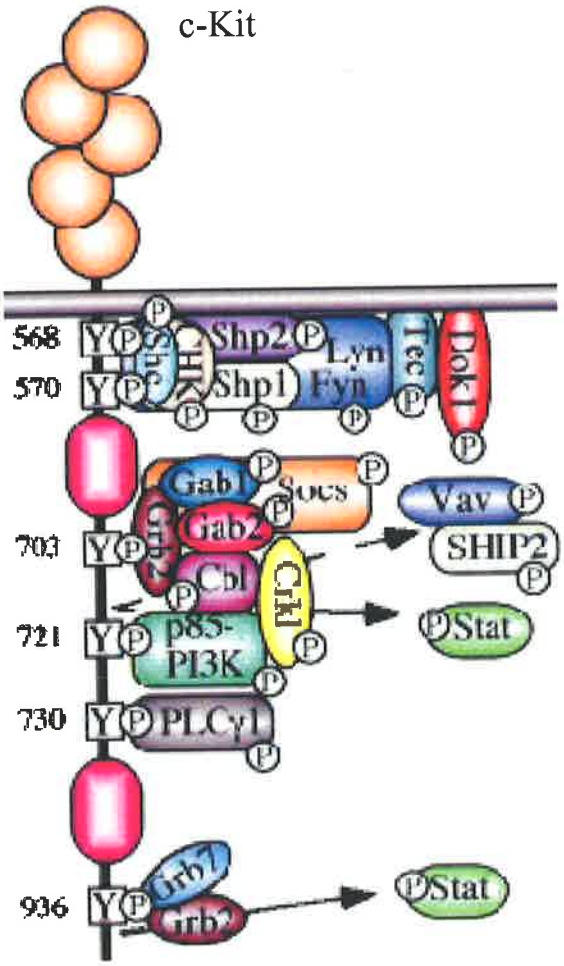

Figure 1.5

Schematic representation of some primary downstream signalling components in the c-Kit signal transduction cascades induced by SCF

Adapted from Scheijen and Griffin, 2002

phosphopeptide competition studies and are homologous to Y719/Y721 (murine/human) of c-Kit.

Stimulation of c-Kit results in recruitment and phosphorylation of the p85 subunit of PI3-K (Blume-Jensen et al., 1994). Mutation of Y719 in murine c-Kit abolished PI3-K activation and diminished c-fos and c-jun induction, which correlated with the impairment of BMMC to adhere to fibronectin in the presence of SCF. However, the mutation had a minimal affect on cell proliferation and survival (Serve et al., 1995). In contrast, deletion of the interkinase domain of the related CSF-1R demonstrated that autocrine induced anchorage-independent growth of NIH3T3 cells was independent of PI 3-K association (Taylor et al., 1989). The mutation of the two tyrosines involved in p85 binding to the PDGFRβ did not affect mitogenic signalling nor ligand-mediated transformation, but p85 binding to PDGFRβ was required for chemotactic responses (Heidaran et al., 1991). These data demonstrate that PI3-K is involved in the regulation of varied cellular responses depending on the RTK (Kapeller et al., 1994). In addition, PI3-K downstream signalling triggered by the same RTK can vary depending on the cellular context. Stimulation of c-Kit expressed on SCF dependent haemopoietic stem cell like lines activated Raf and Erk, as well as PKB/Akt in a PI3-K dependent manner. In mature mast cells stimulated with SCF, activation of Raf and Erk were independent of the PI3-K pathway, with PKB/Akt activation remaining PI3-K dependent (Wandzioch et al., 2004).

1.7.2. Phospholipase C-γ1

c-Kit has also been shown to associate and weakly phosphorylate phospholipase C-γ1 (PLC-γ1) (Blume-Jensen et al., 1994; Lev et al., 1991; Rottapel et al., 1991).

Although Rottapel *et al* (Rottapel et al., 1991) showed PLC-γ1 association with c-Kit in murine mast cells, Koike *et al*, (Koike et al., 1993) demonstrated phospholipase D (PLD) rather than PLC-γ1 association in rat mast cells. Unlike PI3-K, which was found to associate with all members of the type III RTKs, PLC-γ1 was unable to associate with CSF-1R (Downing et al., 1989a). It has been reported that PI3-K p85 subunit and PLC-γ1 compete for association to their binding sites on c-Kit with the former exhibiting higher affinity, however these proteins bind simultaneously to the PDGFRβ (Herbst et al., 1995b).

1.7.3. RAS-MAPK

The Ras MAPK pathway is activated by c-Kit and increased phosphorylation of ERK has been shown to be correlated with c-Kit activity (Funasaka et al., 1992; Miyazawa et al., 1991). Grb2 is first to associate with c-Kit at Y703 and Y936 and Grb7 binds Y936 (Thommes et al., 1999). Grb2 recruits SOS (a guanine nucleotide exchange factor) (Brizzi et al., 1996) which activates Ras (Duronio et al., 1992). Activated Ras recruits Raf (MAP Kinase Kinase Kinase) to the membrane leading to its increased serine phosphorylation (Blume-Jensen et al., 1994, Okuda, 1992 #186; Hallek et al., 1992; Lev et al., 1991). This leads to the continuing cascade of activation of MAP Kinase Kinase (or MEK) (Dent et al., 1998) and MAP Kinase (or ERK) (Dent et al., 1998; Funasaka et al., 1992; Garrington et al., 1999; Hallek et al., 1992; Welham et al., 1992). Activated ERK phosphorylates nuclear (Avruch et al., 1994; Davis, 1993; Vojtek et al., 1998) and cytoplasmic (Davis, 1993; Hazzalin et al., 1997; Sanchez et al., 1994; Vojtek et al., 1998) proteins.

The Ras GTPase-activating protein (GAP) (a negative regulator of the RAS MAPK pathway) is also recruited to activated c-Kit (Duronio et al., 1992; Herbst et al., 1991). This weak association of GAP has been demonstrated in human embryonic kidney fibroblast cells, 293T (Herbst et al., 1991), and haemopoietic cells (Duronio et al., 1992) but no association was found in mast cells (Rottapel et al., 1991). Weak association/phosphorylation with GAP was also shown to occur with the flk2 and CSF-1 receptors (Dosil et al., 1993; Reedijk et al., 1992) whereas GAP association/phosphorylation with the PDGFR was very strong (Kaplan et al., 1990) .

1.7.4. Protein Kinase C

Serine phosphorylation is also induced by SCF stimulation of c-Kit. In contrast to tyrosine phosphorylation, which increases the kinase activity of the receptor, serine phosphorylation induced by protein kinase C (PKC) acts as a negative regulator of tyrosine autophosphorylation but does not affect ligand binding affinity (Blume-Jensen et al., 1994) . S741 and S746 (located in the interkinase domain), S821 (close to the major autophosphorylation site – Y823) and S959 (in the carboxyl terminus) have been identified as serine phosphorylation sites in human c-Kit (Blume-Jensen et al., 1995). PKC activation by c-Kit was shown to be required for SCF induced cell motility (chemotaxis/migration) but not proliferation (Blume-Jensen et al., 1993). The EGFR is also negatively regulated by PKC induced phosphorylation of serine and threonine residues inhibiting both kinase activity and ligand binding affinity (Lin et al., 1986).

1.7.5. *Src Family Kinases*

Src family kinases Lyn and Fyn have been shown to associate with Y568 and Y570 of human c-Kit (Y567 and Y569 in murine c-Kit) (Linnekin et al., 1997; Timokhina et al., 1998). These investigators have shown that the Src family kinases are essential for SCF mediated proliferation. Inhibition of Src family kinases is effected by phosphorylation of their c-terminal tyrosine (Avraham et al., 1995) by c-terminal Src Kinase Homologous Kinase (CHK) or Megakaryocyte-associated Tyrosine Kinase (MATK) (Jhun et al., 1995). CHK interacts through Y568 and Y570 as well. This poses the question as to which molecule binds c-Kit directly – CHK or Lyn/Fyn? One or other may be performing an "adaptor" function or be acting as a scaffold (Jhun et al., 1995; Price et al., 1997a).

1.7.6. *Other*

SCF induces phosphorylation of a number of other substrates in a variety of cell backgrounds. These include: Tec kinase in M07e cells (Tang et al., 1994) , p95vav in M07e and TF-1 cells (Alai et al., 1992), Grb2/Sem-5 (Blume-Jensen et al., 1994), phosphotyrosine phosphatase in melanocytes (Funasaka et al., 1992) and the haemopoietic phosphatase (HCP) in haemopoietic cells (Yi et al., 1993). Stimulation of c-Kit also transiently associates with and activates Jak2 (a Janus kinase) and also activates Stat1 (Deberry et al., 1997; Linnekin, 1999).

The diversity of pathways recruited to c-Kit in part explains the diversity of biological responses generated from c-Kit including: cell survival (Bendall et al., 1998; Colucci

et al., 2000; Ricotti et al., 1998); proliferation (Colucci et al., 2000; Ikeda et al., 1993; Tsai et al., 1991b); differentiation (Ferrao et al., 1997; Ricotti et al., 1998; Tsai et al., 1991a); adhesion (Kinashi et al., 1994; Levesque et al., 1995; Simmons et al., 1994b; Yuan et al., 1997); and chemotaxis (Blume-Jensen et al., 1993; Meininger et al., 1992).

It is clear that c-Kit demonstrates a broad range of signalling partners, some of which have been outlined in the previous sections. The responses induced by c-Kit upon SCF stimulation may potentially be influenced by any number of the following: a) the set of signalling molecules present or absent within a particular cellular background; b) the degree of stimulation by varying SCF concentrations or type (membrane vs soluble); c) the level of the receptor expressed at the cell surface; d) the duration of activation of certain signal molecules or; e) the combination of other receptors present in the cell which may synergise or antagonise pathways triggered by c-Kit signalling. It is interesting to note that since SCF exists as both a soluble and membrane-bound ligand, the binding of c-Kit to membrane-bound SCF may prevent c-Kit/SCF internalisation. This was shown to be the case by Miyazawa *et al.* Membrane-bound SCF was able to prolong the life span of c-Kit and induce more persistent tyrosine kinase activation in comparison to soluble SCF (Miyazawa et al., 1994), which may explain the biological differences seen between the SCF forms.

1.8. Downmodulation of c-Kit expression/activation

There are numerous mechanisms employed to ensure tight control/down modulation of c-Kit signalling. Following ligand binding it has been shown that the receptor-ligand complexes are endocytosed via clathrin coated pits. The receptor is then either

recycled to the cell surface, targeted to lysosomes where it is degraded, or degraded by proteosome dependent pathways following polyubiquitination. Internalisation of the receptor-ligand complex can be seen as a way of reducing the life span of the receptor and thereby downmodulating ligand-induced activation of the receptor. Downmodulation of c-Kit induced by SCF stimulation has been reported by several groups and has been found to be the result of number of different, but not mutually exclusive, mechanisms described below.

1.8.1. PKC

The binding of soluble SCF to c-Kit has been shown to induce c-Kit/SCF complex internalisation in mast cells and the megakaryocytic cell line, M07e (Adachi et al., 1995; Miyazawa et al., 1994; Yee et al., 1993) resulting in reduced levels of c-Kit on the cell surface. Internalisation could also be induced by phorbol 12-myristate 13-acetate (PMA), a PKC activator, with a concomitant decrease in c-Kit RNA expression (Adachi et al., 1995; Ogawa et al., 1995). Asano *et al*, (Asano et al., 1993) demonstrated that decreased c-Kit mRNA expression in a human erythroleukaemia cell line, HEL, upon 12-0-tetradecanoylphorbal-13-acetate (TPA) stimulation, was a result of post-transcriptional mechanisms involving induction of a RNA destabilising protein. PKC has also been shown to downregulate the SCF-induced activation of c-Kit by inhibiting tyrosine autophosphorylation and the phosphorylation of the associated PI3-K subunit p85 (Blume-Jensen et al., 1994; Blume-Jensen et al., 1993).

1.8.2. *Extracellular domain shedding*

c-Kit can also be downmodulated by the shedding of the extracellular domain (100 kD) from the cell surface. This latter mechanism is induced by PKC dependent and independent pathways (Adachi et al., 1995; Brizzi et al., 1994; Yee et al., 1993) and it is independent of kinase activity which is in agreement with results obtained with CSF-1R (Downing et al., 1989b; Yee et al., 1994a). Src family kinases are also implicated in c-Kit internalisation as PP1 (an inhibitor or Src) prevented Src induced c-Kit internalisation (Broudy et al., 1999). It should be noted, however, that PP1 has since been shown to directly inhibit c-Kit and Bcr-Abl (Tatton et al., 2003), casting doubt on these findings.

1.8.3. *Ubiquitination*

Internalisation and degradation of the c-Kit/SCF complex has been shown to be reduced in kinase defective c-Kit and receptor ubiquitination was shown to be dependent on kinase activity (Miyazawa et al., 1994; Yee et al., 1994a). Similar observations have been made with the CSF-1 and PDGF receptors (Carlberg et al., 1991; Mori et al., 1992; Mori et al., 1993). For c-Kit to be internalised and degraded, the receptor is first ubiquitinated on Lysine residues. Ubiquitin (Ub) is a commonly used 'tag' to identify proteins for destruction by the proteosome or lysosomal pathways (Hicke, 1999). Upon SCF stimulation, c-Kit is rapidly ubiquitinated, as seen by increased molecular weight on SDS-Poly Acrylamide Electrophoresis (SDS-PAGE) analysis and this is dependent on a functional kinase domain in c-Kit (Miyazawa et al., 1994). One potential candidate Ub ligase for c-Kit is c-Cbl. Upon

stimulation of c-Kit with SCF, c-Cbl is phosphorylated and associated with c-Kit (Brizzi et al., 1996). c-Cbl is an E3 Ub protein ligase (capable of conjugating Ub to target proteins) (de Melker et al., 2001; Ettenberg et al., 2001; Sanjay et al., 2001). The adaptor protein APS recruits c-Cbl to the Insulin Receptor, PDGF Receptor β, EPO Receptor and Y568 of c-Kit (Wollberg et al., 2003). c-Cbl is also responsible for the downregulation via polyubiquitination of the RTK Ron, the receptor for macrophage stimulating protein (Penengo et al., 2003).

The mode of ubiquitination, until recent times, was presumed to be polyubiquitination (addition of polyubiquitin chains to the target protein), and this mode is known to target the tagged protein for degradation by the proteosome (Katz et al., 2002; Mosesson et al., 2003). In a recent study of EGF receptor, monoubiquitination of EGFR, mediated by c-Cbl, led to receptor endocytosis and lysosomal degradation in a mechanism distinct from the proteosome dependent polyubiquitination process (Mosesson et al., 2003). The importance of this mechanism of down regulation of RTKs was evident when Y1045 of EGFR (docking site of c-Cbl) was mutated, resulting in an enhanced mitogenic response. Ubiquitination of this mutant EGFR was still possible via indirect recruitment of c-Cbl by Grb2 (Waterman et al., 2002). The c-Cbl molecule could be evaluated for its role in c-Kit regulation using the model system developed in this thesis in Chapter 4.

1.8.4. Phosphatases

Phosphatases also have an obvious role in downmodulation of c-Kit function, removing phosphates from target proteins that have been added by the activated kinases in the signalling cascade, as well as phosphotyrosines on the activated

receptor itself. Phosphatase activity is regulated in an analogous fashion to kinases (Hunter, 1995). For example, SHP-1 (a phosphatase highly expressed in haemopoietic cells) associates with c-Kit upon SCF stimulation (Yi et al., 1993). Mutation of Y569 (murine c-Kit) abolishes the association of SHP-1, and results in hyperproliferation in response to SCF (Kozlowski et al., 1998). Studies by Lorenz *et al* in the murine system clearly showed a cell type specific modulation of c-Kit by SHP-1. In this study, mice heterozygous for a kinase defective c-Kit (*Wv*/+) were crossed with mice heterozygous for a null allele of *motheaten* (SHP1) – (*me*/+). These 2 mutations were shown to complement each other and reverse the phenotypes of the parent strains for haemopoietic progenitor cells, but not mature mast cells (Lorenz et al., 1996). These findings were confirmed in the studies of Paulson *et al* (Paulson et al., 1996). Another phosphotyrosine phosphatase, Syp, also associates with activated c-Kit and may play a role in the downstream signalling cascade initiated by c-Kit (Tauchi et al., 1994).

1.8.5. Others

Downregulation of c-Kit mRNA can also be induced by several cytokines such as IL-3 and GM-CSF in murine bone marrow derived mast cells (Welham et al., 1991), IL-4 in the human mast cell line, HMC-1, and AML cells (Sillaber et al., 1991), transforming growth factor-β (TGF-β) in CD34+ cells (Sansilvestri et al., 1995) and erythroid differentiation factor/activin A in murine erythroleukaemia cells (Hino et al., 1995).

1.9. Mechanisms inducing signalling diversity by the RTK

1.9.1. c-Kit Isoforms

Human c-Kit exists in 4 isoforms, produced by differential splicing at two sites in the human *c-Kit* gene. The first site is an alternate splice sequence at the 3' end of exon 9 (encoding the extracellular domain adjacent to the membrane) (Giebel et al., 1992; Hayashi et al., 1991; Vandenbark et al., 1992). This alternate splice results in the presence/absence of 12bp in the mRNA encoding glycine-asparagine-asparagine-lysine (GNNK). These will be referred to throughout the thesis as GNNK+ and GNNK-. The second site of alternate splicing is at the 3' end of exon 15 (Crosier et al., 1993), resulting in the presence/absence of 3 bp (encoding a serine in the interkinase domain). This will be referred to as S+ and S- throughout the thesis. In murine c-Kit, the alternate acceptor site does not exist (Qiu et al., 1988), and all mRNA encode the S- form (Crosier et al., 1993). Figure 1.6 indicates the location of the 2 alternate splice sites in human c-Kit.

These isoforms are co-expressed in many tissues, but limited quantitative analysis as to the actual distribution of each isoform has been performed. In bone marrow, melanocytes and haemopoietic tumour cell lines, GNNK- appears to dominate (Crosier et al., 1993; Giebel et al., 1992; Piao et al., 1994). S+ also appears to be predominant (Crosier et al., 1993). Murine placenta and mast cells also appear to express more of the GNNK- isoform (Reith et al., 1991).

Differential cellular responses of the isoforms of c-Kit have been previously evaluated (Caruana et al., 1999). In this study, c-Kit isoforms were introduced into NIH3T3

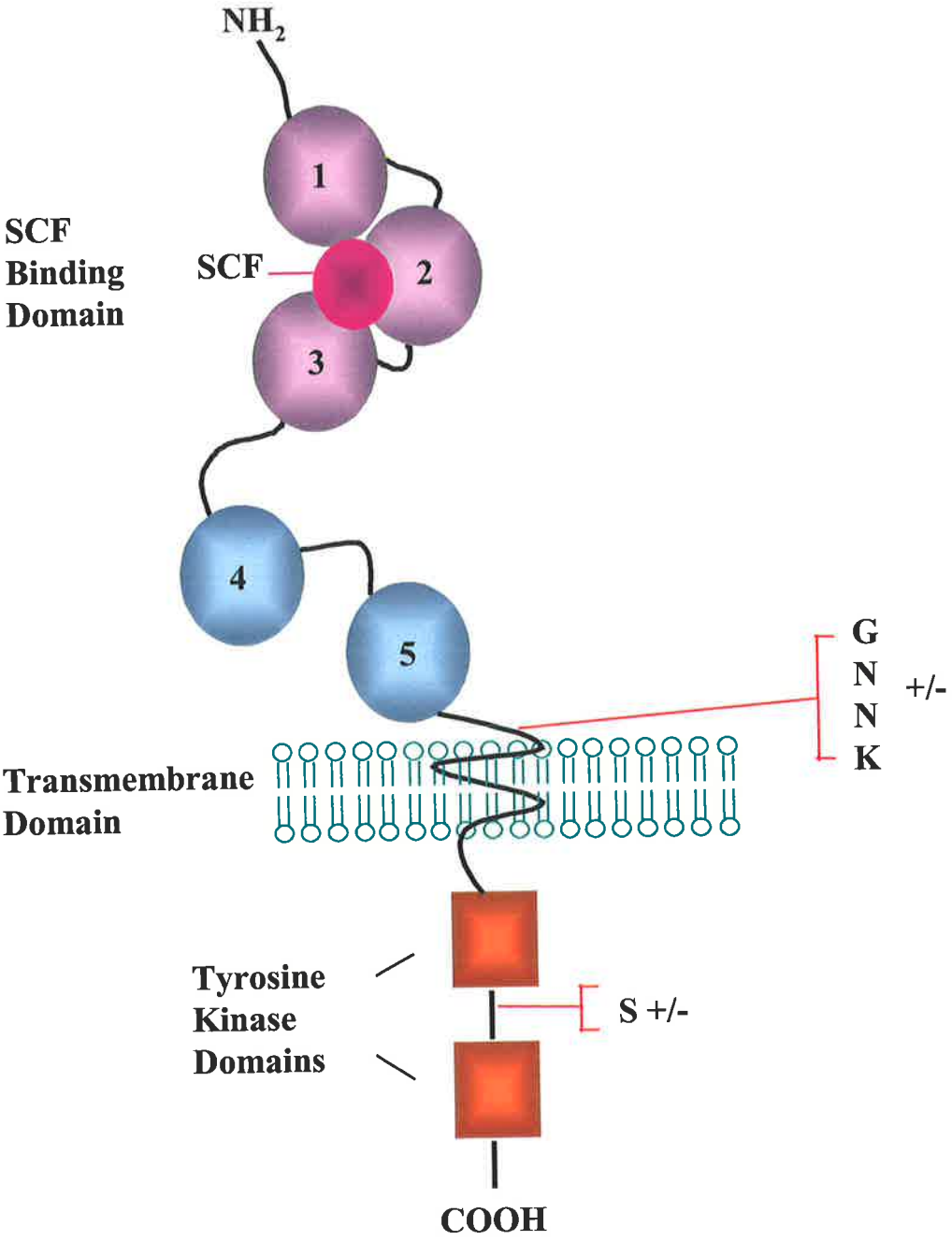

Figure 1.6

Schematic representation of c-Kit receptor showing positions of GNNK and S variant sequences of isoforms

cells. GNNK-S+ c-Kit was potently transforming and induced focus formation, anchorage independent growth (colony formation) and tumourigenicity in nude mice – all the conventional hallmarks of transformation in the NIH3T3 model. GNNK+S+ was very poor at induction of focus formation and tumourigenicity, but induced anchorage independent growth. GNNK+S- could only induce focus formation. These observations demonstrated that the classical readouts for transforming potential were not uniform indicators. These anomalies required detailed biochemical analysis of c-Kit isoform signalling in order to correlate various components of the signal transduction pathway with the phenomena described. This was a primary aim of the studies for this PhD Thesis.

1.9.2. Heterodimerisation

Heterodimerisation of mutant receptors or ligand subunits has provided evidence of how RTK function to transmit their signal. The heterodimerisation of kinase-defective receptor subunits with wild type receptor molecules have displayed dominant-negative effects similar to the underlying mechanism of mutant c-Kit in the heterozygous W mutant mice (Chabot et al., 1988; Reith et al., 1990). This shows the importance of dimerisation as a prerequisite for the induction of transphosphorylation and subsequent association and activation of signalling molecules. The PDGF ligands, like other ligands binding to type III RTK, exists as a dimer. Heterodimerisation of a mutant and wild type PDGF ligand substantially reduced the affinity of the heterodimer for its receptor, supporting the theory that the bivalency of the ligand is important for stable dimerisation of the receptor and to produce high affinity ligand binding (Vassbotn et al., 1993).

Heterodimerisation can also increase the repertoire of signalling pathways a receptor complex can activate. Heterodimerisation between two different ligand isoform monomer subunits (for example PDGF-A and B) or two functional receptors belonging to the same family (for example members of the ErbB family) can occur, resulting in an increase in signal diversity. PDGF exists as three different isoforms, which are made up of disulphide bonded homo- and heterodimers, composed of A and B polypeptide chains (PDGF-AA, PDGF-AB and PDGF-BB). The PDGF isoforms exert their biological effects by binding with different affinities to two distinct cell surface receptors. PDGFRα binds all three isoforms with high affinity whereas the PDGFRβ only binds PDGF-BB with high affinity and PDGF-AB with lower affinity. PDGFRα and β are able to activate unique and common signalling pathways. The subsequent biological outcome depends on the combination and level of expression of the different PDGF isoforms and/or PDGFR expressed within the cell (reviewed by Betsholtz (Betsholtz et al., 2001)). This can explain how one receptor is able to provide a diverse range of functions within different cell types (Claesson-Welsh, 1994; Heldin, 1995; Lemmon et al., 1994).

The increase in recruitment of signalling molecules that can associate with receptor complexes has also been shown through the ErbB family (RTK I), in which different receptors belonging to this group are able to heterodimerise. In addition, their ligands display the ability to cross-bind with other receptors belonging to this family, overall providing a model of trans-regulation. The ErbB family consists of ErbB1 (EGFR), ErbB2 (HER-2/neu), ErbB3 (HER-3) and ErbB4 (HER-4) (Lemmon et al., 1994). EGFR was able to bind several ligands including EGF, TGF-α, amphiregulin,

heparin-binding EGF and betacellulin. The ligand for ErbB3 and 4 was neu differentiation factor (NDF) or the human equivalent, heregulin, which has 10 isoforms produced by alternative splicing that bind with different affinities to their receptors (Wen et al., 1994). It was shown that the ErbB1 is able to heterodimerise with the ErbB2 receptor and that this was induced by EGF binding to ErbB1 as EGF does not bind to ErbB2 receptor. This heterodimerisation induces phosphorylation of the ErbB2 receptor by transphosphorylation (Goldman et al., 1990; Wada et al., 1990). Heterodimerisation has also been shown to occur between ErbB1 or ErbB2 with ErbB3 or ErbB4 due to the binding of NDF to the latter two receptors, since it does not bind to ErbB1 or ErbB2 (Heldin, 1995; Lemmon et al., 1994). The binding affinity of EGF to a NDF occupied heterodimer is reduced therefore heterodimerisation can favour the binding of one ligand over another and this may avoid excessive or even opposing growth regulatory signals.

If both receptor molecules within the heterodimer are able to associate with different SH2 signalling molecules, this will increase the diversity of the response. This is indeed the case with the PDGFRα and β, which not only associate and activate both common and unique molecules as homodimers but upon heterodimerisation autophosphorylate different tyrosine residues within the receptor complex enabling the association with a another set of SH2 containing proteins (Heldin, 1995; Lemmon et al., 1994). Similarly the EGFR is able to associate with other SH2 containing proteins when complexed with other members of the RTK I family. The ErbB3 receptor introduces another peculiarity as it has an impaired tyrosine kinase activity but nevertheless possesses several putative consensus sequences for the binding of the p85 subunit of PI3-K, unlike the other three members of this family.

Heterodimerisation of ErbB3 with other members of the RTK I receptor would then enable coupling to PI3-K (Carraway et al., 1995).

Several isoforms of c-Kit also exist, however it has not yet been shown whether these isoforms are able to heterodimerise. It is possible that heterodimerisation may be able to alter the biochemical events achieved upon c-Kit activation or trans-regulate SCF-dependent and/or -independent responses in a similar fashion to those achieved by other RTK described in this section.

1.9.3. Receptor levels

Receptor densities have been shown to determine the biological response of a cell by influencing the signalling events that follow ligand-stimulation. EGF stimulation of several carcinoma and transfectant cell lines expressing high levels of the EGFR results in the inhibition of proliferation, in contrast to cells expressing lower receptor levels (Kawamoto et al., 1984; Lupu et al., 1990; Riedel et al., 1987). Inhibition of proliferation was associated with an increase in tyrosine kinase activity of the EGFR (Kawamoto et al., 1984). This phenomenon may be explained by data demonstrating that overexpression of the EGF or insulin receptors in the phaeochromocytoma PC12 cells results in sustained activation of MAPK, which is associated with the differentiation of the cells. Low receptor levels on the other hand result in transient activation of MAPK leading to a proliferative cellular response (Dikic et al., 1994; Marshall, 1995; Traverse et al., 1994). These studies also revealed that EGF stimulation of cells overexpressing EGFR inhibited proliferation analogous to the results of Kawamoto *et al* (Kawamoto et al., 1984) described above.

The amplitude or duration of the signal generated as a consequence of receptor density may also result in the activation/association of other signalling molecules that interact with the receptor with low affinity. For example the association of the EGFR with PLC-γ1 required the presence of high receptor levels (Margolis et al., 1989; Wahl et al., 1988). This may result in a different cellular response due to the induction of new signalling pathways. The strength of the signal generated may also be the underlying mechanism involved in the induction of transformation by many RTK when expressed at high levels. It is possible that different cellular responses generated from the same receptor can also be achieved by variation in the concentration of ligand available for binding (Kawamoto et al., 1984). Thus, variations in receptor and/or ligand concentrations may alter the duration or strength of the signal and/or induce the interaction with different signalling molecules. It has been demonstrated that higher concentrations of SCF are required for the proliferation of mast cells than for maintaining their survival (Yee et al., 1994b) and that lower levels are required for cell adhesion than for proliferation (Kinashi et al., 1994).

The level of surface expression of c-Kit is regulated during haemopoiesis. It is possible that similar mechanisms to those described above may determine the biological response (for example cell survival, proliferation, chemotaxis, adhesion or differentiation) upon SCF stimulation. W mutations resulting in reduced levels of functional c-Kit (eg. $W^{/+}$, W^{44}, W^{57} and W^{sh}) have already implied that c-Kit densities may differentially affect certain attributes of these mutant mice.

It has been shown in several systems (as referenced in this section) that the level of receptor expression influences the ability of that receptor to transform target cells. In

NIH3T3 murine fibroblast cells, overexpression of the normal c-Kit or EGF receptor transforms the cells. At physiological levels these receptors are not transforming, supporting the hypothesis that the biological outcomes of receptor signalling changes as the "level" of signal changes. This is likely explained by the fact that these receptors interact with a variety of downstream effectors, all with different affinities and therefore different thresholds of activation. Changing the intensity or duration of a stimulus will most likely modify which cascades are triggered and for how long (as demonstrated in the PC12 model of differentiation (Dikic et al., 1994; Traverse et al., 1994).

1.10. Aims

The aim of this project was to investigate the signalling initiated through the RTK c-Kit, and to correlate the results with the biological outcomes (proliferation/ differentiation/ survival/ transformation). Firstly, two distinct isoforms of the receptor (GNNK+S+ and GNNK-S+) were chosen for analysis and both qualitative and quantitative differences between the isoforms were to be determined. Care was taken at all times to control the level of c-Kit expressed in the cell lines to eliminate variations in biological responses attributable to receptor levels as discussed in 1.9.3.

A second aim was to develop a more sophisticated murine haemopoietic cell model for the expression/analysis of c-Kit. To control c-Kit expression, a chimaeric c-Kit was constructed containing the human extracellular domain and murine transmembrane and intracellular domains. It was hypothesised that the background, ligand-independent signalling observed in previous studies using human c-Kit in

murine cells could be due to a loss of control of c-Kit by the host cell as a result of subtle sequence differences between the species. Use of this chimaeric receptor places the "correct" species receptor in the host cell, and also allows stimulation of the chimaeric c-Kit without interference from any endogenous murine c-Kit, as only the chimaeric molecule can be stimulated with exogenous human SCF – refer section 1.4.

In addition to generating chimaeric c-Kit, a murine factor dependent early haemopoietic cell line model was modified and developed to allow the introduction and functional analysis of the chimaeric c-Kit in a physiologically relevant cell line. This model allowed investigation of several biological outcomes in the same cell (survival, proliferation and differentiation), and lends itself to exploiting gene knockout technology, creating new lines identical to WT but missing one component of the signalling cascade. In particular, the Src family kinase Lyn was investigated.

A third aim of the work was to elucidate the expression patterns of these GNNK+/- isoforms of c-Kit in various subsets of haemopoietic cells. Subsets of CD34 positive haemopoietic cells were analysed to determine the relative expression levels of each isoform. This will serve to further the understanding of the relevance of the various c-Kit isoforms in haemopoiesis. In addition, a series of peripheral blood stem cell apheresis specimens from poor vs good mobilisation groups were analysed. c-Kit downmodulation is commonly observed in mobilised stem cells (To et al., 2003) and it was of value to determine if isoform expression patterns played a role in the mobilisation phenomena. This was measured at the mRNA and protein levels to help determine how c-Kit is downregulated in mobilisation.

2 Materials and Methods

2.1. Tissue Culture

Reagents used were of analytic grade unless specified otherwise. All solutions were prepared using Milli-Q purified water (Milli-Q water) generated by deionising distilled water using a Milli-Q RO60 system (Millipore Corporation, Bedford, MA) and then further purified by passing through two beds of ion exchange resins, a carbon filter and an organic filter using a Milli-Q system (Millipore Corporation).

2.1.1. Tissue Culture Media and Solutions

Dulbecco's Modified Eagle's Medium (DMEM) was prepared by mixing one sachet of DMEM powder (GibcoBRL, Rockville, MD, Cat. No. 12800-017) and 3.7 g $NaHCO_3$ (BDH, USA, Cat. No. 10247) in 900 ml of Milli-Q water. To the solution, N-2-Hydroxyethylpiperazine N`-2-ethanesulphonic acid (HEPES) pH 7.2 (Boehringer-Mannheim, Australia, Cat. No. 737151) was added from sterile stock solutions to a final concentration of 15 mM. Likewise, penicillin (Sigma, St Louis, MO, Cat. No. P3032) and streptomycin sulphate (Sigma, Cat. No. S9137) was added to final concentrations of 50 IU/ml and 50 µg/ml respectively. The pH of the solution was adjusted to 7 by the addition of 4 ml 1 M hydrochloric acid (HCl) and the volume adjusted to 1 L with Milli-Q water. The medium was filter sterilised using an Acrocap™ 0.22 µm filter unit (Gelman Sciences, Ann Arbor, MI, Cat. No. 4480) and a Millipore pump with a filling bell (Millipore, Cat. No. SVGB1010) and stored at 4°C. Prior to use, media was supplemented with 10-20% foetal calf serum (FCS) (CSL, Parkville, Victoria, Australia) which had previously been heat inactivated at

56°C for 30 minutes. To medium that had been stored at 4°C for more than 7 days, glutamine was added to yield a final concentration of 2 mM. As an alternative, DMEM with pyruvate and high glucose, but without glutamine (JRH Biosciences, Lenexa, KS, Cat. No. 45042301) was supplemented with 15 mM HEPES (JRH Biosciences, Cat. No. 44811901), 50 U/ml penicillin, 50 µg/ml streptomycin sulphate (JRH Biosciences, Cat. No. 05081901) and 200 mM glutamine (JRH Biosciences, KS, Cat. No. 44831901).

Iscove's Modified Dulbecco's Medium (IMDM) was prepared by adding one sachet of IMDM powder (GibcoBRL, Cat. No. 12200-036) and 2 g of $NaHCO_3$ in 900 ml of Milli-Q water. As with DMEM, sterile stock solutions of HEPES, penicillin and streptomycin sulphate were added as above and filter sterilised as previously indicated. The pH was adjusted to 7.4 with 2.5 ml of 1 M HCl and the volume made to 1 L.

RPMI 1640 medium was prepared the same way as for IMDM using RPMI 1640 powder (GibcoBRL, Cat. No. 31800-02).

Double strength IMDM was prepared by dissolving one sachet of IMDM powder (Cytosystems, Australia, Cat. No. 50-016-PA) and 0.2 g L-asparagine in 390 ml of Milli-Q water. Sterile stocks of penicillin, streptomycin sulphate, DEAE-Dextran (Pharmacia, Sweden, Cat. No. 17-0350-01) were added to give a final concentrations of 100 IU/ml, 100 µg/ml and 0.19 mg/ml respectively. 5.9 µl β-mercaptoethanol was also added. Medium was filter sterilised and stored up to 6 months at 4°C.

Hank's balanced salt solution (HBSS) contained 0.14 M NaCl, 5 mM KCl, 0.3 mM Na_2HPO_4, 0.4 mM KH_2PO_4, 4.2 mM $NaHCO_3$, 5.5 mM glucose, 1% Phenol Red (in 0.1 M NaOH) in Milli-Q water, with a final pH of 7.4. The solution was sterilised by autoclaving at 121°C for 20 minutes and stored at 4°C. An alternative HBSS without calcium, magnesium, with phenol red (JRH Biosciences, Cat. No. 55021-500M) was also used.

Tissue culture grade phosphate buffered saline (TC-PBS) contained 0.14 M NaCl, 3 mM KCl, 8 mM Na_2HPO_4 and 1 mM KH_2PO_4 in sterile tissue culture grade Milli-Q water, with a final pH of 7.4. Solution was sterilised by autoclaving and stored at 4°C. A sterile 10x stock of PBS without calcium and magnesium (JRH Biosciences, Cat. No. 45312301) diluted in Milli-Q water, sterilised by autoclaving and stored at 4°C was also used.

A solution used for removing adherent cells from the base of tissue culture flasks and dishes consisted of 0.054% w/v trypsin and 0.54 mM ethylenediaminetetra-acetic acid (EDTA) in HBSS. Once dissolved, the solution was filtered through a low protein binding 0.22 μm filter (Millipore, Cat. No. SLGV025LS). To prevent inactivation of the trypsin, the solution was stored at –20°C. Also used was 0.5% trypsin with 0.02% EDTA (JRH Biosciences, Cat. No. 44732301).

Semi-solid medium containing methylcellulose was used for colony growth. To sterilise methylcellulose, 8.1 g of A4M premium grade 400 centipose powder (DOW Chemical Company, Midland, MI), was added to a 500 ml bottle with a tissue culture flea and autoclaved at 121°C for 15 minutes. When cool, 270 ml of sterile single

strength IMDM was added to the bottle while stirring and the mixture left to stir at room temperature in the dark for 3 days with occasional shaking. During this time, bovine serum albumin (BSA) solution was made by dissolving 20 g BSA (Sigma, Cat. No. 2153) in 88.4 ml Milli-Q water in a conical flask at 4°C overnight. Duolite mixed resin beads (BDH, Cat. No. 55057) were used to deionise the BSA solution at 4°C. This involved the addition of 4 g of beads to the BSA solution, with mixing every 15 minutes for about 2 hrs or until beads became yellow. The solution was decanted into a fresh conical flask to remove expired beads. The process was repeated twice or until the beads did not change to yellow after incubation for 2 hrs. The BSA solution was decanted and an equal volume of double-strength IMDM was added, and the solution filter sterilised. Aliquots were stored at -20°C if not used immediately, with a small aliquot collected to check for sterility. To the dissolved methylcellulose, 60 ml of the BSA solution and 180 ml of FCS was added and left to stir for a further 4 hrs. The methylcellulose mixture was aliquoted and stored at –20°C until required. Small aliquots of methylcellulose were set aside for sterility checks and batch testing to ensure comparative batches were used.

2.1.2. *Cytokines and growth factors*

Cytokine units were defined such that 50 Units results in 50% of the maximal number of colonies in soft agar cultures containing $5x10^4$ murine bone marrow cells. Purified recombinant human SCF (huSCF) produced in E. coli, was supplied by Amgen Corporation (Thousand Oaks, CA). Recombinant murine granulocyte macrophage - colony stimulating factor (muGM-CSF) ($5x10^5$ U/ml) synthesised by insect cells infected with a recombinant baculovirus vector sourced from Dr A Hapel, John Curtin School of Medicine, ANU. Recombinant murine interleukin-3 (muIL-3) ($7.5x10^5$

U/ml) synthesised by insect cells infected with a recombinant baculovirus vector from Dr A Hapel. Recombinant murine colony stimulating factor -1 (CSF-1) (5000 U/ml) synthesised by insect cells infected with a recombinant baculovirus vector was provided by Elizabeth MacMillan (IMVS). The culture supernatant for all cytokines produced by baculovirus were extensively dialysed into serum free DMEM. Conditioned medium containing either recombinant human GM-CSF or IL-3 was obtained from cultured CHO cells transfected with the respective expression plasmids, kindly provided by Professor Angel Lopez (IMVS).

2.2. Culture Maintenance of Cells

Tissue culture work was performed in Class II Biosafety Cabinets, using reagents prewarmed to 37°C in a water bath. Cell cultures were incubated in a humidified atmosphere containing 5% CO2 in air at 37°C. Cell density and viability was determined using a haemocytometer with an aliquot diluted 1:2 in 0.8% w/v trypan blue (in saline). Cell cultures were maintained for approximately three to six weeks before initiating new cultures from cryopreserved stocks.

2.2.1. Psi 2 cell line maintenance

The murine ecotropic retrovirus packaging cell line Psi 2 (Mann et al., 1983) was obtained from Professor Tom Gonda (IMVS) and was used for production of ecotropic retrovirus for transduction of murine target cells. Cells were maintained as sub-confluent monolayers in DMEM containing 10% FCS. Cultures that were approximately 70% confluent were harvested and subcultured into a new flask. To harvest cells, the adherent monolayer was rinsed once in HBSS and then incubated for 1 minute in trypsin diluted 1/2 in HBSS. After incubation, cells were dislodged by

repeated aspiration, and trypsin activity was stopped by the addition FCS diluted in DMEM to 10%. Cells were then seeded into new flasks at appropriate densities.

2.2.2. FDC-P1 cell line maintenance

The non-adherent factor dependent cell line FDC-P1 (Dexter et al., 1980), also obtained from Professor Tom Gonda (IMVS) was maintained in DMEM containing 10% FCS supplemented with 62.5 U/ml baculovirus derived muGM-CSF. Cells were maintained at densities between $5x10^4$/ml to $1x10^6$/ml and were sub-cultured every 2-3 days.

2.2.3. NIH3T3 cell line maintenance

Low passage NIH3T3 cells obtained from ATCC were maintained identically to Psi2 cells as described in section 2.2.1 . Passage numbers were recorded at all stages. For NIH3T3 cells expressing human c-Kit constructs, multiple ampoules of a working stock culture were cryopreserved, and fresh cultures were initiated from this stock for each experiment to eliminate genetic drift and replicate the non transformed phenotype of the low passage NIH3T3 clones at the commencement of each experiment.

2.2.4. Maintenance of Myb Immortalised Haemopoietic Cell (MIHC) lines

Non-adherent murine MIHC were created by transducing day 14 foetal livers with pRUF containing an activated form of cMyb cDNA (pRUF CT3-Myb) (Gonda et al., 1989b). MIHC were selected for long term muGM-CSF/muIL-3 dependent growth. These cells were cultured in DMEM supplemented with 20% foetal calf serum with

250 U/ml baculovirus derived muGM-CSF alone or further supplemented with 50 U/ml muIL-3. Cells were maintained at densities between $1x10^5$/ml to $1x10^6$/ml and were sub-cultured every 2-3 days.

2.2.5. *Maintenance of MO7e*

The factor dependent human megakaryocytic leukaemic cell line, MO7e (Avanzi et al., 1988; Miniero et al., 1987) was obtained from Dr. P. Crozier (Department of Molecular Medicine, School of Medicine, University of Auckland, Auckland, New Zealand). Cells were maintained between $1x10^5$/ml to $1x10^6$/ml in DMEM with 10% FCS supplemented with conditioned medium from CHO cells transfected with either human GM-CSF or human IL-3 cDNA.

2.2.6. *Cryopreservation of Cells*

Cells were cryopreserved in the presence of 10% dimethylsulphoxide (DMSO) as cryoprotectant to prevent fracturing of the cellular membrane. Cells in mid-log phase were passaged as above and resuspended in the appropriate growth medium to approximately $1x10^7$/ml. Immediately prior to freezing, an equal volume of "freezing mix" (30% FCS, 20% analytical grade DMSO (BDH, Cat. No. 10323) and 50% RPMI-1640) was added dropwise to the cells. 1 ml aliquots of the cell suspension was dispensed into cryotubes (Nunc, Denmark, Cat. No. 3-66656) which were frozen at a controlled rate in an ultracold freezer (-70°C) overnight (wrapped ampoules in cotton wool). The next day, vials were transferred to liquid nitrogen storage vessels (-196°C).

2.2.7. Thawing of Cryopreserved Cells

Cryotubes removed from liquid nitrogen were snap thawed in a 37°C water bath. The contents were transferred to a 10ml centrifuge tube and 4ml growth medium was added dropwise while shaking the tube. The tube was left for 3 minutes and 3ml medium was added dropwise prior to centrifuging (200 g for 5 minutes at 25°C). The supernatant was removed and cells were seeded into the appropriate growth medium.

2.2.8. Cytology, Cytochemistry and Histology

Cytocentrifuge smears containing $5x10^4$ cells were prepared from cultured cells. Cells were harvested, centrifuged at 200 g and resuspended in 100% filtered FCS. Aliquots of 75 µl were cytocentrifuged at 28 g at room temperature for 5 minutes onto ethanol cleaned glass microscope slides in a Cytospin 3 (Shandon Scientific, Cheshire, England). Cell smears were allowed to air dry before being stored at 4°C in air tight slide boxes containing dessicant (silica gel (Ajax Chemicals, Australia, Cat. No. 3681).

2.2.9. Morphological characterisation of cells

To observe general cellular morphology, cytocentrifuge smears were stained with Wright-Giemsa through the automated system of the Division of Clinical Pathology, IMVS. Briefly, the slides were immersed in Jerner's stain for 2 minutes, Giemsa stain for 6 minutes and washed in a buffer of pH 7, before air drying. For photography, slides were mounted in glycerol-glycine mountant (see 2.9.1)

2.2.10. Phenotypic characterisation of cells – esterase staining

To determine the phenotype of cells in culture, the expression of lineage specific esterases was analysed. Mature macrophages express 'non-specific' (α-naphthyl acetate) esterase while mature neutrophils express chloroacetate esterase. The method used to detect these lineage specific enzymes was adapted from a technique described by (Yam *et al* (Yam et al., 1971). Cytocentrifuged cell smears were fixed in ice cold esterase fixative (see 2.9.1) for 30 seconds upright in a Coplin jar and then washed in distilled water with 3 changes over 5 minutes. The slides were then allowed to stain for 45 minutes at room temperature in a freshly made solution of 'non-specific' esterase substrate solution (see 2.9.1). The slides were washed as above and stained for 1 hour at room temperature in a freshly made 'chloroacetate' esterase substrate solution (see 2.9.1). Slides were washed as above and counterstained in Dako™ methyl green solution (Dako, Carpinteria, CA, Cat. No. S1962) in which the contaminating methyl violet had been removed by two extractions with an equal volume of chloroform. For photography, slides were mounted in glycerol/glycine (see 2.9.1). Cells expressing 'non-specific' (α-naphthyl acetate) esterase were detected by a red-brown colouring and those expressing 'chloroacetate' (naphthol-AS-D-chloroacetate) esterase by a blue colouring.

2.3. Immunoassays

2.3.1. *Antibodies*

Name	Type	Specificity	Source	Reference
1DC3	IgG1 Mab	Human c-Kit	Prof LK Ashman, IMVS	(Aylett et al., 1995)
1B5	IgG1 Mab	Giardia (neg control)	Prof G Mayrhofer, Dept of Molecular Biosciences, University of Adelaide, Australia.	
ACK2	Rat Mab	Murine c-Kit	GibcoBRL	(Ogawa et al., 1991)
F4/80	Rat Mab	Mature murine macrophages	Dr A Hapel, John Curtin School of Medical Research, Canberra, Australia	(Austyn et al., 1981)
biotinylated RB6 8C5	Rat Mab	GR-1 to detect mature neutrophils	Dr. I. Bertoncello, Peter MacCallum Institute, Melbourne	(Conlan et al., 1994)
M1/70	Rat Mab	MAC-1 to detect monocytes	Dr. I. Bertoncello, Peter MacCallum Institute, Melbourne	(Springer et al., 1979)
30H12	Rat Mab	Thy1	from Dr. I. Kotlarski, University of Adelaide, Australia	(Ledbetter et al., 1979)
Anti-mMCP-5	Rabbit Ab	murine mast cell protease-5 (mMCP-5)	Dr. Patrick McNeil, University of New South Wales, Sydney	(McNeil et al., 1992)
Anti Phospho MAPK	Rabbit Ab	Phospho MAPK (Erk 1 and 2)	New England Biolabs	
Anti MAPK	Rabbit Ab	MAPK (Erk 1 and 2)	New England Biolabs	
Anti Phospho AKT	Rabbit Ab	Phospho AKT (Thr 308)	New England Biolabs	
Ant Akt	Rabbit Ab	AKT	New England Biolabs	
1C1	Murine Mab	Human c-Kit	Dr H-J Buhring, Univeristy of Tubingen, Germany	(Buhring et al., 1995)
Anti Ub	Murine Mab	Ubiquitin	Zymed Laboratories Cat No. 13-1600	
4G10	Murine Mab	Phosphotyrosine	Upstate Biotechnology Cat No. 05-321X	
PY20	Murine Mab	Phosphotyrosine	Transduction Laboratories	
Anti PI3-K p85	Rabbit Ab	P85 subunit of PI3-K	Upstate Biotechnology Cat No. 06-195	
Kit4	Murine Mab	Human c-Kit	Ashman Laboratory	

Antibody was diluted in 10% normal human serum in PBS containing 1% BSA (Sigma, St Louis, MO, Cat. No. A-7906) and 0.1% w/v sodium azide (Sigma, St Louis, MO, A-7906) as follows: ACK2, 1μg/ml; F4/80, undiluted, RB6 8C5, 1/160; M1/70, 1/320 and 30H12, 1/160 prior to a 1/2 dilution into cells in the indirect immunofluorescence assay. The rabbit polyclonal antibody raised mMCP-5 was used at 1/50 in 10% normal goat serum to detect murine mast cells.

Murine monoclonal antibodies were detected using affinity-isolated fluorescein isothiocyanate (FITC)-labelled F(ab')2 sheep antibody to mouse immunoglobulin (Silenus, Australia, Cat. No. DDF) or affinity purified R-phycoerythrin (PE) - labelled goat F(ab')2 anti-mouse Ig (Southern Biotechnology Associates, Inc. Birmingham, AL, Cat. No. 1030-09) both diluted 1/50 in 10% normal rabbit serum. Rat monoclonal antibodies were detected with goat anti-rat IgG-R-PE (Southern Biotechnology Associates, Cat. No. 3030-09) diluted 1/100 in 10% normal human serum. Biotinylated antibodies were detected with 1/50 dilution of streptavidin-R-PE (Caltag Laboratories, Cat. No. SA 1001-4) in 10% normal human serum.

2.3.2. *Immunofluorescence Assay*

Indirect

Target cells were harvested and washed twice in 2 ml ice cold PBS/BSA/Az by centrifuging at 200 g for 5 minutes at 4°C. Cells were then resuspended at approximately $1x10^7$ cells/ml in PBS/BSA/Az supplemented with 10% heat inactivated normal rabbit serum (NRS) or 10% normal human serum in order to block antibodies binding to surface Fc receptors. Aliquots of 50 μl were dispensed into round-bottomed plastic tubes and placed on ice. Saturating levels of purified antibody

or culture supernatant (50 µl) were added to cell suspensions, mixed and then incubated on ice for 60 minutes. Cells were washed twice in 2 ml PBS/BSA/Az, after the final wash, the supernatant was removed leaving about 50 µl in the tube. Tubes were mixed prior to the addition of 50 µl of secondary fluorescent tagged antibody diluted in PBS/BSA/Az supplemented with 10% NRS or 10% normal human serum. Cell suspensions were mixed and incubated on ice for 60 minutes in the dark. Following the incubation, cells were washed twice with 2 ml PBS/BSA/Az and fixed in 0.5 ml of 1% paraformaldehyde in PBS. The samples were stored for up to three weeks at 4°C in the dark. (Note: Where cells were to remain viable and be sorted by Fluorescence Activated Cell Sorting (FACS), PBS/BSA/Az was replaced with ice cold HBSS supplemented with 5% FBS, and sorted cells were caught in this media as well. Cells were not fixed.) Samples were analysed by flow cytometry using either a Profile II or EPICS XL-MCS flow cytometer (Coulter, Hialeah, FL).

Direct

Where antibodies were directly conjugated to a fluorescent marker, the assay was performed exactly as described above, with the omission of the steps to wash and then incubate with secondary fluorescent reagents.

2.3.3. *Alkaline Phosphatase Anti-Alkaline Phosphatase Technique*

The Alkaline Phosphatase Anti-Alkaline Phosphatase (APAAP) technique was used to detect the expression of both intracellular and surface expressed antigens and was a derivation of that described by Cordell *et al* (Cordell et al., 1984).

Slides were prepared as detailed in section 2.2.8. Using a wax pen (Dakopatts, Glostrup, Denmark, S2002), a ring was drawn around the cell smear to localise the applied solutions. Cells were fixed for 30 seconds in ice cold standard APAAP fixative (see 2.9.1) then immediately washed by agitation in Tris buffered saline (TBS) (see 2.9.1) with 3 changes over a 5 minute duration. To avoid high background staining, cell smears were not allowed to dry out from this point on. Excess TBS was removed with a paper towel and 50 µl of hybridoma supernatant diluted 1/2 in 10% NRS in PBA was added within the wax ring. This was incubated overnight in a humidified box at 4°C.

Primary antibody was removed by three washes in TBS over a 5 minute duration. To the cell smear 30 µl of rabbit anti-mouse Ig bridging antibody (Dakopatts, Cat no. Z259) diluted 1/50 in 10% NRS in PBS/BSA/Az was added and incubated for 1 hour at room temperature. Slides were washed as above then incubated with 30µl of APAAP complex (murine anti-alkaline phosphatase Mab conjugated to alkaline phosphatase) (Dakopatts, Cat no. D0651) diluted 1/100 in 10% NRS in PBS/BSA/Az. Smears were washed and incubated with two more rounds of bridging antibody and APAAP complex with 10 minute incubations for each. After the final wash, slides were incubated upright in a coplin jar with alkaline phosphatase chromogenic substrate (see 2.9.1) for 20 minutes and then rinsed with distilled water. Slides were either dried or counterstained immediately.

For counter staining, pre-wet slides were immersed in Dako™ Mayer's Haematoxylin (Lillie's Modification) (Dako, Cat. No. S3309) for 5 to 10 minutes. Slides were briefly rinsed in a large volume of distilled water prior to a 3 second immersion in

acid water (0.5% HCl in distilled water). Slides were again rinsed in a large volume of distilled water prior to immersion in Scott's gentle alkaline solution (see 2.9.1) for 2 minutes. Slides were rinsed in water, mounted with glycerol-glycine (see 2.9.1) and stored at room temperature. Cells exhibiting antibody binding appeared reddish pink with the Haematoxylin stained nucleus appearing purple.

For murine mast cell protease 5 staining, cells were fixed as above and incubated with anti-mMCP-5 diluted 1/50 in 10% normal goat serum in PBS/BSA/Az and incubated for 1 hour in a humidified chamber at room temperature. Slides were washed as above and incubated with biotinylated goat anti-rabbit (Chemicon, Aust. Cat no. AP124B) diluted 1/250 in 10% normal goat serum for 2 hours at room temperature. Washed slides were then incubated with streptavidin alkaline phosphatase (Dako, Cat No. K0391) and incubated with APAAP substrate (see 2.9.1) for 20 minutes. Slides were counterstained with haematoxylin as above and mounted in glycerol/glycine (see 2.9.1).

2.3.4. Quantitative confocal microscopy for determination of endogenous muSCF levels

NIH3T3 transfectants were plated onto glass Chamber slides (Nunc) at a density of 3 x 10^4 per well and incubated at 37°C for 24hrs in DMEM 10% FCS. The medium was then aspirated and cells fixed for 30 sec on ice with 47.5% Acetone, 47.5% Methanol, 5% Formaldehyde. Chambers were immediately rinsed three times with ice-cold PBS pH 7.4. Rabbit anti-mu-SCF (Genzyme, Cambridge, MA), 10µg/ml in 10% normal human serum (NHS) in PBS was then added and incubated on ice for 1 hr. Chambers were again rinsed three times in ice cold PBS. A 1% solution of

biotinylated donkey anti-rabbit Ig (Amersham, Cat no. RPN 1004) in PBS 10%NHS was then added and incubated on ice for a further hour. Chambers were then rinsed three times in ice cold PBS, and then incubated for 1hr in a 1/500 dilution of streptavidin-Tricolor (Caltag Laboratories, Cat No. SA1006) in PBS 10% NHS. Chambers were again rinsed three times, and the cells fixed in ice cold 1% paraformaldehyde in PBS for 15 mins on ice. The chamber wells were then removed and the slides analysed with a MRC-600 confocal microscope (Bio-Rad, Hercules CA) using an excitation wavelength of 488nm and a 600nm long pass filter. A minimum of 50 cells were analysed for total fluorescence for each cell population and treatment.

2.3.5. *Confocal Microscopy – visualisation of receptor internalisation*

Analysis of cell surface and intracellular antigen distribution was performed by confocal microscopy. In all cases, the NIH3T3 cells were plated into Lab-Tek™ Chamber Slides (Nunc) at 2 x 10^4 /chamber in DMEM with 10% FCS and cultured overnight. The cells were starved of serum for 2 hours, then pulsed with 100ng/ml SCF at 37° for the times indicated. Cells were fixed for 30 seconds in permeabilising fixative (47.5% methanol, 47.5% acetone, 5% formaldehyde) or for 15 minutes in non-permeabilising fixative (1% paraformaldehyde in PBS) at 4°C. Cells were then rinsed 5 times in ice cold PBS, and murine primary antibodies, diluted in 10% normal rabbit serum (NRS), were added and incubated at 4°C for 2 hours. Cells were again rinsed 4 times in ice cold PBS and sheep anti-mouse Ig - FITC (Chemicon) secondary antibody was added (in 10% NRS) for 1 hour at 4°C. Slides were rinsed 3 times,

fixed for 15 min in 1% paraformaldehyde and analysed on a MRC 600 confocal microscope (Bio-Rad) using 488nm excitation and a 520nm Band Pass Filter.

2.4. Analysis of cell survival, proliferation and growth by PKH assay

The technique and data analysis was essentially carried out as described by Ashley *et al* (Ashley et al., 1993). The procedure relies on the incorporation of a fluorescent lipophilic dye into the cellular membrane. Cellular division results in equal distribution of the dye between the two daughter cells, hence the level of fluorescence on a given cell is an indication of the number of divisions it has undergone. A standard number of fluorescently labelled beads is mixed into each sample prior to analysis by flow cytometry and they are used to calculate the total number of cells present in the sample. This cell count together with the Mean Fluorescence Intensity (MFI) is used to calculate the cell survival based on the yield of fluorescence remaining in the viable cell gate within the population.

Cells were labelled using the PKH26 Red Fluorescent Cell Linker kit (Sigma, Cat No. PKH26-GL) as per manufacturers instructions. Cells were harvested from culture at equivalent densities and washed three times in serum free DMEM and then resuspended to $2x10^7$/ml in Diluent C (supplied in kit). The staining procedure was optimised for each cell line to maximise staining whilst maintaining viable cell yields from the procedure. For FDC-P1 cells, an equal volume of $2x10^{-5}$ M PKH dye diluted in diluent C was added to the cells and incubated at room temperature for 3 minutes with gentle mixing every 30 seconds. For MIHC, an equal volume of $1x10^{-5}$ M PKH26 dye diluted in diluent C was added to the cells and incubated at room temperature for 3 minutes with gentle mixing every 30 seconds.

To stop dye incorporation, an equal volume of 100% FCS was added and incubated for 1 minute followed by the addition of an equal volume of 10 to 20% FCS in DMEM with a further incubation of 1 minute. The volume was then made to 10 ml and viability and number of cells were determined using a haemocytometer and trypan blue exclusion. Cells were centrifuged at 200 g and resuspended to $4x10^5$/ml in appropriate growth medium and incubated overnight to stabilise the cells before commencing analysis.

Cells were harvested about 15 hours post staining and washed three times in serum free DMEM and then factor deprived by resuspension to $1x10^6$/ml in serum free DMEM for 2 hours at 37°C. Cells were counted and resuspended to $2x10^5$/ml in appropriate medium and 100 µl aliquoted in triplicate into 96 well tissue culture trays already containing factors to give a final volume of 200 µl and a final density of $1x10^5$/ml. At appropriate time points the wells were harvested (200 µl) and 400 µl 1% Paraformaldehyde in PBS was added. Samples were vortexed before storage at 4°C in the dark.

On the day of analysis, $2.5x10^3$ Standard-Brite™ calibration beads (Coulter, Cat. No. PN 660414) diluted in PBS/BSA/Az were added to each tube immediately prior to analysis. The cell count, bead count and the mean fluorescence intensity (MFI) for each sample was analysed on a flow cytometer. The total cell number was calculated using the formula: Cell Density (cells/ml) = (viable cell count / bead count) x (volume of the beads / volume of the cells) x (concentration of the beads). Since each division results in halving of the fluorescence of individual cells, the average number of

divisions was calculated based on the MFI at each time point relative to the MFI at day 0. The formula used was: Number of Divisions = (log (MFI at day 0 / MFI at that day)) / log (2). The survival or maintenance as the percentage retention of fluorescence relative to day 0 was calculated by the formula: Cell maintenance = (MFI at that day x total viable cells at that day) / (MFI at day 0 x total cells at day 0) x 100. This calculation is possible as no dye from dead cell membranes is able to re-incorporate into live cells and dead cells are excluded from analysis on the flow cytometer.

2.5. Saturation Binding Analysis (Scatchard Analysis)

Recombinant human SCF (Amgen) and murine SCF (Immunex Corp., Seattle, WA) were iodinated using the iodine monochloride method (Contreras et al., 1983). 4μg of recombinant protein was processed in the reactions, and the iodinated proteins were separated from free iodide ions on a Sephadex G-25 PD-10 column (Pharmacia) and eluted with PBS containing 0.02% Tween 20 and stored for up to three weeks at 4°C.

Binding assays were done on the NIH3T3 transfectants grown to 80% confluency in 24 well tissue culture plates over a concentration range of 6pM to 3nM ^{125}I-labelled SCF in binding medium (RPMI-1640 supplemented with 0.5% Bovine Serum Albumin (BSA) and 0.1% Sodium Azide) with non-specific binding determined at each concentration with excess unlabelled SCF (10nM). After incubation at 4°C for 4 hours, radioligand was removed and the wells washed twice in cold binding medium (RPMI 1640, 0.5% BSA, 0.1% Sodium Azide). Specific counts were determined after lysis of the cell monolayer (Lysis buffer 1% NP40 10mM Tris, 150mM NaCl) with

subsequent transfer to tubes for counting on a γ-counter (Cobra Auto Gamma, Packard Instruments Co., Meridien, CT).

Where binding assays were performed on non adherent cells (FDC-P1 transfectants, MO7e, HEL), 50,000 cells were added to borosilicate tubes in 50μl of binding media, and binding assays performed in a total volume of 100μl. These tubes were incubated at 4°C on an orbital shaking platform, and then centrifuged through neat FCS to separate cell bound SCF from free SCF. The tubes were cut off and the segment containing the cell pellet was transferred to counting tubes for analysis on a γ-counter. Dissociation constants and copy number were determined by Scatchard analysis.

2.6. Protein Analysis

2.6.1. Preparation of cellular lysates

Cells grown in log phase were harvested and starved in DMEM without serum at $1x10^6$/ml for 2 hours at 37°C. After serum deprivation, cells were resuspended to 1-2 $x10^7$/ml in serum free DMEM. Cells were stimulated with 100 ng/ml huSCF at 37°C and pelleted immediately in a microfuge by centrifugation at 14000 g for 2-5 seconds. Tubes were immediately placed on ice, the supernatant aspirated and cells lysed in 1 ml of 1% NP40 lysis buffer (see 2.9.2) with thorough mixing. Lysed cells were incubated on ice for 30 minutes with vortexing every 5 minutes to ensure complete lysis. Lysates were then centrifuged at 14000 g for 30 minutes at 4°C to pellet nuclei. The lysate was transferred to a fresh tube and a small portion was removed and stored at -20°C for protein determination. The remainder was immunoprecipitated (see 2.6.2).

2.6.2. *Immunoprecipitation*

Immunoprecipitation of 1ml lysates was performed with 5 μg of primary antibody mixed with 25 μl of a 50% slurry of Protein A Sepharose in PBS with 0.1% azide at 4°C on a rotating platform for 2 hours. Immunoprecipitates were washed five times in the lysis buffer (including protease inhibitor cocktails - see 2.9.2) supplemented with 5 mM sodium orthovanadate. After the final wash, the Protein A Sepharose pellet was resuspended in an equal volume of double strength reduced loading buffer (see 2.9.2). Samples were boiled for 2 minutes and then processed by SDS Polyacrylamide Gel Electrophoresis (SDS PAGE).

2.6.3. *Determination of the amount of protein within lysates*

Protein determination was carried out on whole cell lysates using Micro BCA Protein Assay Reagent Kit (Pierce, Rockford, IL, 23235) according to manufacturer's instructions. In the presence of peptides and aa side chains, a purple reaction product is obtained absorbing at 562 nm. BSA (supplied with kit) was serially diluted in PBS with concentrations ranging from 1.56 μg/ml to 200 μg/ml. Protein determination was performed on frozen lysates after centrifugation for 15 minutes at 14000 g at 4°C. Samples were diluted 1/20 or 1/30 in PBS. For the correction of background absorbance, blanks consisting of PBS only or 1% NP-40 diluted 1/20 or 1/30 dilution in PBS were used. Standards, lysates and blanks (75 μl) were loaded in triplicate into wells of 96 well tissue culture treated trays. All standards and blanks were replicated on all trays used. To the wells, 75 μl of BCA reagent (50% reagent MA, 48% reagent MB, and 2% reagent MC) was added and trays incubated at 37°C for 2 hours in a humidified box. Microtitre plates were read on a Bio-Rad microtitre plate reader (Bio-Rad, model 3550) at absorbance 570nm.

2.6.4. Size determination of proteins – SDS PAGE

The size of proteins was estimated by comparison of their relative mobilities with commercially available molecular weight markers. Two different sets of markers were deployed, both prestained for monitoring progression of electrophoresis. These were SDS-PAGE Standards, High Range (Bio-Rad, Cat. No. 161-0309) and SeeBlue™ Pre-Stained Standard (Invitrogen, Cat. No. LC5625). The estimated sizes of these molecular weight markers in kDa are as follows:

Prestained SDS-PAGE Standards, High Range: 204; 123; 80; 48

SeeBlue™ Pre-Stained Standard: 250; 98; 64; 50; 36; 30; 16; 6; 4

Immunoprecipitates as described in section 2.6.2 above were size fractionated under reducing conditions on 8% polyacrylamide gels (see 2.9.2) overlayed with a stacking gel (see 2.9.2). Gels were assembled in mini vertical gel tanks, according to manufacturer's instruction, and immersed in protein electrophoresis buffer (see 2.9.2). Boiled immunoprecipitates (including Sepharose) were loaded onto gels and electrophoresed at 15 mA/gel through the stacking gel and 20 mA/gel through the resolving gel. Whole cell lysates diluted 1/2 in double strength reduced loading buffer were size fractionated under reducing conditions on 10% polyacrylamide gels (see 2.9.2) overlayed with a stacking gel (see 2.9.2). Samples were boiled for 2 minutes prior to loading and were electrophoresed at 15 mA/gel through the stacking gel and 20 mA/gel through the resolving gel.

2.6.5. *Transfer of proteins to PVDF*

Proteins size fractionated on 8% or 10% gels by SDS-PAGE were electroblotted to polyvinylidene difluoride (PVDF) Hybond membrane (Amersham, Cat. No. RPN 303F) prewetted in 100% methanol (chosen for its low fluorescence) using a fully submerged electrophoretic transfer in Tris/Glycine/Methanol transfer buffer (see 2.9.2) with 20% methanol for PVDF. Proteins were transferred at 30 mA overnight or 250 mA for 2 hours.

2.6.6. *Visualisation of blots*

Membranes to be probed were washed twice in 1x TBS (see 2.9.2) with 0.1% Tween20 for 10 minutes. To prevent non-specific antibody binding, the membranes were incubated on a rocker in 2.5% membrane blocking solution (Amersham, NIF833) in TBS for 1 hour at room temperature. The membrane was washed in TBS with 0.1% Tween20 (2 quick rinses followed by a 15 minute incubation and two 5 minute incubations) on a fast rocking platform at room temperature. The membrane was then incubated with primary antibody diluted in 2.5% membrane blocking solution for at least 2 hours in a covered container (to prevent evaporation) on a slow rocking platform at room temperature. After washing as above, the membrane was incubated with secondary antibody conjugated to alkaline phosphatase for at least 1 hour in a covered container on a slow rocking platform at room temperature. Membranes were then washed 5 times as above followed by two rinses of 5 minutes in TBS alone. The membrane was incubated protein side down with 1 ml/mini gel of enhanced chemifluorescence substrate (ECF) (Amersham, Cat. No. RPN 5785) for 30 seconds to 1 minute then placed protein side down on the glass plate of the

FluorImager595 (Amersham) and scanned immediately using a 488nm excitation and 570nm band pass emission filter.

2.6.7. *Quantitation of protein bands*

Digital images produced by the FluorImager were quantitated using ImageQuant™ software (Amersham). Background values for each band were determined using an equivalent size analysis region in the same lane. The background value in relative fluorescence units was subtracted from the intensity of the band of interest.

2.7. Manipulation of DNA

2.7.1. *Restriction Endonuclease Digestion*

Plasmid DNA was digested with restriction endonuclease(s) in a final volume of 10 - 40 µl. Digests were performed for 1 - 3 hours in 1X digestion buffer (supplied with enzyme as a 10x concentrated stock) at the optimal temperature as indicated by the manufacturer. The extent of digestion was determined by visualisation of the DNA fragments by gel electrophoresis. Following digestion, enzymes were inactivated as specified by the manufacturer. If DNA was to be digested by multiple enzymes, then this was done simultaneously if the enzymes had compatible buffer conditions. If not, the DNA was purified by phenol chloroform extraction (see section 2.7.4) after digestion with the first enzyme and before digestion with the subsequent enzyme.

2.7.2. *Electrophoresis of DNA*

DNA was separated by electrophoresis on agarose gels made in 1X TAE (see 2.9.3) with the percentage of the gel dependent on the size of the DNA products to be detected. Gel loading buffer (see 2.9.3) was added to the DNA and the samples loaded

on horizontal gels immersed in a submarine electrophoresis tank containing 1X TAE (see 2.9.3). Gels were electrophoresed at 80 - 100 V until the bromophenol blue dye had migrated three quarters the length of the gels. Gels were then removed, stained with ethidium bromide solution (2 μg/ml in water) for 5 minutes and destained in water for 5 minutes. DNA bands were visualised using FluorImager 595 (Amersham) using a 488nm excitation and a 610 long pass filter.

2.7.3. *Size determination and quantitation of DNA fragments*

Calculation of the size of DNA fragments was by a comparison of their relative mobilities by electrophoresis with DNA of known size. The commercially available molecular weight markers used were *Bacillus subtilis* bacteriophage SPP1 DNA digested with EcoRI (GeneWorks, Australia, Cat. No. DMW-S1) and plasmid pUC19 DNA digested with HpaII (GeneWorks, Cat No. DMW-P1). The estimated sizes of these molecular weight markers in kilobases are as follows:

EcoRI digested SPP1: 8.51; 7.35; 6.11; 4.84; 3.59; 2.81; 1.95; 1.86; 1.51; 1.39; 1.16; 0.98; 0.72; 0.48; 0.36

HpaII digested pUC19 DNA: 0.501; 0.489; 0.404; 0.331; 0.242; 0.190; 0.147; 0.111; 0.110; 0.067; 0.034; 0.026

The concentration of DNA in solution was determined by spectrophotometry with absorbance at 260nm (OD of 1 = 50ng/μl DNA). Alternatively, DNA was electrophoresed and the intensity of the ethidium bromide stained bands was compared to those with known molecular weight markers using a FluorImager.

2.7.4. Purification of DNA

Two techniques were used in the purification of DNA. Firstly, GENECLEAN was used to purify DNA excised from agarose gels. The second technique was phenol chloroform extraction used for purifying DNA after restriction enzyme digests.

GENECLEAN™

For purification of target DNA from contaminating DNA fragments after restriction endonuclease digestion, samples were electrophoresed and stained with ethidium bromide as in section 2.7.2. The gel was then scanned on the FluorImager 595 and a 100% scaled printout of the gel was produced. This printout was placed beneath a glass plate the gel was resting on and the fragment of interest was excised from the gel. The gel was then rescanned to ensure the entire band had been excised. This eliminates any exposure of the DNA to UV (from a transilluminator), enhancing the quality of DNA for subsequent ligation into vectors – 488nm light will not induce nicks in the nucleic acid).

This method was used to purify DNA between 0.5 and 3 KB from molten agarose and was a modification of the manufacturer's instructions (BIO 101, La Jolla, CA, Cat. No. 3105). The excised gel slice containing the DNA fragment was placed into a microfuge tube and weighed (assuming 1 mg is equivalent to 1 ml). To this, 2.5-3 volumes of sodium iodide (NaI) solution (supplied by manufacturer) were added and the agarose melted at 55°C. To the molten agarose, 5 µl of glassmilk suspension (supplied by manufacturer) (for 5 µg or less of DNA) was added and the sample mixed on a rotator at 4°C for 15 to 30 minutes. DNA bound to the silica matrix was pelleted in a microcentrifuge for 5 seconds (14000 g) and the NaI supernatant was

removed. The pellet was resuspended and washed 3 times with 'NEW WASH' (NaCl/Ethanol/Water; as supplied by the manufacturer) and resuspended in 10 - 20 µl Milli-Q water by heating the tube at 55°C for 10 minutes. The glassmilk was pelleted and the supernatant containing the DNA was transferred to a fresh tube.

Phenol extraction

The DNA to be purified was made up to a minimum volume of 100 µl. To this, 2 µl of glycogen (2 mg/ml) (Roche, Mannheim, Germany, Cat. No. 901393) was added as a carrier to aid in visualisation of the purified DNA when pelleted. An equal volume of phenol/chloroform (50% phenol, 50% chloroform) was added, vortexed and incubated on ice for 2 minutes to allow separation of the two phases. The solution was then centrifuged at 4°C at 14000 g for 5 minutes and the top aqueous phase transferred to a new centrifuge tube. To precipitate the DNA, 0.1 volumes of 3 M sodium acetate (pH 5.2) and 2.5 volumes of 100% ethanol were added and incubated on ice for 20 minutes prior to centrifuging at 14000 g for 20 minutes at 4°C. The precipitated DNA was washed once with 500 µl of 70% ethanol and allowed to air dry or dry under vacuum and then resuspended in water or TE (see 2.9.3).

2.7.5. *Dephosphorylation of DNA*

Dephosphorylation of vector DNA was performed to prevent vector religation. This procedure used calf intestinal alkaline phosphatase (CIP) (Amersham, Cat No. E2250Y) which removed the 5' phosphates of DNA. Phosphatase treatment was performed in 10 µl reaction comprising DNA, 1X OnePhorAll buffer (Amersham , Cat No.. 27-0901-02) and 1 U of CIP per 1 µg of DNA. Phosphatase reactions for 'sticky ends' were carried out at 37°C for 30 minutes and then inactivated by the

addition of EDTA (pH 8) to a final concentration of 5 mM and incubation at 75°C for 10 minutes. DNA was purified using the GENECLEAN™ method.

2.7.6. Ligation

Ligation of DNA was performed using T4 DNA Ligase (Amersham, Cat No. E70005Y). Ligation reactions were carried out with a 1 - 3 fold molar excess of insert DNA to vector DNA in the presence of 10 mM dATP, 66 mM Tris HCl (pH 7.6), 6.6 mM $MgCl_2$, 10 mM 1,4-Dithiothreitol (DTT), 150 mM NaCl, and 6 U of T4 ligase to a final volume of 10 µl and incubated at 4°C overnight. To terminate the reaction, it was heated at 65°C for 10 minutes and then DNA was purified using phenol chloroform procedure (see 2.7.4) and resuspended to 10µl in sterile water.

2.7.7. Production of chemical competent bacterial cells

A single colony of *E. coli* DH10α was cultured in ψ broth (see 2.9.3) and cultured overnight at 37°C with shaking. This was subcultured into 100ml pre warmed ψ broth and grown with shaking to an OD_{600} of 0.5 – 0.6. The culture was then chilled on ice 15 minutes before centrifugation at 5500 g at 4°C for 5 minutes. The pellet was resuspended in 40ml ice cold Tfb I (see 2.9.3) and incubated for 5 minutes on ice. Cells were again centrifuged at 5500 g for 5 minutes at 4°C and the pellet resuspended in 4 ml ice cold Tfb II (see 2.9.3). Cells were incubated 15 minutes on ice, and dispensed into 1.5ml reaction tubes embedded in dry ice to snap freeze chemical competent cells. These were stored at -70°C for future use.

2.7.8. Transformation of chemical competent cells

Chemical competent bacteria were slowly thawed on ice and incubated a further 10 minutes on ice. 0.1 – 0.5µg of purified DNA (or the total ligation mix as prepared in section 2.7.6) for transformation was added to the cells, mixed and incubated 30 seconds on ice. Cells were then heat shocked at 42°C for 90 seconds, and returned to ice for a further 2 minutes. To this mix was added 200µl of SOC media (see 2.9.3) and the cells were cultured for 45 minutes at 37°C to establish expression of selectable marker. The cells were then plated onto LB Agar plates (see 2.9.3) with appropriate selection media and incubated overnight at 37°C.

2.7.9. Expansion of plasmid DNA

Small scale plasmid preparation

Single colonies were plucked asceptically from agar plates and grown overnight in 10 ml centrifuge tubes containing 3 ml of luria broth (see 2.9.3) with 100 µg/ml ampicillin unless otherwise indicated. Cultures were chilled on ice for 5 minutes and 100 µl of culture transferred to a microfuge tube and stored at 4°C. The remaining cells were centrifuged at 2000 g for 10 minutes at 4°C. The supernatant was removed and pellet resuspended in 250 µl of fresh lysis buffer (50mM Tris HCl, pH 7.5; 62.5mM EDTA, pH 8; 0.4% Triton X100; 2.5M LiCl), vortexed, transferred to 1.5 ml microfuge tubes and incubated on ice for 5 minutes. To this, 20 µl of lysozyme (10 mg/ml) was added, vortexed for 3 seconds, boiled in a waterbath for 1 minute and immediately placed on ice for 15 minutes. Chromosomal DNA and protein was pelleted by centrifugation at 14000 g for 20 minutes at 4°C. The supernatant

containing the plasmid DNA was transferred to a fresh tube and precipitated with 2 volumes of 100% ethanol with $1/10^{th}$ volume 3M Sodium Acetate. The plasmid DNA was pelleted at 14000 g for 15 minutes at 4°C. The pellet was washed with 1 ml of 70% ethanol, dried and resuspended in 30 µl of Milli-Q water.

Midiprep DNA preparation

Midiprep DNA preparation was carried out using a QIAGEN Midi Kit (QIAGEN, Germany, Cat. No. 12143) according to manufacturers instructions. A 100 ml 2x YT bacterial culture (see 2.9.3) containing 100 µg/ml ampicillin was innoculated with bacterial culture using a sterile loop and incubated overnight at 37°C with shaking. The culture was centrifuged at 4°C for 10 minutes at 1800 g. The supernatant was removed and the pellet resuspended in 4 ml Buffer P1 containing RNase A. Cells were lysed by the addition of 4 ml Buffer P2, mixed and incubated for 5 minutes at room temperature. The chromosomal DNA and protein were precipitated by the addition of 4 ml Buffer P3 with gentle inversion and incubated on ice for 15 minutes. Samples were centrifuged at 31000 g for 30 minutes at 4°C. The supernatant was transferred to a fresh tube and re-centrifuged at 31000 g for 10 minutes at 4°C. This supernatant was then applied to a QIAGEN-tip that had been pre-equilibrated with 10 ml of Buffer QBT. The column was washed twice with 10 ml of Buffer QC before the elution of plasmid DNA using 5 ml Buffer QF. Eluted DNA was precipitated with 0.7 volumes of room temperature isopropanol and centrifuged at 14000 g in a JLA25.500 rotor for 30 minutes at 4°C. The supernatant was removed and the DNA pellet air dried briefly. The pellet was then resuspended in 400 µl of TE and transferred to a microfuge tube. The DNA was then re-precipitated with the addition

of 40 µl 3 M sodium acetate and 1 ml of 100% ethanol and centrifuged at 14000 g for 30 minutes at 4°C. The pellet was washed in 70% ethanol, centrifuged for 10 minutes at 14000 g at 4°C and dried under vacuum. The pellet containing the plasmid DNA was resuspended in 100 µl of TE.

Glycerol stocks were made of all midiprep cultures. 3 ml of culture was centrifuged at 1800 g for 10 minutes at 4°C and supernatant removed. The pellet was resuspended in 1 ml of 20% glycerol in LB and transferred to a 1ml cryotube for storage at -20°C.

2.7.10. Polymerase Chain Reaction

All reagents were aliquoted using aerosol barrier tips in order to reduce contamination. Reactions were prepared in 0.5 ml dome cap microcentrifuge tubes to a final volume of 50 µl for use in heated lid thermal cyclers. For amplification of plasmid DNA, reactions containing 0.1 to 1 ng DNA, 100 ng each of forward and reverse primers, 0.2 mM each of dATP, dTTP, dCTP and dGTP (Pharmacia, Cat. No. 27-20(5-8)0-02), 50 mM KCl, 10 mM Tris HCl (pH 8.3), 1.5 mM $MgCl_2$ and 2.5 U of AmpliTaq DNA Polymerase (Perkin Elmer, Boston, Massachuesetts, Cat. No. N801-0060) made to a final volume with sterile Milli-Q water were set up. Different DNA polymerases were used at times and are detailed in the following sections.

DNA was amplified using Hot Lid Thermal Cyclers with an initial 7 minute denaturation step at 94°C followed by 30 rounds of denaturation, primer annealing and elongation, finishing with a final extension at 72°C for 7 minutes. Completed reactions were stored at 4°C.

The temperature selected for the annealing of primers was 1-5°C lower than the average melting temperature for the two oligonucleotide primers and was optimised for each set of primers. The melting temperature was calculated using the formula:

Melting Temperature (°C) = 2(A+T)+4(C+G)

2.7.11. Generation of anti-sense murine SCF

A 630bp fragment incorporating the 5' 420 bases of the coding region of murine SCF (Anderson et al., 1990) was excised from pBSSKMGF10.1 (Immunex) by restriction endonuclease treatment with EcoR1. This fragment was gel purified using GENECLEAN™ (see Section 2.7.4) and ligated into the EcoR1 site of the pCXN2 expression vector (Niwa et al., 1991).

Insert orientation was determined using restriction endonuclease Pst1. This enzyme cut the insert at position 60, and cut pCXN2 535 bp downstream of the EcoR1 ligation site. Several clones were isolated, and the two selected for the experiment were (sense) pCXNC8 and (anti-sense) pCXNC12.

In order to select cells expressing these new sense and antisense SCF constructs, the NIH(mu-Kit) cells were cotransfected with excess (10μg) pCXNC8 or pCXNC12 and 1μg pRUFpuro per dish of cells containing 50000 cells using calcium phosphate co-precipitation (See Section 2.7.17). Cotransfectants were selected using 2μg/ml Puromycin over two weeks in culture. Selection was then removed and cells subjected to anchorage independence assay. The assay was set up in quadruplicate,

and the new NIH mu-Kit pools expressing sense and anti sense mu-SCF were evaluated for colony formation in the presence or absence of mu-SCF.

To verify expression of anti-sense SCF transcript, the Puromycin-resistant pools of pCNXC12 and pCXNC8 expressing cells were plated into 10cm dishes. Upon reaching confluence, RNA was prepared in situ using TRIzol (See Section 2.8.1). Yields of RNA from respective pools of cells was:

WT NIH3T3	160μg
WT NIH3T3 + pCXNC8 (sense)	164μg
WT NIH3T3 + pCXNC12 (antisense)	164μg
NIH3T3 mu-Kit	44μg
NIH3T3 mu-Kit + pCXNC8 (sense)	170μg
NIH3T3 mu-Kit + pCXNC12 (antisense)	184μg

Each preparation was analysed for OD 280:OD 260, and this exceeded 2:1 indicating high quality RNA. 15μg of each RNA as well as 10ng pBSSKMGF10.1 vector DNA cut with EcoR1 (as a positive control) was loaded onto the gel for the Northern Blot analysis and this was electrophoresed and blotted as per Section 2.8.

2.7.12. *Chimaeric c-Kit Generation – Step 1 PCR conditions*

The basic strategy for generation of chi-c-Kit is illustrated in Figures 2.1 and 2.2. A PCR based strategy was chosen and Figure 2.1 shows a schematic layout of the template DNAs.

Figure 2.1

Strategy for Chimaeric c-Kit generation – schematic representations of cDNA and primers used.

Schematic representations of Human and Murine c-Kit cDNA domain structure, indicating location of GNNK sequence. Primers A1, B1, A2, B2 shown schematically to indicate their orientation and the placement of engineered restriction sites. Refer to 2.7.12 for a detailed explanation of the strategy employed. Colour coded arrows alongside each primer are for reference to Figure 2.2.

Template cDNAs for Chimaeric c-Kit generation

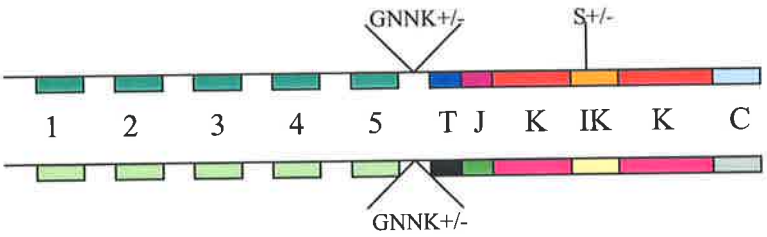

Human c-Kit

Murine c-Kit

Legend

1-5 - Extracellular Ig Like Domains
T - Transmembrane Domain
J - Juxtamembrane Domain
K - Kinase
IK - Interkinase Domain
C - c Terminal

Primers for Chimaeric c-Kit generation

A1 - BCXHUKITFWD 39mer

CGC GGA TCC ATC GAT CTC GAG GCT ACC GCG ATG AGA GGC

Bam H1 Cla I Xho I Kozac Start

B1 – HUKITAS1 35mer

AG CAG CGG CGT GAA CAG GGT GTG GGG ATG GAT TTG

Murine TM seq Human

A2 - XNXMUKITRV 41mer

CT AGT CTA GAG CGG CCG CTC GAG TCA GGC ATC TTC GTG CAC

Xba I Not I Xho I Stop

B2 – MUKITS1 35mer

AA ATC CAT CCC CAC ACC CTG TTC ACG CCG CTG CTC

Human Murine TM seq

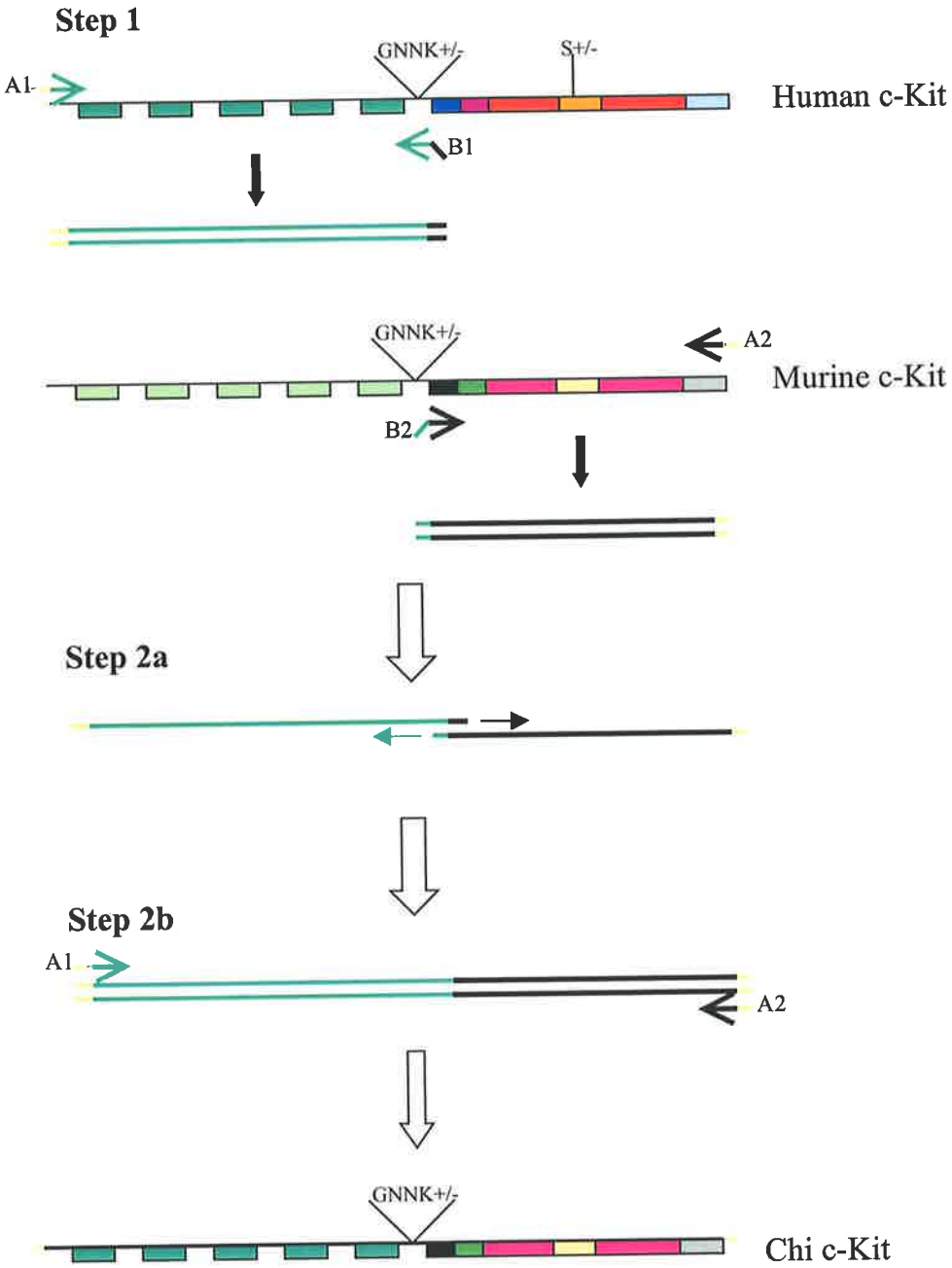

Step 3

Primer ends then digested for ligation into target vectors

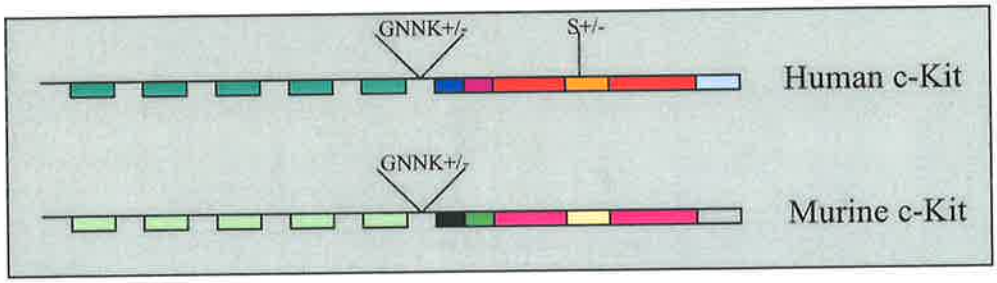

The human c-Kit templates were GNNK± cDNA in the vector pRUFneo, originally generated by Gina Caruana (Caruana, 1996). Primers A1 and B1 were designed to amplify the human extracellular domains from these templates. The murine c-Kit template was a GNNK- murine c-Kit in pSP72 which was also sourced from Gina Caruana (Caruana, 1996). Primers A2 and B2 were designed to amplify the murine transmembrane and intracellular domains.

As depicted in Figure 2.1, primer A1 incorporates 3 restriction enzyme sites with a 5' CGC to facilitate cutting of the Bam H1 site for linear double stranded PCR cDNA product. Also included was the minimal Kozac sequence, the c-Kit start codon and 6bp of coding region.

The B1 primer is comprised of the last 6 codons of human sequence prior to the human transmembrane domain, and 17bp of murine transmembrane sequence. This is to create an overlap in the PCR product to allow fusion of this product with the murine transmembrane/intracellular domain cDNA generated by primers A2 and B2.

The A2 primer also incorporates 3 restriction enzyme sites with a 5' CTAG to facilitate cutting of the Xba 1 site for linear double stranded PCR cDNA product. Also included was the stop codon and the last 5 codons of murine intracellular domain coding sequence.

Primer B2 is comprised of the last 17 bases of human sequence prior to the human transmembrane domain, and 18 bases of murine transmembrane sequence. This is to

create an overlap in the PCR product to allow fusion of this product with the human extracellular domain cDNA generated by primers A1 and B1.

The restriction enzymes were chosen based on the fact that none of them will cut the new chimaeric c-Kit cDNA coding regions, and their placement was such that this would facilitate easy directional cloning into the final retroviral vector used to transduce target haemopoietic cells for analysis.

Figure 2.2 illustrates the 3 steps to generate chimaeric c-Kit. In step 1, Primers A1 and B1 are used to generate double strand cDNA of the human c-Kit extracellular domain. The template cDNA is either GNNK + or GNNK – human c-Kit in pRUFneo. At the same time, primers A2 and B2 were used on the murine c-Kit cDNA in pSP72 to generate murine transmembrane and cytoplasmic domain coding cDNA.

For these reactions, it was critical to have a proof reading polymerase, and PFU polymerase was employed in the reactions. The reaction mix was as follows:

Template cDNA (1ng/μl in water)	5μl
2mM dNTPs	5μl
Primer 1 (0.1μM)	3.2μl
Primer 2 (0.1μM)	3.2μl
10 x PFU Buffer	5μl
Water	27.6μl

This reaction mixes were transferred to a thermal cycler and denatured at 94°C for 5 mins. 1μl PFU polymerase (Stratagene, La Jolla, CA, Cat No. 600135) was then

added (ie HOTSTART). Following addition of PFU polymerase, amplification proceeded with 35 cycles of 94° C for 45 secs, followed by 55° C for 45 secs, followed by 72° C for 7 mins. A final extension of 72°C for 10 min concluded the reaction.

PCR product was cleaned through Bresaspin columns as per manufacturer's direction and the approx 1.5kb products were gel purified as described in section 2.7.4.

2.7.13. *Chimaeric c-Kit Generation – Steps 2 and 3*

Step 2 in the generation for the GNNK± chi-c-Kit generation was also a PCR reaction. Due to the engineered overlaps of the human extracellular domain products (primed by A1/B1) with the murine transmembrane/intracellular domain products (primed by A2/B2), these fragments will anneal in the Transmembrane domain and prime the polymerase to complete double stranded full length chimaeric cDNA as shown in Figure 2.2, step 2a. The reaction also includes primers A1 and A2, which will then amplify the full length chimaeric cDNA as illustrated in step 2b. The reaction conditions used in all reactions for step 2 are detailed below. There are 2 A1/B1 products, one using GNNK+ template , 1 using GNNK – template.

10x PFU buffer	5µl
2mM dNTPs	5µl
A1 primer (.075µM)	2.3µl
A2 primer (.075µM)	2.3µl
A1/B1 product	1µl
A2/B2 product	1µl
Water	32.4µl

This reaction mix was transferred to a thermal cycler and denatured at 94°C for 5 min. 1µl PFU polymerase (Stratagene) was then added (ie HOTSTART). Following addition of PFU polymerase, amplification proceeded with 35 cycles of 94° C for 45 secs, followed by 60° C for 45 secs, followed by 72° C for 7 mins. A final extension of 72°C for 10 mins concluded the reaction.

PCR product was cleaned through Bresaspin columns as per manufacturer's direction and the approx 3kb products were gel purified as described in section 2.7.4.

As indicated in Step 3 of Figure 2.2, chimaeric c-Kit (GNNK + or GNNK -) had been generated with short restriction site sequences at either end (Bam H1 – Cla 1 – Xho 1 5', and Xho 1 – Not 1 – Xba – 1 3'). These sites would facilitate ligation of the cDNA into vectors pBluescript SK and pRUFpuro (Figure 2.3). pBS-SK was selected as it is a relatively small vector with restriction sites suitable for easy ligation of the chimaeric c-Kit cDNA. The cDNA is easily sequenced off this vector (using T3 and T7 primers as well as several internal cDNA primers), and the substantial polylinker provides more flexibility in excising the cDNA to shuttle it to other vectors, including pRUFpuro. pRUFpuro was selected as it is a retroviral vector suitable for transduction of the haemopoietic target cells, and has Puromycin resistance as a selectable marker. This selection was necessary as the mouse knockout cells were G418 resistant, as gene disruption was carried out using a Neomycin resistance selectable targeting sequence.

The full length products from Step 2 (Figure 2.2) were digested with Bam H1 and Xba 1 to facilitate cloning into pBS-KS. The digestion reaction mix was precipitated

Figure 2.3

Plasmid maps.

Maps including Multiple Cloning Site region details for the 2 vectors used to propagate chimaeric c-Kit cDNA (pBluescript II SK (+)) and transduce Myb Immortalised Haemopietic Cells with chimaeric c-Kit (pRufPuro).

f1 (+) origin 135–441
β-galactosidase α-fragment 460–816
multiple cloning site 653–760
***lac* promoter** 817–938
pUC origin 1158–1825
ampicillin resistance (*bla*) ORF 1976–2833

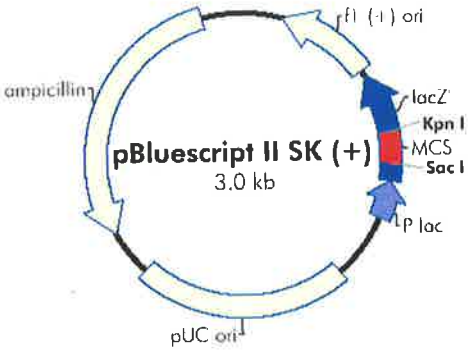

pBluescript II SK (+/–) Multiple Cloning Site Region (sequence shown 598–826)

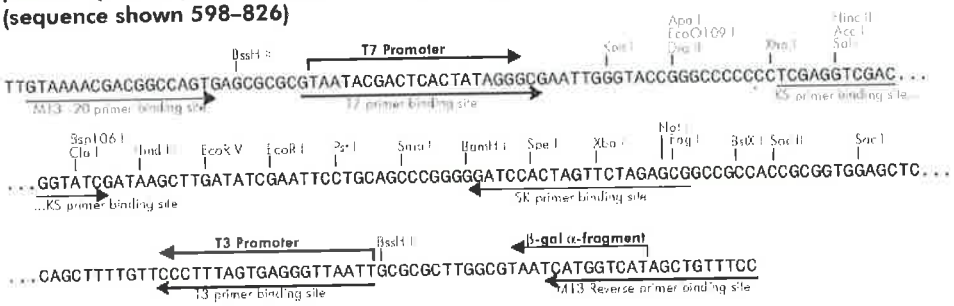

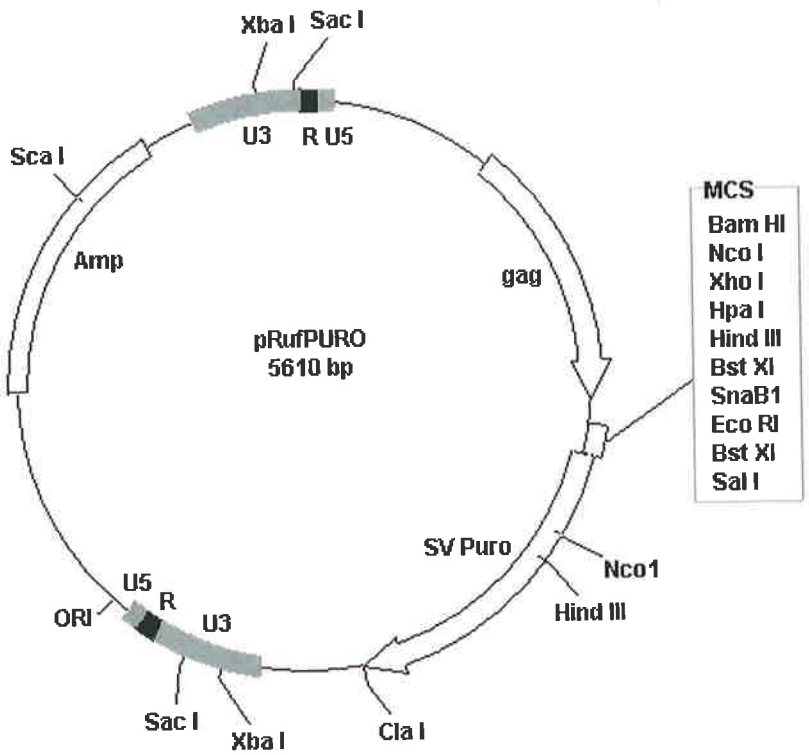

using 3M Sodium Acetate and Ethanol precipitated (Section 2.7.4), and resuspended to 10µl. Approximately equimolar amounts of Bam H1/Xba 1 digested pBS-KS and GNNK+ or GNNK- chimaeric c-Kit cDNA insert were ligated using T4 DNA Ligase (Section 2.7.6) overnight at ambient temperature. The ligation was heat inactivated 65°C for 20 minutes, and 1/3rd of the ligation was used to transform chemically competent XL-10 Gold E. coli (Section 2.7.8).

2.7.14. PCR Site Directed Mutagenesis of chimaeric c-Kit cDNA

The chimaeric c-Kit generation described in the preceding section led to the derivation of a single GNNK+ clone (chi 12+ 10 c-Kit) and a single GNNK- clone (chi 12- 3 c-Kit). These clones were fully sequenced as shown in Figure 2.4 and a number of point mutations were identified (Figure 2.5 (A)). The strategy chosen to resolve these mutations is outlined in Figure 2.5 (B). Clone Chi 12+ 10 was chosen as the source cDNA to generate correct GNNK+ and GNNK- chimaeric c-Kit cDNA. Using PCR site directed mutagenesis, this clone would have the cytoplasmic mutation GGC corrected to GCG. A second round of site directed mutagenesis would be used to correct the extracellular deletion at 1350. This would create a complete and correct GNNK + chimaeric c-Kit cDNA. This would then be subjected to a third round of PCR site directed mutagenesis to remove GNNK (12bp) from this clone to create a complete GNNK – chimaeric c-Kit.

As already stated, Chi 12+ (10) was chosen for PCR site directed mutagenesis of GGC back to GCG. The approach used was to create large sense and anti-sense primers to the same sequence (40mers) with the targeted base for change in the centre of each primer. The PCR would then completely replicate the entire cDNA and

A	387:	ATG	AGA	GGC	GCT	CGC	GGC
B	388HUSENSE:	GAC	AAC	GAC	ACG	CTG	GTC
C	787HUSENSE:	CAT	CAC	GGT	GAC	TTC	AAT
D	765:	AGT	GAA	CTT	CAT	CTA	ACG
E	1142:	CTA	GTG	GTT	CAG	AGT	TCT
F	1773MUSENSE:	GGA	AAG	ACA	TTG	GGA	GCT
G	2157 MUSENSE:	TAT	ATG	GAC	ATG	AAG	CCT
H	2524MUSENSE:	AGC	TGC	GTG	TAC	ACA	TTT

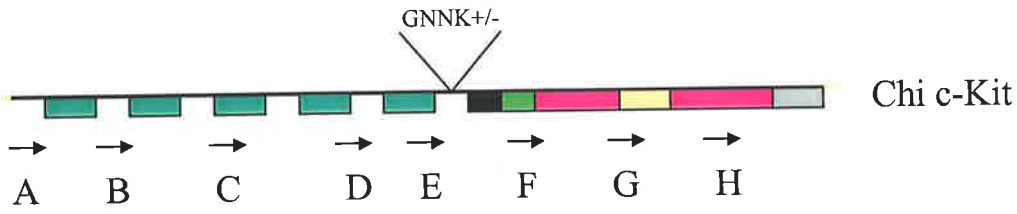

Figure 2.4

Primers used in sequencing of chimaeric c-Kit cDNA

Detailed sequences of primers used for Big Dye ™ sequencing reactions to verify full coding region sequence of all chimaeric c-Kit clones generated. Also shown is a schematic representation of the spatial positioning of each primer. In all sequencing reactions, sufficient sequence was obtained to overlap the next sequence initiation site.

Figure 2.5

Errors in chimaeric c-Kit constructs and strategy for repair

A. Schematic representation of mutations generated in process of generating chimaeric c-Kit cDNAs (GNNK±).
B. Schematic representation of strategy to remove introduced mutations by site directed PCR mutagenesis as described in section 2.7.14.

A

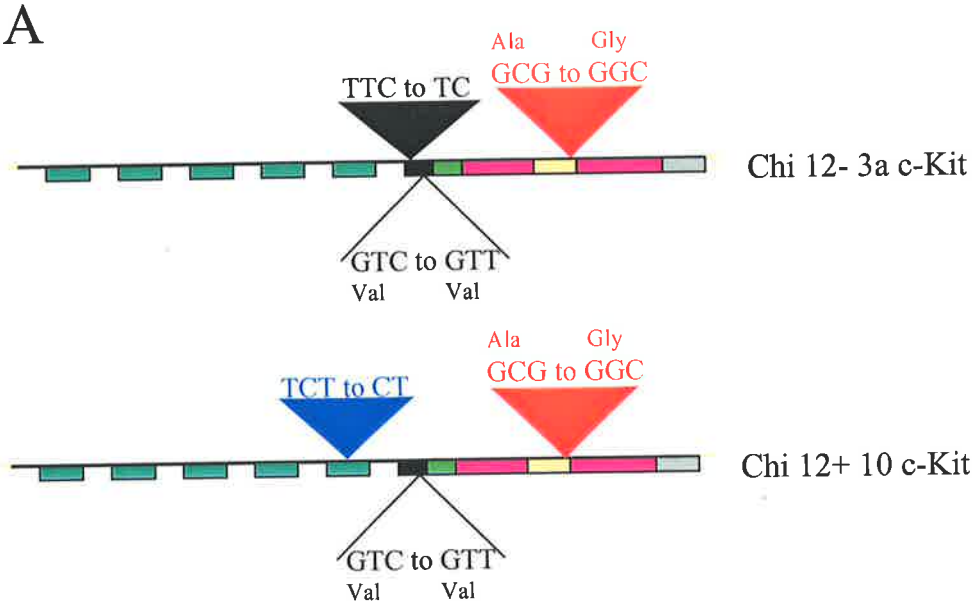

B – **Planned Repairs to Chi 12 + 10 c-Kit**

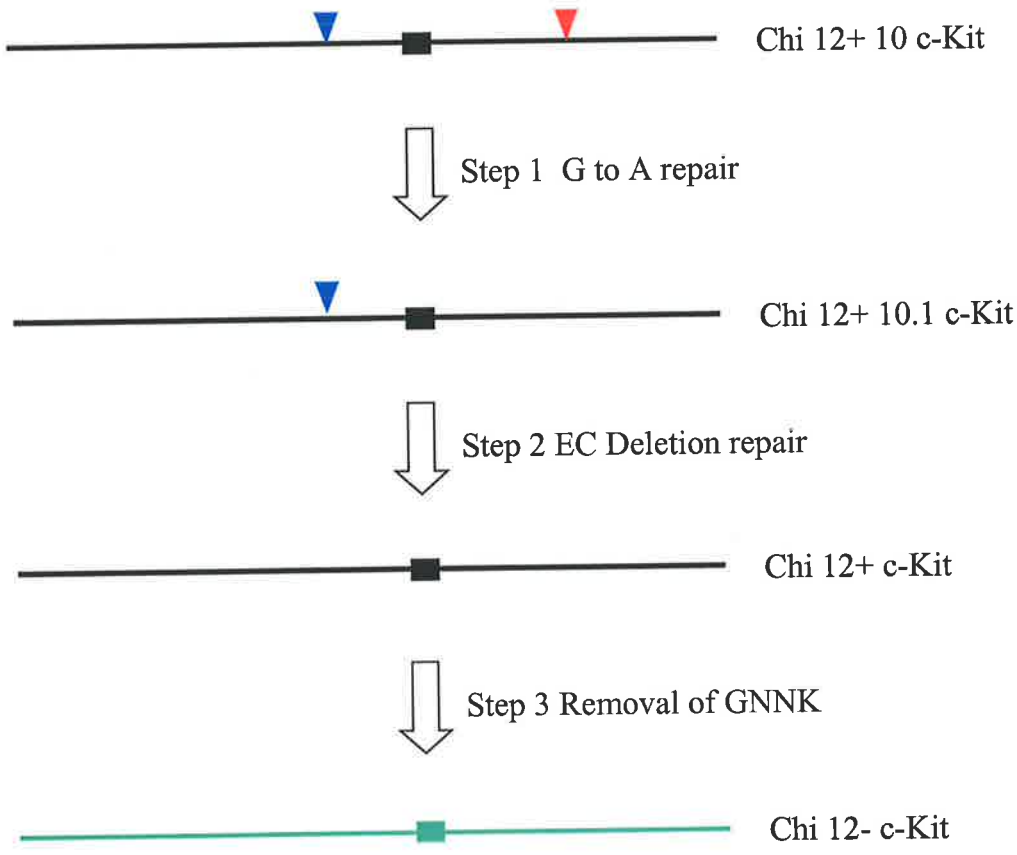

vector (6Kb), with all product having the corrected sequence. This is depicted schematically in Figure 2.6. The primers used for all steps in the correction process are also shown in this figure. Reaction mixes were set up as follows:

10x PFU buffer	5µl
10mM dNTPs	1µl
sense primer (125ng)	0.3µl
αsense primer (125ng)	0.3µl
Template (mutant cDNA)50ng	1µl
Water	41.4µl
PFU Turbo (Stratagene)	1µl

This reaction mix was transferred to a thermal cycler and denatured at 95°C for 30 secs. Amplification proceeded with 18 cycles of 95° C for 30 secs, followed by 55° C for 60 secs, followed by 68° C for 20 mins. A final extension of 68°C for 20 mins concluded the reaction.

PCR product was cleaned through Bresaspin columns, and approx 1/3 used to transform E. coli (Section 2.7.8). A number of clones (both GNNK+ and GNNK-) were selected for analysis and all showed full length chi c-Kit inserts by restriction enzyme analysis. These clones were then sequenced with primers 1142 (verify GNNK status) and 2157 (check cytoplasmic domain for correction of mutation). One clone of each isoform of chimaeric c-Kit was then selected (clones chi 12+ F1 and chi 12- F1) and these were verified as correct by sequencing the full length of the cDNA insert in pBS SK+.

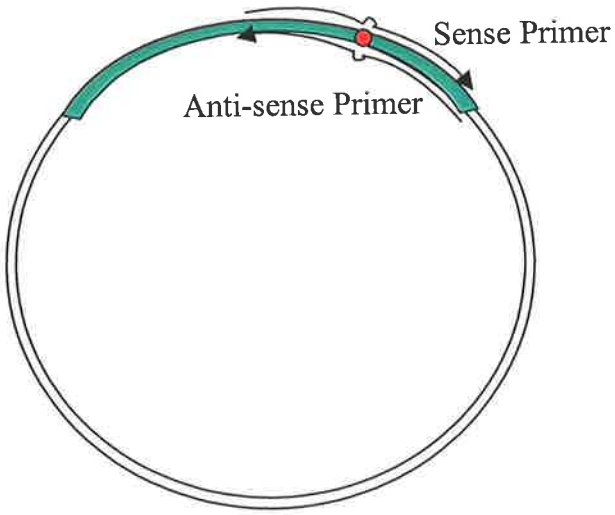

Step 1 Primers

GA Sense C TCC TAC CAG GTG GCC AAG **GCG** ATG GCG TTC CTC GCC TCC

GA Antisense GGA GGC GAG GAA CGC CAT **CGC** CTT GGC CAC CTG GTA GGA G

Step 2 Primers

ECDELSense GGA ACT GAG CAG AGA TGC **TCT** GCT TCT GTA CTG CCA GTG

ECDELAntisense CAC TGG CAG TAC AGA AGC **AGA** GCA TCT CTG CTC AGT TCC

Step 3 Primers

GNNK Sense GCC TAT TTT AAC TTT GCA TTT AAA GAG CAA ATC CAT CCC CAC

GNNK Antisense GTG GGG ATG GAT TTG CTC TTT AAA TGC AAA GTT AAA ATA GGC

Site of removal of GNNK sequence (GGT AAC AAC AAA)

Figure 2.6

Site directed PCR mutagenesis – schematic representation of strategy employed and primers used.

Step 1 - primers repair cytoplasmic domain mutation in cDNA
Step 2 - primers repair point deletion in extracellular domain of cDNA
Step 3 - primers are for excision of GNNK coding sequence to generate GNNK-cDNA

The restriction enzymes Bam H1 and Not 1 were used to excise the GNNK+ and GNNK- chimaeric c-Kit cDNAs from pBS-SK for ligation into pRUFpuro. pRUFpuro was digested with Bam H1 and Hpa 1 to create a directional ligation target. The chimaeric cDNAs in pBS-SK were digested with Not1, end filled with Klenow fragment to create a blunt end, and then digested with BamH1. The 3Kb insert was then ligated into pRUFpuro, and 2 clones were selected from each ligation after several diagnostic restriction enzyme digests. pRUFpuro chi 12+1 and pRUFpuro chi 12- 1 were both fully sequenced and verified as correct chimaeric c-Kit cDNAs.

2.7.15. Q-PCR

The ABI Prism 7700 Sequence Detection System (Perkin Elmer) uses fluorogenic probes to quantitate specific sequences using real time quantitative PCR. Target cells are lysed, RNA isolated using TRIzol (see 2.8.1), cDNA generated by reverse transcription, and quantitative real time PCR performed using primers flanking the target sequence in conjunction with specific fluorogenic probes to the target sequence.

Cells were sorted on the FACStar^{PLUS} (Becton Dickinson) using monoclonal antibodies as indicated in the relevant sections of Chapter 5. RNA from sorted cells was extracted as detailed in Section 2.8.1.

RT-PCR to generate cDNA was performed using Superscript II Rnase H- Reverse Transcriptase (Invitrogen Cat no. 18064-014) and random hexamer primers (Geneworks – Cat no. CS-104). Up to 1μg of RNA in 11μl DEPC treated water was placed into 1.5ml reaction tubes together with 1μl 250ng/ml random hexamer primers and heated to 70°C for 10 minutes, and then placed on ice to chill rapidly. To each

sample was added 4µl of 5X First Strand Buffer, 2µl 0.1M DTT, 1µl 10mM dNTPs mix and 1 µl Super Script II reverse transcriptase. This mix was incubated at room temperature for 10 minutes, 42°C for 50 minutes, and 70°C for 10 minutes. cDNA was then stored at -20°C until required for use.

To perform the quantitative PCR, the following reagents and master mix was prepared.

Two common primers were used in all QPCR reactions:

Forward Primer: CAA CGA TGT GGG CAA GAC TTC

Reverse Primer: CAT CAT GCC AGC TAC GAT TAC G

The isoform specific probes used were 6-FAM labelled probes with a minor groove binder motif, used to increase the Tm of the very short probes:

GNNK- c-Kit Probe: 6FAM–CATTTAAAGAGCAAATCC–MGBNFQ

GNNK+ c-Kit Probe: 6FAM–TAAAGGTAACAACAAAGAGCA–MGBNFQ

Universal Master Mix	12.5µl (Applied Biosystems, CA, Cat no. 4305719)
Forward Primer	0.2µM
Reverse Primer	0.2µM
TaqMan MGB Probe	0.1µM
Water	added to 22.5µl final

22.5µl of the above master mix was dispensed into reaction tubes and 2.5µl of target cDNA was then added. To generate standard curves, two specific target cDNAs were used. These were human c-Kit GNNK+ S+ or GNNK- S+ cDNAs in pRUFneo. These were diluted to have 10, 10^2, 10^3, 10^4, 10^5 and 10^6 copies per 2.5µl in water and were incorporated in every quantitative real time PCR run.

The reaction mixes were then loaded into the ABI 7700 thermal cycler and run under the following conditions:

50°C 2 minutes

95°C 10 minutes

then 40 cycles of

95°C 15 seconds

60°C 60 seconds.

To create a standard curve, an amplification threshold of 10x SD of baseline fluorescence is set and the cycle number to cross this threshold is recorded in order to generate a standard curve. The cycle number for unknown samples is then used to determine copy number for that sample of the target sequence.

2.7.16. Sequencing of DNA

The ABIPRISM Dye Terminator Cycle Sequencing Reaction Kit (Perkin Elmer) was used to sequence DNA purified using the QIAGEN midi kit. For a sequencing reaction, 8 µl of Terminator Ready Reaction Mix (A, G, C, T-Dye Terminator, dGTP, dATP, dCTP, dTTP, Tris-HCl, pH 9; $MgCl_2$, thermostable pyrophosphatase AmpliTaq polymerase) was added to 2 µg of template DNA and 3.2 pmol of

sequencing primer. The volume was made up to 20 µl with water. The reaction was performed in a thermal cycler programmed for 96°C for 10 secs, 50°C for 5 secs, 60°C for 4 mins (25 cycles), followed by a 4°C hold step. Following cycle sequencing the DNA was precipitated with 2 µl 3M sodium acetate (pH 4.6) and 50 µl 100% ethanol and incubated on ice for 10 minutes. The DNA was pelleted at 14000 g for 30 minutes at 4°C, washed with 250 µl 70% ethanol and air dried. The sequence was then determined using a Perkin Elmer automated sequencer.

2.7.17. *Calcium phosphate transfection into NIH3T3 cells*

One day prior to transfection, 6 cm dishes were each seeded with $5x10^4$ cells in DMEM supplemented with 10% FCS. In a 10 ml polystyrene tube, a 0.5 ml solution containing 20 µg DNA and 250 mM $CaCl_2$ was prepared. A second solution of equal volume was made in a 20 ml conical polystyrene tube and consisted of 250 mM NaCl, 1.5 mM $NaPO_4$ pH 7 and 50 mM HEPES pH 7.1). The DNA solution was added dropwise to the second solution while bubbling air through the second solution with a 1 ml pipette. The combined solution was incubated at room temperature for 30 minutes until a visible precipitate had formed. 500 µl of the precipitate was added dropwise to a duplicate set of dishes and cultures were incubated at 37°C. After 24 hours, medium was removed from dishes and 1 ml of 15% glycerol in DMEM was added and rocked gently every 30 seconds. After 4 minutes the glycerol/DMEM was removed and cells were gently washed with 5 ml DMEM. After the wash, DMEM containing 10% FCS was added and cells incubated overnight. The following day, cells were harvested and seeded into DMEM containing 10% FCS and geneticin or puromycin as required. Medium was changed twice weekly. Selection was maintained in the culture medium until all mock transfected cells died.

2.7.18. Retroviral infection of suspension cells by co-cultivation

pRUF (neo or puro) retroviral vectors contain a Multiple Cloning Site and rearranged *gag-pol* sequences from the M3Neo(myb) provirus (Rayner et al., 1994), but lack the *gag, env* and *pol* genes (critical for production of functional retrovirus particles) . In their place, cDNA of interest, together with a selectable marker (puromycin or neomycin resistance) are inserted. These genes are found between the two Long Terminal Repeats (LTRs) which are responsible for integrating the viral nucleic acid between them into the host cell genome. In order to produce infectious virus particles, the retroviral cDNA constructs must be transfected into a packaging cell line capable of supplying the missing viral components. Genetically modified cell lines such as Psi2 (Mann et al., 1983), when transfected with retroviral constructs including pRUFneo and pRUFpuro, will secrete retroviral particles into the culture supernatant capable of infecting murine target cells and integrating their "cargo" cDNA between the LTRs stably into the target cell genome. Using other packaging cell lines will alter the specificity of the retroviral particles for target cell type and/or species.

In the systems used in this thesis, semi-confluent monolayers of Psi2 transfectants carrying pRUFpuro c-Kit or pRUF CT3-Myb cDNAs were irradiated at 30 Grays (to block any further proliferation of the cells), harvested and seeded at $1x10^6$ in $25cm^2$ flasks. These cells adhere to the plastic, but do not proliferate. Non-adherent target cells to be transduced were added to these cultures at various densities depending on the cell line in a final volume of 5 ml. A separate "mock transduction" was set up at the same time (no Psi2 cells added). After 2 days co-cultivation, non-adherent cells were collected, washed and cultured in 5 ml DMEM with FCS, mu-GM-CSF and

1mg/ml geneticin or 2μg/ml puromycin (depending on retroviral construct used). Medium was changed twice weekly until all "mock" transduced cells had died.

2.8. Manipulation of RNA

For RNA procedures, materials were maintained RNase free, and gloves were always worn. Plasticware and autoclaved glassware were pretreated with 0.5 M NaOH to destroy any RNase contamination. All Milli-Q water used was treated with 0.1% v/v diethylpyrocarbonate (DEPC) (Sigma, Cat. No. D-5758) at 37°C overnight and autoclaved at 121°C to inactivate the DEPC. All other solutions used were prepared in 'RNase-free' plasticware or glassware. Aerosol barrier tips were used to prevent contamination.

2.8.1. Total RNA Extraction

Total RNA extraction was performed using TRIzol according to the manufacturer's instructions (GibcoBRL, Cat. No. 15596-026). Cells were harvested and washed in PBS. The supernatant was removed and 1 ml TRIzol reagent for up to 1.5 x 10^7 cells was added to the pellet and mixed by pipetting. The samples were left at room temperature for 5 minutes, before transferring them to microcentrifuge tubes and storing frozen at -70°C. For small cell numbers (<10^6), 200μl TRIzol was added irrespective of cell number.

To TRIzol samples that had been thawed to room temperature, 1/5 volume of chloroform was added and vigorously shaken before incubation for 3 minutes. Samples were centrifuged at 12000 g for 15 minutes at 4°C, which resulted in the presence of three phases, a lower red phase, a phenol-chloroform interphase and an

upper colourless aqueous phase containing RNA. The aqueous phase (approximately 50% of volume of TRIzol) was transferred to a fresh tube and the RNA was precipitated with an equal volume of isopropyl alcohol by incubation at room temperature for 10 minutes. The samples were centrifuged at 12000 g for 10 minutes at 4°C. The supernatant was removed and the pellet washed with 1 ml 75% ethanol. Samples were incubated at room temperature for 10 minutes then centrifuged for 5 minutes at 7500 g at 4°C. Pellets were air dried then dissolved in DEPC treated water to the desired volume.

2.8.2. *Quantitation of RNA*

Quantitation of RNA was performed using a spectrophotometer to measure absorbance at A_{260}. The concentration was determined on the assumption that an absorbance at 260 nm of 1 is equivalent to 40 µg/ml (1 cm light path) of RNA.

2.8.3. *Random Oligonucleotide Priming – probe generation*

Double strand DNA probes were labelled using the GIGAprime DNA Labelling Kit (Bresatec, Australia, Cat. No. GPK-1) according to the manufacturer's instructions. 50 - 100 ng of template DNA was made to 7 µl with sterile Milli-Q water and heated at 95°C for 5 minutes to denature the DNA, and then placed on ice to cool. To this was added 6 µl of decanucleotide solution, 6 µl of nucleotide/buffer cocktail, 50 µCi of α^{32}P-dATP (specific activity 3000 Ci/mM) (Bresatec, Cat. No. ADA-2) and 1 µl (5 U) of Klenow DNA polymerase. The solution was mixed and flicked down in a microfuge before incubation at 37°C for 15 minutes. The reaction was terminated by the addition of 1 µl of 0.5 M EDTA and the volume adjusted to 50 µl with sterile Milli-Q water. The probe was purified from the label using Microbio-spin 6

chromatography columns (Bio-Rad, Cat. No. 732-6221). Columns were inverted to resuspend the gel and the tip snapped off and placed in a 2 ml microcentrifuge tube with the top cap removed to allow flow. The column was centrifuged for 2 minutes at 1000 g and then placed in a clean tube. Samples were applied to the column and centrifuged at 1000 g for 4 minutes, to elute the purified labelled probe. The counts per minute of the DNA probe was determined by diluting 1 µl of the probe in 100 µl Milli-Q water and placing into a Bioscan QC-2000.

2.8.4. Northern Blot Transfer

RNA samples (10 µg) were dried in a heated speedvac and then resuspended in 12 µl of sample buffer (see 2.9.3) with 0.2 mg/ml ethidium bromide and mixed. RNA was denatured at 65°C for 5 minutes and then 1 µl of loading buffer (see 2.9.3) was added to the tubes. Samples were electrophoresed in a 1% agarose gel in formaldehyde running buffer (see 2.9.3). The gels were washed by rocking in DEPC treated water for 30 minutes and then ethidium bromide stained RNA contained in the gel was visualised using a FluorImager595 at an excitation wavelength of 488nm, using a 610 nm long pass filter for detection. This was performed to determine the quality of the RNA. The gel was then blotted onto Hybond N+ filters (Amersham, Cat. No. RPN303B) and the RNA transferred by capillary action in 10x SSC (see 2.9.3) overnight. The nylon membrane was rinsed in 2x SSC and allowed to air dry prior to cross-linking the RNA to the filter by exposure to UV light (0.4 J/cm2 in a Hybaid UV crosslinker).

Nylon membranes were placed in 2x SSC, rolled and placed in glass hybaid bottles. Prior to hybridisation with radiolabelled probes, filters were incubated at 68°C for 30

minutes in 10 ml of pre warmed Express Hyb solution (Clontech, Palo Alto, CA, 8015-1) Probes of a final activity of $5x10^6$ cpm/ml were denatured by incubation at 95°C for 10 minutes and then added to 3 ml ExpressHyb. This was added to the bottle containing the membrane and incubated for 1 hour at 68°C whilst rotating.

Filters were washed twice with 2x SSC containing 0.05% SDS with the final wash incubated for 30 minutes at room temperature, whilst rocking. Filters were then washed once in a more stringent solution (0.1x SSC with 0.1% SDS) at 50°C for 30 minutes while shaking. Filters were dried and wrapped in plastic wrap. Hybridisation signals were detected on phosphor storage screens, which were exposed overnight and analysed using a Molecular Dynamics PhosphorImager with ImageQuant™ software (Molecular Dynamics, Sunnyvale, CA). Hybridisation signals were quantified using the GAPDH signals as a loading control.

2.9. Reagents

2.9.1. Immunocytochemistry, Immunohistochemistry and Immunofluorescence Reagents

0.066 M Phosphate Buffer, pH 6.3

3.5 g KH_2PO_4 and 1.1 g Na_2HPO_4 was added to 500 ml of distilled water gradually while stirring. The solution was stored at 4°C.

0.066 M Phosphate Buffer, pH 7.4:

0.087 g KH_2PO_4 and 3.84 g Na_2HPO_4 was added to 500 ml of distilled water gradually while stirring. The solution was stored at 4°C.

APAAP substrate:

Prepared immediately before use. For 100ml: 20mg napthol AS-MX phosphate free acid (Sigma, St Louis, MO, Cat. No. N4875) was diluted to 10 mg/ml in dimethyl formamide. This solution along with 100 µl 1 M levamisole (Sigma, Cat. No. L-9756 diluted in water was added to 100ml 0.1M Tris – HCl pH8.2. 100mg of Fast Red TR salt (Sigma, Cat. No. F-1500) was added to solution and filtered with 3 M Whatman.

'Chloroacetate' esterase substrate solution:

5 mg naphthol-AS-D-chloroacetate (Sigma, Cat. No. N-0758) was diluted in 2.5 ml N-N dimethylformamide and then added to a fresh solution of 38 ml 0.066 M phosphate buffer pH 7.4 containing 20 mg Fast Blue (Sigma, Cat. No. F-0250). Solution was immediately filtered with 3 M Whatman.

Esterase Fixative:

100 mg Na_2HPO_4, 500 mg KH_2PO_4, 225 ml acetone and 125 ml formalin (40% formaldehyde in water) were added to 150 ml distilled water. The solution was stored at 4°C.

Facs Fix:

2% w/v D-glucose, 1% v/v 37 - 40% formaldehyde and 0.02% sodium azide in PBS and stored at 4°C.

Glycerol-glycine mountant:

1.4 g glycine dissolved in water and adjusted pH to 8.6 with NaOH. To 30 ml glycine buffer, added 70 ml glycerol.

'Non-specific' esterase substrate solution:

0.3 ml of pararosanaline solution was mixed with 0.3 ml of 4% sodium nitrite solution and allowed to stand for 1 minute. This was added to a freshly made solution of 30 ml 0.066 M phosphate buffer pH 6.3 containing 1 ml of 10 mg/ml α-naphthyl acetate

(Sigma, Cat. No. N-8505) in acetone. The final pH was adjusted to 6.1 with 5 M NaOH.

Pararosanaline:

0.2 g pararosanaline hydrochloride (Sigma, P-3750) was added to 10 ml of 20% v/v HCl in water and incubated at 56°C for 30 minutes in the dark. The solution was filtered (0.45μm) and stored in the dark at room temperature for no greater than 1 month.

Standard APAAP Fixative:

Acetone: methanol: formaldehyde (47.5:47.5:5 v/v). Solution was stored at 4°C.

Scott's gentle alkaline solution:

3.5 g $NaHCO_3$ and 20 g $MgSO_4.7H_2O$ was dissolved in 1 L water.

TBS (for APAAP):

1.5 M NaCl solution was buffered to pH 7.6 with 0.5 M Tris-HCl.

2.9.2. Reagents For Protein Analysis

0.5 M Activated Sodium Orthovanadate:

0.5 M solution made in Milli-Q water and the pH of the solution adjusted to 11.1 with 0.5 M HCl. Solution was heated, cooled to room temperature and adjusted to the original volume with Milli-Q water three times. The pH of the solution was then adjusted to 10.05, filtered (0.45 μm) and stored in aliquots at –20°C.

1% NP40 in TSE:

50 mM Tris, 150 mM NaCl, 1 mM EDTA was dissolved in water and solution adjusted to a pH of 8. NP40 was added (1% v/v final) and solution filtered (0.45 μm) and stored at 4°C.

10x TBS (for westerns):

199 mM Tris, 1.5 M NaCl dissolved in water, pH adjusted to 7.5 with 10 M HCl. For use, this stock was diluted to 1x in Milli-Q water.

Double Strength Reduced Loading Buffer:

125 mM Tris-HCl, pH6.8; 20% glycerol; 4% SDS; 10% β-mercaptoethanol; 0.0025% bromophenol blue.

SDS PAGE electrophoresis buffer:

25 mM Tris, 192 mM glycine, 0.1% SDS, should be pH 8.3 without further adjustment.

Lysis Buffer:

1% v/v NP40 with 5 mM sodium fluoride, 5 mM tetrasodium pyrophosphate, 5mM sodium vanadate, 1 mg/ml leupeptin, 1 mg/ml aprotinin, 1 mM phenylmethyl sulphonyl fluoride (PMSF) and Complete Protease Inhibitor Cocktail (Roche, Cat. No. 1836145)

Resolving Gel:

% gel	8	10
Acrylamide-bis (37.5:1)	8%	10%
Tris - HCl pH 8.8	0.4 M	0.4 M
SDS (in water)	0.1%	0.1%
Ammonium persulphate (in water)	0.1%	0.1%
TEMED	0.0006%	0.0004%
Made in water		

Stacking Gel:

Acrylamide-bis (37.5:1)	5%
Tris - HCl pH 6.8	125 mM
SDS (in water)	0.1%

Ammonium persulphate (in water)	0.1%
TEMED	0.001%

Made in water

Tris/Glycine/Methanol Transfer Buffer:

25 mM Tris, 192 mM glycine with 20% methanol in water.

2.9.3. *Molecular Biology Reagents*

ψ broth

2% w/v Bacto-tryptone (Difco, Sparks, MD), 0.5% w/v Bacto-yeast extract (Difco), 0.5% w/v $MgSO_4$, pH 7.6 in water.

2x YT:

2% w/v Bacto-tryptone (Difco), 1% Bacto-yeast extract (Difco), 1% NaCl in water.

50x TAE:

100 ml 0.5 M EDTA, pH 8 was mixed with 57.1 glacial acetic acid and made to 1 L with water, to which 242 g Tris was added and dissolved. Stock solution was diluted as required.

100x TE:

1 M Tris, 100 mM EDTA with pH of solution adjusted to 7.5 prior to the addition of EDTA.

Gel Loading Buffer:

0.25% bromophenol blue, 0.25% xylene cyanol FF, 30% glycerol in water.

Luria Agar plates:

1.5% w/v Bacto-agar in Luria Broth was autoclaved. Agar was cooled to ~ 55°C prior to the addition of 100 μg/ml ampicillin and then poured onto petri dishes. Plates were allowed to set and stored at 4°C.

Luria Broth medium:

1% Bacto-tryptone, 0.5% Bacto-yeast extract , 1% NaCl in water and pH adjusted to 7 - 7.2 and autoclaved.

RNA agarose gels (containing formaldehyde)

10 x Mops Buffer
200mM MOPS

10mM EDTA

50mM NaAc

made in DEPC water

** store at RT in the dark

1 x Running Buffer
1 x Mops Buffer

2.2M Formaldehyde 18% v/v

made in DEPC water

** store at RT

Sample Buffer
1 x Mops Buffer

50% Formamide

2.2M Formaldehyde 18% v/v

made in DEPC water

1% agarose gel with formaldehyde
Agarose (RNase free)

1 x Mops Buffer

made in DEPC water to 82% final volume

Heat to dissolve agarose, allow to cool to ≤ 60°C then add formaldehyde

2.2M Formaldehyde 18% v/v

SOC medium:

2% Bacto-tryptone, 0.5% Bacto-yeast extract, 10 mM NaCl and 2.5 mM KCl in water were autoclaved. When cool, 10mM $MgCl_2$, Mg SO_4 and 20 mM glucose were added and the medium filter sterilised through a 0.22 μm filter unit.

20x SSC Buffer

NaCl	3M
NaCitrate	0.3M

Final pH 7.0 (using 1M HCl)

TfbI buffer

KOAc	30mM
KCl	100mM
$CaCl_2$	10mM
$MnCl_2$	50mM
Glycerol	15%, v/v

Final pH 5.8 (using 0.2M Acetic Acid) and sterile filtered (0.22μm)

TfbII

MOPS	10mM
$CaCl_2$	75mM
KCl	10mM
Glycerol	15% v/v

Final pH 6.5 (using 0.5M KOH) and sterile filtered (0.22μm)

3 Transforming Potential of c-Kit - Effects of Copy Number and Isoform

INTRODUCTION

3.1. c-Kit receptor levels

As outlined in Chapter 1, binding of ligand to the extracellular domain of receptor tyrosine kinases induces their dimerisation resulting in activation of the intrinsic tyrosine kinase activity and transphosphorylation of the receptor subunits. Subsequent phosphorylation and association of downstream signalling molecules occurs leading to a biological response (Heldin, 1995; Ullrich et al., 1990; Yarden et al., 1988). Mutation and transduction of the genes encoding several RTKs by retroviruses has resulted in constitutive activation of the receptors and oncogenesis. An example discussed in Chapter 1 is v-kit in the Hardy-Zuckerman-4 strain of feline sarcoma virus (FeSV), which induced fibrosarcomas in cats (Besmer et al., 1986) as a result of several alterations compared with its normal cellular counterpart, c-Kit (Herbst et al., 1995a). Like c-Kit, genes encoding other RTKs, eg. c-fms and c-erbB which encode CSF-1R and the Epidermal Growth Factor receptors respectively (Type I RTKs), have counterparts in retroviral oncogenes (Yarden et al., 1987a).

Activating mutations of cellular genes encoding RTKs is not the only path leading to oncogenicity. Elevated expression levels of several "Wild Type" RTK have been implicated in the progression of human malignancies. There are several examples of the EGF receptor family being expressed at elevated levels in carcinomas (Kern et al., 1990; Liu et al., 1992; Paik et al., 1990; Slamon et al., 1987; Slamon et al., 1989), and overexpression of the HER-2/*neu* receptor in breast and ovarian cancers is associated with poor prognosis (Slamon et al., 1987; Slamon et al., 1989).

The potential role of overexpression of the HER-2/*neu* and the EGF receptors in carcinogenesis was demonstrated by their ability to induce transformation of NIH3T3 cells. Cells expressing low receptor levels did not display transformed behaviour, in contrast to those expressing high levels, which were also tumourigenic in nude mice (Di Fiore et al., 1987; Hudziak et al., 1987; Velu et al., 1987).

Similar results have been obtained with c-Kit, which is expressed on very early progenitor cells within the bone marrow. During haemopoiesis, the c-Kit receptor is lost as progenitor cells differentiate into more mature lineage committed cells with the exception of mast cells which retain very high levels of c-Kit expression (Galli et al., 1994; Irani et al., 1992; Mayrhofer et al., 1987). Patients with acute myeloid leukaemia (AML) accumulate blast cells within their bone marrow, which have been blocked in the differentiation process, frequently at a stage still retaining c-Kit expression. A sub-group of 25-30% of adult AML patients displayed high levels of surface c-Kit protein on their blast cells at presentation, as detected by the monoclonal antibody (Mab), YB5.B8. This high level c-Kit expression was correlated with resistance of the disease to chemotherapy and poor prognosis (Ashman et al., 1988).

3.2. Ectopic expression of c-Kit in the NIH3T3 model: Previous findings in this laboratory

Previous studies in this laboratory investigated the effects of murine c-Kit expression levels (GNNK - isoform) on its transforming potential in NIH3T3 and its tumourigenicity in nude mice (Caruana, 1996). The findings of that study are in this section.

3.2.1. Overexpression of c-Kit

Ectopic expression of murine c-Kit in NIH3T3 cells transformed them in anchorage independent assays. In the absence of ligand, cells expressing mu c-Kit displayed a plating efficiency of 27%, which increased to 40% with saturating doses of ligand (muSCF) (Caruana et al., 1998). These data clearly demonstrated the transforming potential of c-Kit when overexpressed in NIH3T3 cells. Addition of a ligand blocking Ab to mu c-Kit (ACK2) or Ab to muSCF (rabbit polyclonal Ab) significantly reduced exogenous muSCF induced colony formation but not "factor independent" colony formation (Caruana et al., 1998), suggesting that this activity is truly ligand independent activation of the receptor, as opposed to endogenous (autocrine) SCF stimulation. Experiments described later in this chapter demonstrate that factor independent transformation was indeed occurring.

3.2.2. Transformation potential of Human c-Kit isoforms

In the experimental work described above, much of the focus was on c-Kit expression levels, and the effects this had on transformation and tumourigenesis in the NIH3T3 model. Caruana extended this work using human c-Kit in the NIH3T3 model, this time evaluating the contributions made to transformation by each of the naturally occurring isoforms of c-Kit. Given the effects of receptor density demonstrated above for mu c-Kit, and also for human c-Kit (Caruana et al., 1998), extreme care was taken in the studies to control the receptor expression levels. The effects of c-Kit receptor density on NIH3T3 transformation was investigated using a series of clones expressing increasing levels of c-Kit mRNA and surface protein. These were analysed for their ability to induce anchorage independent growth in the presence of muSCF. Clones expressing less than $2.5x10^4$ receptors/cell were generally unable to

form colonies under these conditions. Intermediate levels of c-Kit expression resulted in colony growth which was generally enhanced as the surface expression increased up to about $8x10^4$ copies/cell, and a positive correlation existed between the level of c-Kit protein in these clones and colony number in the presence of muSCF (RS = 0.58; $p<0.01$ (Caruana et al., 1998)). Clones expressing the highest levels of c-Kit mRNA and among the highest levels of c-Kit protein in this study produced few colonies even in the presence of muSCF. This phenomenon is discussed later.

Two specific isoforms of human c-Kit (GNNK+S+ and GNNK-S+) were examined. These pools were generated by Caruana as described below: cDNAs for GNNK+S+ and GNNK-S+ c-Kit were subcloned into the retroviral vector pRufMC1neo (Rayner et al., 1994), packaged in Psi2 cells, and viral supernatants were used to infect early passage NIH3T3 cells. G418-selected cells were screened for expression of c-Kit by indirect immunofluorescence using monoclonal antibody (Mab) 1DC3 (data not shown). Analysis of mRNA showed similar levels of transcript of the predicted sizes (Figure 3.3 A). That the correct isoforms were expressed was confirmed in each case by PCR analysis (Figure 3.3 B). Despite numerous attempts, Caruana was never able to obtain surface expression of the GNNK-S- isoform of c-Kit in any cell model system even though mRNA expression was demonstrated (Figure 3.3 A). Therefore, the GNNK isoforms were compared on the S+ background.

Caruana generated pools of cells comprising the top 10%, 5% and 2% of each population of infectants by sequential fluorescence activated cell sorting (FACS). These pools were expanded and, after checking their expression of c-Kit, were cryopreserved. All experiments performed by Caruana or for this thesis were

performed on cells expanded for no more than two weeks from these frozen stocks, ensuring the oligoclonality and consistency of the cell populations.

The c-Kit-expressing cell populations described above were assayed for their ability to grow in an anchorage-independent fashion (colony formation in soft agar), and for the loss of contact inhibition (focus formation) in the presence/absence of saturating doses of SCF. Early passage NIH3T3 cells expressing murine GNNK- c-Kit (as previously described (Caruana et al., 1998)) were included for comparison. Anchorage independent growth was observed in cells expressing both isoforms, and the yield of colonies was lower at high levels of expression. This supported the data generated using inducible vectors expressing human c-Kit described earlier (Caruana et al., 1998).

When cell populations were assayed for a loss of contact inhibition, the GNNK- isoform was much more efficient at induction of focus formation. This formation was substantially SCF-dependent at lower receptor levels. In contrast to the results of the colony assay, increasing focus formation was observed with increasing receptor levels for both isoforms. Consistent with the loss of contact inhibition, cells expressing GNNK- or, to a lesser extent, GNNK+ c-Kit grew to a higher density than cells infected with empty vector (Caruana et al., 1998).

In summary, Caruana had successfully generated a series of cell lines expressing murine and human c-Kit, and had characterised some of the cellular responses to SCF. In this thesis, the cellular responses in these cell lines were further characterised, and the processes involved were studied at the biochemical level.

RESULTS

3.3. Ectopic expression of Murine c-Kit in NIH3T3 Model

3.3.1. Quantitation of mu c-Kit surface expression

In experiments investigating the effect of receptor levels on transformation of NIH3T3 cells, Caruana (Caruana, 1996) characterised relative c-Kit expression based on Mab binding and flow cytometry. To determine the absolute surface expression of mu c-Kit, a saturation binding assay was performed. The average number of mu SCF receptors per cell, as determined by Scatchard Analysis of the saturation binding data (see section 2.5), was 2.3×10^4 receptors per cell with a binding affinity of 1.43×10^{-9}M (Figure 3.1). This analysis was used to assign copy number to all clones and pools analysed in this study, comparing relative Mean Fluorescence Intensity of tested pools and clones with the standard pool analysed here.

3.3.2. Autocrine stimulation

A possible mechanism for factor independent colony formation as seen by Caruana was autocrine stimulation of the ectopically expressed mu c-Kit. To address this question, Caruana expressed mu c-Kit in *Sl/Sl* –3T3 cells (Fujita et al., 1989) (murine fibroblasts lacking any functional mu SCF genes). However, the parental cells proved resistant to transformation by mu c-Kit, even in excess mu SCF (data not shown) (Caruana, 1996).

To address this question, anti-sense mu SCF constructs were generated and introduced into the mu c-Kit NIH3T3 pools as described in Section 2.7.11. Briefly, a 630bp

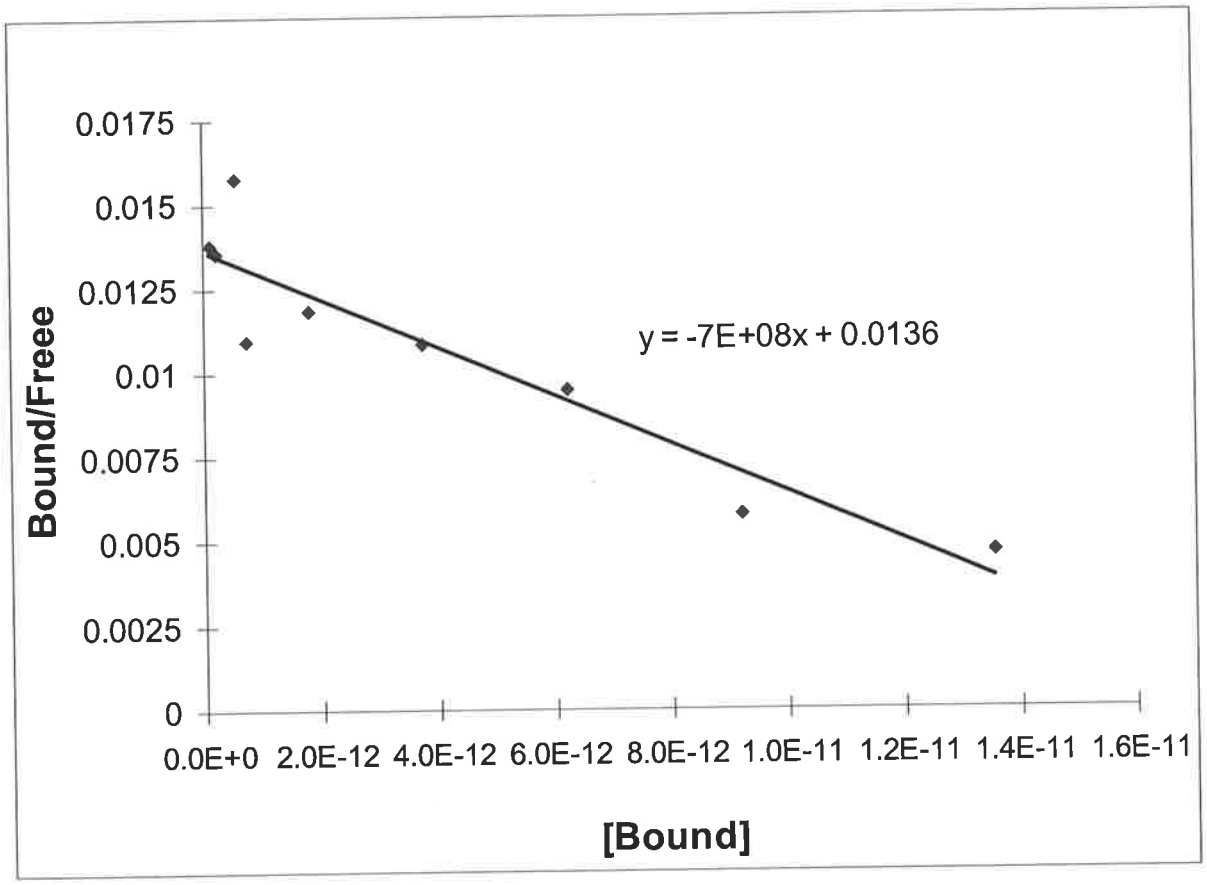

Figure 3.1

Saturation Binding Analysis of I^{125} labelled muSCF on NIH3T3 pool cells expressing mu c-Kit.

Saturation binding studies and Scatchard analyses were performed as described in section 2.5. Binding affinity (Kd) of muSCF for mu c-Kit on this standard pool was determined from the slope of the illustrated line to be 1430pM. Copy no. was determined from the B_{max} of 1.94×10^{-11} M, which represents 23400 copies per cell in this analysis.

This pool of cells was used as a reference in indirect immunofluorescence analysis to assign copy number for mu c-Kit to the various other pools analysed the study.

fragment incorporating the 5' 420 bases of the coding region of murine SCF (Anderson et al., 1990) was ligated into the pCXN2 expression vector (Niwa et al., 1991). Several clones were isolated, and the two selected for these experiments were (sense) pCXNC8 and (anti-sense) pCXNC12. In order to select cells expressing these new sense and antisense SCF constructs, the NIH(muKit) cells were cotransfected with excess pCXNC8 or pCXNC12 and limiting pRUFpuro and cotransfectants were selected for Puromycin resistance.

The two resultant NIH muKit pools expressing sense and anti sense muSCF were evaluated for colony formation in the presence or absence of muSCF. Results from a representative experiment are shown in Table 3.1, and clearly demonstrate that removal of endogenous muSCF had no effect on muSCF independent colony formation.

It was important to verify expression of anti-sense SCF transcript. To do this, northern blot analysis was performed as described in Section 2.8 on the Puromycin-resistant pools of pCNXC12 and pCXNC8 expressing cells. The probe chosen for the Northern Blot was the same 630bp SCF fragment used to generate the sense and anti-sense constructs. Figure 3.2 clearly shows very weak, but detectable endogenous muSCF transcript in all pools of cells. The approx 420bp transcript of the sense/antisense constructs is clearly visible in the each pool expressing the sense or antisense constructs, confirming the successful transcription of these constructs in the target cell pools.

Table 3.1: Effects of anti-sense mSCF on colony formation

cell line	SCF	construct		
		none	SCF α-sense	SCF sense
		colony no./10^4 cells		
NIH(*neo*)	-	0.0 ± 0.0	1.0 ± 0.5	0.5 ± 0.3
	+	0.0 ± 0.0	3.0 ± 1.0	0.8 ± 0.6
NIH(mu*kit*) pool	-	20.5 ± 8.1	130 ± 10	46 ± 22
	+	758 ± 15	964 ± 294	1404 ± 33

NIH muKit pools of cells expressing pCXNC8 (sense muSCF) or pCXNC12 (anti sense muSCF) were generated as described in Section 2.7.11. 10^4 cells plated in 0.33% soft agar in the absence or presence of 100ng/ml mSCF and colonies scored on day 14. Colony number presented as the mean ± S.E.M. of quadruplicate cultures.

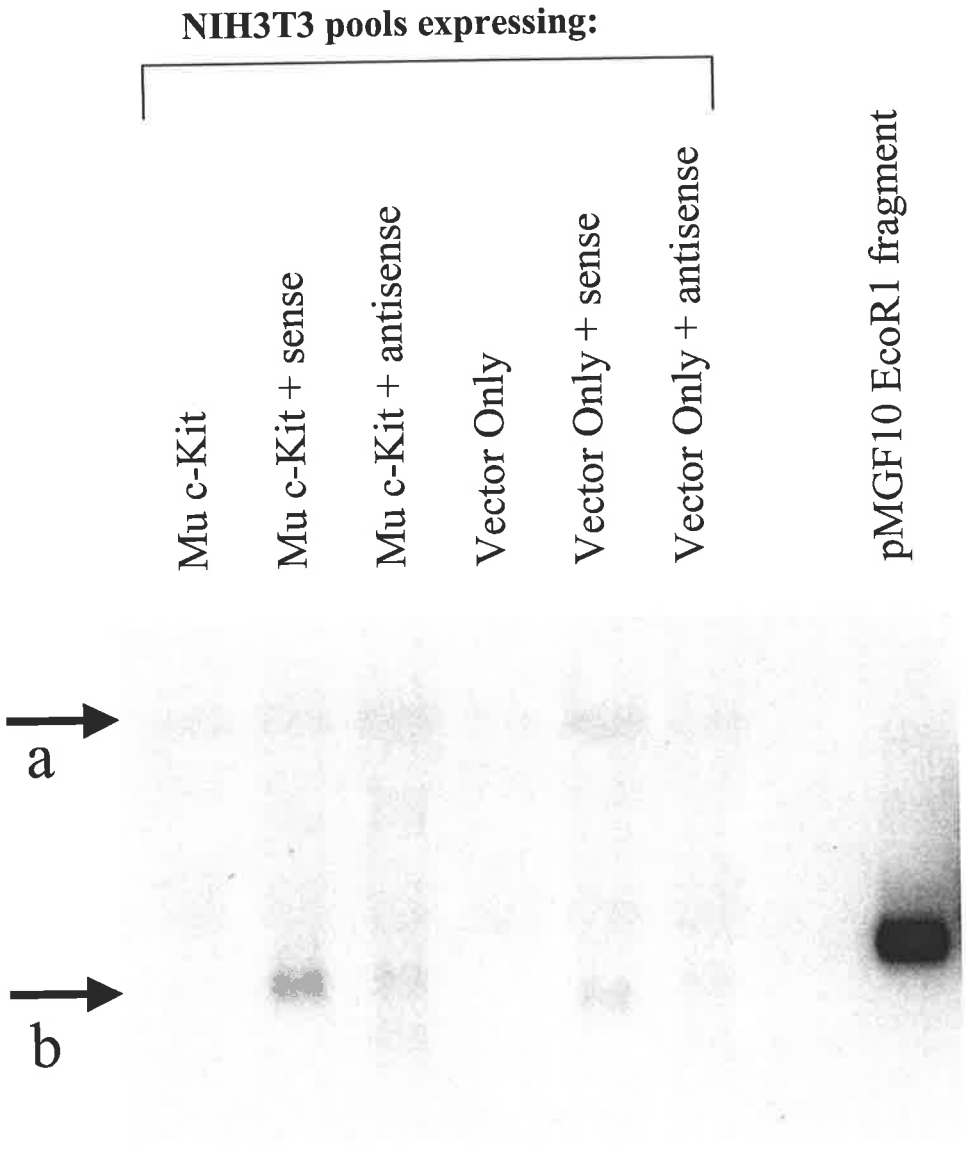

Figure 3.2

Northern Blot Analysis to verify expression of sense and antisense muSCF constructs in NIH3T3 cells expressing mu c-Kit or vector only (pZenNeo).

15µg of each RNA together with 10ng pBSSKMGF10.1 vector DNA cut with EcoR1 (as a positive control) was loaded onto the gel for the Northern Blot analysis and this was electrophoresed and blotted as per section 2.9.

(a) indicates endogenous muSCF transcript detected in NIH3T3 cells. A second transcript (b) was detected only in cells transfected with sense or anti sense constructs. The 630bp EcoR1 fragment from pBSSKMGF10.1 is clearly detectable in the right hand lane.

The probe was the same 630bp fragment from pBSSKMGF10.1 labelled as detailed in Section 2.8.3

To evaluate the efficacy of the anti-sense construct in reducing endogenous muSCF levels, NIH muKit pools cells expressing sense and anti sense muSCF were analysed by quantitative confocal microscopy. Due to the extremely low levels of muSCF expression in these cells (as evidenced by the low abundance of mRNA demonstrated in Figure 3.2 above) extremely high gains were needed to visualise the signals from the anti-muSCF antibody, generating very high background fluorescence values when scoring pixels for each cell. Despite this, as seen in Table 3.2, endogenous SCF could be visualised and quantitated, and this was reduced to background levels (equivalent fluorescence to negative control Ab) when the antisense construct was expressed in the cells. Clearly, antisense muSCF, in this series of experiments was successful in substantially eliminating endogenous muSCF expression. It did not, however, eliminate exogenous ligand independent colony formation.

3.3.3. *Human c-Kit Isoforms*

As discussed in Chapter 1, different isoforms of c-Kit exist as a result of alternate mRNA splicing events. In the murine system, two isoforms are known and differ only in the inclusion/exclusion of four amino acids, GNNK, in the juxtamembrane region of the extracellular domain (Hayashi et al., 1991; Reith et al., 1991). These variants arise due to the use of alternative 5' splice donor sites at the exon/intron junction of exon 9 (Hayashi et al., 1991) and they appear to be co-expressed in a variety of tissues (Reith et al., 1991). The GNNK+/- variants also exist in human c-Kit with the GNNK- form being more abundant (Crosier et al., 1993). A second site of alternate splicing is at the 3' end of exon 15 (Crosier et al., 1993), resulting in the presence/absence of 3 bp (encoding a serine in the interkinase domain). These

Table 3.2: Effects of anti-sense mSCF on SCF expression

cell line	Antibody	construct		
		none	SCF α-sense	SCF sense
		fluorescence units/cell [$]		
NIH (mu*kit*) pool	NRS	22.05±0.06	22.15±0.08	22.50±0.07
	α-muSCF	25.52±0.17	22.65±0.10	24.15±0.11

[$] 3×10^4 cells cultured on chamber slides were fixed, permeabilised and stained with either Rabbit α-SCF or NRS. Bound Rabbit Ig was detected with biotinylated donkey α-Rabbit Ig/Streptavidin-Tricolor. Immunofluorescence was visualised and quantitated by Confocal microscopy. Total Fluorescence Intensity of individual cells (n=50) ± SEM is shown. NIH (mukit) pool cells and pool cells expressing α-sense SCF were not significantly different when stained with control antiserum (NRS) in background fluorescence (P=0.14 - one tailed Students t-Test), but were significantly different when stained with α-muSCF (P< 0.0001). The pool expressing α-sense SCF showed an 85% reduction in levels of SCF compared to the parent pool after correction for background fluorescence. Pool cells expressing α-sense SCF also differed significantly from pool cells expressing sense SCF (P< 0.0001).

isoforms were confirmed in other studies (Furitsu et al., 1993; Piao et al., 1994; Zhu et al., 1994).

Little was known about whether functional differences exist between the isoforms. When transiently expressed in COS cells, GNNK-, but not GNNK+, murine c-Kit displayed some constitutive tyrosine phosphorylation and association with PI3-K (Reith et al., 1991). However these isoforms had similar ability to restore survival, proliferation and adhesion responses muSCF in W*sh* mast cells (Serve et al., 1995).

In this section of the study, all NIH3T3 pools used were generated previously by Caruana (see section 3.2.2).

3.3.4. *Establishment of c-Kit copy number on cell pools*

It was critical to establish a reliable copy number for human c-Kit in these studies. Indirect immunofluorescence analysis on 4 standard pools of cells showed low levels of surface expression for all isoforms except GNNK-S- (see Figure 3.3C). The GNNK+S+ and GNNK-S+ pools were subjected to saturation binding and Scatchard Analysis using ^{125}I- huSCF (see section 2.5). Copy number for all pools analysed were derived from these standard pools of cells by direct comparison of mean fluorescence intensity using indirect immunofluorescence using the same Mab. Mean copy numbers for the different populations of pools are included in Table 3.3 and were in the range 6.8 - 46 x 10^3/cell.

Figure 3.3

A and B:
Expression of c-Kit isoforms in NIH3T3 pools.

A:
poly A+ c-Kit mRNA was extracted from pools of NIH3T3 cells expressing each of the 4 isoforms of human c-Kit. 2μg was loaded onto each track and subjected to agarose gel electrophoresis and Northern blotting with full-length GNNK+S+ cDNA probe and a 780bp GAPDH probe. The 6.3 and 5.1 kb fragments are the predicted size for transcripts generated from the vector pRUFMC1neo containing c-Kit cDNA (3kb).

This data was generated by Gina Caruana and is presented to illustrate the successful expression of each isoform's cDNA cloned in pRUFMC1neo in NIH3T3 pools.

B:
Confirmation of the GNNK± status of each pool was done by reverse transcription from 200 ng of poly A+ selected mRNA used above in A) using the protocol described by the manufacturers of the First-Strand cDNA Synthesis Kit (Pharmacia). 2nd strand cDNA products were generated by PCR using primers flanking the 12bp region (GNNK) in the juxtamembrane region of c-Kit. These products were run on a 4% agarose gel and visualised with Ethidium Bromide.

These data were generated by Caruana, 1996.

* pools used in subsequent experimentation

C:
Indirect Immunofluorescence on NIH3T3 cells for human c-Kit

NIH3T3 cells expressing each isoform of c-Kit were analysed by indirect immunofluorescence with Mab 1DC3 (anti c-Kit) ····· or isotype matched negative control Mab ——— to assess relative surface expression of each isoform of c-Kit. Fixed cells were analysed on a Coulter Profile II Flow Cytometer.

A

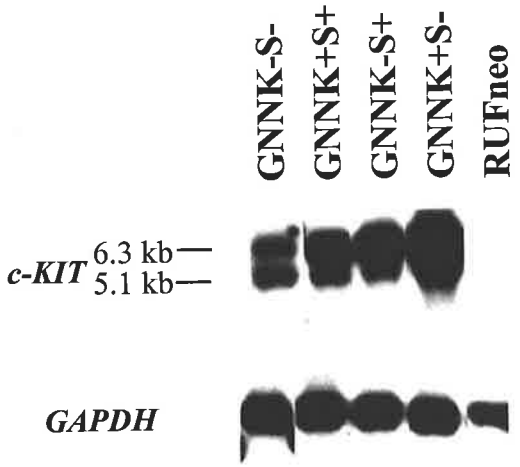
GNNK-S-
GNNK+S+
GNNK-S+
GNNK+S-
RUFneo
c-KIT 6.3 kb
5.1 kb
GAPDH

B

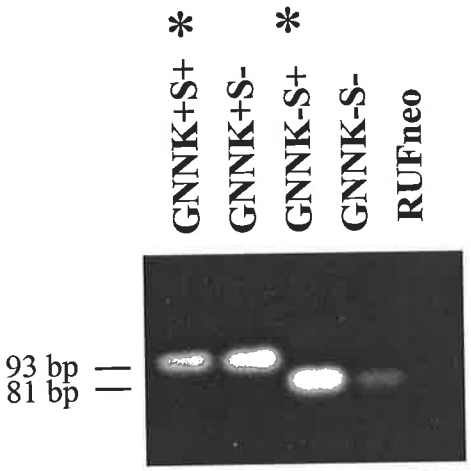
*
*
GNNK+S+
GNNK+S-
GNNK-S+
GNNK-S-
RUFneo
93 bp
81 bp

C

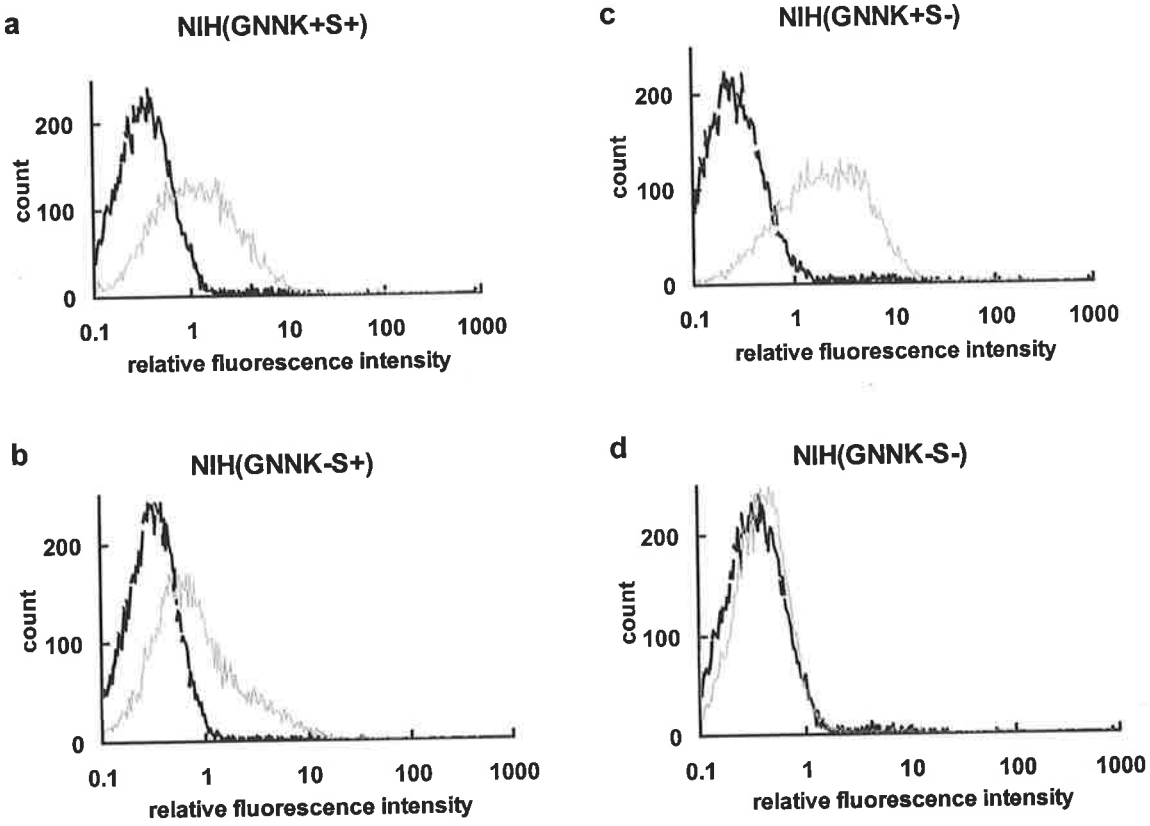
a
NIH(GNNK+S+)
c
NIH(GNNK+S-)
b
NIH(GNNK-S+)
d
NIH(GNNK-S-)
count
200
100
0
0.1
1
10
100
1000
relative fluorescence intensity

Table 3.3: Properties of the NIH3T3 cell lines expressing the c-KIT isoforms

NIH3T3 infectant	receptor no. x 10^3*	Colonies/ per 10^4 cells plated*		Foci/ $5x10^4$ cells plated*		no. of tumours/ no. of injections**
		-SLF	+SLF	-SLF	+SLF	
RUFMC1neo	<1	7.25 ± 1.8	6.75 ± 1.5	0	0	0/6
(GNNK+) -A	10.7	82.00 ± 5.7	97.75 ± 6.3	0	7	0/6
(GNNK+) -B	23.0	40.50 ± 2.9	49.75 ± 2.2	nd	nd	nd
(GNNK+) -C	38.1	17.25 ± 2.9	35.75 ± 5.4	7	49	nd
(GNNK-) -A	6.8	57.70 ± 3.8	77.50 ± 7.2	17	144	nd
(GNNK-) -B	9.2	13.25 ± 2.3	17.75 ± 1.9	15	137	4/6
(GNNK-) -C	45.8	7.00 ± 1.2	36.00 ± 4.0	115	>200	nd
Zen(neo)	0.0[$]	0.00 ± 0.0	0.00 ± 0.0	0	0	0/6[$]
Zen(mukit)	23.0[$]	12.75 ± 1.9	204.30 ± 25.2	0	dense monolayer	5/6[$]

$ Data from Caruana et al, 1998

* Data as published in Caruana et al, 1999

** Tumourigenesis data completed by Tony Cambareri.

Shaded area – data of Caruana, 1996

3.3.5. *Affinity of isoforms of human c-Kit for SCF*

Saturation binding of ^{125}I-SCF and Scatchard analysis was also used to determine the relative affinity of the 2 isoforms of c-Kit for SCF. Results of 5-7 separate experiments on each isoform, carried out using NIH3T3 cells (n=2), PC12 cells (n=2-4) and FDCP1 cells (n=1) are summarised in Figure 3.4, and show that there was no significant difference in dissociation constant (Kd=57±13 pM and 87±26 pM for the GNNK+ and GNNK- isoforms respectively) for SCF. This clearly demonstrates that any differences in signal output from these isoforms is not as a result of variations in affinity for ligand.

3.3.6. *Transformation of NIH3T3 cells expressing c-Kit isoforms*

As already summarised in 3.2.2, Caruana demonstrated differences between the isoforms in terms of anchorage independent growth and contact inhibition. To further the analysis, NIH3T3 cells expressing comparable levels of human c-Kit protein for each isoform were tested for their ability to give rise to tumours in nude mice. To assess this, 8 x 10^6 low passage cells were injected subcutaneously into the hind flank of nude mice. Only cells expressing the GNNK- isoform were tumourigenic *in vivo* with a latency period of approximately 42 days (Table 3.3). As previously reported (Caruana et al., 1998), NIH3T3 cells expressing murine GNNK- c-Kit also induced tumours, in this case with an average latency of 50 days.

Figure 3.4

Saturation binding analysis of the affinity of GNNK± c-Kit isoforms

Representative Scatchard plots for both GNNK+ and GNNK- c-Kit expressed in NIH3T3 pools are shown in the top 2 panels. Analysis was performed on NIH3T3 pools (n = 2), PC12 pools (n = 2-4) (PC12 analyses were done collaboratively with Sonia Young), and FDCP1 pools (n = 1) as detailed in Section 2.5. A summary of the affinity (Kd) of c-Kit isoforms for SCF is shown in the bottom panel bar graph as the mean ± s.e.m.

GNNK+ c-Kit has a Kd of 57 ± 13pM and GNNK- c-Kit has a Kd of 87 ± 26pM. There was no significant difference in the affinity of the 2 isoforms (two-tailed t-test, $P > 0.1$).

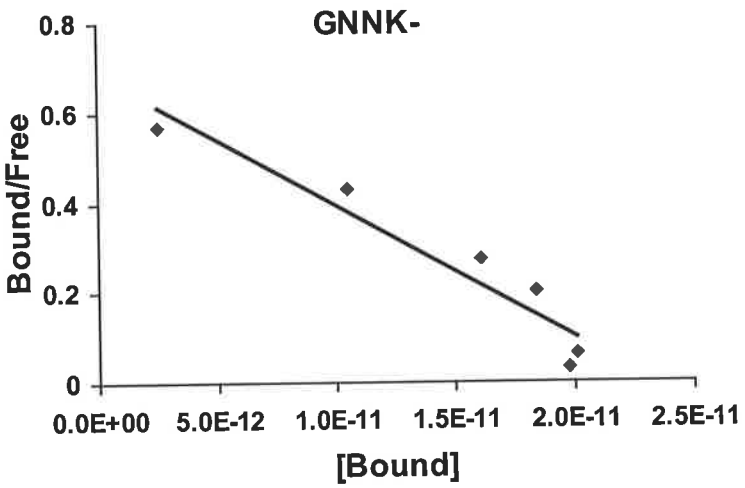
GNNK-
0.8
0.6
0.4
0.2
0
Bound/Free
0.0E+00
5.0E-12
1.0E-11
1.5E-11
2.0E-11
2.5E-11
[Bound]

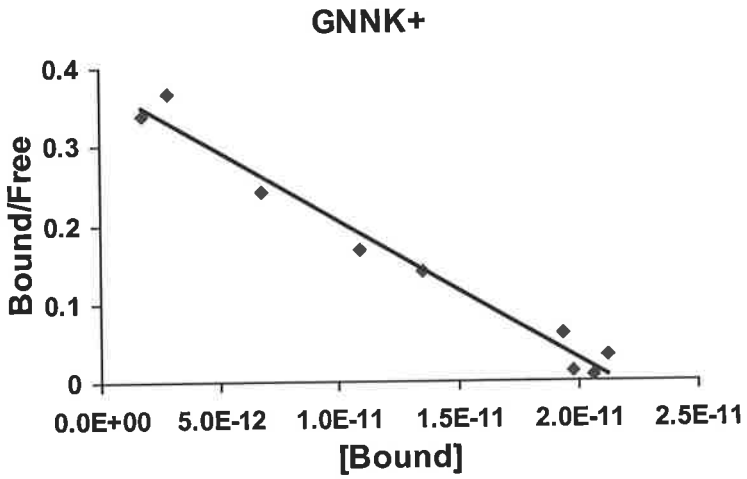
GNNK+
0.4
0.3
0.2
0.1
0
Bound/Free
0.0E+00
5.0E-12
1.0E-11
1.5E-11
2.0E-11
2.5E-11
[Bound]

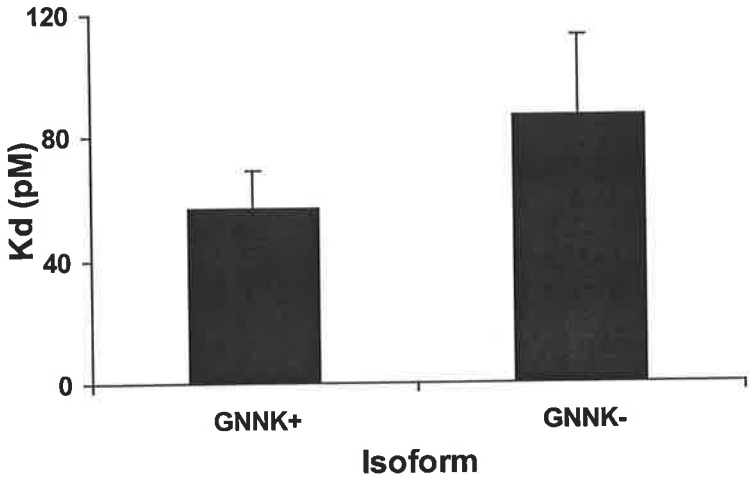
120
80
40
0
Kd (pM)
GNNK+
GNNK-
Isoform

Template cDNAs for Chimaeric c-Kit generation

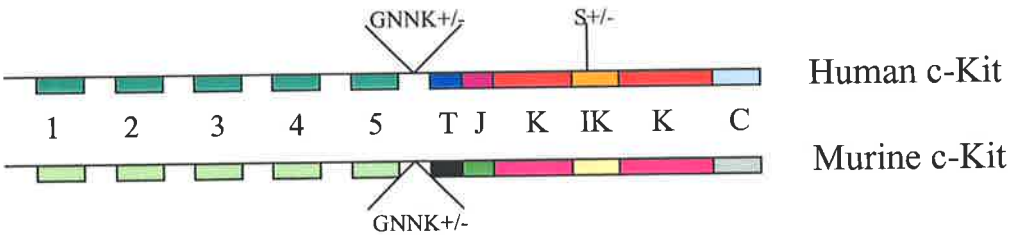

Legend

1-5 - Extracellular Ig Like Domains
T - Transmembrane Domain
J - Juxtamembrane Domain
K - Kinase
IK - Interkinase Domain
C - c Terminal

Primers for Chimaeric c-Kit generation

A1 - BCXHUKITFWD 39mer

CGC GGA TCC ATC GAT CTC GAG GCT ACC GCG ATG AGA GGC
Bam H1 Cla I Xho I Kozac Start

B1 – HUKITAS1 35mer

AG CAG CGG CGT GAA CAG GGT GTG GGG ATG GAT TTG
Murine TM seq Human

A2 - XNXMUKITRV 41mer

CT AGT CTA GAG CGG CCG CTC GAG TCA GGC ATC TTC GTG CAC
Xba I Not I Xho I Stop

B2 – MUKITS1 35mer

AA ATC CAT CCC CAC ACC CTG TTC ACG CCG CTG CTC
Human Murine TM seq

3.4. Biochemical analysis of human c-Kit isoforms signalling

3.4.1. Kinetics of activation of c-Kit isoforms, recruitment of p85 subunit of PI3-K

To begin to address the biochemical basis for the distinct transforming effects of c-Kit isoforms, the kinetics of receptor tyrosine phosphorylation and down-regulation in response to SCF were closely examined. Since the different isoforms were shown to have similar affinity for SCF, a single, saturating dose of 100 ng/ml SCF was used in these experiments. Cells expressing comparable levels (approximately 10^4 copies/cell) of each isoform were cultured to approximately 70% confluence, then starved of serum for three hours prior to pulsing with saturating levels of SCF. After the indicated times, cells were chilled on ice and lysed *in situ* with ice-cold lysis solution as described in Section 2.6. Lysates containing comparable amounts of protein were subjected to immunoprecipitation with the anti-c-Kit Mab, KIT4 (IgG2a), followed by polyacrylamide gel electrophoresis (PAGE) under reducing conditions and western blotting. Parallel blots were probed with Mab to phosphotyrosine (4G10 and PY20) or c-Kit (1C1), and quantitative analysis of blots was performed using Enhanced Chemifluorescence substrate and a FluorImager595 as described in Section 2.6.

Co-immunoprecipitation of PI3-K, which is the dominant downstream effector molecule that associates with c-Kit (Herbst et al., 1995b; Lev et al., 1991; Reith et al., 1991), was detected by probing western blots of c-Kit immunoprecipitations with antibody to the p85 subunit. To standardise quantitation of immunoblots, enabling comparison of data from different experiments, standard aliquots of NP40 lysates of

starved and SCF-pulsed MO7e cells were subjected to immunoprecipitation and analysis in parallel with NIH3T3 infectants. Results of typical blots and data derived by quantitation using ImageQuant™ software are shown in Figure 3.5.

Under the conditions used in this study, a very low level of receptor phosphorylation, and some association with p85, was seen in the absence of SCF. The presence or absence of GNNK had a substantial effect on the kinetics and extent of receptor phosphorylation, with the GNNK+ isoform displaying lower, but more sustained levels of tyrosine phosphorylation. In five independent experiments, the mean ratio of the phosphotyrosine to c-Kit signals at the peak response was 5.7±1.6 for the GNNK- isoform compared with 0.82±0.44 for GNNK+. Furthermore, receptor phosphorylation peaked earlier for the GNNK- isoform (median 2.5 min; range 2-3 min post stimulation) than the GNNK+ isoform (median 7.5 min; range 2.5-10 min).

In contrast, the maximum level of p85 recruitment to the two isoforms was similar (Figure 3.5). Probing blots for c-Kit protein indicated that the GNNK- isoform was more rapidly down-regulated, accounting for the loss of associated p85 and phosphotyrosine at later time points.

3.4.2. *Internalisation of c-Kit following SCF stimulation*

The apparent down-regulation of GNNK- c-Kit protein shown in Figure 3.5 could arise from degradation (for example cleavage of the extracellular domain (Brizzi et al., 1994; Yee et al., 1993)) or from internalisation, cytoskeletal association and incomplete solubilisation in NP40 detergent. Confocal microscopy was used on permeabilised and non-permeabilised cell monolayers to monitor SCF-induced

Figure 3.5

Time course analysis of SCF stimulated NIH3T3 cells expressing GNNK+ and GNNK- c-Kit – c-Kit tyrosine phosphorylation and PI3K p85 subunit recruitment.

Cells serum starved for 2 hours were stimulated with 100ng/ml SCF for the times indicated and lysed *in situ* as per Section 2.6. Lysates containing equivalent amounts of protein were immunoprecipitated with Mab Kit4 (anti c-Kit (IgG2a)) and Protein-A Sepharose. Sepharose pellets were loaded onto SDS-PAGE under reducing conditions, electrophoretically transferred to PVDF membrane and immunoblotted for Phosphotyrosine (4G10 and PY20), c-Kit (1C1) or anti PI3-K p85 (See Section 2.6). Blots were visualised using alkaline phosphatase conjugated secondary antibodies followed by development with ECF (enhanced chemifluorescence) substrate (Amersham) and scanned on a Fluorimager595 (Amersham).

On all gels, a standard c-Kit immunoprecipitate of MO7e cells stimulated for 2 minutes with SCF (M+) was loaded and used as the reference point for comparison analysis across gels. All bands were quantitated using ImageQuant™ software (Amersham) and displayed as relative percent of MO7e control. This information is displayed in the bottom panel of graphs.

Legend:

□ GNNK- c-Kit
■ GNNK+ c-Kit
A c-Kit Tyrosine phosphorylation
B c-Kit protein immunoprecipitated from cells in lysates
C PI3-K p85 subunit co-immunopreciptation

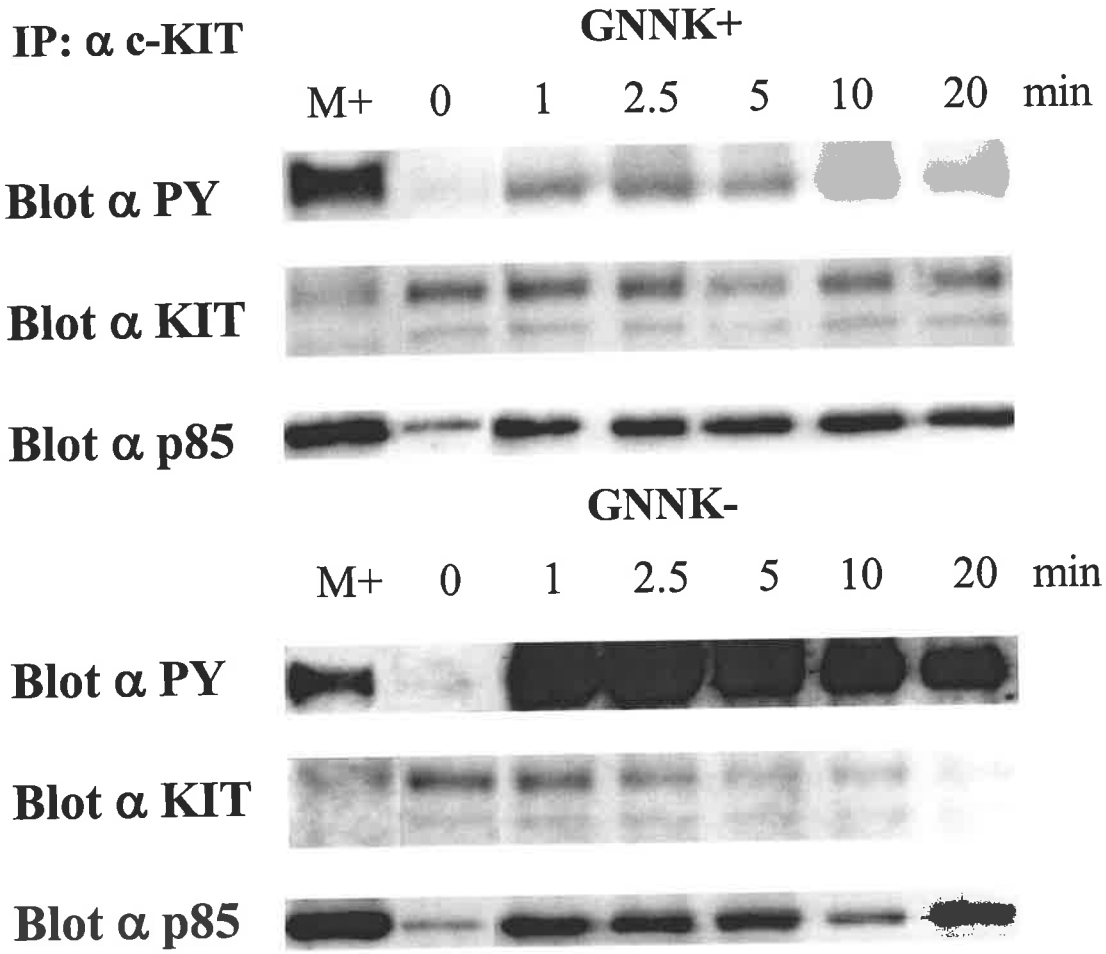
IP: α c-KIT
GNNK+
M+ 0 1 2.5 5 10 20 min
Blot α PY
Blot α KIT
Blot α p85
GNNK-
M+ 0 1 2.5 5 10 20 min
Blot α PY
Blot α KIT
Blot α p85

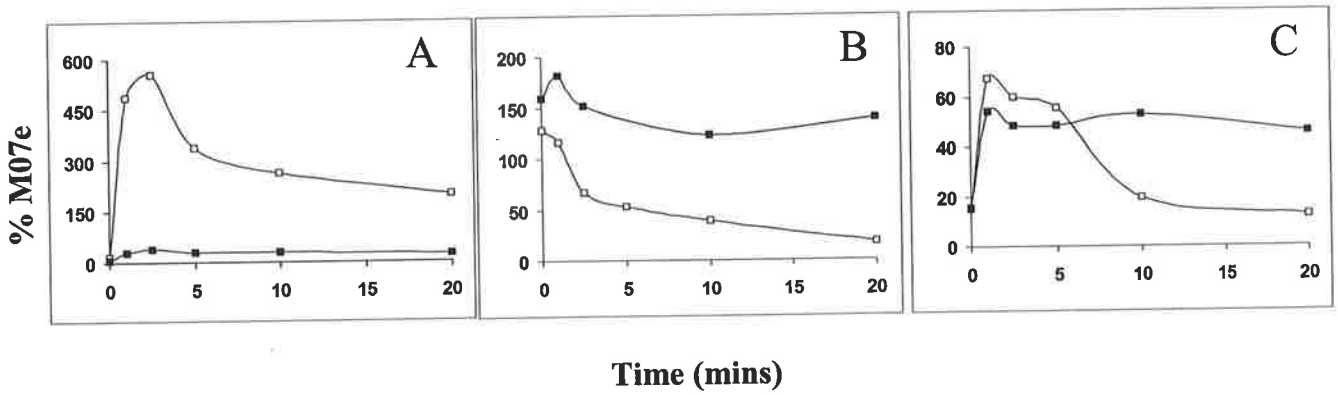
% M07e
A
B
C
600
450
300
150
0
200
150
100
50
80
60
40
20
0 5 10 15 20
Time (mins)

internalisation of the receptor. As illustrated in Figure 3.6, GNNK- c-Kit was completely lost from the cell surface within 10 min of SCF stimulation, while the GNNK+ isoform was still evident at 20 min. Experiments on permeabilised cells indicated that loss of the receptor from the surface was substantially due to endocytosis. Some intracellular c-Kit, possibly newly synthesised, was seen in unstimulated cells expressing both isoforms, although there was a hint of GNNK- c-Kit in endocytic vesicles as indicated by punctate staining. Following SCF stimulation, substantial internalisation of GNNK- isoform could be seen as early as 3 minutes, whereas a comparable level endocytosis of GNNK+ required at least 10 min (Figure 3.7).

3.4.3. *Downstream signalling from c-Kit isoforms*

As shown in Figure 3.5, PI3-K was recruited to a similar extent to both receptor isoforms. As a measure of PI3-K activation, phosphorylation of a known major target, c-Akt in NP40 lysates was examined by western blotting with antibodies specific for the phosphorylated form. Both c-Kit isoforms were capable of activating c-Akt phosphorylation to a similar extent following SCF stimulation (Figure 3.8). As a measure of activation of the Ras-MAP kinase (MAPK) pathway, phospho-MAPK levels were also examined. The GNNK- isoform brought about 4-fold stronger phosphorylation of MAPK than GNNK+ c-Kit, although activation appeared transient (Figure 3.8). Similar results were obtained in three independent experiments. This transience may have been due in part to translocation to the nucleus as observed by Traverse *et al* (Traverse et al., 1992) as nuclear phospho-MAPK was observed at 30 min post SCF stimulation by confocal microscopy. However no appreciable

Figure 3.6

Loss of c-Kit Surface expression by confocal microscopy

Subconfluent cultures of NIH3T3 cells expressing GNNK+ or GNNK – c-Kit in chamber slides were serum starved for 2 hours and then pulsed for the times indicated with 100ng/ml SCF, immediately followed by fixation with a non-permeabilising fixative (1% paraformaldehyde). Cells were then immunostained *in situ* with anti c-Kit Mab (1DC3 – see section 2.3.1), followed by FITC conjugated sheep anti-mouse Ig (Silenus Laboratories) and analysed by confocal microscopy (BioRad MRC600). Surface expression was quantitated by pixel counting using Confocal Assistant™ software analysing 5 random low power fields per timepoint. Data are presented as the mean average pixel value (immunofluorescence units) (expressed as a percentage of unstimulated cells) ± s.e.m.

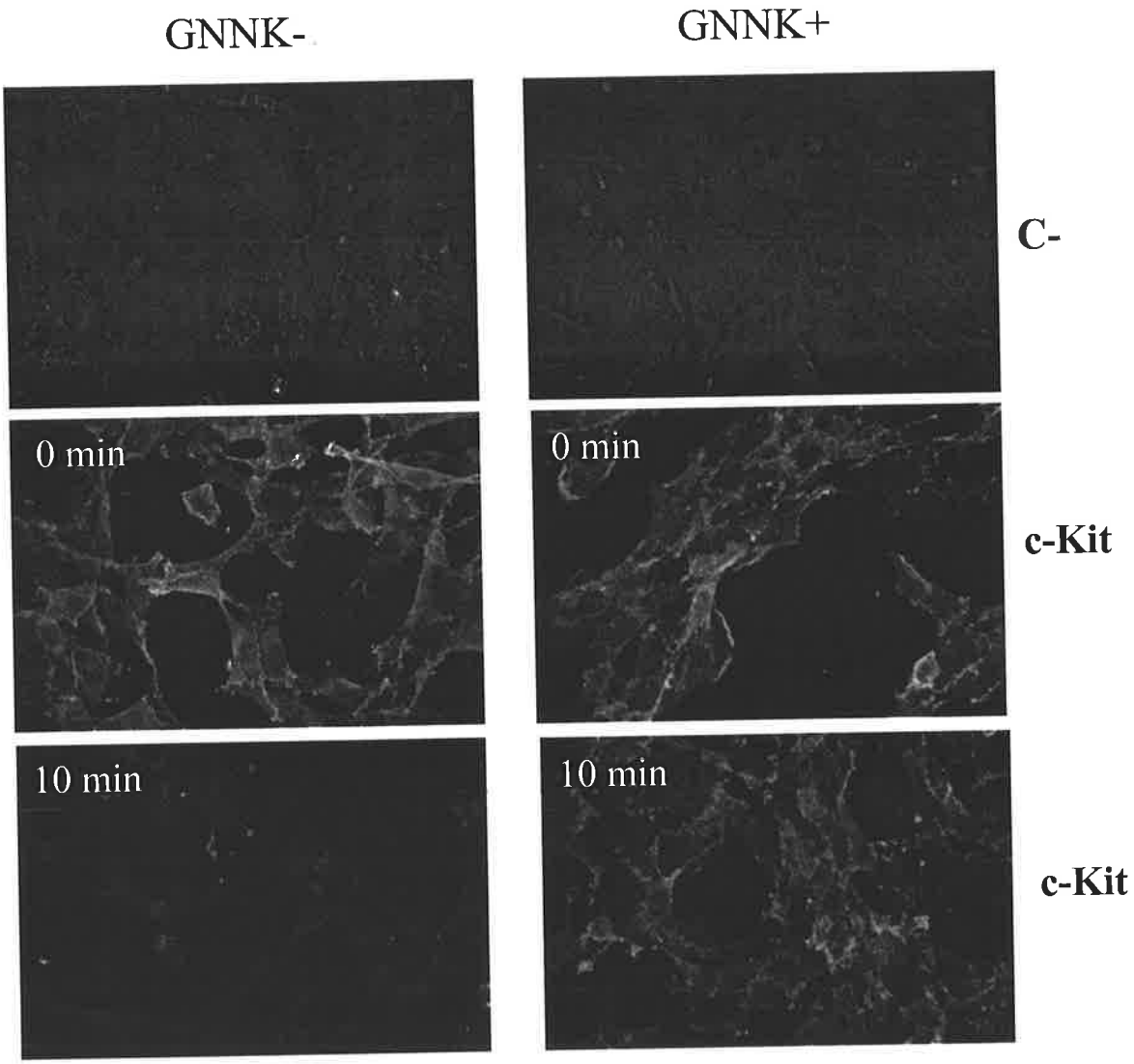
GNNK-
GNNK+
C-
0 min
0 min
c-Kit
10 min
10 min
c-Kit

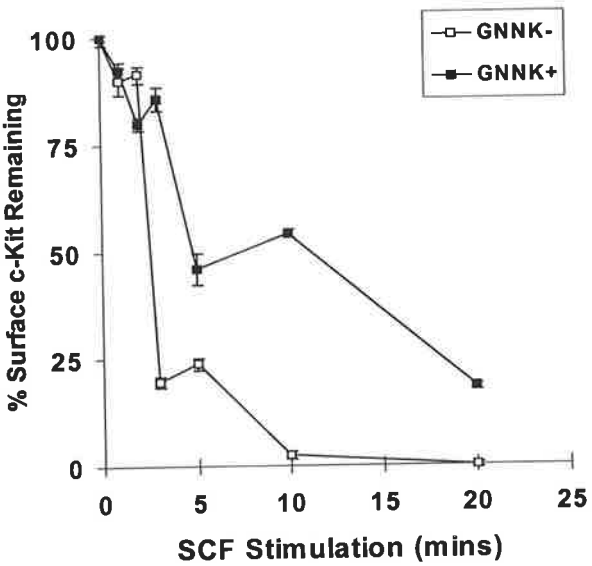
GNNK-
GNNK+
100
75
50
25
0
% Surface c-Kit Remaining
0
5
10
15
20
25
SCF Stimulation (mins)

Figure 3.7

Endocytosis of c-Kit following SCF stimulation analysed by Confocal Microscopy.

Subconfluent cultures of NIH3T3 cells expressing GNNK+ or GNNK – c-Kit in chamber slides were serum starved for 2 hours and then pulsed for the times indicated with 100ng/ml SCF, immediately followed by fixation with a permeabilising fixative (ice-cold 47.5% Methanol, 47.5% Acetone, 5% formaldehyde). Cells were then immunostained *in situ* with anti c-Kit Mab (1DC3), followed by FITC conjugated sheep anti-mouse Ig (Silenus Laboratories) and analysed by confocal microscopy (BioRad MRC600).

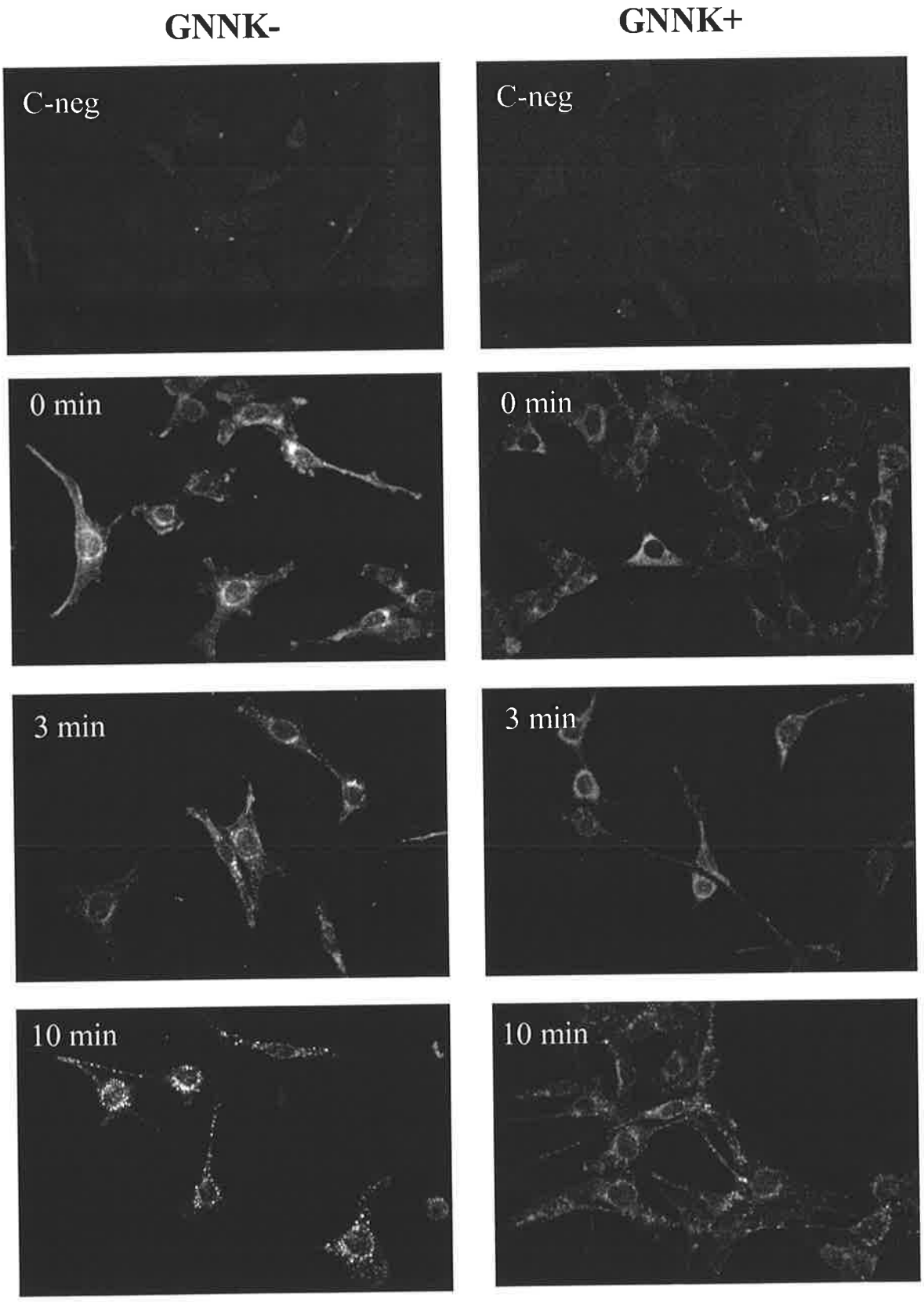
GNNK-
GNNK+
C-neg
C-neg
0 min
0 min
3 min
3 min
10 min
10 min

Figure 3.8

Time course analysis of SCF stimulated NIH3T3 cells expressing GNNK+ and GNNK- c-Kit – MAPK and Akt phosphorylation.

Cells serum starved for 2 hours were stimulated with 100ng/ml SCF for the times indicated and lysed in situ as per Materials and Methods. Lysates containing equivalent amounts of protein were loaded onto SDS-PAGE under reducing conditions, electrophoretically transferred to PVDF membrane and immunoblotted for phosphorylated MAPK (Erk1 and 2), total MAPK (Erk 1 and 2) or phosphorylated Akt (see Section 2.3.1). Blots were visualised using alkaline phosphatase conjugated secondary antibodies followed by development with ECF (enhanced chemifluorescence) substrate (Amersham) and scanned on a Fluorimager595 (Amersham).

On all gels, a standard lysate of MO7e cells stimulated for 2 minutes with SCF was loaded and used as the reference point for comparison analysis across gels. All bands were quantitated using ImageQuant™ software (Amersham) and displayed as relative percent of MO7e control. This information is displayed in the bottom panel of graphs.

Legend:

□ GNNK- c-Kit
■ GNNK+ c-Kit
A Phospho MAPK
B Phospho Akt

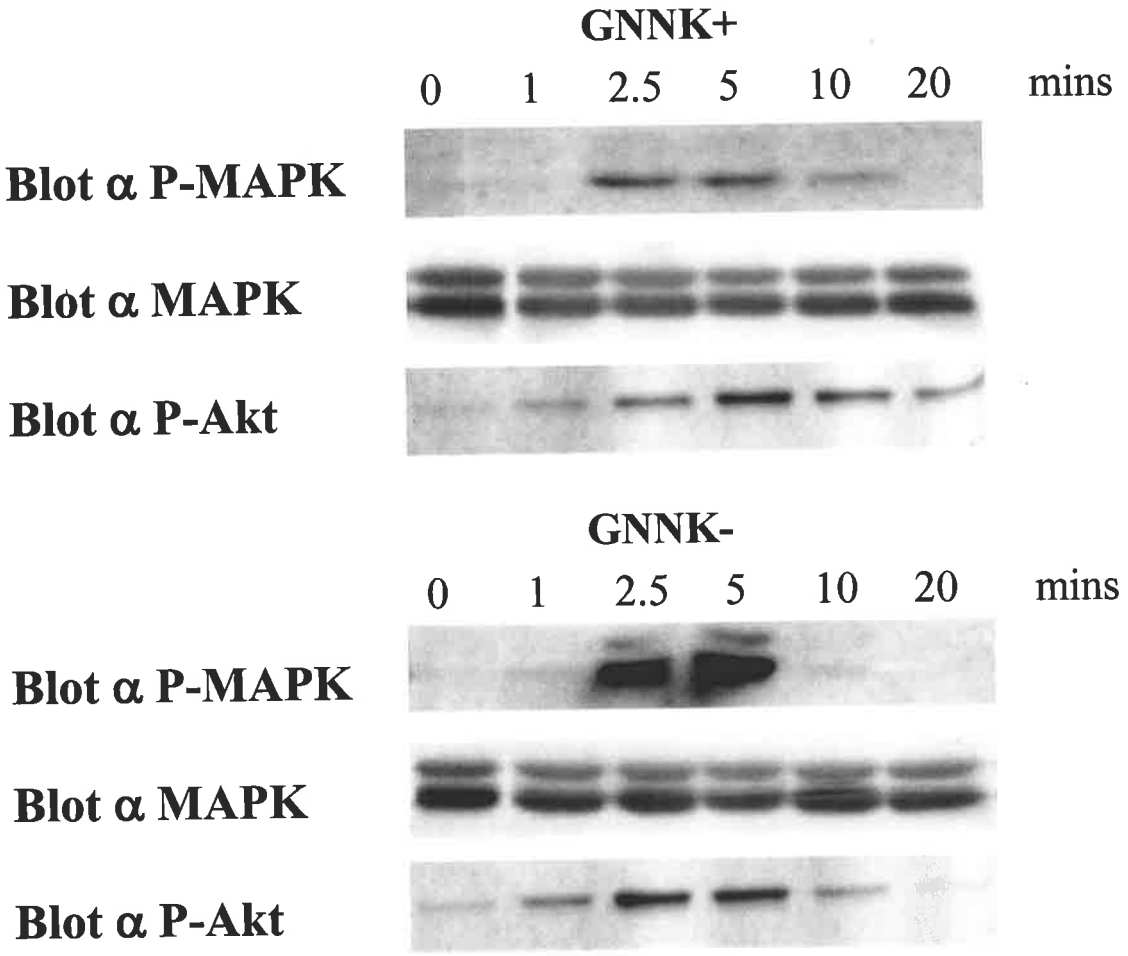
GNNK+
0 1 2.5 5 10 20 mins
Blot α P-MAPK
Blot α MAPK
Blot α P-Akt
GNNK-
0 1 2.5 5 10 20 mins
Blot α P-MAPK
Blot α MAPK
Blot α P-Akt

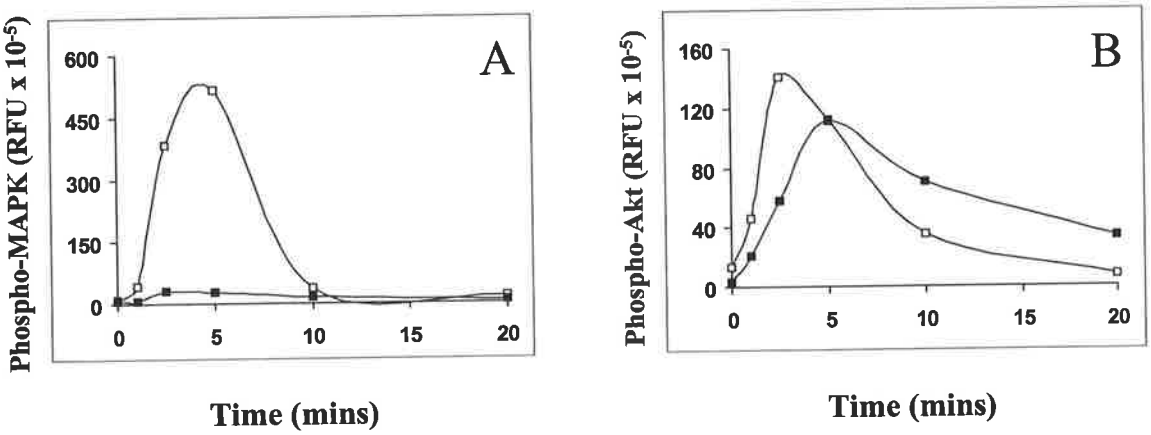
A
Phospho-MAPK (RFU x 10-5)
600
450
300
150
0
0 5 10 15 20
Time (mins)
B
Phospho-Akt (RFU x 10-5)
160
120
80
40
0
0 5 10 15 20
Time (mins)

difference in the extent of nuclear translocation between cells expressing the different isoforms was apparent (Figure 3.9).

3.5. Discussion

3.5.1. c-Kit receptor levels

In this analysis, it was demonstrated that ectopic expression of the unaltered murine c-Kit receptor in NIH(muKit) pools of infectants was able to induce a full range of transformed characteristics (ie. morphological changes, growth in low levels of serum, focus formation, anchorage independent growth in soft agar, and tumours in nude mice) in a substantially factor-dependent manner.

Clones expressing less than about $2.5x10^4$ receptors/cell were generally unable to form colonies under these conditions. Intermediate levels of c-Kit expression resulted in colony growth which was generally enhanced as the level increased up to about $8x10^4$ copies/cell, and a positive correlation existed between the level of c-Kit protein in these clones and colony number in the presence of muSCF. These levels can be compared with an average of $2x10^4$ copies/cell in CD34+ human haemopoietic progenitor cells (Cole et al., 1996); therefore expression of c-Kit at levels only moderately higher than physiological were required to induce anchorage independent growth of the NIH(muKit) cells. Clones which expressed the highest levels of c-Kit mRNA and among the highest levels of c-Kit protein in this study, produced few colonies even in the presence of muSCF (Caruana et al., 1998). Inhibition of colony formation at high receptor levels was also seen with NIH3T3 cell lines expressing human c-Kit up to $1.5x10^5$ per cell (Caruana et al., 1998). In these, optimum colony formation occurred at $5x10^4$ receptors per cell which is near the upper end of the

Figure 3.9

MAPK translocation to nucleus analysed by Confocal Microscopy.

Subconfluent cultures of NIH3T3 cells expressing GNNK+ or GNNK – c-Kit in chamber slides were serum starved for 2 hours and then pulsed for the times indicated with 100ng/ml SCF, immediately followed by fixation with a permeabilising fixative (ice-cold 47.5% Methanol, 47.5% Acetone, 5% formaldehyde). Cells were then immunostained *in situ* with anti phospho-MAPK (Erk1 and 2) polyclonal antisera (see Section 2.3.1), followed by FITC conjugated sheep anti-rabbit Ig (Silenus Laboratories) and analysed by confocal microscopy (BioRad MRC600).

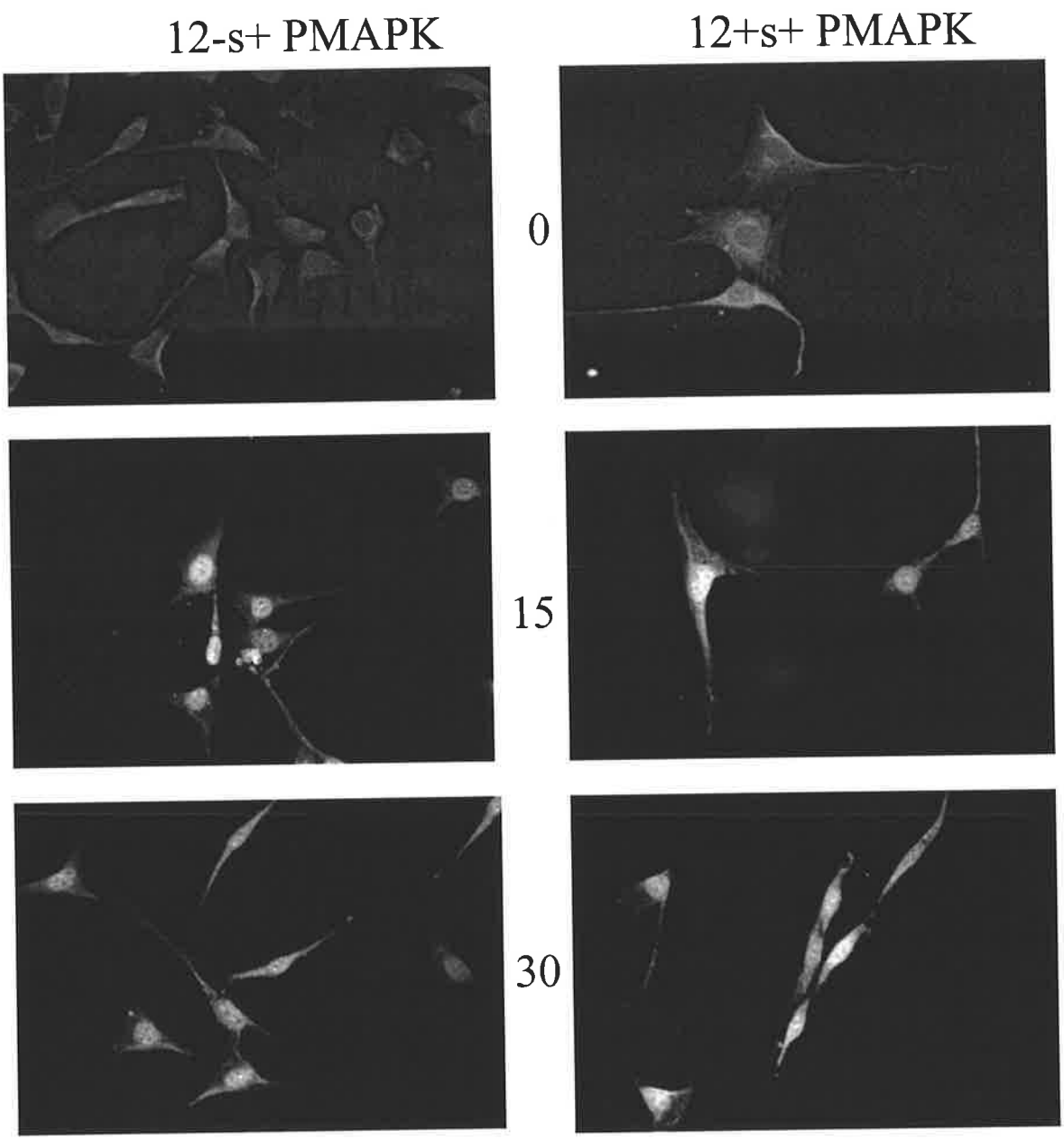
12-s+ PMAPK
12+s+ PMAPK
0
15
30

range observed in the mu c-Kit studies summarised here (Caruana et al., 1998). These results indicate that there is an optimum level of c-Kit expression that is necessary for the production of anchorage-independent growth of NIH3T3 cells.

The mechanism for receptor overexpression resulting in transformation of indicator cell lines is not known, but may be the result of activation of a common signalling pathway. These receptors all activate the Ras/Raf/mitogen-activated protein kinase (MAPK) pathway, many components of which are known proto-oncogenes (Schlessinger et al., 1994). As discussed in Chapter 1, the strength and duration of signal generated by RTKs as a consequence of the variation in receptor density on PC12 cells changes the biological response. (Dikic et al., 1994; Marshall, 1995; Traverse et al., 1994). Decreases in proliferation seen upon stimulation of cells overexpressing the EGF or HER-2/neu receptors were associated with high levels of tyrosine kinase activity, while an enhanced proliferative response was produced when these cells were stimulated with lower ligand concentrations, or by cells expressing lower receptor levels (Kawamoto et al., 1984; Lupu et al., 1990; Riedel et al., 1987), however the receptor copy number at which this was determined was much higher than in our experiments.

Inhibition of anchorage-independent growth was observed at high levels of receptor expression in two series of experiments (one series using mu c-Kit, one using hu c-Kit) by Gina Caruana (Caruana et al., 1998). This may also reflect a 'strength of signal' phenomenon. Although NIH3T3 cells do not undergo differentiation, other data indicate that an optimum level of stimulation of the Ras/MAPK pathway is required for transformation. While moderate Raf kinase activity was associated with

proliferation and transformation in these cells, high constitutive activity led to p21Cip1 induction and cell cycle arrest (Woods et al., 1997). Similarly, there appears to be an optimum level of signalling through c-Kit for transformation.

A significant level of apparently factor-independent colony formation was observed with pools and clones of NIH3T3 cells expressing relatively high levels of c-Kit. This could have been due to autocrine SCF (Jozaki et al., 1991). Firstly, the effects of an antagonistic anti-c-Kit Mab and a partially neutralising anti-muSCF antibody on colony production by the NIH(muKit) pools in the absence of exogenous SCF were examined. Both antibodies inhibited the response to exogenous muSCF but did not influence 'factor-independent' colony yield. This is inconclusive, as antibodies vary in their ability to functionally block receptor/ligand interactions depending on their affinity for the antigenic epitope, and the epitope's position relative to the interaction sites of the ligand/receptor. As the "factor independent" activity is quite low, it is likely that any deficiency in blocking of the antibodies used may allow sufficient interaction to produce a survival/proliferation signal to the cells. Therefore, to confirm this result, a retroviral anti-sense SCF cDNA construct was generated to block autocrine SCF production. No inhibition of 'factor-independent' colony growth was observed, indicating a low level of ligand independent c-Kit activation in these cells.

In conclusion, the data presented here indicate that ectopic expression of normal c-Kit is capable of contributing to oncogenic transformation. c-Kit is ectopically expressed in some human solid tumours as discussed in Section 1.1.3, and is highly expressed in some AMLs where it is associated with poor prognosis (Ashman et al., 1988). How it

contributes to the development of these cancers is not known, but analysis of the signalling pathways in the model system described here should provide valuable information on the molecular relationship between receptor density, ligand-dependence and transformation.

3.5.2. *Hu-c-Kit isoforms*

As previously stated, alternative splicing of mRNA encoding human c-Kit occurs in an apparently tissue non-specific fashion (Crosier et al., 1993) and its significance is unknown. To investigate the function of the different isoforms, a retroviral vector was used to introduce cDNAs encoding different isoforms of human c-Kit into NIH3T3 fibroblasts, which do not express endogenous (murine) c-Kit. As already shown, stable expression of human or murine c-Kit in these cells induces several characteristics of transformation (Caruana et al., 1998) (see Table 3.3). Thus, the resulting infectants could be used to compare cellular responses elicited by binding of SCF to the different receptor isoforms. Any differences could then be explored at the level of signal transduction.

The GNNK- c-Kit was more strongly transforming than the GNNK+ isoform when expressed at similar levels (approximately 10^4 copies/cell). Interestingly, dissociation of the different correlates of transformation was observed. While the GNNK+ isoform was at least as effective as GNNK- in inducing anchorage-independent growth (colony formation in soft agar) it was relatively poor at overcoming contact inhibition (focus-formation assay), and was non-tumourigenic in nude mice.

3.5.3. *Biochemical analysis*

In order to gain some insight into the biochemical basis for these different cellular responses, receptor activation in response to SCF was examined. Saturation binding analysis indicated that both isoforms have similar affinity for SCF. Therefore subsequent experiments were performed with a single saturating level of SCF (100 ng/ml). The presence or absence of the GNNK tetrapeptide had a profound effect on the kinetics and extent of receptor phosphorylation, being extremely rapid for GNNK- (peaking at 2-3 min) followed by downregulation which involved internalisation of the receptor. In contrast, the GNNK+ isoform displayed later peak tyrosine phosphorylation (around 7.5 min) and showed little dephosphorylation or down-regulation by 20 min. A marked difference was observed in the relative level of phosphorylation, which was 7-fold, higher for the GNNK- isoform. Whether this reflects a lower efficiency of phosphorylation overall, or the lack of phosphorylation of specific sites is not known.

Despite the low level of phosphorylation of GNNK+ c-Kit, PI3-K was recruited similarly to both forms of the receptor and similarly activated based on phosphorylation of its major down-stream effector c-Akt. Recruitment of PI3-K to another type 3 RTK, the platelet-derived growth factor receptor (PDGFR), was previously reported to have the least requirement of several substrates for receptor phosphorylation (Rankin et al., 1994). In contrast, phosphorylation of MAPK paralleled that of c-Kit and was much stronger with the GNNK- isoform.

The relationship between hyperphosphorylation of GNNK- c-Kit and its more rapid endocytosis is unclear. Experiments with endocytosis-defective cells indicated that maximal phosphorylation of the EGF receptor requires internalisation. Furthermore, efficient MAPK phosphorylation and activation required receptor endocytosis while activation of phospholipase Cγ was more efficient in endocytosis-defective cells (Vieira et al., 1996). Thus the different rates of internalisation of the c-Kit isoforms may contribute to their altered specificity of signalling.

The results presented here differ from those of Reith *et al* (Reith et al., 1991) with murine GNNK+ and GNNK- isoforms transiently expressed in COS cells. These workers observed some constitutive tyrosine phosphorylation of the GNNK- isoform, but not GNNK+, in the absence of ligand. In contrast, receptor phosphorylation in the absence of SCF was very low for both isoforms in this study. One possible explanation is that the levels of receptor expression, which were not determined by Reith *et al*, were probably somewhat higher than in our study. However, a significant level of factor-independent receptor activation can occur for both the GNNK+ and GNNK- isoforms of human c-Kit, as is evident from the results of the colony assays described here (Table 3.3) where relatively high frequencies of factor-independent colonies were observed. Based on studies of factor independent mu c-Kit activation (Caruana et al., 1998) and results presented in Section 3.3.2, these are unlikely to arise as a result of autocrine stimulation by murine SCF produced by NIH3T3 cells, especially since muSCF is less active than huSCF on human c-Kit (Lev et al., 1993).

Strong stimulation of certain signalling pathways may be inhibitory to NIH3T3 proliferation through induction of p21Cip1 (Sewing et al., 1997; Woods et al., 1997).

In contrast to the colony assay, NIH3T3 infectants grown attached to the dish in the assay for focus formation showed much less evidence of factor-independent c-Kit activation. The conditions in this assay are comparable to those under which the biochemical assays were performed. Furthermore, inhibition at higher receptor levels was not observed in this assay (Table 3.3). These results indicate a complex interplay between signals via c-Kit and adhesion molecules. It has been reported that proliferation of fibroblasts induced by Ras required Rho activation to prevent p21Cip1 induction (Olson et al., 1998). Since Rho is also involved in cell adhesion processes, it may be that this pathway is operative in the focus formation assay, but that repression of p21Cip1 is defective in contact-deprived cells, ie. in the colony assay.

The differences between the isoforms in their transforming ability could be correlated with differences in signalling. The GNNK- isoform, which induced anchorage-independence, loss of contact inhibition and tumourigenicity, displayed stronger receptor phosphorylation, more rapid internalisation, and stronger activation of the MAPK pathway following SCF stimulation than the GNNK+ isoform. In contrast, the GNNK+ isoform induced anchorage-independent growth with similar efficiency to GNNK- c-Kit, but was much less effective in inducing other attributes of transformation. The fact that SCF binding to the GNNK+ isoform efficiently recruited and activated PI3-K suggests that this pathway is particularly important in preventing death of cells deprived of contact with extracellular matrix ("anoikis" (Ruoslahti et al., 1994)).

Indeed PI3-K induced activation of c-Akt has been demonstrated to be a major mechanism of promoting cell survival in response to growth factors (Kennedy et al., 1997) and cell adhesion (Khwaja et al., 1997). There are strong parallels between GNNK+ c-Kit and R-Ras in both signalling and their ability to induce different attributes of transformation *in vitro*. Activated R-Ras was as effective as H-Ras in promoting growth of NIH3T3 cells in soft agar, but was much less effective in inducing focus formation (Cox et al., 1994). Furthermore, activated R-Ras stimulates the PI3-K pathway but, in contrast to other Ras proteins, has little effect on the MAPK pathway in fibroblasts (Marte et al., 1997).

The molecular mechanisms by which these relatively minor sequence differences between the c-Kit isoforms lead to such remarkably different activation characteristics and biological behaviour are unknown. For example, it is unclear how the GNNK+/- variation in the juxtamembrane region of the extracellular domain influences the rate of receptor phosphorylation and internalisation, but it seems likely that it must modulate interactions with other membrane proteins. Since the isoforms have similar affinity for ligand, it seems improbable that the tetrapeptide has an appreciable effect on receptor homodimerisation. The data presented here imply major differences between the isoforms in their interaction with signal transducing molecules. It will be important to investigate their interactions with phosphatases such as SHP-1 which is associated with c-Kit (Yi et al., 1993) and a range of proteins including Shc (Matsuguchi et al., 1994), Lyn (Linnekin et al., 1997), PLCγ1 (Herbst et al., 1995b; Rottapel et al., 1991), p120CBL (Wisniewski et al., 1996), and others that are known to be recruited or activated on SCF binding to c-Kit.

With reference to Shc and Lyn mentioned above, a recent study by Voytyuk *et al* (Voytyuk et al., 2003), demonstrated that Src family kinases were differentially activated by two c-Kit isoforms (GNNK+S+ and GNNK-S+). The GNNK- isoform lead to 3 fold higher phosphorylation of Shc (downstream of Src family kinases) than that stimulated by the GNNK+ isoform. This analysis also confirmed activation of Erk was higher by the GNNK- isoform of c-Kit (as already shown in this thesis) in a Src family kinase dependent manner (this was inhibitable with the specific Src kinase inhibitor SU6656).

3.5.4. *Future experiments*

These experiments highlighted a need to develop an alternative model system to more closely examine cellular responses to c-Kit as the NIH3T3 model can only provide information on the transformation potential of the receptor and is a cell type that does not normally express the receptor. This may, in fact, be the cause of the ligand independent behaviour of c-Kit in this model, simply due to an inappropriate repertoire of downstream signalling moieties – down modulation/negative regulation of the receptor may not be as tight as in haemopoietic or other cells that normally express c-Kit. This model also fails to measure many of the normal cellular responses to SCF. In Chapter 4, an improved model is developed to redress some of these shortfalls. This model is derived from cells of haemopoietic origin, and has the potential to measure proliferation, differentiation and survival in response to SCF stimulation of c-Kit.

4 Development of chimaeric c-Kit isoforms for expression in new Myb Immortalised Haemopoietic Cell (MIHC) Lines

INTRODUCTION

In this chapter, a novel cell line model was adapted from a model established in the IMVS previously by Professor T Gonda and Dr P Ferrao, where an oncogenic form of c-Myb was used to immortalise murine foetal liver cells. This model was intended to generate immortalised murine immature haemopoietic cells with the express purpose of studying cellular responses to exogenously added SCF. The cell lines would be engineered to express the GNNK+ and GNNK – isoforms of newly created chimaeric (murine/human molecule) c-Kit responsive to human SCF. Importantly, any endogenous c-Kit in these cells will not be stimulated by the exogenous human SCF used in experimentation.

It was hypothesised that these lines would be capable of differentiation, proliferation, and survival responses, and the lines could be used to measure these parameters in response to exogenously added human SCF. Once these cellular responses were evaluated in normal cells, similar lines could be generated from knockout mice missing one downstream effector of the c-Kit signalling pathways. This was to be a systematic approach to analysing critical downstream effector molecules in the c-Kit signalling pathway and assigning cellular responses to distinct pathways of the c-Kit signalling cascades. The knockout strain chosen to evaluate this approach lacked Src family tyrosine kinase member Lyn, a known downstream component of c-Kit

signalling pathways. Comparisons between WT and Lyn -/- cell lines would potentially show the cellular responses to exogenous SCF that are affected by Lyn.

4.1. Myb-immortalisation of haemopoietic cells

4.1.1. Myb gene family

The *Myb* gene was first discovered as the transforming oncogene of the Avian myeloblastosis retrovirus (AMV) first isolated by Hall *et al* in 1941 (Hall et al., 1941). A 2nd virus was identified later and named E26. E26 induced erythroid and myeloid leukaemias in Quails (Reviewed Oh *et al* (Oh et al., 1999)).

AMV was later shown to result from a recombination between the myeloblastosis-associated virus type I (MAV-1) and chicken c-Myb cDNA sequences. AMV v-Myb was a 45kD product (Baluda et al., 1994) compared to c-Myb (75kD). E26 produced a viral gag-Myb-Ets-1 fusion protein of 135kD (Leprince et al., 1983a; Leprince et al., 1983b; Nunn et al., 1983).

The discovery of these two v-Myb genes led to the cloning and isolation of the normal cellular counterpart, c-Myb. This gene is highly conserved through all species (Lipsick, 1996). The gene product (viral and cellular Myb) is localised in the nucleus and has specific DNA binding activity. Its function is as a transcription regulator.

There are 3 members of the Myb gene family – A-Myb, B-Myb and c-Myb (Ness, 2003). These genes have high sequence homology, but have quite different tissue expression patterns. A-Myb is strongly expressed in male germ cells and breast epithelial cells (Mettus et al., 1994; Toscani et al., 1997). B-Myb is ubiquitously

expressed and has been shown to play a role in inhibiting collagen gene expression in vascular smooth muscle cell (Hofmann et al., 2004) and fibroblasts (Cicchillitti et al., 2004; Luchetti et al., 2003). In addition, B-Myb activity is regulated by cyclinA/Cdk2 (stimulator) and cyclinD1 (inhibitor) (Joaquin et al., 2003a; Joaquin et al., 2003b; Schubert et al., 2004), and a significant gene target of B-Myb is the c-Myc gene (Tashiro et al., 2004).

c-Myb is largely restricted to immature haemopoietic cells (Gonda et al., 1982; Westin et al., 1982) and has also been shown to regulate collagen gene expression (Luchetti et al., 2003). Its role in regulation of growth and differentiation is accepted, but how c-Myb is itself regulated is still poorly understood. Recent studies have demonstrated that c-Myb is sumoylated, increasing its activity, and that it associates with promyelocytic leukemia (PML) protein localised in PML nuclear bodies. Overexpression of PML IV was shown to increase c-Myb activity (Dahle et al., 2004). As with B-Myb, c-Myb has been shown to target the *c-Myc* gene promoter. Where c-Myb is overexpressed, granulocytic differentiation was blocked, and there was a concomitant increase in the level of c-Myc expression and activity. Of interest, overexpression of c-Myc alone was unable to block differentiation, yet the differentiation block was dependent on c-Myc as demonstrated by the reversal of this c-Myb induced block by addition of a dominant negative c-Myc (Kumar et al., 2003).

4.1.2. c-Myb structure

The gene product of c-Myb is a 636 amino acid (75kD) protein localised to the nucleus, and it is expressed in most haemopoietic tissues (Gonda et al., 1982; Westin et al., 1982). An alternative splice product of 89kD (expressed in avian, murine and

human haemopoietic cells) was later identified (Dasgupta et al., 1989; Dudek et al., 1989a; Dudek et al., 1989b). The alternate splice adds 369bp to the mRNA between exons 9 and 10. It is also nuclear localised (Dudek et al., 1989a; Dudek et al., 1989b) and functional as a transcription regulator (Sakura et al., 1989; Weston et al., 1989). A schematic representation of the 4 known translated gene products is shown in Figure 4.1 (adapted from Oh *et al* (Oh et al., 1999)).

All Myb proteins have an N-terminal domain (DNA Binding Domain) that is conserved and consists of 3 tandem 50 amino acid repeats (R1, R2, R3) (Saikumar et al., 1990; Sakura et al., 1989). Deletion analysis showed that R2 and R3 were essential for DNA binding (Howe et al., 1991; Saikumar et al., 1990) and Tanikawa *et al* (Tanikawa et al., 1993) later demonstrated that R1 played a role in stabilisation of DNA binding interaction. The DNA Binding Domain has a sequence specificity of PyAACG/TG (Biedenkapp et al., 1988), and this sequence is found in target promoter regions (Nakagoshi et al., 1990; Ness et al., 1989). Surrounding sequences influence the specificity of each Myb family member (Oh et al., 1999).

A transactivation domain of 52 aa is present in c-Myb and A-Myb , and there is some conservation between the 2 proteins in this region. A-Myb transactivation is believed to be more potent than c-Myb (Golay et al., 1994). B-Myb also has a transactivation domain, but has little homology to the other two family members, and is not functionally equivalent (Oh et al., 1999; Watson et al., 1993).

The C terminal regulatory domain is missing in v-Myb, which led to the suggestions that it was a negative regulatory domain. Sakura *et al* (Sakura et al., 1989) and

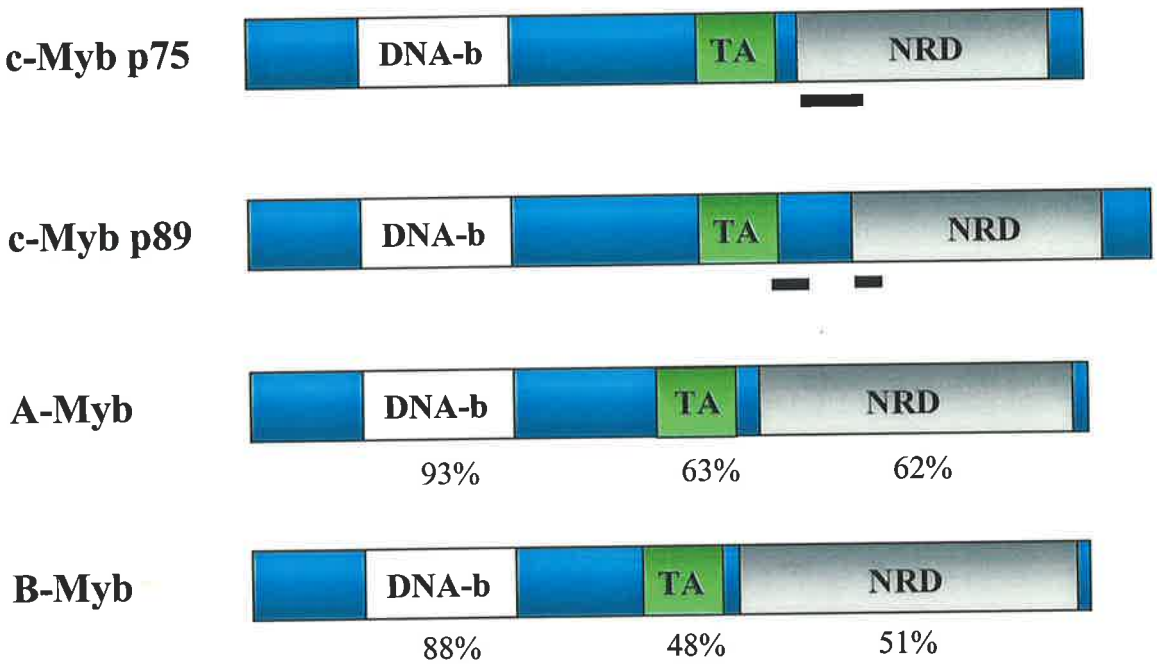

Figure 4.1

Structural comparison of Myb gene family products.

▬ Represents Leucine Zipper domains in c-Myb. The values shown below A- and B-Myb are percent homology to c-Myb.

DNAb = DNA binding domain.
TA = trans activation domain.
NRD = negative regulatory domain.
RD = regulatory domain.

Adapted from Oh et al, 1998

Weston *et al* (Weston et al., 1989) both demonstrated this by deleting the domain and demonstrating marked increases in transactivational activity. Increased transformation potential was also demonstrated for these deletion mutants (Gonda et al., 1989a; Grasser et al., 1991; Hu et al., 1991). Within this domain is a leucine zipper region which is believed to function in homo- and/or heterodimer formation (Biedenkapp et al., 1988). This leucine zipper region is disrupted in the 89kD splice variant form of c-Myb, and this form demonstrates higher transactivational activity compared to the normal 75kD c-Myb (Woo et al., 1998). This domain is highly conserved within the Myb family across species (Katzen et al., 1985; Sleeman, 1993) and its deletion has the same effects in A-Myb as it does in c-Myb (Oh et al., 1997; Takahashi et al., 1995). In contrast, deletion of this domain in B-Myb reduced its transactivation activity (Oh et al., 1998).

Ser 528 in the c-Myb regulatory domain is the target of a proline directed kinase and its phosphorylation negatively regulates c-Myb activity. ERK1 can mimic this kinase in vitro, but is unlikely to be the kinase *in vivo* (Aziz et al., 1995; Taylor et al., 1996). This serine is within a PEST sequence postulated to target c-Myb for ubiquitination and degradation. When c-Myb is truncated to remove the regulatory domain, its half-life is substantially increased, supporting this postulate (Bies et al., 1997). c-Myb, with the regulatory domain removed (termed CT3Myb in this thesis), was utilised for the work performed in this chapter, as it has superior activity when overexpressed compared to full-length c-Myb and had been used successfully in this laboratory previously (Ferrao et al., 1997).

4.1.3. Cellular targets of c-Myb

A number of gene targets for c-Myb have been identified over the past 10-15 years. These include mim-1, which has 3 Myb binding sites within its promoter. This gene is highly expressed in promyelocytes and poorly expressed in macrophages (Ness et al., 1989; Tomita et al., 1998). Nicolaides *et al* (Nicolaides et al., 1991) demonstrated that Myb transactivated the *c-Myb* gene promoter itself (which has 3 Myb binding sites). In contrast to this finding, Guerra *et al* (Guerra et al., 1995) demonstrated a negative regulation of the *c-Myb* gene promoter. Overexpressing c-Myb in T cells lead to increased expression of c-Myc. This had no effect, however, on cell cycle rates or factor dependence of T cells (Evans et al., 1990). Some other demonstrated target genes for c-Myb are CD4 (Nakayama et al., 1993; Siu et al., 1992), CD34 (He et al., 1992; Melotti et al., 1994a; Melotti et al., 1994b), p34cdc2 (Furukawa et al., 1990), DNA polymerase alpha (Venturelli et al., 1990a; Venturelli et al., 1990b), and GATA-1 and EpoR (Lin et al., 1996).

4.1.4. c-Myb regulation of proliferation and differentiation

Original studies of colony formation from human bone marrow mononuclear cells (soft agar assays) demonstrated an absolute requirement for c-Myb to enable proliferation of the cells. Inclusion of antisense c-Myb reduced colony size (ie cell number) but had no effect on the differentiation progression of progeny within the colony (Gewirtz et al., 1988). Similarly, mitogen stimulation of T cells was blocked with antisense c-Myb (Gewirtz et al., 1989). There have been doubts cast over the oligonucleotides used in these experiments, with suggestions the effects were a non-specific inhibition of cell cycle. However, Jarvis *et al* (Jarvis et al., 1996) used

ribozymes targetted to c-Myb RNA to demonstrate cell cycle arrest. Added to this, c-Myb knockout mice developed normally *in utero* to day 13, but were dead by day 15 suffering severe anaemia. It was shown that embryonic haemopoiesis from the yolk sac was normal, but that long term erythropoiesis, which first appears in the foetal liver, is extremely dependant on c-Myb (Mucenski et al., 1991).

c-Myb is highly expressed in immature haemopoietic cells (Gonda et al., 1984), and expression is cell cycle dependent, peaking at late G1 to S phase (Catron et al., 1992; Thompson et al., 1986). It, together with B-Myb, plays a crucial role in the cell cycle progression from G1 to S phase (Oh et al., 1999).

c-Myb expression, whilst high in immature haemopoietic cells, is down regulated during terminal differentiation (Gonda et al., 1984). Cytokine or artificial stimulation of differentiation also down regulates c-Myb (Gonda et al., 1984; Kuehl et al., 1988; Ramsay et al., 1986). Neuroblastoma cell lines capable of differentiation in response to Retinoic Acid also down regulate c-Myb, and overexpression of c-Myb in these lines blocked the differentiation response (Clarke et al., 1988; Todokoro et al., 1988). Not only is c-Myb expression down regulated, but also its transactivation activity is reduced. Retinoic acid treatment inhibited transactivation of a Myb responsive reporter gene, despite Myb retaining the same DNA binding activity (Smarda et al., 1995). Overexpression of c-Myb in 32Dc13 cells induced with G-CSF blocked the normal growth arrest and differentiation response of these cells (Bies et al., 1995).

4.1.5. *Activated c-Myb immortalisation of primitive haemopoietic cells*

As has already been discussed, c-Myb has roles in growth and differentiation of haemopoietic cells (reviewed (Gonda, 1991)). Activated forms of c-Myb have the ability to immortalise murine myeloid cells, enabling continuous factor-dependent growth (reviewed (Gonda, 1991)). The most potent form of Myb in this system is different in two aspects to WT c-Myb. Firstly it is constitutively expressed (usually from the long terminal repeats of a retrovirus such as AMV) and, secondly, it is truncated to remove the regulatory domain.

Murine Foetal Liver Cells (FLC) were shown to be immortalised by truncated overexpressed c-Myb giving rise to long term cell lines were established that were factor dependent (Gonda et al., 1989a; Hu et al., 1991). These cell lines retain an immature myelomonocytic phenotype, suggesting that c-Myb exerts a differentiation blocking effect as well as its role in proliferation.

4.2. Lyn – a member of the Src Family of Tyrosine Kinases

Src family tyrosine kinases are involved in many signal transduction pathways. These cytoplasmic proteins operate downstream of various surface receptors, facilitating the process of cellular responses to external stimuli. These are associated with various transmembrane receptors such as hormone receptors, cytokine receptors and cell adhesion molecules (Tatosyan et al., 2000).

The first identified Src family member was Src itself, and this was identified as the activated v-Src in the Rous Sarcoma Virus (Jove et al., 1987). Other members of the

Src family include Fyn and Yes (expressed widely in the body) and Fgr, Lyn, Hck, Lck, Blk and Yrc (which have more restricted expression profiles). Lyn, which is the subject of investigations in this chapter, is predominantly expressed in haemopoietic cells (Hibbs et al., 1997) and was first identified in 1987 (Yamanashi et al., 1987).

4.2.1. Src Family Kinase Structure

Figure 4.2 shows a schematic structure for Src. This organisation is conserved for all Src family members (reviewed (Tatosyan et al., 2000)).

The SH4 domain (15-17aa) is located at the N terminal of the protein, and contains a myristylation site facilitating membrane association, however all protein is not membrane associated (Tatosyan et al., 2000) .

The unique domain (approx 66aa) is divergent amongst all family members and is believed to be responsible for the target specificity of the kinase (Tatosyan et al., 2000; Thomas et al., 1997).

The SH3 domain (approximately 55aa) is required for interactions with proline rich regions of target proteins. It also provides intramolecular binding sites necessary to downregulate kinase activity (Pawson, 1995).

The SH2 domain (approx 120aa) is also required for interactions with various target proteins, recognising a short peptide sequence containing a phosphorylated tyrosine (Songyang et al., 2001). This module adds specificity to that already imposed by the

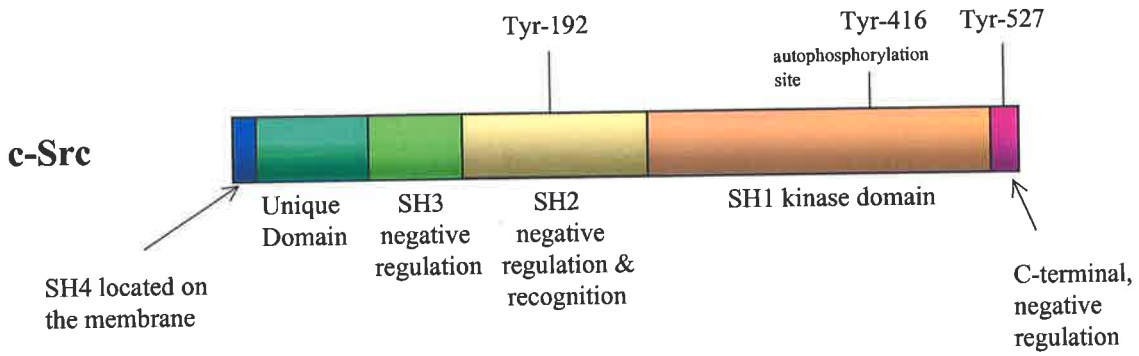

Figure 4.2

Domain Structure of c-Src.

Adapted from Tatosyan et al, 2000

unique and SH3 domains, restricting further the number of potential target proteins a particular Src family kinase may interact with.

The Kinase domain (approx 250aa) is responsible for the activity of the molecule and imposes the last level of specificity for target substrates. Within this site is a conserved Tyrosine (Tyr 416 in Src), which is an autophosphorylation target of the kinase. Phosphorylation of this tyrosine is required for full activation of the kinase, achieved by causing a conformation change in the activation loop (Tatosyan et al., 2000).

The c-Terminal region (approx 20aa) has a conserved peptide sequence surrounding a Tyrosine residue (Tyr 527 in Src) which is highly conserved and critical for negative regulation of the kinase activity. When this residue is phosphorylated, kinase activity is inhibited 98%, irrespective of the phosphorylation status of Tyr416 (in Src) in the catalytic domain (van Hoek et al., 1997). It is this region that is substituted or missing in v-Src (Dorai et al., 1991; Reynolds et al., 1987; Yaciuk et al., 1986).

Tyr 527 is phosphorylated by the cytoplasmic kinase Csk (Okada et al., 1991), and it is believed that the phosphorylated Tyr 527 interacts with the SH2 domain of the kinase to generate a "closed" conformation incapable of catalysis (Xu et al., 1999) (See Figure 4.3). The SH3 domain makes an independent association with the c-Terminal region further stabilising the closed conformation (Xu et al., 1999). This form of regulation will also block the SH2 and SH3 domains from interacting with target proteins, adding a further level of control to Src kinase function (Tatosyan et al., 2000). Activation is believed to be triggered by interactions between target

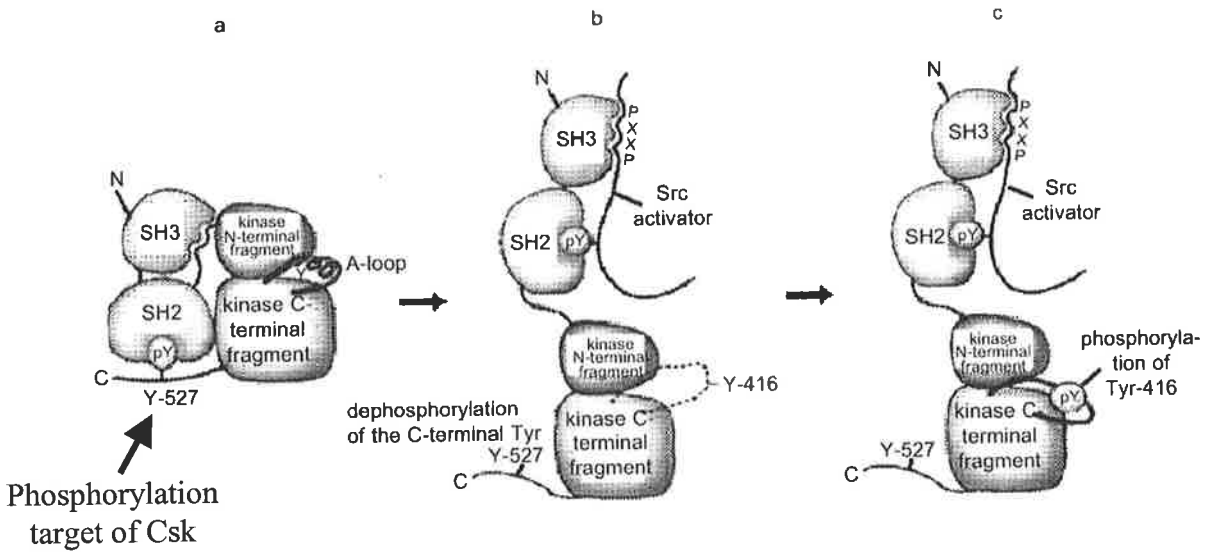

Figure 4.3

Regulation of Src

a. Closed auto-inhibited state.
b. Open intermediate state induced by either interactions of the SH3 and SH2 domain with Src protein partners or by dephosphorylation of the c-terminal Tyr-527. Tyr-416 is now accessible for phosphorylation
c. Open activated form with phosphorylated Tyr-416

Adapted from Tatosyan et al, 2000

proteins and the SH2/SH3 domains, together with dephosphorylation of the c terminal Tyrosine. Full activation follows with autophosphorylation of the catalytic domain Tyrosine (Tatosyan et al., 2000)) (Figure 4.3)

4.3. Lyn and c-Kit

The juxtamembrane region of c-Kit has two Tyrosine residues (568 and 570), which bind to Src family kinases Lyn and Fyn (Linnekin et al., 1997; Price et al., 1997b). Csk homologous kinase (CHK) and the adaptor Shc also bind to these two sites, as do the phosphatases SHP1 (Tyr-570) and SHP2 (Tyr 568) (Kozlowski et al., 1998). A number of kinases and phosphatases have all been clearly linked to this very small section of c-Kit, and it is unclear as to precisely how these molecules interact with each other and c-Kit. Lyn is also shown to associate with Tec and p62Dok1 in a PI3-K dependent manner (van Dijk et al., 2000). Hypothetical interactions between Kit and downstream molecules are illustrated in Figure 4.4 (Scheijen et al., 2002)). This figure illustrates the main regions for association of downstream signalling in c-Kit – namely the juxtamembrane region and the interkinase domain (Grb 2, PI3-K and PLCγ associations). Mutants in the juxtamembrane region of c-Kit (Frost et al., 2002; Kitayama et al., 1995; Lasota et al., 2003a; Lasota et al., 2003b; Nakahara et al., 1998) can be transforming, highlighting the importance of this region in normal signal transduction. It is possible that SHP1 and SHP2 behave as a scaffold structure for the association of Shc, CHK and Lyn, and that Tec and Dok associate via Lyn (van Dijk et al., 2000). Given Lyn is centrally placed with downstream signalling components from this region of c-Kit, its putative action in c-Kit downregulation (Broudy et al., 1999), and our access to Lyn knockout mice (a kind gift from Dr M Hibbs and Dr A Dunn), it was decided that signalling of c-Kit would be investigated in a background devoid of Lyn.

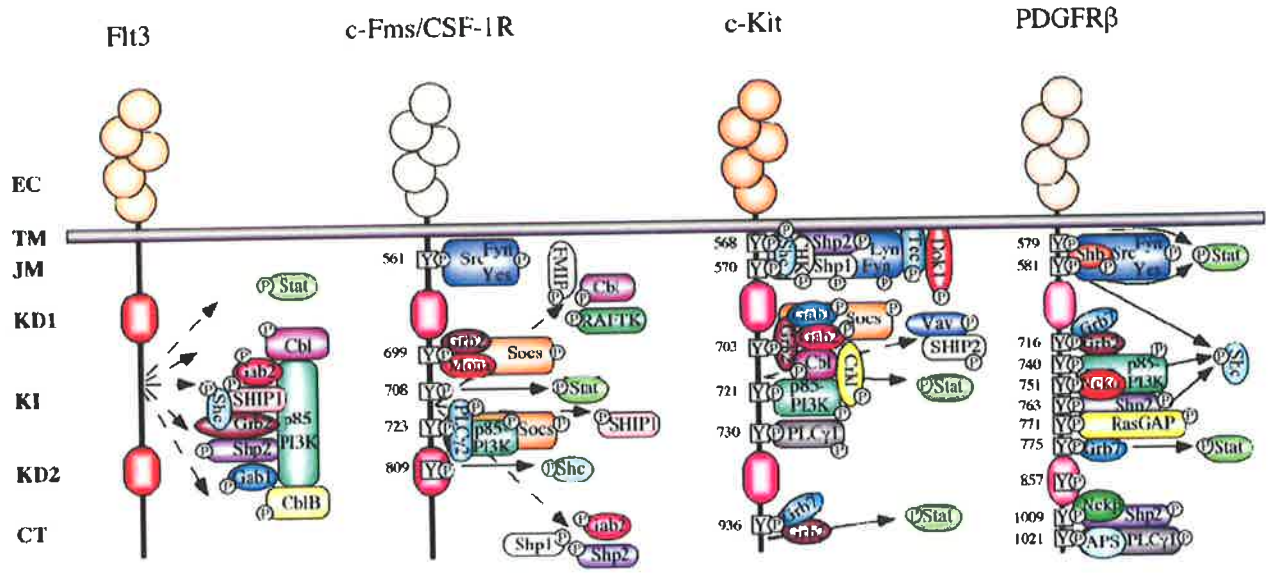

Figure 4.4

Hypothetical interactions of signalling molecules with human type III receptor tyrosine kinases.

EC – 5 Ig like domains in extracellular domain
TM – transmembrane domain
JM – juxtamembrane domain
KD1 & 2 – split kinase domain
KI – kinase insert
CT – c-terminal tail

Characterised autophosphorylation sites are shown, along with potential adaptor and effector signalling molecules.

Dashed arrows indicate substrate phosphorylation through characterised phosphotyrosine interaction sites

Solid arrows implicate indirect mechanisms of phosphorylation.

Adapted from Scheijen and Griffin, 2002

4.3.1. *Lyn knockout mice*

Lyn is predominantly expressed in haemopoietic cells as already mentioned. It is associated with many haemopoietic cell receptors including the B Cell Antigen Receptor (Burkhardt et al., 1991; Yamanashi et al., 1991a; Yamanashi et al., 1991b), CD40 (Ren et al., 1994), the LPS receptor (Stefanova et al., 1993), FcεR1 complex (Eiseman et al., 1992), G-CSF receptor (Corey et al., 1994), Erythropoietin receptor (Tilbrook et al., 1997) and c-Kit (Linnekin et al., 1997; Price et al., 1997a).

Hibbs *et al* (Hibbs et al., 1995) generated homozygous Lyn null mice to investigate B cell receptor signalling. This was achieved by disruption of the Lyn gene promoter using a PGKneo cassette. RT-PCR was utilised to verify the abrogation of any Lyn transcription in the homozygous knockout mice. It was demonstrated that B lymphocyte lineages were abnormal in these mice, as was mast cell function. There were decreased numbers of circulating B cells, yet the mice were IgM hyperglobulinaemic. The mice fail to raise an allergic response to IgE receptor crosslinking, and had circulating autoantibodies. Many of the mice developed severe glomerulonephritis caused by IgG immune complex deposition in the kidney, demonstrating Lyn's crucial roles in immunoglobulin mediated signalling and induction of B cell tolerance. This has recently been shown to be dependent on IL-5 signalling. Lyn deficient mice were crossed with IL-5 Receptor α deficient mice. The double knockout progeny had significantly lower B1 cell numbers and splenomegaly (Moon et al., 2004).

The role of Lyn in mast cell function was attributed solely to FcεR1 (Hibbs et al., 1995). With the more recent knowledge of Lyn's association with c-Kit, which is

highly expressed in mast cells (Mayrhofer et al., 1987), the possibility of additional down modulation of mast cell function through c-Kit signalling (in Lyn -/- mice) is plausible. To this end, O'Laughlin-Bunner *et al* (O'Laughlin-Bunner et al., 2001), demonstrate impairment of SCF-induced responses in Lyn-deficient mast cells and progenitor cells. Lyn deficient mast cells are, however, less prone to apoptosis in response to cytokine withdrawal (Hernandez-Hansen et al., 2004), and this has been attributed to Lyn involvement in mediating cell cycle arrest via the JNK pathway in Lyn deficient fibroblasts (Shangary et al., 2003).

Lyn deficient mice also demonstrate platelet defects, due to a loss of negative regulation of alpha(IIb)beta(3) integrin . This was related to the recruitment of the phosphatase SHP-1 (Cho et al., 2002; Maxwell et al., 2004). Similarly, Lyn deficient neutrophils were demonstrated to be hyper-responsive to integrin engagement, and Lyn was shown to be essential for recruitment of SHP-1 to modulate the response (Pereira et al., 2003).

RESULTS

4.4. Generation of Human/Mouse Chimaeric c-Kit

To analyse c-Kit in the MIHC model system, it was imperative to have c-Kit appropriately expressed and controlled in the murine cell lines that were being generated. It had already been demonstrated in Chapter 3 that full length human c-Kit expressed in murine cells displayed some ligand independent activity, possibly indicating inadequate control of the human molecule in murine cell lines. In addition to this, it was expected that the cell lines to be generated, being of immature haemopoietic phenotype, would express endogenous murine c-Kit. The use of

ectopically expressed human extracellular domain c-Kit together with human SCF, which is inactive on murine c-Kit, enabled us to study different isoforms of c-Kit (eg. GNNK+ and GNNK-) without interference from the endogenous receptor.

To achieve this, a chimaeric c-Kit was generated. The human extracellular domain was fused to the murine c-Kit transmembrane and intracellular domains. This created a chimaeric c-Kit receptor, which will be referred to as chi-c-Kit. Chi-c-Kit was postulated to be responsive to exogenously added human SCF and to appropriately interact with the murine intracellular signalling machinery. It was also hypothesised that chi-c-Kit should be appropriately controlled in the absence of exogenous ligand. Endogenous murine c-Kit is not responsive to human SCF (Lev et al., 1993).

4.4.1. Strategy

The approach used to generate chimaeric GNNK+ and GNNK- c-Kit is fully detailed in sections 2.7.12-13. Briefly, the human c-Kit templates for generation of the human extracellular domain of chi-c-Kit were GNNK± c-Kit cDNA in the vector pRUFneo, originally generated by Gina Caruana (Caruana, 1996). The murine c-Kit template was a GNNK- murine c-Kit in pSP72, which was also sourced from Gina Caruana .

Primers A1 and B1 (see section 2.7.12) were used to generate double strand cDNA of the human c-Kit extracellular domain. The primers introduce restriction sites upstream of the start codon and Kozac sequence, and also incorporate the 1st 17bp of the murine transmembrane sequence in the PCR product. Primers A2 and B2 (see Section 2.7.12) were used to generate double strand cDNA of murine c-Kit

transmembrane and cytoplasmic domains. These primers introduce restriction sites at the 3' end of the cDNA, and the 5' primer contains a 17bp segment of the last 17bp of human extracellular domain.

Step 2 in the generation for the GNNK± chi-c-Kit generation was also a PCR reaction. Due to the engineered overlaps of the human extracellular domain products with the murine transmembrane/intracellular domain products described above, the two PCR products anneal in the TM region and prime the polymerase to complete double stranded full length chimaeric cDNA (see Section 2.7.13). The PCR reaction also included primers A1 and A2, which will then amplify the full-length chimaeric cDNA.

Step 3 of generating chimaeric c-Kit (GNNK + or GNNK -) utilised the introduced restriction sites at either end of the new chi-c-Kit cDNAs to facilitate ligation of the cDNAs into vectors pBluescript SK and pRUFpuro (See Section 2.7.13). pBS-SK was selected as it is a relatively small vector with restriction sites suitable for easy ligation of the chimaeric c-Kit cDNA. The cDNA is easily sequenced off this vector (using T3 and T7 primers as well as several internal cDNA primers), and the substantial polylinker will provide more flexibility in excising the cDNA to shuttle it to other vectors, including pRUFPuro. pRUFpuro was selected as it is a retroviral vector suitable for transduction of the haemopoietic target cells, and has puromycin resistance as a selectable marker. Traditionally, pRUFneo would be used in this laboratory, but conventionally, mouse knockout cells are likely to be G418 resistant, as gene disruption is typically carried out using a Neomycin resistance selectable targeting sequence.

4.4.2. *Cloning chi-c-Kit GNNK ± into pBS-SK*

The full-length products from Step 2 were digested with Bam H1 and Xba 1 to facilitate ligation into pBS-KS. Efficiencies of successful full-length ligation of chi-c-Kit (GNNK±) into pBS-SK were very low – only 1 in 24-30 clones had complete 3Kb inserts that satisfied a series of diagnostic restriction enzyme digestions verifying that they were full-length and in the correct orientation. Two clones were finally selected chi 12+ (10) and chi 12- (3a). Due to the poor efficiencies it was decided to sequence the full length of each cDNA to verify the correct isoform (GNNK±) and check for any mutations. The sequencing primers chosen are detailed in Section 2.7.14, Figure 2.4.

Clone chi 12+ (10) had 3 mutations introduced into the wild type sequence. These are depicted in figure 2.5 (A) (see section 2.7.14). Firstly, in the human extracellular domain 5, a point deletion at 1350 created a frameshift TCT to CT. A second silent mutation was detected in the murine transmembrane domain at 1603 – GTC to GTT (Val to Val). A third mutation was detected at 2334 – GCG to GGC (Ala to Gly) (See Figure 2.5, section 2.7.14).

Clone chi 12- (3a) also had 3 mutations – 2 identical to chi 12+ (10). The unique mutation was at 1564 in the mouse transmembrane domain – TTC – TC, creating a different frameshift to chi 12+ (10). It also had the silent mutation at 1591 (1603 in chi 12+ (10)) and the GCG to GGC mutation at 2322 (2324 for chi 12+ (10)) (See Figure 2.5).

This pattern indicates that the murine fragment of the chimaera generated by primers B2 and A2 must have generated the silent mutation in the TM domain and the substitution in the cytoplasmic domain. The unique mutations (TM deletion for chi 12- (3a) and EC domain deletion for chi 12+ (10)) were a result of the PCR joining the original 2 products primed with A1 and A2. It was decided to tolerate the common silent mutation, as codon usage charts did not suggest a preference to translate this codon compared to the published sequence codon.

4.4.3. Mutation corrections

PCR site directed mutagenesis was the approach chosen to resolve these mutations as described in Section 2.7.14. Briefly, the cytoplasmic mutation GGC in clone chi 12+(10) was corrected to GCG in the first round of site directed mutagenesis. A second round of site directed mutagenesis corrected the extracellular deletion at 1350. This created a complete and correct GNNK + chimaeric c-Kit cDNA (pRUFpuro chi 12+1). This was then subjected to a third round of PCR site directed mutagenesis to remove GNNK (12bp) from this clone to create a complete GNNK – chimaeric c-Kit (pRUFpuro chi 12- 1).

4.4.4. Generation of MIHC c57 and Lyn -/- (use of mIL-3)

The strategy for generation of Myb Immortalised Haemopoietic Cells (MIHC) is outlined in Figure 4.5. In essence, the truncated constitutively activated c-Myb (CT3Myb) was introduced into target murine primitive haemopoietic cells (D14 foetal liver cells) by means of co-culture of Psi2 cells (ecotropic retrovirus packaging cell line) stably transfected with the defective retroviral construct pRUF(CT3Myb) as

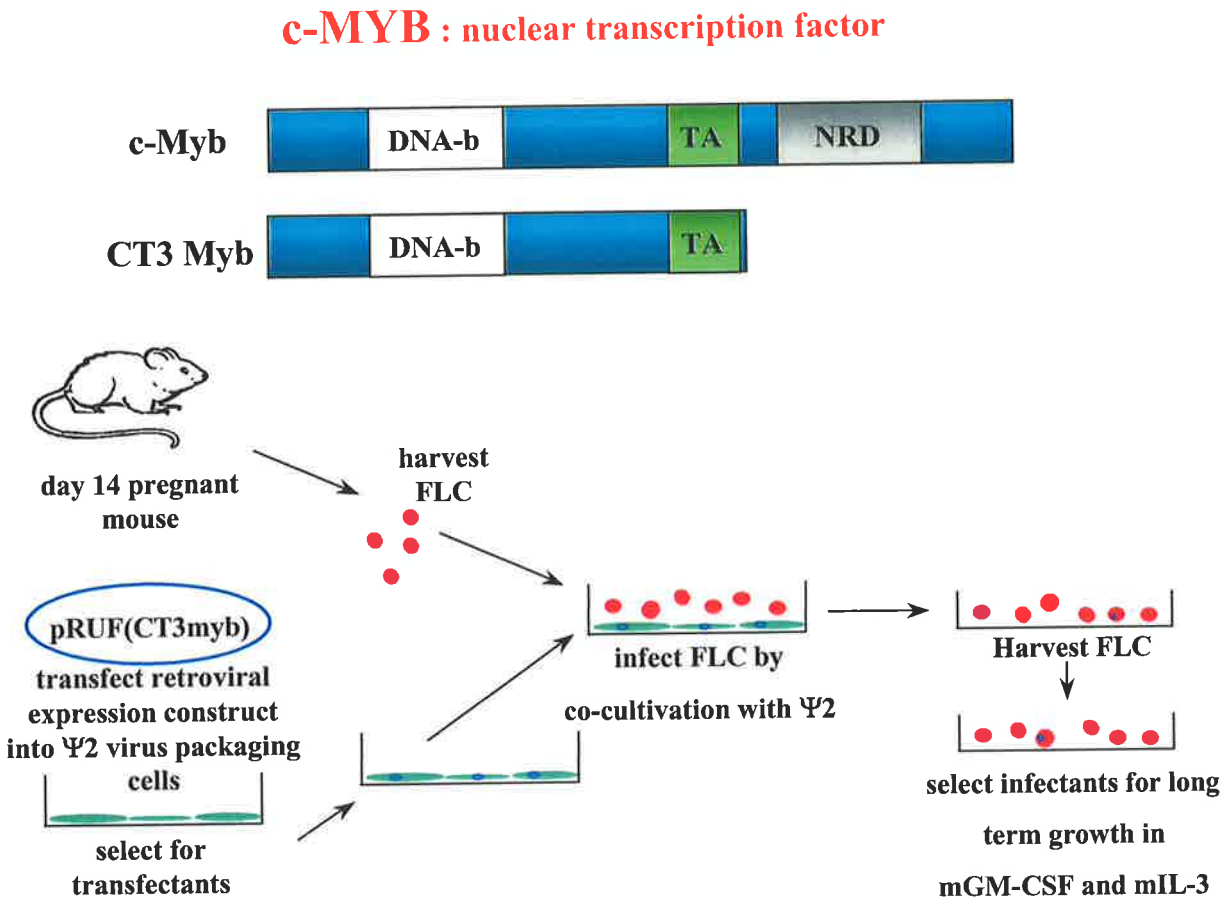

Figure 4.5

Schematic representation of the process used for generation of CT3-Myb immortalised haemopoietic cells (MIHC).

described in Section 2.7.18. The Psi2 pRUF(CT3Myb) cell line was kindly provided by Professor Tom Gonda (IMVS).

The target foetal liver cells were harvested from timed mated Lyn -/- (provided by Dr Margaret Hibbs, Ludwig Institute, Melbourne) or C57BL/6 mice (as a wild type control population) day 14 pregnant mice. C57 mice were chosen as the control, as the homozygous Lyn null mice had been extensively backcrossed (6 back crosses) onto the C57BL/6 background (Dr M Hibbs, personal communication), and this was believed to be the closest genotype to the knockout mouse foetal liver cells.

After two days co-culture with the retroviral packaging cells, foetal liver cells were harvested and resultant MIHC were selected for long term factor dependent growth in culture (in these experiments, all MIHC were maintained in a mixture of 400 u/ml mGM-CSF and 100 u/ml mIL-3). Within 2-4 weeks of co-culture, successfully transduced immature, factor dependent haemopoietic cells grow out in the cultures. These cells typically grow in clumps and are small, spherical in shape and grow in suspension. As soon as culture conditions deteriorate (typically through factor exhaustion), the cells adhere to the culture vessel, differentiate and eventually die. Typical culture micrograph images are shown in Figure 4.6.

The MIHC model was originally set up in Professor Gonda's laboratory with cells maintained in recombinant mGM-CSF alone, and the mGM-CSF was of yeast origin. The supply of factor for these experiments was actually derived from a Baculovirus source (due to the superior yields of factor from this system and the very high rate of usage of factor for these cell lines). In retrospect, it was found that the quality of the

Figure 4.6

Phase contrast micrographs of C57 MIHC – comparison of growth in yeast and baculovirus derived mGM-CSF

40X magnification phase contrast micrographs of 6-week-old cultures of C57 derived MIHC cultured continuously in either Yeast or Baculovirus derived mGM-CSF. Both factor preparations were titrated for activity on the factor dependent line FDC-P1, and equivalent doses of each factor (400u/ml) were added. The top image is representative of yeast derived factor stimulated cultures – continuous rapid growth and typically small spherical cells growing freely and in large aggregates. The lower image is representative of a culture stimulated in Baculovirus derived mGM-CSF for 6 weeks – cells lose their proliferative potential and the small, spherical, clumpy cell phenotype. They progressively differentiate and adhere to the plastic.

Yeast derived mGM-CSF

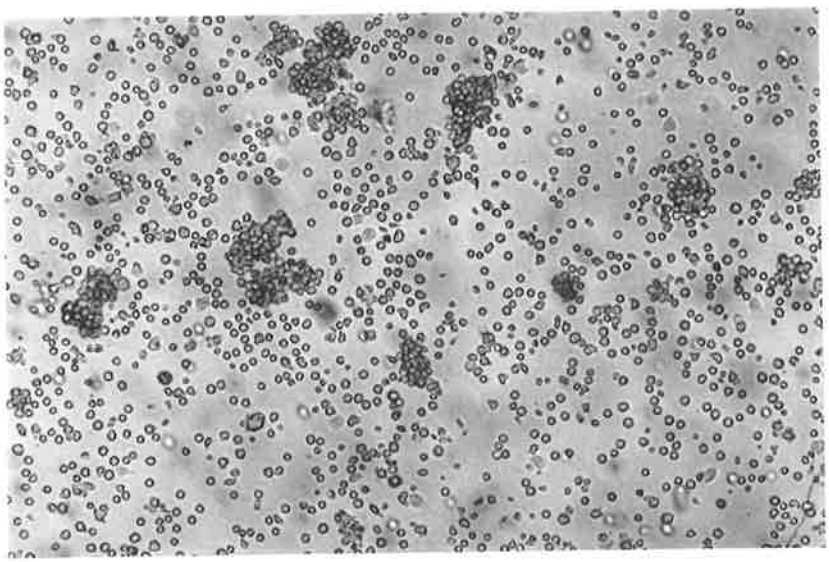

Baculovirus derived mGM-CSF

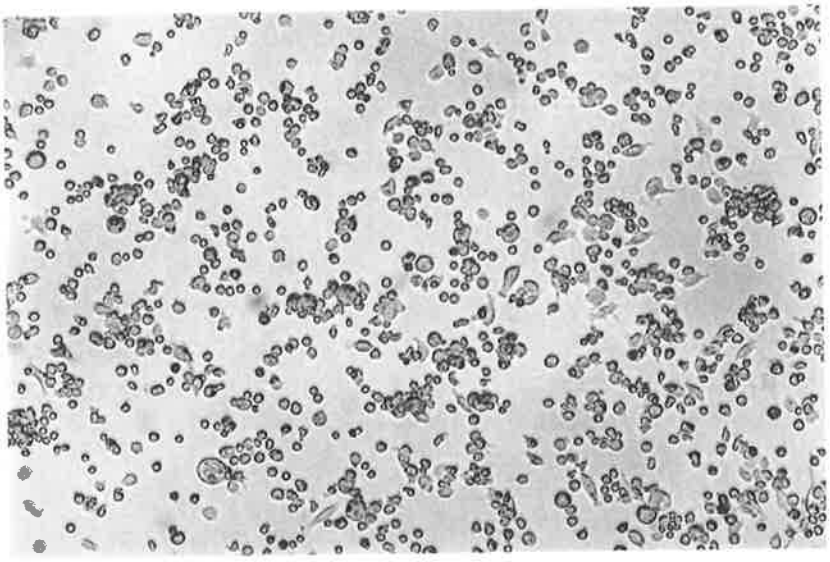

mGM-CSF from Baculovirus for these culture systems was inferior, and the cultures often differentiated and ceased to proliferate, despite being used at the same levels of activity as Yeast derived factor (as determined by titration against the factor dependent line FDC-P1). Four separate MIHC derivations using Baculovirus mGM-CSF as sole growth factor failed to generate stable MIHC pools capable of sustained growth beyond 2 months in cultures. An example of this is shown in the 4X phase contrast micrographs in Figure 4.6. In the Baculovirus GM-CSF panel, the clusters of small spherical suspension cells after 3 weeks in culture have diminished (size of clusters and number of clusters), and adherent cells are evident.

This problem was circumvented by supplementation of Baculovirus mGM-CSF cultures Baculovirus derived mIL-3. This restored the growth characteristics of the cultures to a level similar to the original Yeast derived mGM-CSF, with cultures capable of sustained continual growth with minimal differentiation for periods up to 6 months.

It was not clear in the development of these MIHC cell lines, whether or not the cultures were clonal. To exclude clonal variation as an explanation for any differences observed, three separately derived MIHC lines were developed from both Lyn -/- and C57 day 14 foetal liver cells. All subsequent analysis was performed on all lines generated, and all lines responded to stimuli in the same manner. Representative data are presented in this chapter.

4.4.5. *Morphology of MIHC lines*

As stated in the introduction to this chapter, the reason for development of these cell lines was to have a model capable of differentiation, proliferation and survival in response to exogenous factor (human SCF in this case).

It was important to have an indication of the current level of differentiation in these cells, prior to the introduction of chimaeric c-Kit and exogenous human SCF. To evaluate this, cytocentrifuge slides were prepared and stained with Giemsa. Histochemistry to detect the levels of Non-specific esterase (NSE - brown staining in these experiments) or chloro-acetate esterase (CAE - blue staining in these experiments) were also performed, as was immunohistochemistry to detect murine mast cell protease 5 (mMCP-5). All methodology is described in Sections 2..2.8-10. Giemsa staining provided overall morphology information on the cells, NSE would be indicative of cells differentiating into monocytes, CAE would indicate cells differentiating into the neutrophil lineage, and mMCP-5 was used to confirm that the cultures were not murine mast cell lines, as it is possible for these to develop when culturing primary primitive murine haemopoietic cells with mIL-3 present in the system (Kawanishi et al., 1986).

Figure 4.7 shows a representative series of micrographs of a C57 MIHC line and Lyn -/- MIHC line after approximately 3 months in culture. As can be seen in the C57 Giemsa panel, there was evidence of some differentiation in these cultures, but there was also a pool of approximately 35% undifferentiated cells (range 30 – 42%, n = 9), which presumably were the source of progeny for the continuing culture. 25% of the

Figure 4.7

Histochemical and immunohistochemical comparisons of C57 MIHC and Lyn -/- MIHC.

100X micrographs of cytocentrifuge preparations of representative parental MIHC pools stained with May-Grunwald Giemsa (Giemsa). The second panels (Esterase) are the same cells stained for Non-specific (red-brown) and Chloro-acetate (blue) Esterases (monocyte and neutrophil specific respectively). The 3rd panel is immunostained with mMCP5 (anti mast cell granule). Refer to 4.4.5 for detail. The positive control panel demonstrates the strong red staining of granules in murine bone marrow IL-3 derived mast cells (kindly provided by Dr R Wilkinson, IMVS).

Parent Lines

C57 MIHC

Lyn -/- MIHC

Giemsa

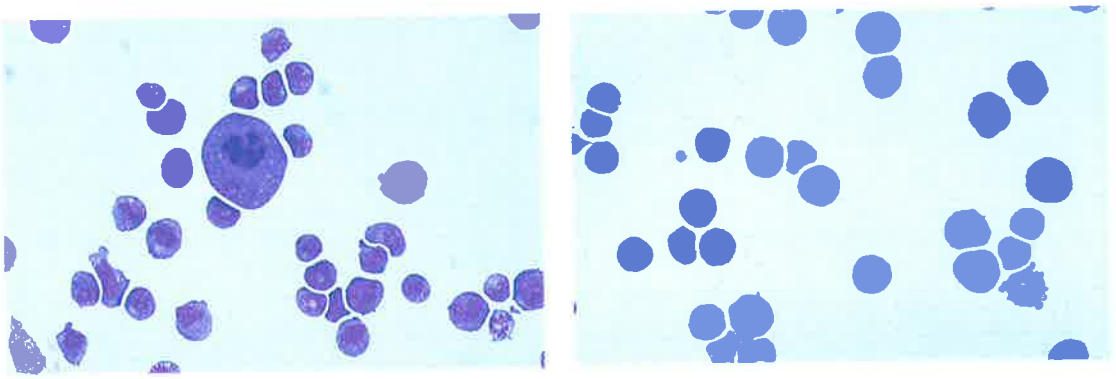

Esterase

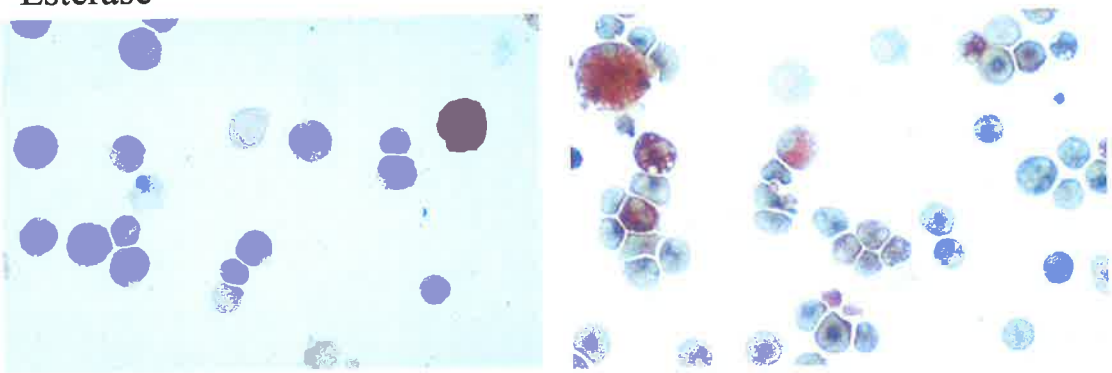

mMCP5

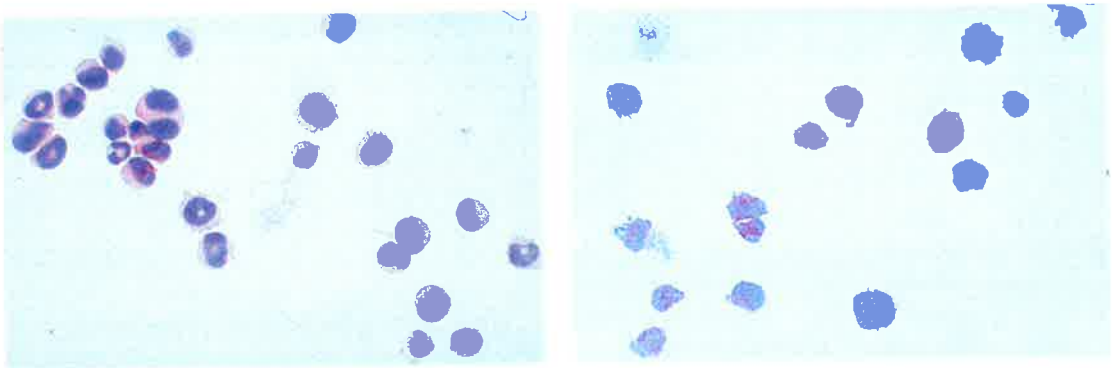

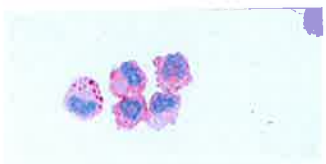

mMCP-5
Positive Control

50µm

cells appeared to be expressing NSE (range 20-45%, n = 9), and 15% weakly expressed CAE (range 5 – 25%, n = 9), suggesting that the cells were more mature than desirable and were proceeding predominantly down the monocyte differentiation pathway. mMCP5 was negative (when compared to the positive control panel demonstrating the typical granular staining pattern for this marker), confirming that the culture was not a mast cell line. The Lyn -/- MIHC line also shows evidence of differentiation (30% undifferentiated (range 27 – 40%, n = 8). In this series of micrographs, approximately 25% express NSE (range 18 – 40%, n = 8) and 10% express CAE (range 5 – 30%). Again, no mMCP-5 positive granule staining was evident in cells from these pools.

The evidence suggested that the lines are definitely immortalised – the cultures continue to grow exponentially well past 3 months in continuous culture, with a doubling time of approximately 18 hours (quite rapid), and in fact did not slow in rate for the duration of experimentation in continuous culture. It is also evident, however, that the culture has a higher than desirable proportion of cells maturing and differentiating, and in fact the composition of the mature cell pool varies with time (CAE and NSE percentages vary – data not shown). This diminished the value of these cell lines for the evaluation of differentiation responses of Kit-transduced cells to exogenous SCF.

4.5. Introduction of chi c-Kit GNNK+/- into Lyn -/- and C57 MIHC

The constructs (pRUFpuro Chi 12+ 1 and pRUFpuro Chi 12- 1) were stably transfected into the Psi2 packaging cell line (See section 2.7.17). Stable transfectants were selected by culture with Puromycin selection (2μg/ml) over 14 days. These Psi2

transfectants were then co-cultured with each of the C57 and Lyn -/- MIHC lines. Nonadherent MIHCs were harvested from the co-cultures and subjected to indirect immunofluorescence staining with Mab 1DC3 (anti Human c-Kit) as described in Section 2.3.2. These stained cells were sorted on a FACStar^{PLUS} (Becton Dickinson) and sorted pools cultured for 30 days prior to cryopreservation of large stocks for use in experimentation (to minimise genetic drift and maximise oligoclonality). Again, it is reiterated that experiments were performed on MIHC from three independent CT3Myb immortalisations to eliminate clonal variation from the analyses.

As has already been discussed in Chapter 3, it was important to select pools of MIHCs expressing comparable levels of chimaeric c-Kit to eliminate quantitative variations in the strength of signal emanating from the chimaeric c-Kit, which may change the cellular responses seen. Figure 4.8 shows the relative levels of surface expression of chimaeric c-Kit (GNNK ±) on C57 and Lyn -/- MIHC. This analysis was performed at 1 month post selection for chi-c-Kit expression by FACS sorting after labelling by indirect immunofluorescence using Mab 1DC3. As can be seen, relative fluorescence intensities for the 4 pools shown are very similar. Data from these pools is presented in the remaining figures and are representative of all MIHC derivations.

It was important to determine the differentiation status of the newly derived chi-c-Kit expressing MIHCs. Figure 4.9A and 4.9B shows the morphology of these populations one month after selection for chi-c-Kit expression. It can be seen, as in Figure 4.7, that there were various states of differentiation within the populations, but all remain within the ranges stated above for the parental cell lines (4.4.5), indicating that introduction of chi-c-Kit did not alter the phenotype of the cells in the absence of

Figure 4.8

Surface expression of chimaeric c-Kit on C57 and Lyn -/- MIHC

C57 MIHC and Lyn -/- MIHC expressing chimaeric c-Kit (GNNK±) were stained with Mab 1DC3 (anti human c-Kit) by indirect immunofluorescence, using a Sheep anti-mouse Ig – FITC (Silenus) secondary reagent. Cells were analysed on an EPICS XL flow cytometer. The forward scatter (FS) vs side scatter (SS) dot plot illustrates the live cell gate used for analysis, and each cell line is depicted in a single parameter histogram showing relative fluorescence intensity.

— Isotype matched negative control Mab (1B5 – anti Giardia IgG1)

▬ IDC3 Mab (anti human c-Kit – IgG1)

C57 MIHC chi-c-Kit GNNK- :	MFI	480
C57 MIHC chi-c-Kit GNNK+ :	MFI	988
Lyn -/- MIHC chi-c-Kit GNNK- :	MFI	491
Lyn -/- MIHC chi-c-Kit GNNK+ :	MFI	384

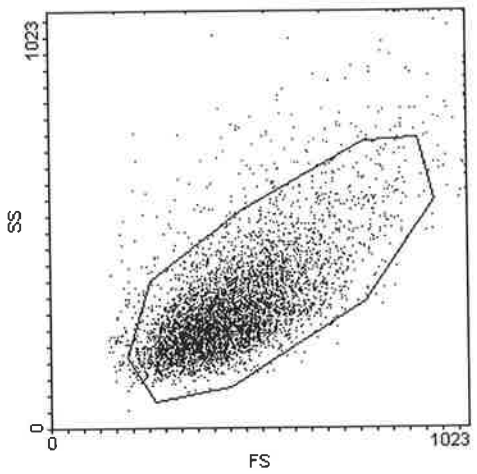

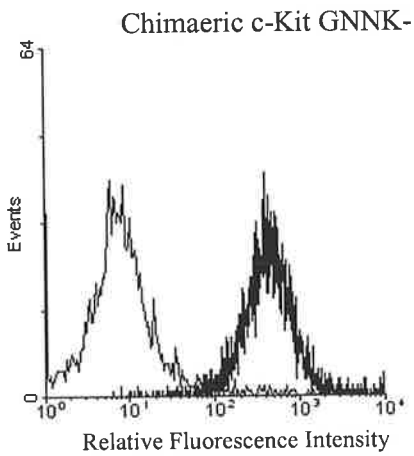

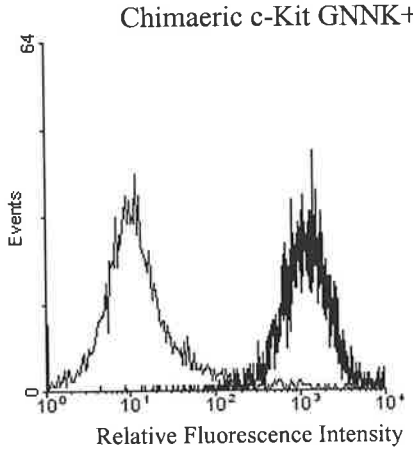

C57 MIHC

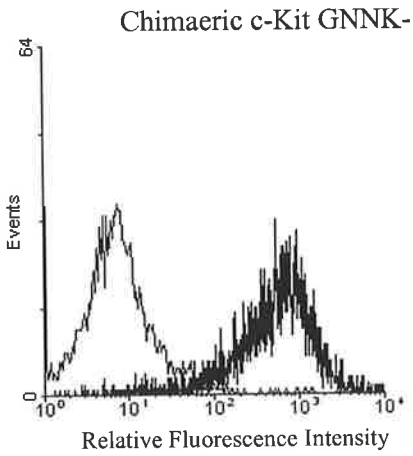

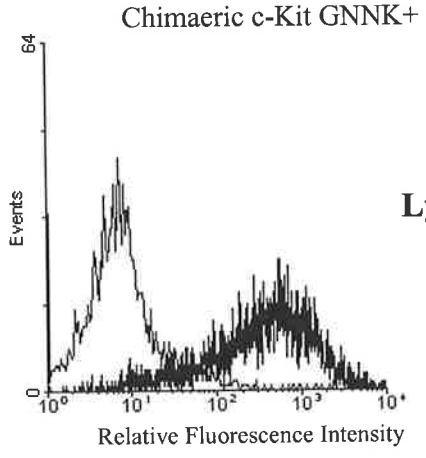

Lyn -/- MIHC

Figure 4.9

Histochemical and immunohistochemical comparisons of C57 MIHC and Lyn -/- MIHC expressing chimaeric c-Kit (GNNK±).

100X micrographs of cytocentrifuge preparations of representative MIHC pools stained with May-Grunwald Giemsa (Giemsa). The second panels (Esterase) are the same cells stained for Non-specific (red brown) and Chloro-acetate (blue) Esterases (monocyte and neutrophil specific respectively). The 3rd panel is immunostained with mMCP5 (anti mast cell granule). Refer to 4.5 for detail. The positive control panel demonstrates the strong red staining of granules in murine bone marrow IL-3 derived mast cells (kindly provided by Dr R Wilkinson, IMVS).

4.9A – C57 and Lyn -/- MIHC expressing chimaeric c-Kit GNNK –

4.9B – C57 and Lyn -/- MIHC expressing chimaeric c-Kit GNNK +

4.9A

Chimaeric c-Kit GNNK-

C57 MIHC

Lyn -/- MIHC

Giemsa

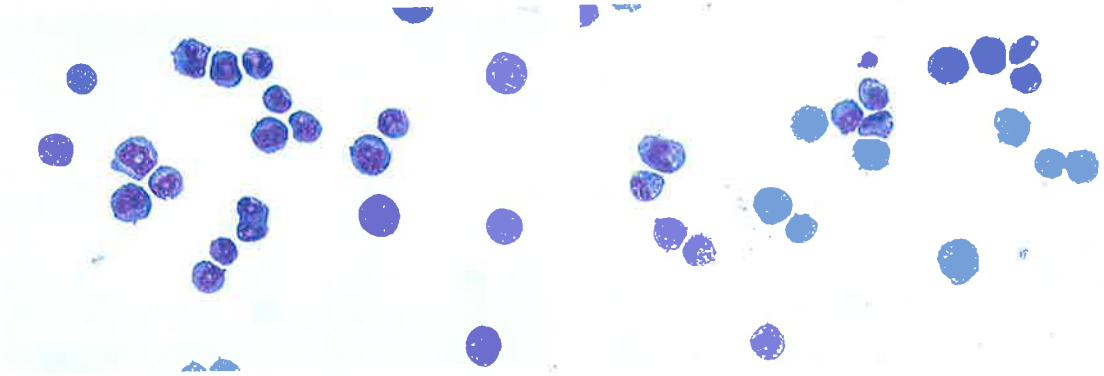

Esterase

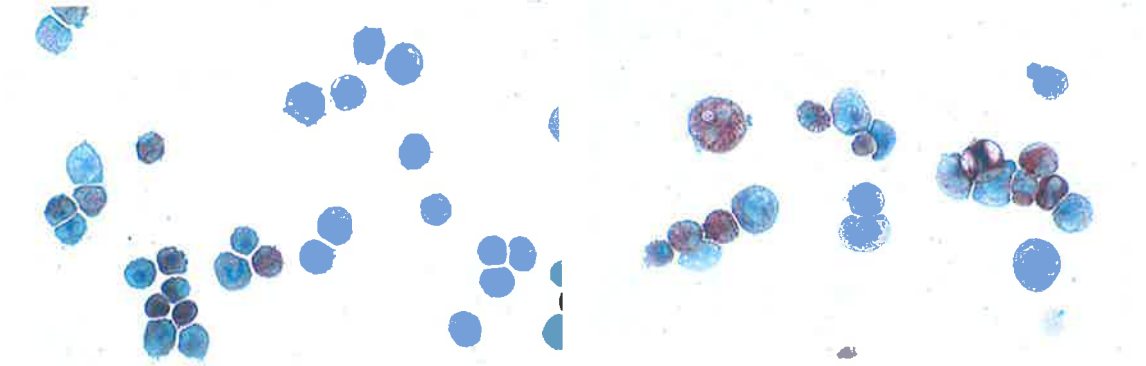

mMCP5

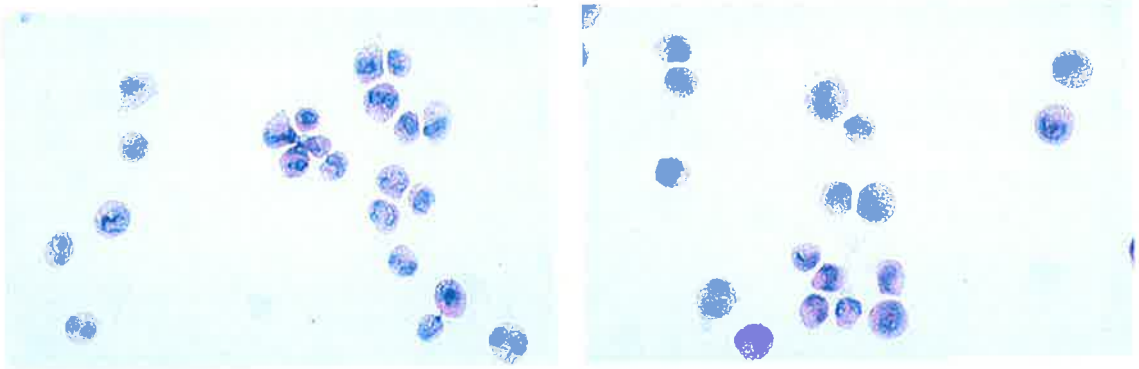

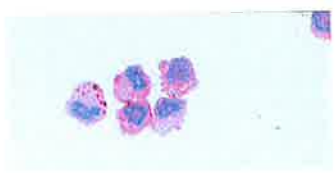

mMCP-5
Positive Control

50µm

4.9B

Chimaeric c-Kit GNNK+

C57 MIHC

Lyn -/- MIHC

Giemsa

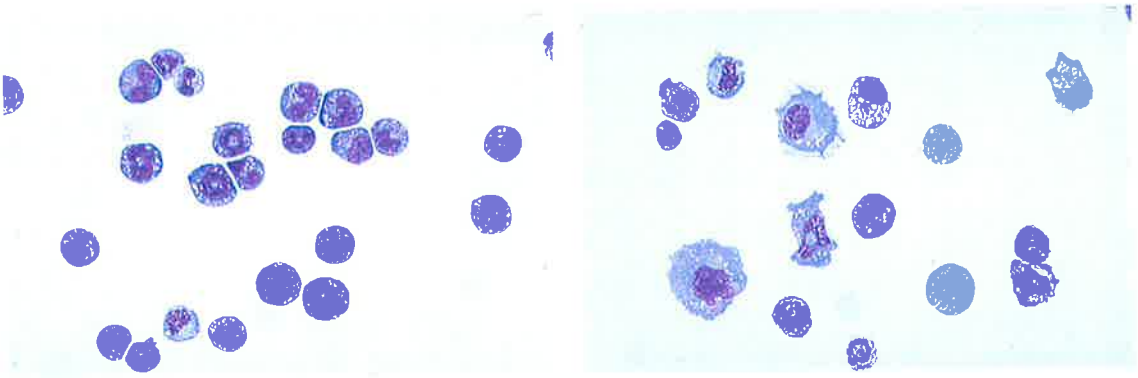

Esterase

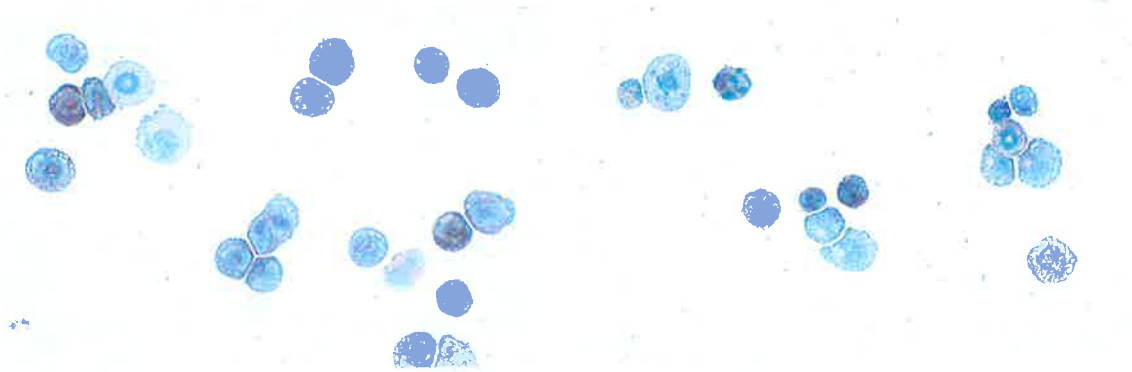

mMCP5

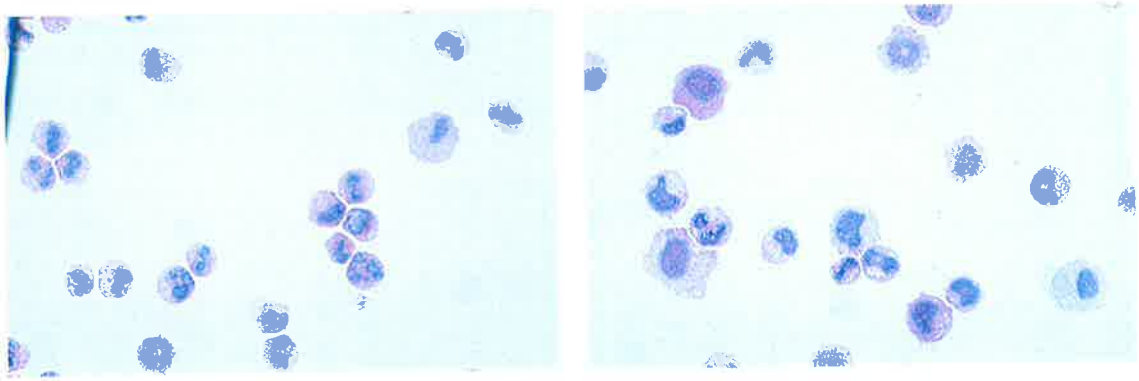

mMCP-5
Positive Control

50µm

human SCF. Furthermore, these lines were still negative for mMCP-5 in the continued presence of mIL-3.

The variability observed in NSE (non specific esterase – monocyte) and CAE (chloro-acetate esterase – neutrophil) staining is most likely attributed to culture condition variance. As has already been observed, factor levels, when inadequate, caused rapid degeneration of the early MIHC lines generated through differentiation and later death. As these cultures grow very rapidly (turnover rate of 18hrs), it is possible that the cultures periodically undergo factor deprivation to varying degrees, despite the very high levels of factor used in the system and the frequent (two to three day) subculture. This may generate waves of differentiation to monocytes and neutrophils. Monocytes will persist in culture for several days to weeks, but neutrophils will persist only very short times in culture. These phenomena may explain the variation observed in the proportions of NSE and CAE positive cells in these long-term cultures. The consequence, though, of this high and variable background of mature cells was that it was impractical to use this model to assess differentiation responses to exogenous human SCF as it was impossible to define a baseline state of differentiation of the pool under analysis. A possible solution to this may be to culture cells in a system permitting constant perfusion of fresh media and factors, but this was not investigated further in the analyses presented here.

In addition to histochemical/immunohistochemical morphology, the 4 pools analysed in Figure 4.9 were phenotyped by indirect immunofluorescence as shown in Figures 4.10A – D. As a second verification of the mast cell status of these cultures, Mab ACK2 (anti Murine c-Kit highly expressed on murine mast cells) was examined. It

Figure 4.10

Phenotyping (by surface expression analysis) of C57 and Lyn -/- MIHC expressing chimaeric c-Kit (GNNK±)

C57 MIHC and Lyn -/- MIHC expressing chimaeric c-Kit (GNNK±) were stained with Abs ACK2 (anti murine c-Kit), F4/80 (mature murine macrophage marker), M1/70 (murine monocyte marker), Thy-1 (murine haemopoietic progenitor cell marker) and GR-1 (murine granulocyte marker).

The forward scatter (FS) vs side scatter (SS) dot plot illustrates the live cell gate used for analysis, and results for each Ab are depicted in single parameter histograms showing relative fluorescence intensity.

—— Isotype/species matched negative control Ab

▬ Ab as indicated

4.10A – Lyn -/- MIHC expressing chimaeric c-Kit GNNK-
4.10B – Lyn -/- MIHC expressing chimaeric c-Kit GNNK+
4.10C – C57 MIHC expressing chimaeric c-Kit GNNK-
4.10D – C57 MIHC expressing chimaeric c-Kit GNNK+

4.10A

Lyn -/- MIHC
Chimaeric c-Kit GNNK-

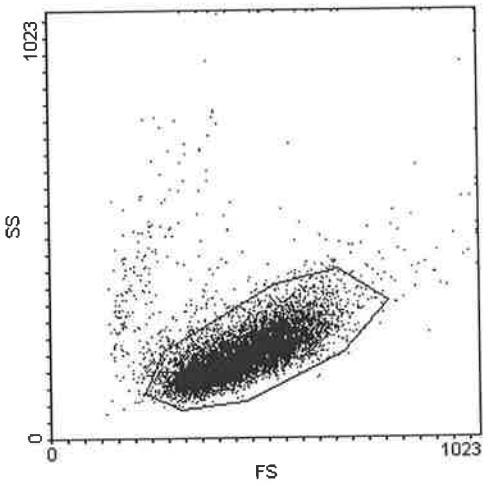

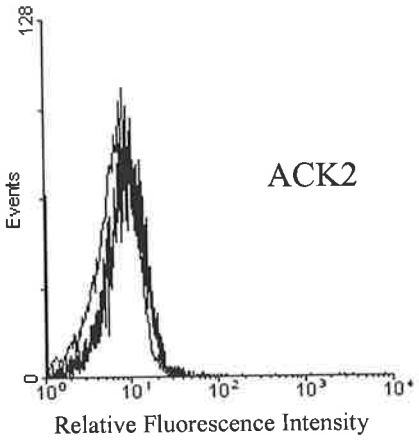

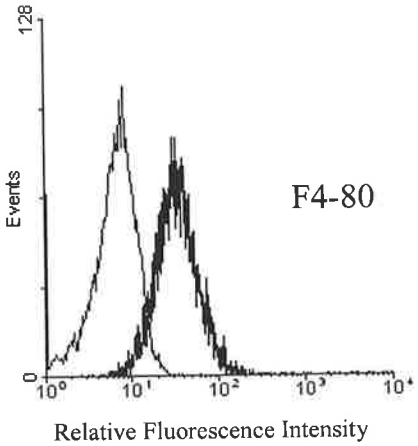

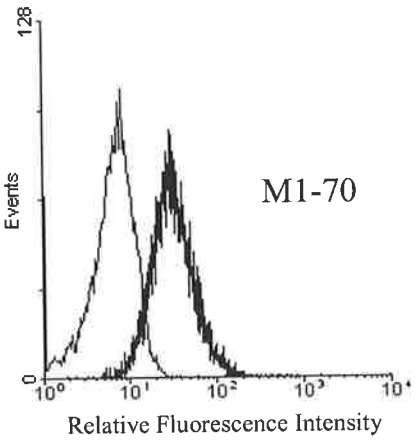

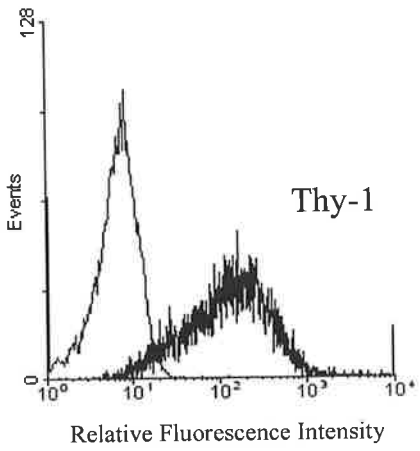

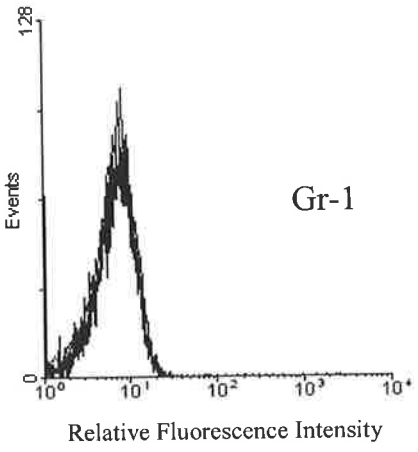

4.10B
Lyn -/- MIHC
Chimaeric c-Kit GNNK+

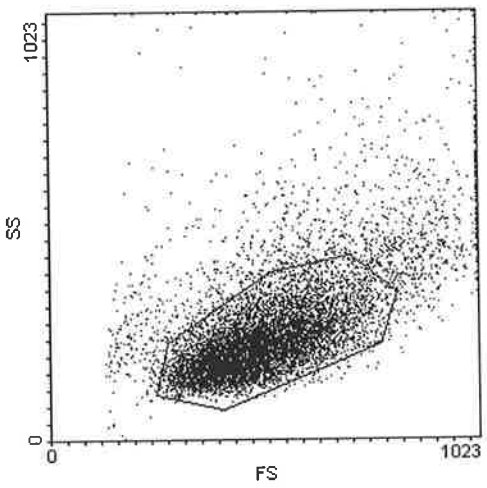

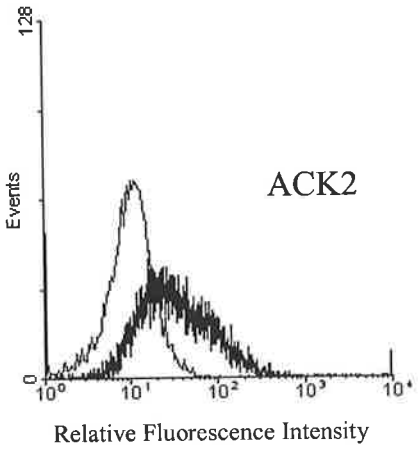

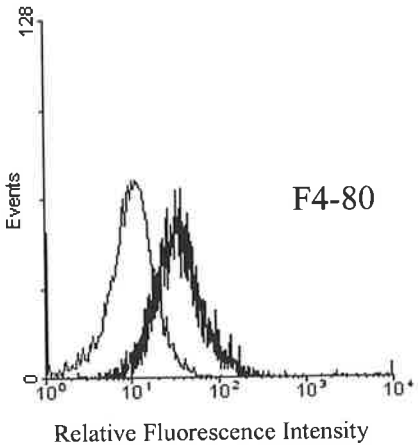

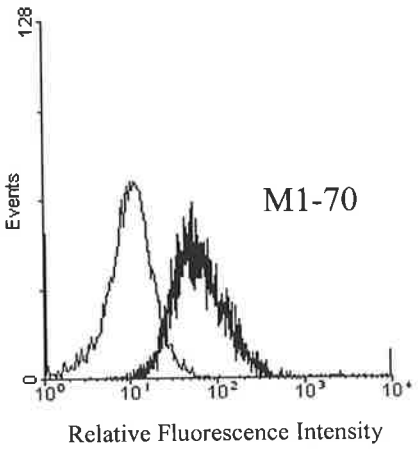

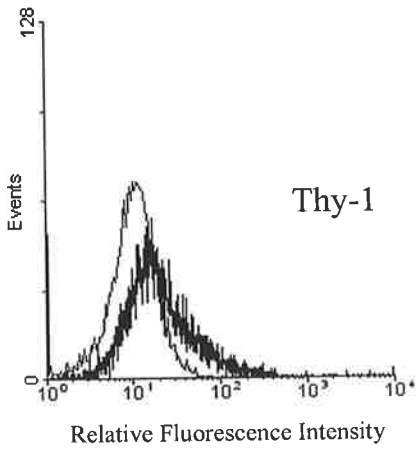

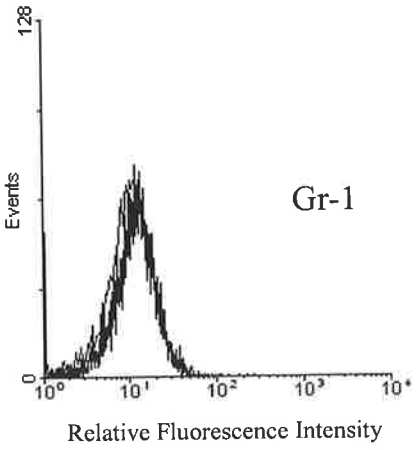

4.10C
C57 MIHC
Chimaeric c-Kit GNNK-

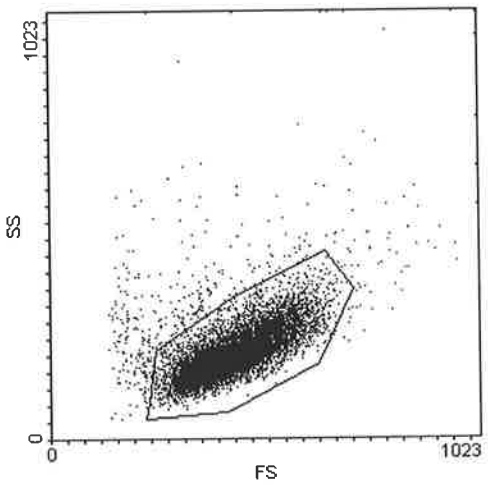

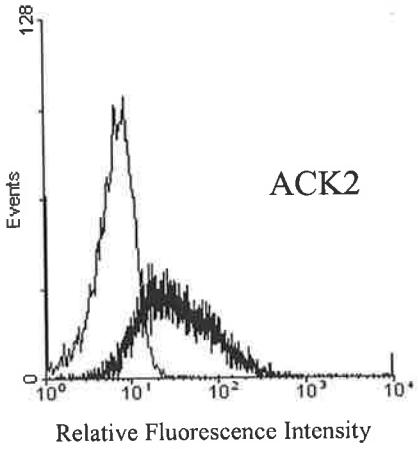

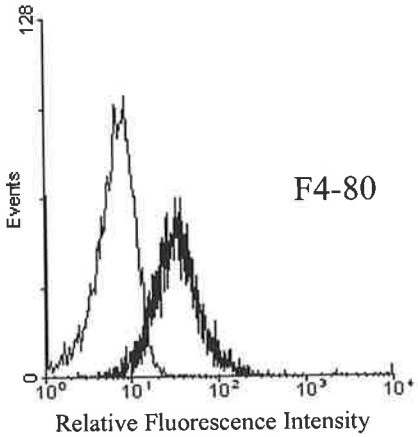

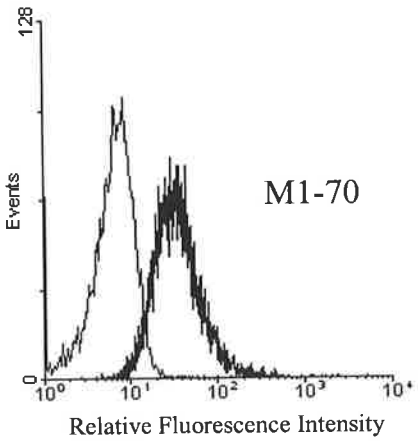

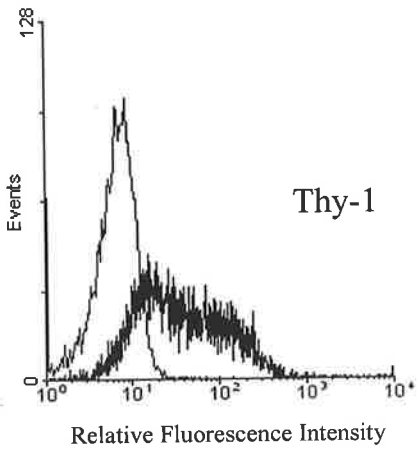

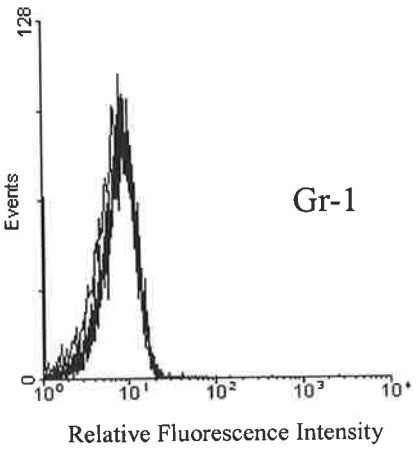

4.10D
C57 MIHC
Chimaeric c-Kit GNNK+

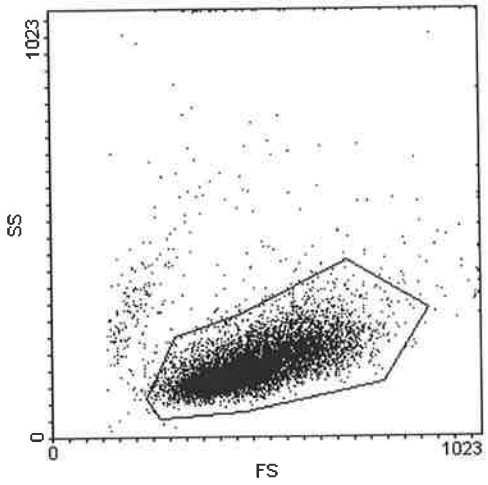

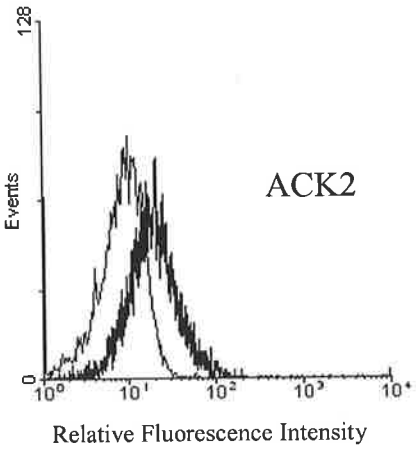

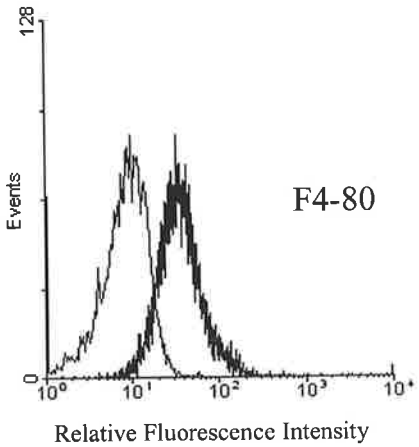

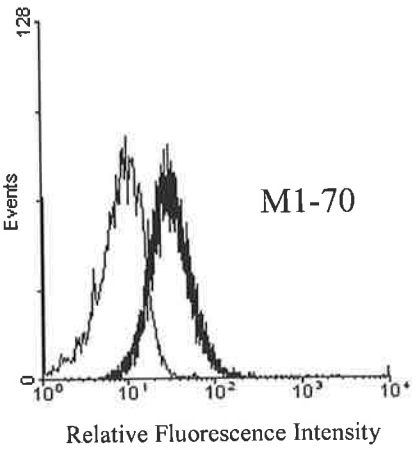

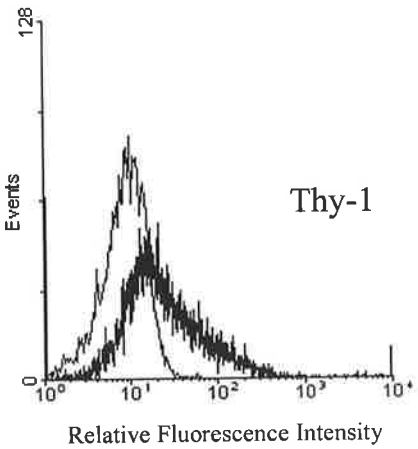

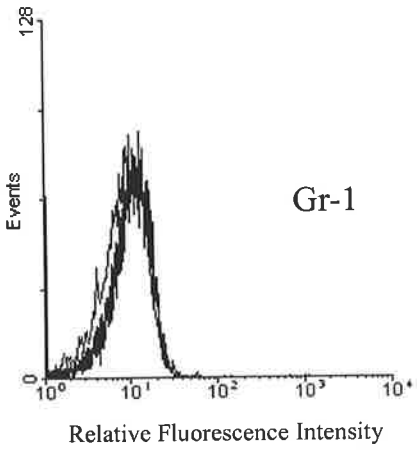

was expected that immature haemopoietic cells would express a low level of surface staining for murine c-Kit, which was indeed the case for all 4 pools of cells (MFI range from 1 to 5.5, mean 3.1, n = 16). F4/80 (mature murine macrophage marker) and M1/70 (murine monocyte marker) are markers for monocytic differentiation. It is evident in all 4 pools that they are all at least partially differentiated along the monocyte/macrophage differentiation pathway. Interestingly, all pools were negative for Gr-1 (murine granulocyte marker), although neutrophils, as already mentioned, are short lived in culture, and the process of indirect immunofluorescence staining may have removed them from the analysis, giving a false impression for the lack of presence of mature granulocytes. Of interest, Thy-1 (murine progenitor marker) was variably expressed in all 4 pools. In the C57 MIHC chi 12- c-Kit pool, Thy-1 appeared to delineate 2 subpopulations. This was not a consistent observation with other equivalent pools, and this supports the concept of the cyclical conditions of the Baculovirus derived mGM-CSF/mIL-3 supported cultures. These data show only a snap-shot of the culture composition at any point in time.

Due to the substandard culture conditions imposed on the MIHCs by using Baculovirus derived growth factors, this model was unreliable for assessing differentiation in response to SCF. It was still a very useful tool, however, to evaluate short term proliferation and survival responses to human SCF, and also useful to use for basic biochemical analysis of c-Kit signalling, comparing pools expressing or lacking Lyn. These are now addressed.

4.6. Response of Chimaeric c-Kit to human SCF in C57 and Lyn -/- MIHCs

4.6.1. Chimaeric c-Kit Internalisation in response to human SCF

Human GNNK - c-Kit was rapidly internalised upon stimulation with SCF. GNNK+ c-Kit was also internalised at a slower rate (Figure 3.9). In Figure 3.9, human c-Kit was expressed in the murine fibroblast line NIH3T3. Being adherent, confocal microscopy was used to perform the analysis of surface versus internalised protein. This approach, however, is not feasible with the MIHC pools in use here, which grow in suspension.

To analyse chimaeric c-Kit internalisation, an adaptation of standard indirect immunofluorescence staining using Mab 1DC3 was employed. In brief, cells were stimulated for varying periods of time at 37°C in media with 100ng/ml human SCF or 10ng/ml mGM-CSF (saturating doses). At the set time points, the sample was rapidly cooled to 4°C on ice, and 3 volumes of ice cold PBS with 0.4% Sodium Azide added and mixed to effectively stop any membrane transport mechanisms, blocking further capping or internalisation of c-Kit. These cells were then fixed with a non permeabilising fixative and subjected to standard indirect immunofluorescence to evaluate surface chimaeric c-Kit remaining (see section 2.3.2).

As can be seen in Figure 4.11, C57 MIHC expressing GNNK- chimaeric c-Kit very rapidly internalised most of the surface c-Kit. As was seen in Figure 3.9, the GNNK+ chimaeric c-Kit also internalised, but did so at a slower rate, and to a lesser extent over the course of the experiment (approx 70% internalisation compared to 90% with

Figure 4.11

Comparison of Lyn -/- and C57 MIHC surface expressed chimaeric c-Kit (GNNK±) internalisation in response to Human SCF.

C57 MIHC and Lyn -/- MIHC expressing chimaeric c-Kit (GNNK±) were stained by indirect immunofluorescence with Mab IDC3 (anti human c-Kit) after stimulation of cells for varying times with 100ng/ml human SCF or 10ng/ml mGM-CSF (saturating doses) as indicated. Cells were rapidly chilled and sodium azide added at each time point to immediately block completion of membrane internalisation/capping mechanisms.

Data are presented relative to unstimulated cells stained immediately with Mab 1DC3.

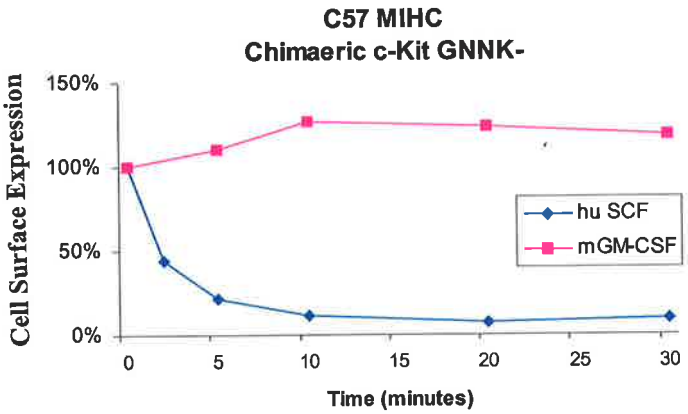
C57 MIHC
Chimaeric c-Kit GNNK-
Cell Surface Expression
150%
100%
50%
0%
0
5
10
15
20
25
30
Time (minutes)
hu SCF
mGM-CSF

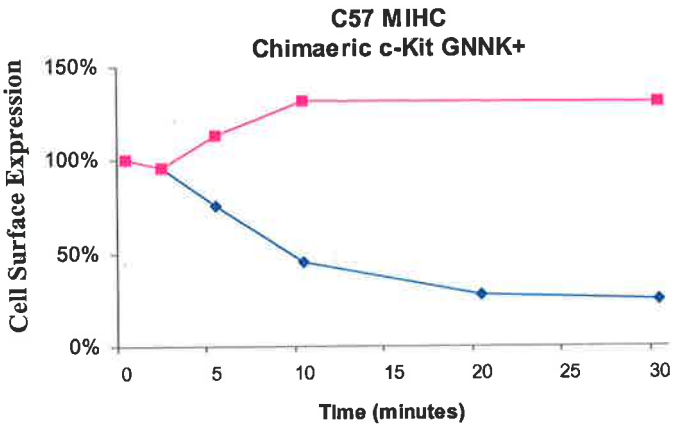
C57 MIHC
Chimaeric c-Kit GNNK+
Cell Surface Expression
150%
100%
50%
0%
0
5
10
15
20
25
30
Time (minutes)

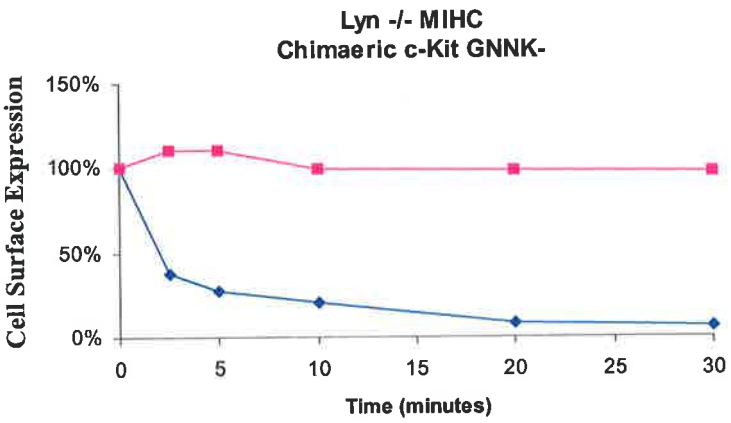
Lyn -/- MIHC
Chimaeric c-Kit GNNK-
Cell Surface Expression
150%
100%
50%
0%
0
5
10
15
20
25
30
Time (minutes)

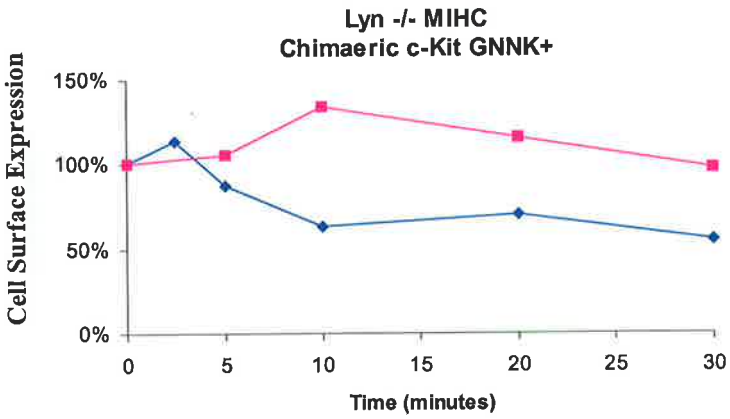
Lyn -/- MIHC
Chimaeric c-Kit GNNK+
Cell Surface Expression
150%
100%
50%
0%
0
5
10
15
20
25
30
Time (minutes)

GNNK-). In the Lyn -/- MIHC expressing GNNK- chimaeric c-Kit, there was again very rapid internalisation of 90% of surface expressed chimaeric c-Kit. There was no apparent alteration in the kinetics of this internalisation. Similarly, GNNK+ chimaeric c-Kit in Lyn -/- MIHC was more slowly and less completely internalised than GNNK- chimaeric c-Kit in Lyn -/- MIHC. In addition, the GNNK+ isoform was not internalised to the same extent in Lyn -/- MIHC as in C57 MIHC. In all cases, treating the cells with mGM-CSF instead of Human SCF had no effect at all on surface chimaeric c-Kit expression as expected. This experiment demonstrated that the chimaeric c-Kit molecules were responsive to exogenously added human SCF, and that the isoforms behaved in a similar manner to the human c-Kit previously expressed in NIH3T3 cells. There was an indication that in Lyn -/- MIHC, internalisation of the chimaeric c-Kit receptors was less than the WT C57 MIHC counterparts. This is supported by the recent findings of Voytyuk *et al* using Src kinase inhibitors (Voytyuk et al., 2003).

4.6.2. *Proliferation and Survival in response to Human SCF*

In order to evaluate the proliferative responsiveness of the Lyn-/- and C57 MIHCs expressing chimaeric c-Kit to Human SCF, a flow cytometric analysis for proliferation and survival utilising the lipophilic dye PKH26 was employed. This analysis is described in Section 2.5. This analysis allows quantification of the number of divisions of cells during the experiment, as well as net survival, as it is able to quantify total dye retained in viable cells (dead cells and associated debris are excluded in the analysis, and dye from dead cells and debris is not available for re-incorporation into the viable culture (Ashley et al., 1993)).

In these experiments, all cells were harvested from mGM-CSF/mIL-3 cultures, labelled with PKH26, and then re cultured overnight in mGM-CSF/mIL-3 cultures to stabilise the dye loaded into the cells. Cells were then extensively washed to remove all exogenous factor, and replated into either the original mGM-CSF/mIL-3 conditions, 100ng/ml human SCF alone or no factor. Triplicate cultures were harvested and analysed at days 1, 2 and 3. All data are plotted as the mean value ± SEM of the triplicate cultures. These times were chosen to ensure factor deprivation did not skew the analysis. Figure 4.12A shows the growth curve data for each isoform of chi-c-Kit in C57 and Lyn -/- MIHC. It is quite clear form these data that irrespective of the presence or absence of Lyn, GNNK- chi-c-Kit elicits superior growth of the MIHCs in response to human SCF. It is also evident that, in the absence of Lyn, the growth curves are inferior to WT (C57 MIHC). As can be seen in figure 4.12B, withdrawal of factor resulted in completion of the cells' current cell cycle and by Day 1 the viable cells in the system had undergone 1 cell division. Data were unavailable for "no factor" cells after day 1, as the cultures were no longer viable, verifying the factor dependent nature of the MIHCs. It is clear that human SCF had the same proliferative stimulus potential as mGM-CSF/mIL-3 in both isoforms of chimaeric c-Kit irrespective of the presence or absence of Lyn in the MIHCs. This suggests that firstly, the proliferative signal from c-Kit is the same irrespective of isoform (GNNK±) and secondly, Lyn plays no active role in the proliferative response of c-Kit to exogenously added SCF.

Figure 4.12C shows the survival analysis on the same samples. A number of differences became apparent. The mGM-CSF/mIL-3 culture conditions, over 3 days, demonstrated 100% maintenance of the MIHCs irrespective the isoform of chimaeric

Figure 4.12

PKH26 flow cytometric analysis – proliferation and survival response to human SCF of C57 and Lyn -/- MIHC expressing chimaeric c-Kit (GNNK±)

MIHC were stained with lipophilic dye PKH26 24 hrs prior to experiments. Cells were then harvested, washed and set up in triplicate cultures in 96 well plates in either mGM-CSF/mIL-3, 100ng/ml human SCF or no factor and harvested for analysis as described in Section 2.4 on an EPICS XL flow cytometer at Days 0, 1, 2 and 3. Data are presented as mean ± SEM (n= 3).

4.12A – Total Cell Yield Data

4.12B – Cell Division Data of same sample

4.12C – Cell Survival Data of same sample

4.12A

Total Cell Yield

Cell Count

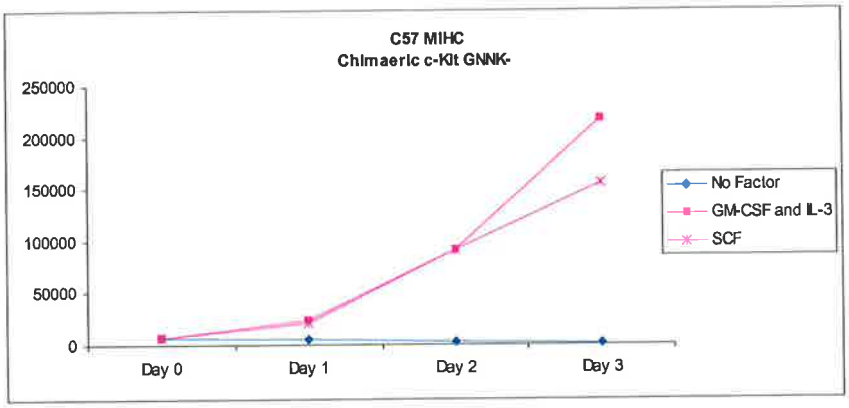

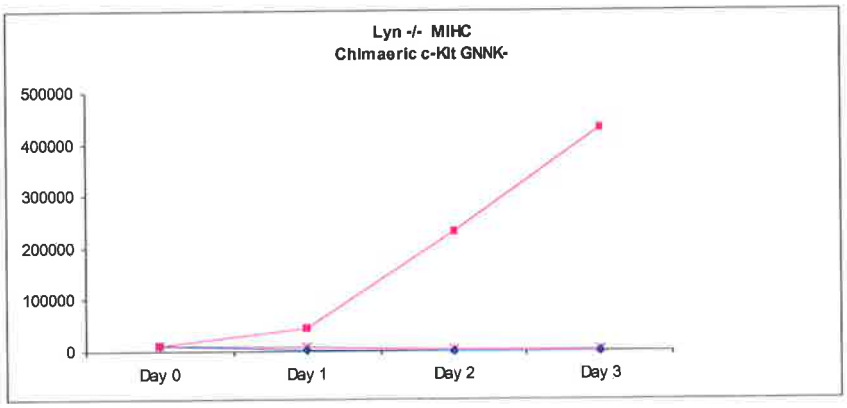

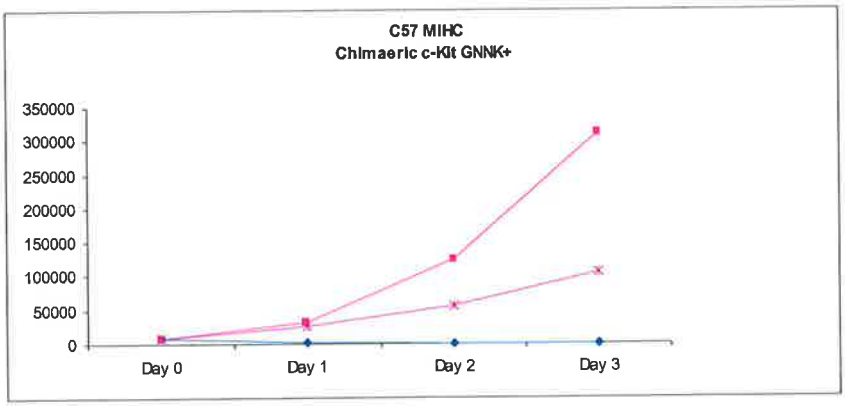

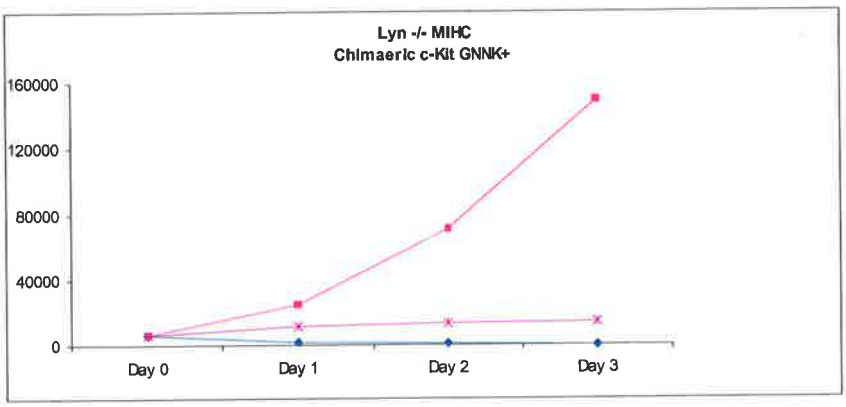

4.12B

Cell Divisions

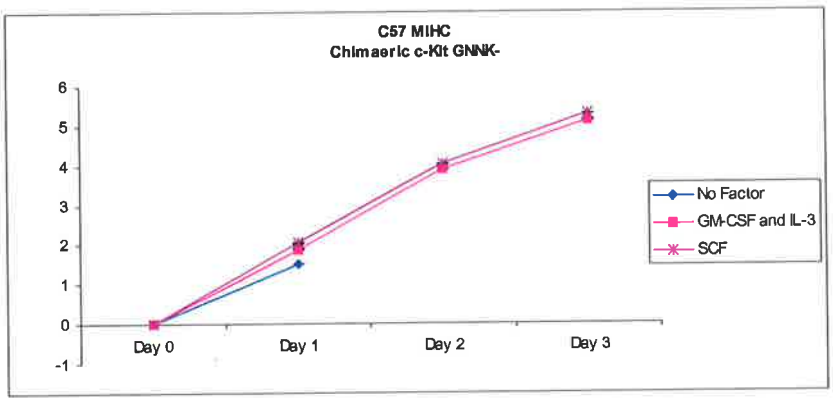

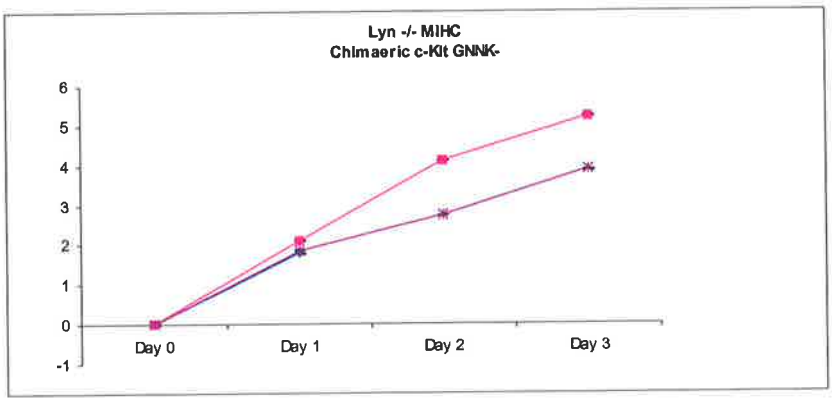

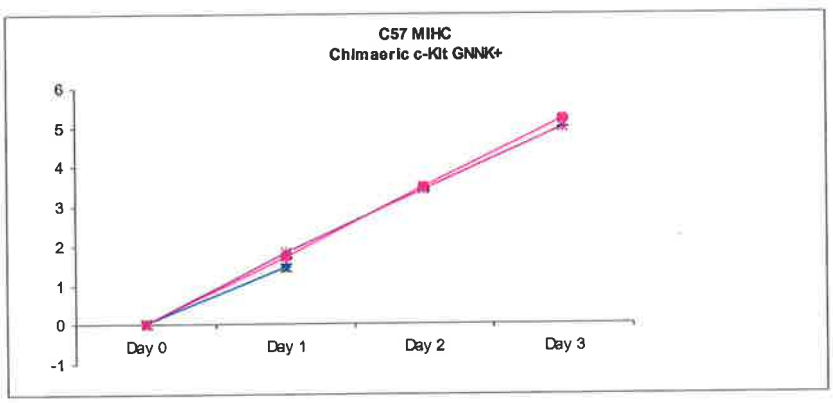

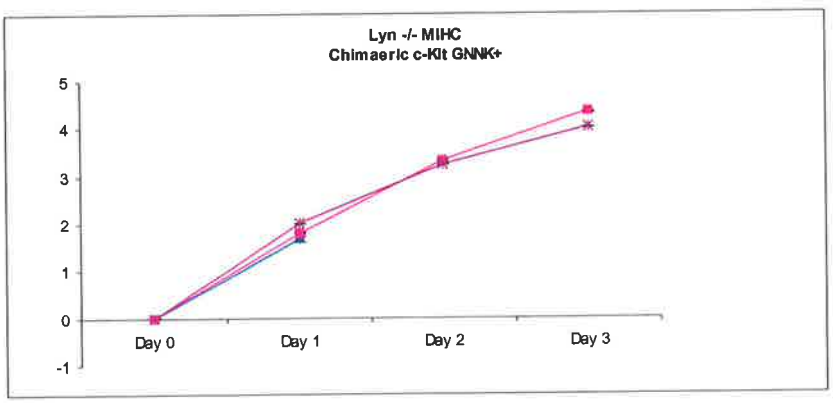

4.12C

Cell Survival

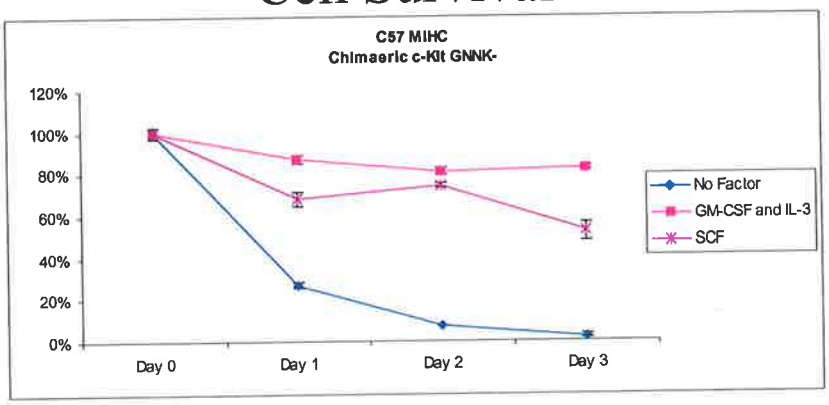

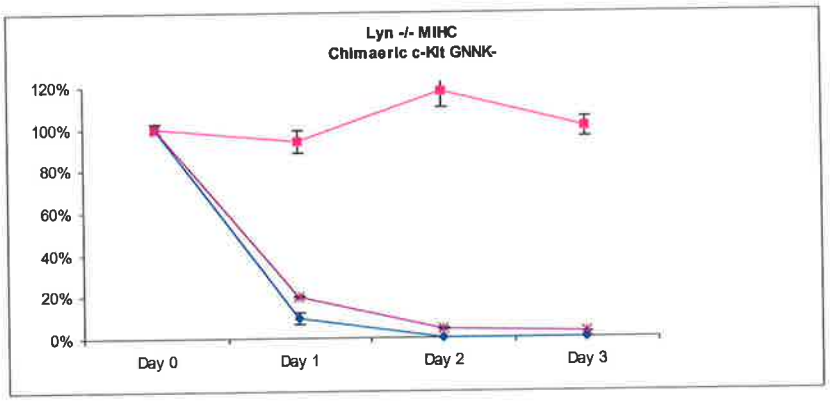

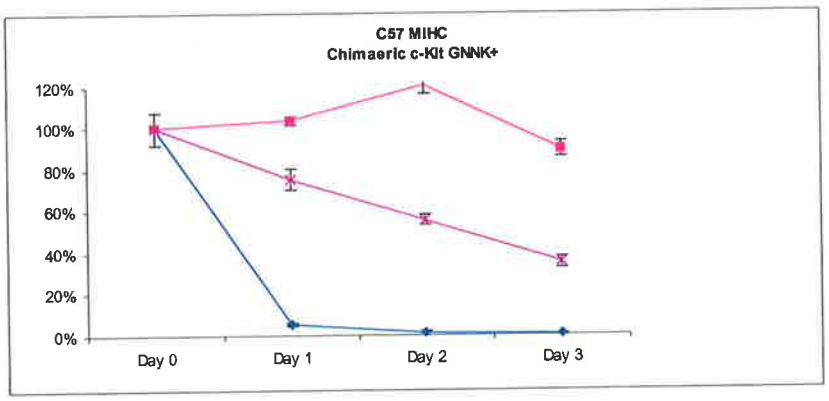

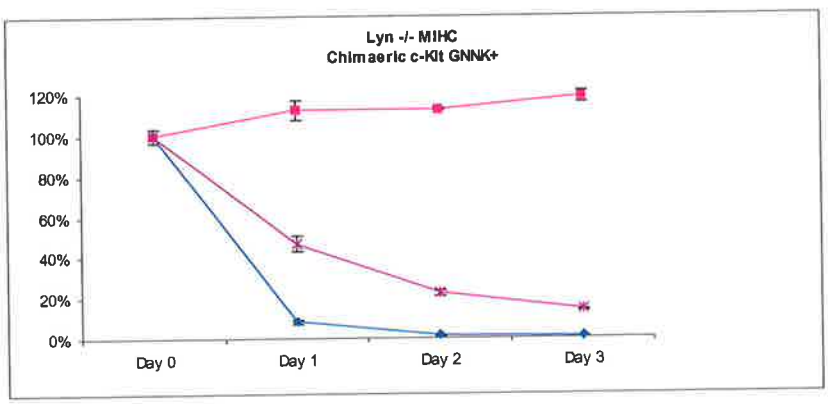

c-Kit expressed or the presence/absence of Lyn as expected. When cultured in human SCF, the GNNK- isoform in C57 MIHC is capable of maintaining 70-80% viability over 3 days, in contrast to GNNK+ in C57 MIHC (only 40% viability at day 3). In the absence of Lyn (Lyn -/- MIHC), survival of cells expressing either isoform of chimaeric c-Kit was reduced compared to the C57 MIHC counterparts. This lead to the conclusion that the survival signal emanating from the 2 isoforms of c-Kit is qualitatively different and that the presence of Lyn may contribute to this survival response, as both isoforms performed less effectively in maintaining survival in the Lyn -/- MIHCs.

4.7. Chimaeric c-Kit Downstream Signalling Analysis- Lyn-/- vs C57 MIHCs

To further understand the signalling kinetics/alterations resulting from the two isoforms of chimaeric c-Kit in the presence/absence of Lyn, a large series of biochemical analyses were performed on the MIHC pools. These analyses were the same range of treatments and immunoblots performed in chapter 3 on NIH3T3 cells expressing the human GNNK± c-Kit isoforms. Briefly, cells were starved for 2 hours, then stimulated with a saturating dose of human SCF (100ng/ml) for various times up to 20 minutes. Cells were then lysed, immunoprecipitated (as required) with KIT-4 Mab, separated on 8% SDS-PAGE, electro-blotted onto PVDF membrane and probed as indicated. The immunoprecipitates or lysates were split over 4 replicate gels to allow simultaneous immunoblotting and eliminate the need for stripping membranes to reprobe with new primary antibodies. The methodology is described in full in section 2.6.

Total c-Kit levels for Lyn -/- MIHCs expressing either isoform of chimaeric c-Kit were indistinguishable and approximately the same level as that of the control MO7e c-Kit immunoprecipitate used in this series of experiments. This can be seen in panel (i) of Figures 4.13 A and B. The C57 MIHCs expressing either isoform of chimaeric c-Kit had chi-c-Kit levels 3-4 fold higher than the control sample (panel (i) in Figures 4.13 C and D. This is higher than was expected, given the surface expression data shown in Figure 4.8, and is suggestive of a larger intracellular pool of c-Kit in these cells.

In all cases, upon SCF stimulation, chimaeric c-Kit protein smeared to higher molecular weight irrespective of the presence/absence of Lyn at approx 1-2.5 minutes (GNNK- chimaeric c-Kit – 4.13 A and 4.13 C) and 5 - 10 minutes (GNNK + chimaeric c-Kit – 4.13 B and 4.13 D). This is attributed to ubiquitination, shown in panel (iii) of figures 4.13 A-D, which shows identical kinetics and molecular weight to c-Kit protein. These data support the previous kinetic information for human c-Kit in NIH3T3 cells shown in chapter 3, Figure 3.8.

There was no difference evident in the rate of degradation of the chimaeric c-Kit isoforms when comparing Lyn MIHCs to C57 MIHCs. Lyn -/- MIHCs have degraded chimaeric c-Kit (50% for GNNK- and 25% for GNNK+) after 20 minutes stimulation with human SCF (4.13 A(i) and 4.13 B(i)). Approximately 50% of the chimaeric c-Kit (either isoform) in C57 MIHCs was degraded at 20 minutes (Figures 4.13 C(i) and 4.13 D(i)). This parallels data shown for surface internalisation in Figure 4.11.

Figure 4.13

Biochemical analyses of signalling induced by Hu SCF on C57 and Lyn -/- MIHC expressing chimaeric c-Kit (GNNK±).

Cells were serum/factor deprived for 2 hrs prior to stimulation with 100ng/ml human SCF for the times indicated. At each time interval, an equivalent number of cells (protein levels were validated to be equivalent using the Micro BCA assay for protein estimation – see Section 2.6.3) were lysed in 1% NP40 with protease and phosphatase inhibitors, and c-Kit immunoprecipitated with Mab Kit4 (anti-human c-Kit, IgG2a). Immunoprecipitates were separated on reducing SDS-PAGE and western blotted for:

i) c-Kit
ii) Phosphotyrosine
iii) Ubiquitin
iv) P85 subunit of PI3K

Western blots were developed using Alkaline Phosphatase coupled secondary reagents (anti Mouse or rabbit Ig (Silenus)) and ECF Substrate (Amersham), then visualised on a Fluorimager 595 (Amersham). Blots were quantitated using ImageQuant Software.

In all experiments, an aliquot of "reference control" was included (MO7e stimulated for 2 mins with Human SCF and c-Kit immunoprecipitated with Kit-4 MAb). This serves as an internal reference control for individual blots, permitting direct comparisons of quantitative data derived from each blot. All data is expressed as a percentage of this reference control.

4.13A – Lyn -/- MIHC expressing chimaeric c-Kit GNNK-
4.13B – Lyn -/- MIHC expressing chimaeric c-Kit GNNK+
4.13C – C57 MIHC expressing chimaeric c-Kit GNNK-
4.13D – C57 MIHC expressing chimaeric c-Kit GNNK+

4.13A

Lyn -/- MIHC
Chimaeric c-Kit GNNK-

i)

M+ M- 0 1 2.5 5 10 20

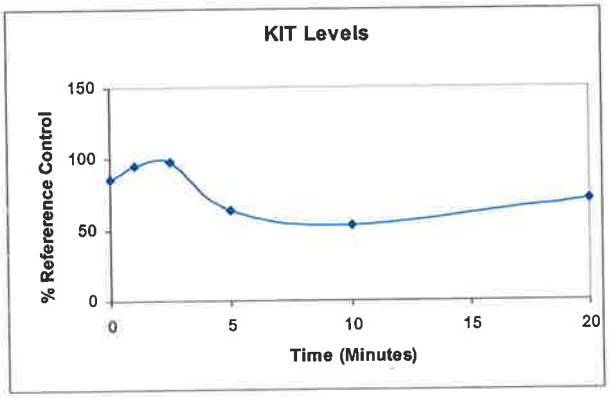

ii)

M+ M- 0 1 2.5 5 10 20

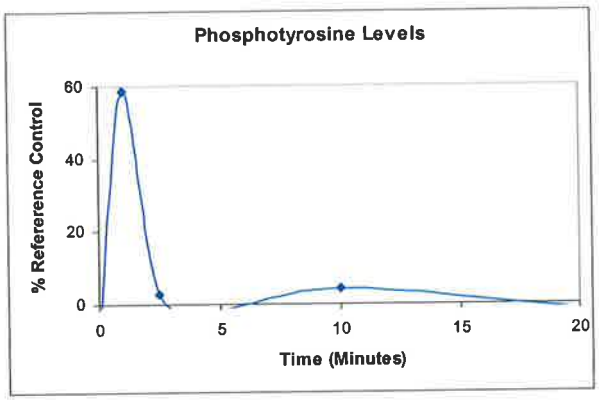

iii)

M+ M- 0 1 2.5 5 10 20

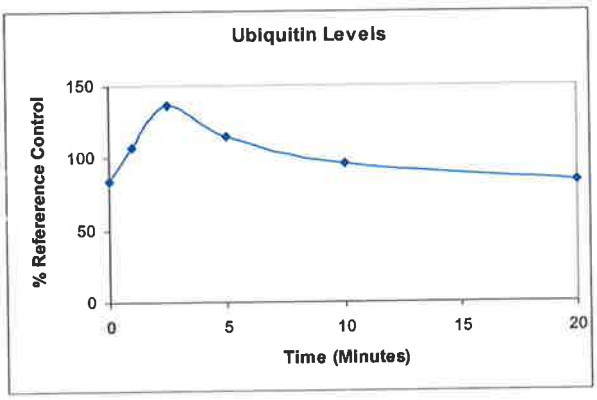

iv)

M+ M- 0 1 2.5 5 10 20

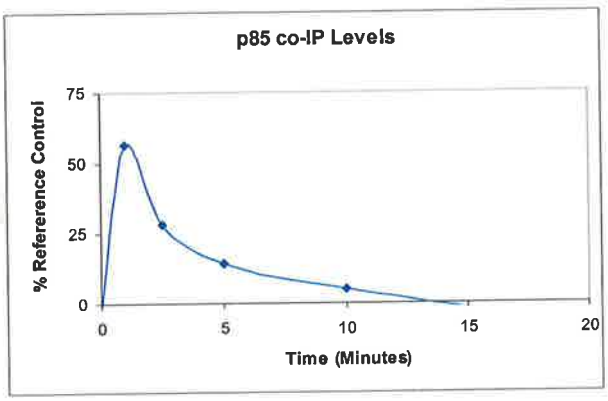

4.13B

Lyn -/- MIHC
Chimaeric c-Kit GNNK+

i)

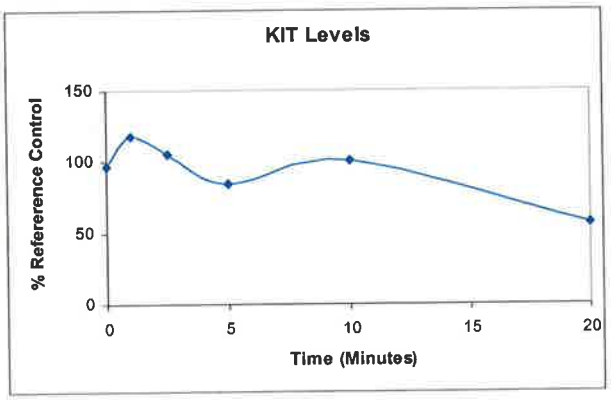

ii)

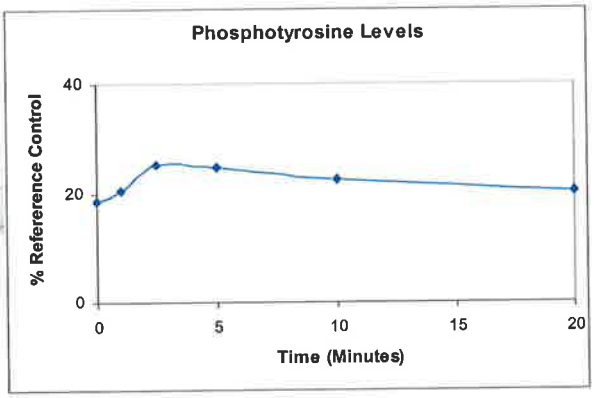

iii)

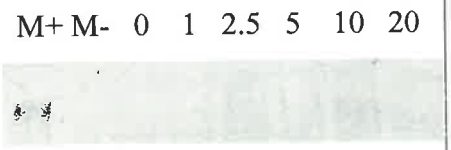

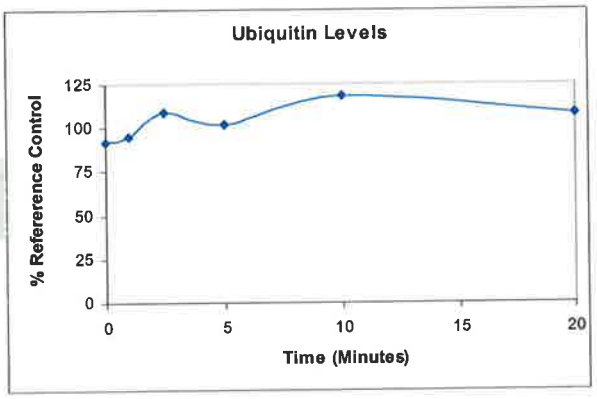

iv)

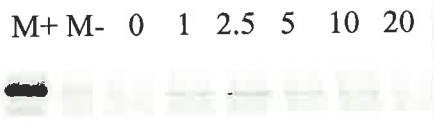

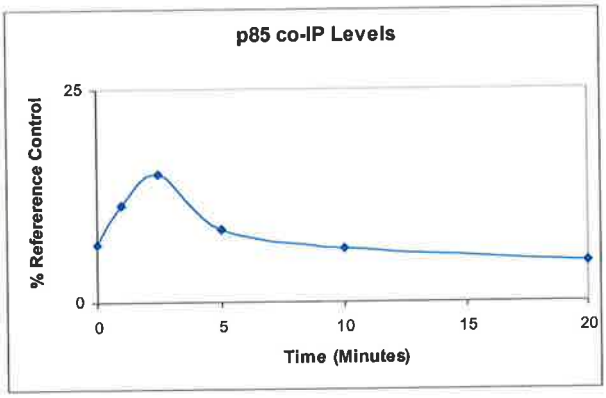

4.13C

C57 MIHC
Chimaeric c-Kit GNNK-

i)

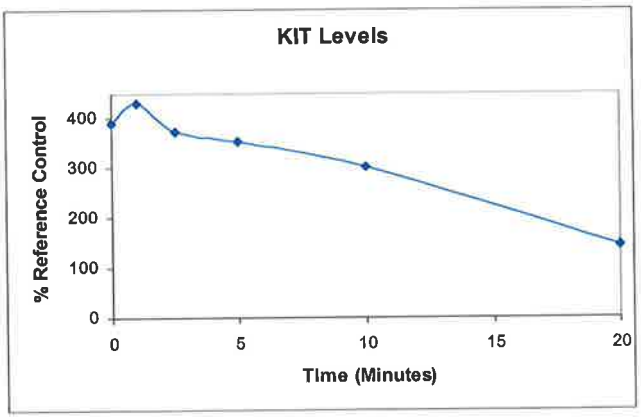

ii)

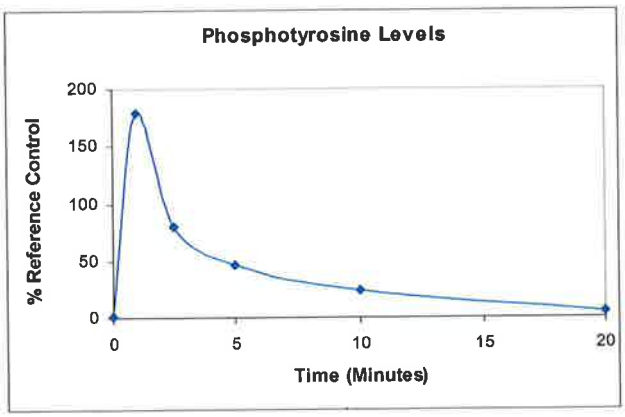

iii)

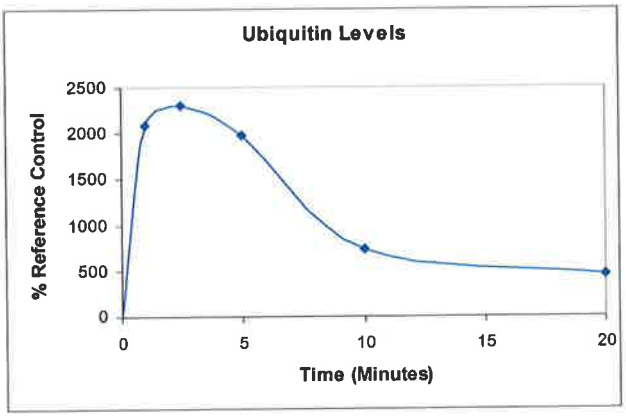

iv)

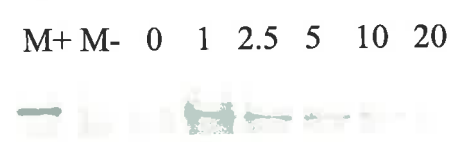

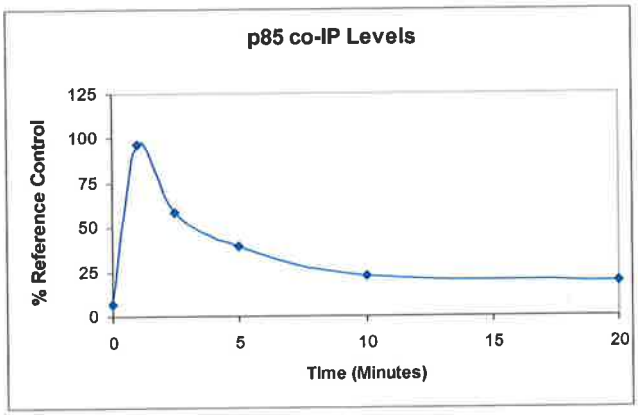

4.13D

C57 MIHC
Chimaeric c-Kit GNNK+

i)

M+ M- 0 1 2.5 5 10 20

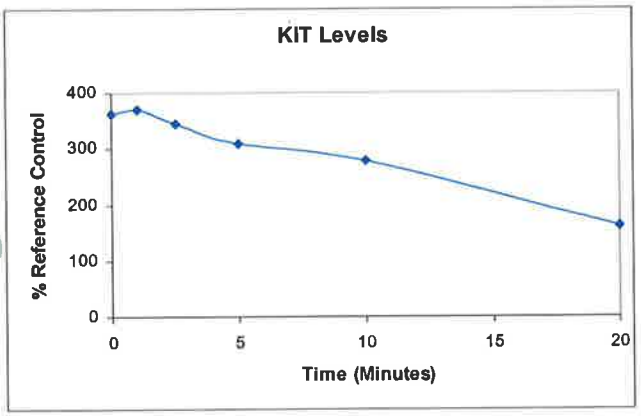

ii)

M+ M- 0 1 2.5 5 10 20

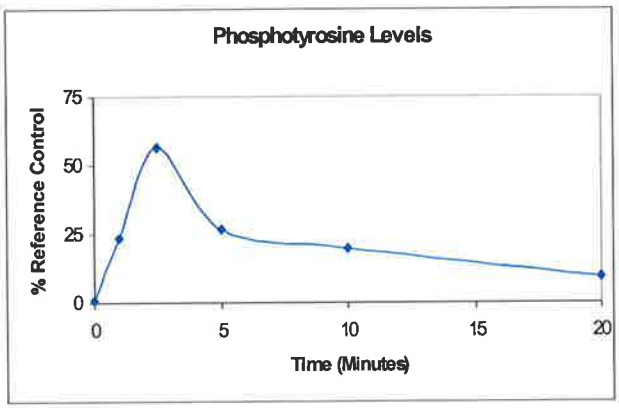

iii)

M+ M- 0 1 2.5 5 10 20

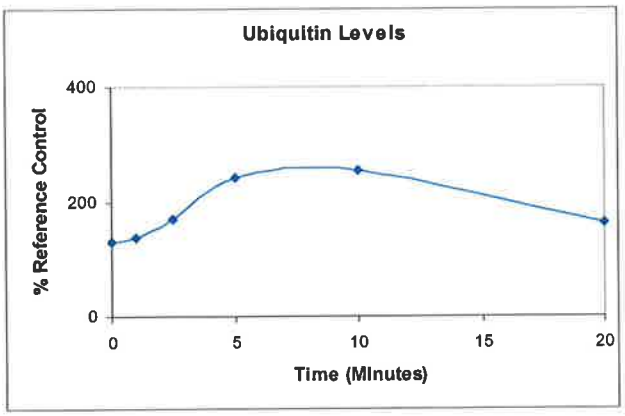

iv)

M+ M- 0 1 2.5 5 10 20

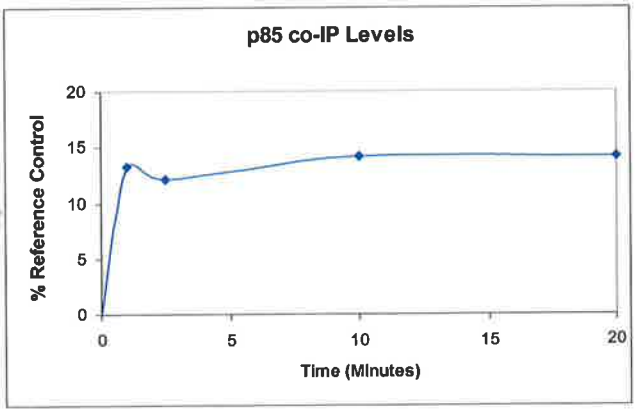

Total phosphorylated chimaeric c-Kit is illustrated in figures 4.13 A-D in panel (ii). Lyn -/- MIHC chi-c-Kit GNNK- displayed peak phosphorylation at 1 minute at approx 60% of control levels (4.13 A (ii)). Lyn -/- MIHC chi-c-Kit GNNK+ displayed peak (very weak) phosphorylation at 2.5 minutes at 20-25% control levels (4.13 B (ii)). In WT C57 MIHC chi-c-Kit GNNK-, Kit phosphorylation also peaked at 1 minute (approx 180% control levels – Figure 4.13 C (ii)) and C57 MIHC chi-c-Kit GNNK+ again at 2.5 minutes (55% control levels – Figure 4.13 D (ii)).

The 3 fold difference in levels of chi-c-Kit between Lyn and C57 are comparable to the levels of c-Kit in these cells (as already demonstrated). These data shows kinetics slightly faster than that previously shown for the 2 isoforms of human c-Kit in NIH3T3 cells (figure 3.8), but confirms that GNNK- c-Kit is more rapidly and more extensively phosphorylated than GNNK+ in the presence or absence of Lyn. This faster kinetics may simply be due to more efficient signalling being possible in this system – the chimaeric c-Kit has an appropriate murine c-Kit sequence in the cytoplasm of cells which would be expected to have c-Kit expressed and functional (ie immature murine haemopoietic cells), as distinct from the system used in chapter 3 where human c-Kit was expressed in a murine fibroblast cell type that would not normally express c-Kit and therefore not necessarily have in place all the appropriate downstream signalling components in appropriate concentrations.

The ability to recruit the p85 subunit of PI3-K was also assessed in Figures 4.13 A-D, panel iv. Lyn -/- MIHC chi-c-Kit GNNK- was very efficient at recruiting p85 (approx 60% of control at 1 minute Fig 4.13A (iv)), when compared to Lyn -/- MIHC chi-c-Kit GNNK + (approx 15-20% of control at 2.5 minutes - Fig 4.13 B (iv)). C57

MIHC chi-c-Kit GNNK- was higher, recruiting 100% of reference control p85 at 1 minute (Figure 4.13 C (iv)) and C57 MIHC chi-c-Kit GNNK+ recruited 15% of control p85 at 2.5 minutes (Figure 4.13 D (iv)). It is quite clear that there is direct correlation between the level and kinetics of phosphorylation achieved of the chimaeric c-Kit and the level of p85 subunit recruited. The presence or absence of Lyn had no influence on p85 recruitment as expected, given these two molecules associate at distant sites on the cytoplasmic domain of c-Kit (Figure 4.4), and any indirect effects of the presence/absence of Lyn are unlikely to be seen in the short time course of these experiments.

MAPK and phosphorylated MAPK levels were also investigated in this series of experiments. As shown in Figures 4.14 A-D panel i, total MAPK levels in all cell types (Lyn -/- or C57 MIHCs expressing either isoform of chimaeric c-Kit) were similar (4-7 times control levels) as expected. Lyn -/- MIHC chi-c-Kit GNNK- efficiently elicited phosphorylation of MAPK (p42 and p44) at 1- 2.5 minutes (approx 300% control Figure 4.14 A (ii)). Lyn -/- MIHC chi-c-Kit GNNK+ was approx 1/3 the efficiency at 2.5 minutes (100% of control Figure 4.14 B (ii)). C57 MIHC chi-c-Kit GNNK- elicited peak phosphorylation of MAPK at 1 minute (1000% control Figure 4.14 C (ii)) and C57 MIHC chi-c-Kit GNNK+ approx 500% of control at 2.5 minutes Figure 4.14 D (ii)). The difference in levels of activation can be attributed to the c-Kit levels and extent of phosphorylation of c-Kit. This infers that the presence or absence of Lyn has had no effect on the ability of the chimaeric c-Kit to stimulate MAPK activation, and the only determining factor is the GNNK± isoform status. This is supported in the previous study using human c-Kit in NIH3T3s shown in Figure 3.8.

Figure 4.14

Biochemical analyses of signalling induced by Hu SCF on C57 and Lyn -/- MIHC expressing chimaeric c-Kit (GNNK±).

Cells were serum/factor deprived for 2 hrs prior to stimulation with 100ng/ml human SCF for the times indicated. At each time interval, an 4 x 10^5 cells (equivalent protein levels validated by Micro BCA assay – see section 2.6.3) were lysed in 1% NP40 with protease and phosphatase inhibitors. Lysates were separated on reducing SDS-PAGE and western blotted for:

i) P42/P44 MAPK
ii) Phosphorylated P42/P44 MAPK
iii) Phosphorylated AKT
iv) AKT

Western blots were developed using Alkaline Phosphatase coupled secondary reagents (anti Mouse or rabbit Ig (Silenus)) and ECF Substrate (Amersham), and visualised on a Fluorimager 595 (Amersham). Blots were quantitated using ImageQuant Software.

In all experiments, an aliquot of "standard" was included (MO7e stimulated for 2 mins with Hu SCF and lysed in 1% NP40). This serves as an internal reference control for every blot, permitting direct comparisons of quantitative data derived from each blot. All data is expressed as a percentage of this reference control.

4.14A – Lyn -/- MIHC expressing chimaeric c-Kit GNNK-
4.14B – Lyn -/- MIHC expressing chimaeric c-Kit GNNK+
4.14C – C57 MIHC expressing chimaeric c-Kit GNNK-
4.14D – C57 MIHC expressing chimaeric c-Kit GNNK+

4.14A

Lyn -/- MIHC
Chimaeric c-Kit GNNK-

i)

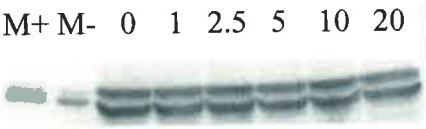

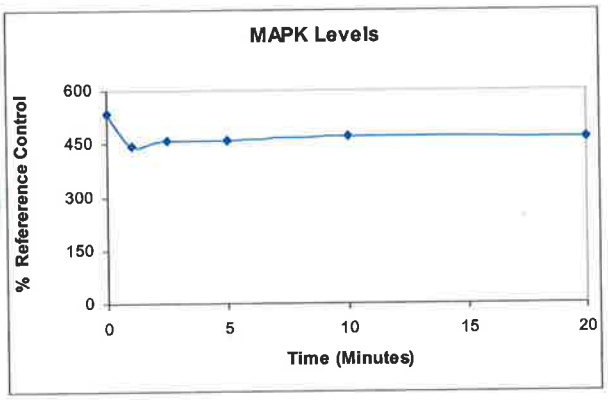

ii)

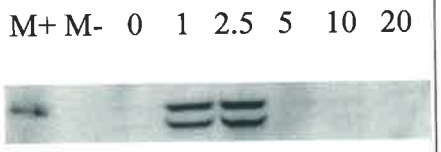

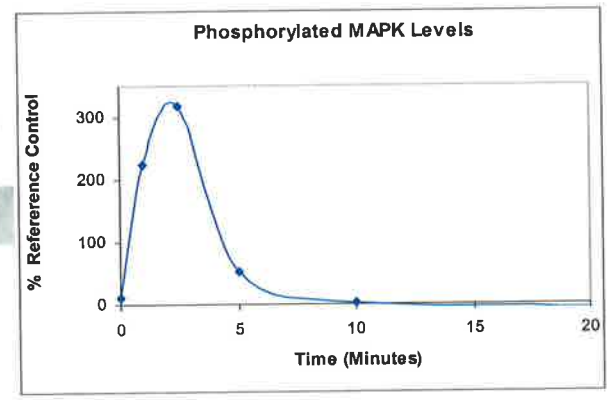

iii)

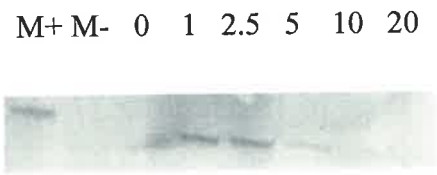

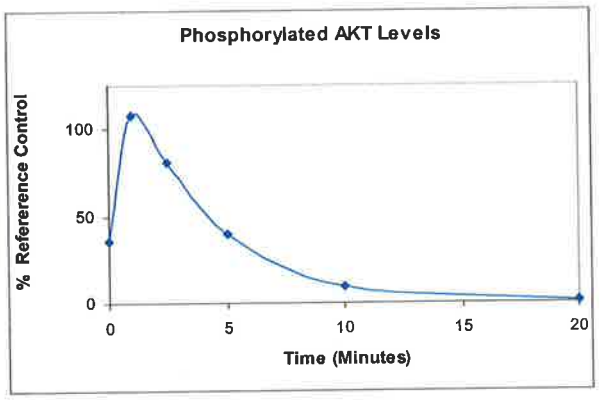

iv)

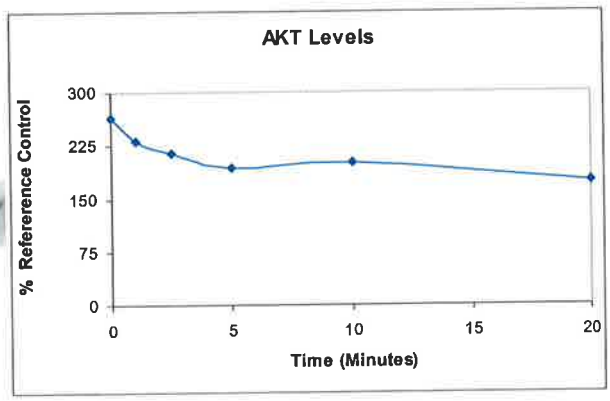

4.14B

Lyn -/- MIHC
Chimaeric c-Kit GNNK+

i)

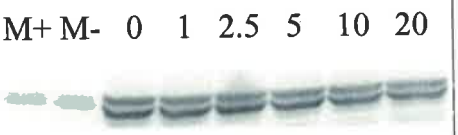

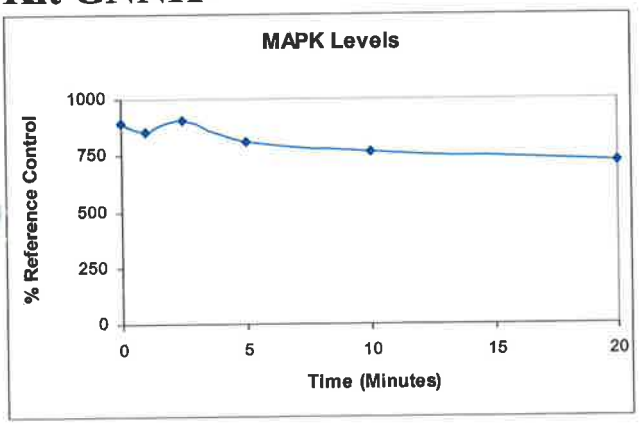

ii)

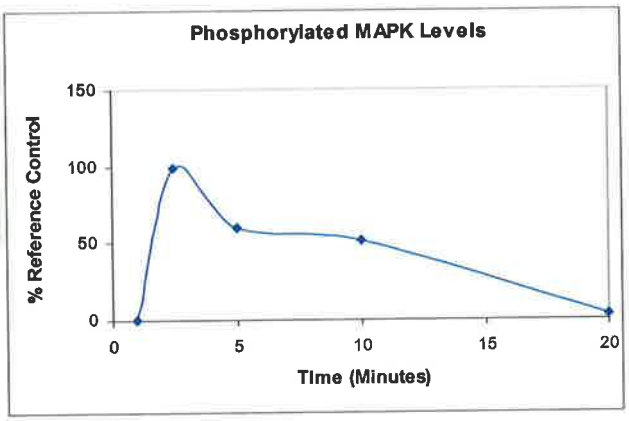

iii)

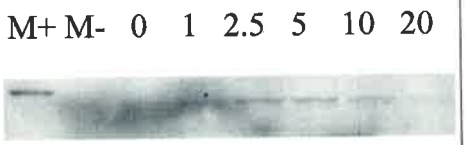

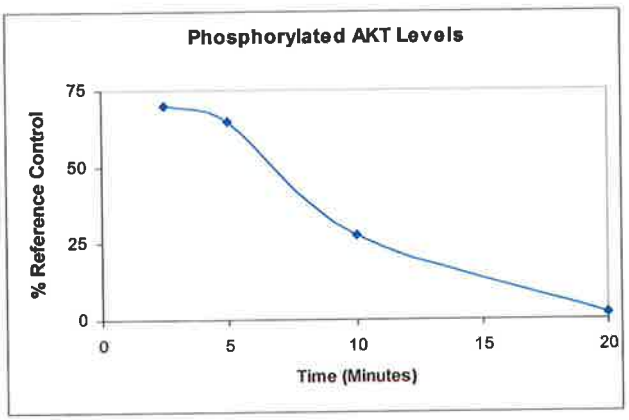

iv)

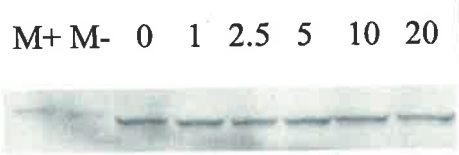

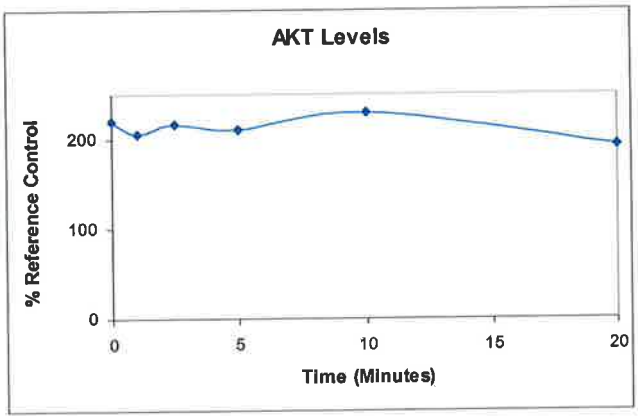

4.14C

C57 MIHC
Chimaeric c-Kit GNNK-

i)

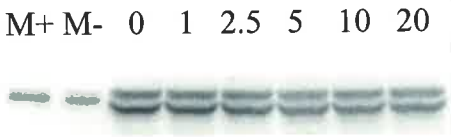

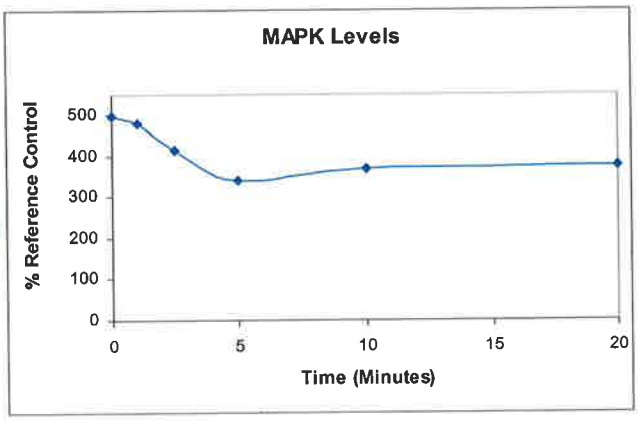

ii)

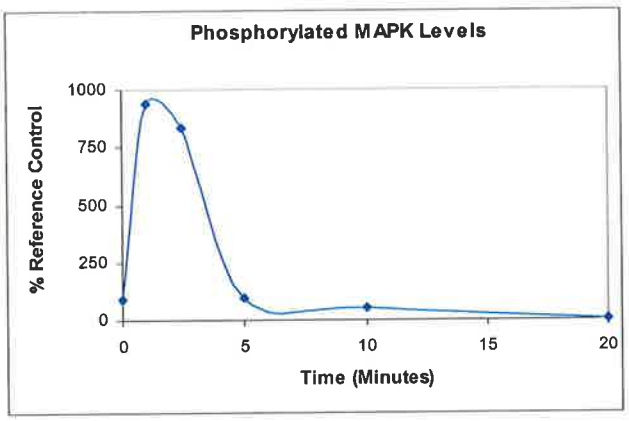

iii)

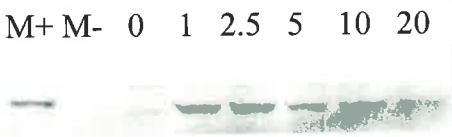

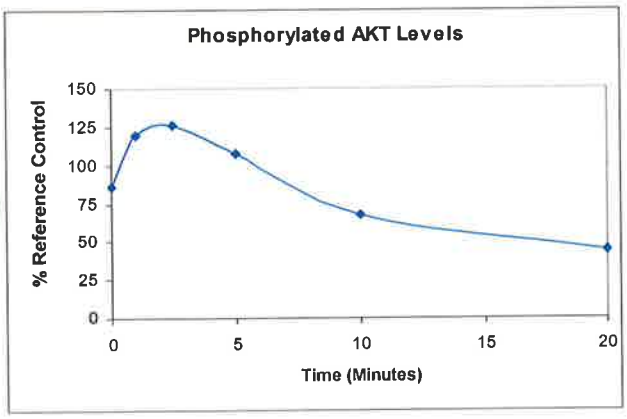

iv)

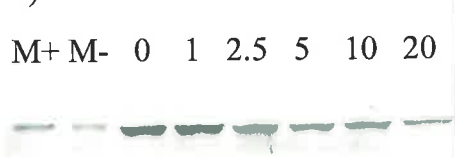

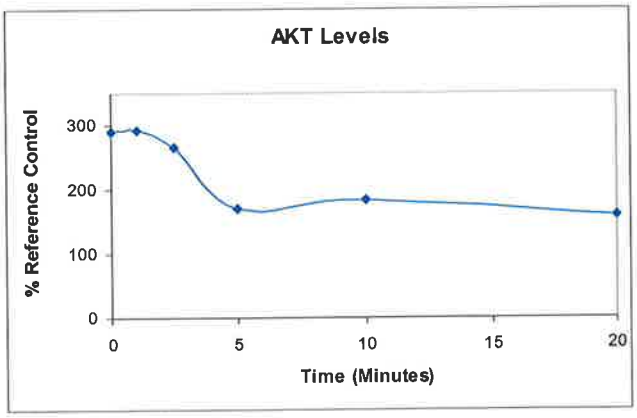

4.14D

C57 MIHC
Chimaeric c-Kit GNNK+

i)

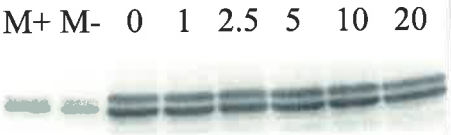

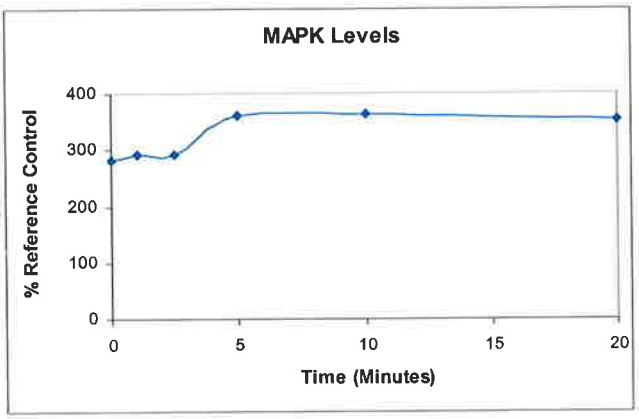

ii)

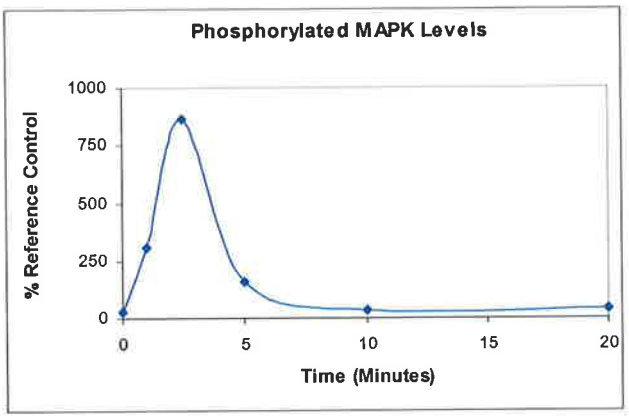

iii)

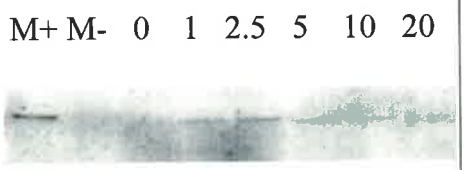

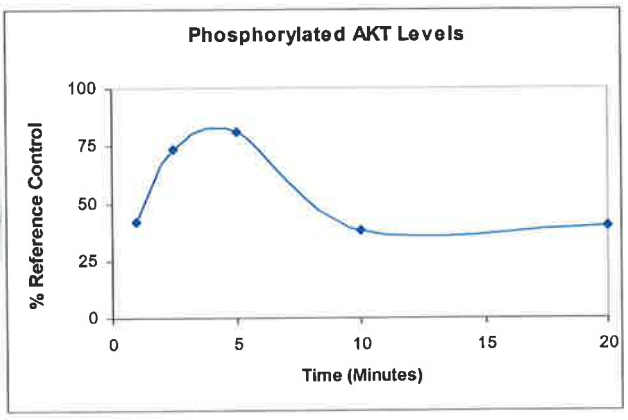

iv)

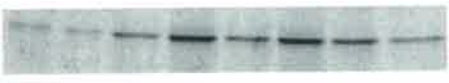

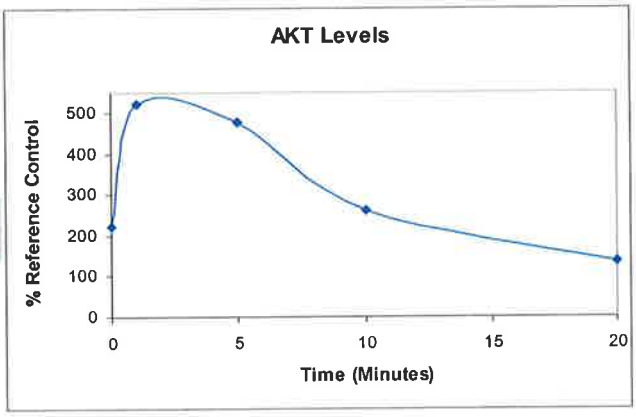

AKT and Phosphorylated AKT levels were similarly analysed. AKT was analysed as a surrogate marker for PI3K activation, lying downstream of activated PI3K in the signalling cascade for c-Kit. Figures 4.14 A-D iv show similar levels of AKT in both cell types expressing either isoform of chimaeric c-Kit as expected (approx 2-3 fold reference control sample). Lyn -/- MIHC chi-c-Kit GNNK- stimulated AKT phosphorylation to approximately 100% of control at 1 minute (Figure 4.14 A (iii)), as compared to 60% for Lyn -/- MIHC chi-c-Kit GNNK+ at 2.5 minutes (Figure 4.14 B (iii)). This compared to AKT phosphorylation of 300% of control for C57 MIHC chi-c-Kit GNNK- at 1-2.5 minutes (Figure 4.14 C (iii)) and 100% for C57 MIHC chi-c-Kit GNNK+ at 2.5 minutes (Figure 4.14 D (iii)). Again, these levels correlate with the kinetics and level of c-Kit phosphorylation, suggesting that the only influence was by the isoform status of c-Kit (GNNK±). The presence or absence of Lyn played no major role in this. The three fold difference observed between Lyn-/- and WT C57 MIHCs would appear to be attributable to higher c-Kit levels in C57 MIHC. However, Lyn -/- MIHC activation of AKT appeared to downregulate faster than the C57 MIHC counterparts. Given the role of PI3-K/AKT in cell survival discussed previously, this may present a mechanism to explain the deficient survival response observed in figure 4.12 for Lyn-/- MIHC.

4.8. Discussion

The aim of the work presented in this chapter was to use a novel model system to further characterise and study c-Kit triggered cellular responses including proliferation, survival and differentiation in a cell type that normally expresses c-Kit. This system was also used to biochemically analyse signalling differences between

the GNNK + and GNNK – isoforms, in backgrounds differing only in the presence or absence of a single c-Kit downstream effector, Lyn.

The MIHC cell line model was successfully established for both WT (C57) and Lyn -/- genotypes. This removed the ambiguity caused by analysis of expression of c-Kit in non-haemopoietic cells. The system proved extremely useful for evaluating proliferation and survival responses to SCF stimulated c-Kit, but was unreliable for analysis of differentiation responses. Added to this, the chimaeric c-Kit molecule functioned in a tightly controlled, human ligand inducible manner. Subtle differences were noted between c-Kit isoforms in the presence/absence of Lyn, demonstrating the potential value of this approach in evaluating the role played by other downstream components in the c-Kit signal cascades.

4.8.1. MIHC Generation

The generation of MIHC was successful with some qualification. It was unclear at the start of this work whether or not D14 Foetal Liver Cells harvested from various strains of mice would immortalise equally well to the model established by Professor Tom Gonda and Dr Petranel Ferrao where CBA mice were used. MIHC were successfully produced from C57BL/6 and Lyn -/- foetal livers, although the state of differentiation of the resultant immortalised cells was higher than desirable as shown in figures 4.6, 4.7, 4.8 and 4.9. This is most likely due to the use of Baculovirus derived murine growth factors. As shown in Figure 4.6, the yeast derived mGM-CSF used previously by Professor Gonda and Dr Ferrao was a superior stimulant of growth without differentiation, even though both sources of factor were equivalent with respect to their potency in stimulating growth of the factor dependent cell line FDC-

P1 (which was used to titrate and normalise all batches of cytokine throughout these experiments).

Despite this technical limitation, a question-mark will remain for the MIHC model as to whether it will ever be useful to evaluate differentiation due to the constitutive overexpression in these cells of activated c-Myb, which is known to have anti-differerentiative effects as outlined earlier in this chapter. It is possible, with overexpression of receptors such as c-Kit, that a strong differentiation signal may over-ride the Myb effects, but the system may become too contrived to confidently interpret differentiation responses at all.

The other positive feature of the MIHC model is the ability to generate a series of different MIHC lines potentially only differing in the presence or absence of one protein, taking advantage of the many knockout mouse strains now available. The principle has been demonstrated clearly in this study using Lyn knockout mice, although refinements are necessary. Firstly, the C57BL/6 and Lyn -/- MIHC used in this study were not strictly identical except for the presence/absence of Lyn. The Lyn -/- mice were extensively backcrossed onto a C57 strain to bring them as close as possible to the C57 genotype. However, this will never generate a pure C57 mouse strain lacking Lyn. As a minimum, genes physically linked to Lyn will be of knockout strain origin, making the backcrossed mice chimaeric. In future, development of MIHC from identical mice strains (one with a targeted gene, the other "wild type") will eliminate this variability.

A second limitation in the approach of using knockout mice as a source of cells for MIHC generation is the problem encountered by knockout technology itself – redundancy. Lyn -/- mice have relatively normal haemopoiesis and are viable despite lacking a downstream component of c-Kit signalling which would be presumed necessary for some aspect of haemopoietic development. This implies that, in the absence of this Src family kinase member, another has stepped in and adequately replaced most functional aspects of Lyn with respect to c-Kit function. This will mask the true effects of removal of a protein to assign functions to it. Therefore, identifying possible redundancies will be important. It may be possible to cross knockout strains to generate double knockouts. Even if these mice are not viable, if homozygous double knockout progeny can reach day 14 of gestation, MIHC could be developed for re-analysis in the system.

4.8.2. *Cellular responses to exogenous Human SCF*

In the analysis done here, differences between GNNK + and GNNK – were investigated in the presence or absence of Lyn. A number of cellular responses were analysed including surface receptor internalisation, survival, and proliferation (differentiation investigations were not performed for the reasons discussed previously in the chapter).

It was shown in Figure 4.11 that both isoforms of chi-c-Kit were internalised in response to human SCF to similar levels, with Lyn -/- MIHC expressing chi-c-Kit GNNK+ showing a small reduction in internalisation compared to the C57 MIHC counterpart. Irrespective of the presence/absence of Lyn, GNNK- isoform internalised more rapidly and extensively than the GNNK+ isoform. The kinetics and

extent of internalisation was dictated by the isoform, supporting the work done previously with murine fibroblasts and human c-Kit shown in Figure 3.9. This was also supported by the biochemical analyses in Figure 4.13, where ubiquitination of the isoforms is shown to be slightly slower for GNNK+ c-Kit compared to GNNK-, and also lower for Lyn-/- MIHC compared to C57 MIHC. Voytyuk *et al* have also demonstrated a small level of downmodulation c-Kit internalisation with the addition of the Src kinase inhibitor SU6656. Direct measurement of c-Kit ubiquitination was not determined in this study. In the related RTK III, PDGFRα, it has been shown that c-Cbl mediated polyubiquitination for degradation was also Src family kinase dependent (Voytyuk et al., 2003).

The ability of all MIHCs (Lyn-/- and C57 expressing either isoform of c-Kit) to proliferate in response to Human SCF was potent and identical to that elicited by mGM-CSF/mIL-3 (Figure 4.12B). The doubling time was very rapid in these cells, achieving 5 divisions in only 3 days. These analyses also demonstrated the continued factor dependence of the MIHCs, as deprivation of factor led to only 1 cycle of cell division (presumably completion of the currently committed cycle whilst growing in mGM-CSF/mIL-3 before factor deprivation) before culture death. The normal proliferation response to SCF of Lyn -/- MIHC, expressing either isoform of c-Kit, suggests no role for Lyn in the proliferative response. This contrasts to the findings of O'Laughlin-Bunner in murine mast cells (O'Laughlin-Bunner et al., 2001). The data also demonstrate that the proliferation signal from GNNK+ and GNNK- c-Kit is identical, despite the large differences in kinetics of phosphorylation of c-Kit itself, MAPK and AKT (all of which are substantially higher in GNNK- compared to GNNK+ c-Kit (Figures 4.13 and 4.14).

These same cells were simultaneously analysed for survival. Figure 4.12C demonstrated that GNNK- chi-c-Kit was superior to GNNK + chi-c-Kit in promoting survival in response to human SCF over the 3 days of the experiment (in the presence or absence of Lyn). However, these experiments also showed that C57 MIHC had better survival percentages than their Lyn-/- MIHC counterparts. The presence of Lyn may contribute to this survival response as roles for Lyn in anti-apoptotic responses have been demonstrated in a variety of cell types (Adachi et al., 1999; Pazdrak et al., 1998; Wei et al., 1996).

In summary, very few cellular responses were influenced by the presence/absence of Lyn in the MIHC model using chimaeric c-Kit (GNNK+ and GNNK- isoforms). The model did provide valuable information on differences in cellular responses between isoforms of c-Kit, and has demonstrated the potential of this model, with refinements, to carefully analyse cellular responses to haemopoietic growth factors. Where major differences can be seen between parental and knockout MIHCs, verification of the need for the "knocked out" protein is possible by re-introduction of the protein (knock in) to demonstrate rescue of the phenotype.

4.8.3. Further experiments

It is important to re-visit this model system using optimal growth factor conditions. Where MIHC can be grown in yeast derived mGM-CSF alone (or an equivalent), and maintain a much more undifferentiated status, it may become possible to evaluate differentiation in response to SCF stimulation. Also, MIHC generated from the original knockout and parental mice strains to eliminate genetic background variation

introduced by backcrossing to C57BL/6) needs addressing. The technical feasibility for this, however, is unknown.

Given the published association of Tec kinase and Dok1 with Lyn (Figure 4.4), it would also be valuable to analyse the activation of these 2 molecules in the model used here. It would be expected that these molecules remain unaltered in the Lyn -/- MIHC upon SCF stimulation. If, however, they are stimulated early (ie directly by SCF activation of c-Kit), it would be indicative of another Src family kinase replacing Lyn in the knockout MIHCs, confirming redundancy in the system. Another approach may be to use specific Src Family kinase inhibitors as employed in the studies of Voytyuk *et al* (Voytyuk et al., 2003) to tease out the contribution of this family of kinases.

5 Analysis of c-Kit isoform expression in primitive human haemopoietic cells

INTRODUCTION

It is clear from the data presented in Chapters 3 and 4 that the GNNK+ and GNNK – isoforms of c-Kit differ with respect to intracellular signalling and cellular responses. Given the diverse range of cellular responses attributed to c-Kit signalling, it was postulated that differential expression of the c-Kit isoforms in different subsets of cells may be a possible mechanism for this.

5.1. Expression of c-Kit isoforms in primitive haemopoietic cells

c-Kit has been demonstrated to be expressed on the cell surface of primitive haemopoietic stem cells (Ashman, 1999b; Ashman et al., 1999; Ashman et al., 2000; Buhring et al., 1999; Escribano et al., 1998; Oertel et al., 1996; Ratajczak et al., 1998; Simmons et al., 1994a). It has varying roles within the haemopoietic system depending on the cell type in question, and this is suggestive that the cellular environment plays a role in determining the cellular responses to stimulation by SCF. A major influence in generation of such diversity from a common trigger will be the repertoire of downstream effectors within different subsets of cells, which will define the cellular response of any given cell type to one stimulus (SCF). In addition, the presence or absence of other signalling receptors can reinforce or negate a specific signalling pathway's influence. Further to this, differential expression of the naturally occurring isoforms of c-Kit may add a 3rd means of generating diversity in cellular responsiveness in the one receptor/ligand signalling system. This aspect will be investigated in more detail in the work that follows.

To investigate this in primitive haemopoietic cells (one of the major cell types in which c-Kit is expressed), human bone marrow mononuclear cells were subdivided on the basis of their expression of the primitive stem cell marker CD34 (Baum et al., 1992; Craig et al., 1993; Murray et al., 1994; Peault et al., 1993) together with markers associated with commitment of progenitor cells to B cells (CD19), T cells (CD7), megakaryocytes (CD61), erythrocytes (Glycophorin A), myeloid committed progenitors (CD33) as well as a subset of the most immature stem cells (CD38 negative). More information on these markers is given in Appendix 1 at the end of this chapter.

5.2. G-CSF mediated Stem Cell Mobilisation – involvement of c-Kit

Several studies have noted a role for c-Kit in mobilisation of haemopoietic stem cells into the peripheral blood using G-CSF or a combination of G-CSF and SCF (To et al., 2003). c-Kit protein was down regulated on mobilised cells, and it was not known if this occurred at the mRNA level. The investigations detailed in this chapter will address this point.

It is also well documented that individuals vary significantly in their ability to mobilise peripheral blood stem cells (CD34 positive) in response to these regimes (To et al., 2003). Given the poorly understood role of c-Kit in this process, analysis of expression of c-Kit isoforms in mobilised CD34+ stem cells was also investigated. This would determine the contribution, if any, of c-Kit isoform expression patterns, to differing abilities to release stem cells from the bone marrow into peripheral circulation. It was hypothesised that c-Kit may be differentially expressed in different

groups of patients and that this may play a role in the variability in mobilisation efficiencies observed.

G-CSF, which mediates its effects through the G-CSF Receptor, is a pivotal cytokine for induction of proliferation and differentiation of normal bone marrow granulocytic precursors. G-CSF receptors are expressed on extremely early progenitor populations, preceding commitment to myeloid lineages, and its expression increases with maturation. CD34+CD33- cells express the least, followed by CD34+CD33+, then CD34-CD33+ (Shinjo et al., 1997).

G-CSF alone, or in combination with chemotherapy, has long been used to mobilise haemopoietic stem cells from the bone marrow to facilitate the harvesting of high numbers of CD34 positive haemopoietic stem cells for use in autologous and allogeneic stem cell transplantation (Juttner et al., 1990; Martinez et al., 1996; Sheridan et al., 1992; To et al., 2003; To et al., 1997; To et al., 1990). A persistent problem in the field of stem cell mobilisation is yield of CD34+ cells, which is regarded as an accurate predictor of successful engraftment (Pecora, 1999; Siena et al., 2000, Cottler-Fox, 2003 #517)). To achieve the optimal stem cell dose, multiple harvests are often required. It has been demonstrated that SCF increases the yield of CD34+ CD33- cells which leads to earlier sustained haemopoietic recovery (Pecora, 1999).

As stated earlier, the mechanism of this mobilisation is poorly understood, and patients undergoing treatment for G-CSF mobilisation vary in their ability to mobilise sufficient CD34+ cells for therapeutic use. G-CSF has been shown to stimulate an

accumulation of granulocyte precursors in the bone marrow, and that there is an accumulation of active neutrophil proteases as a consequence. This accumulation of serine proteases was believed to be responsible for the observed cleavage of the chemokine receptor CXCR4, as well as its ligand, stromal-cell derived factor 1 (SDF-1). This chemokine/receptor combination is responsible for homing and retention of CD34+ cells in the bone marrow (Cottler-Fox et al., 2003; Levesque et al., 2003a). Matrix metalloproteinase-9 (MMP-9), produced by activated neutrophils, has also been postulated to play a role in CD34+ cell mobilisation by G-CSF (Levesque et al., 2004) or IL-8 (Cottler-Fox et al., 2003; Lapidot et al., 2002). These proteases are suspected of cleaving various cytokines and their receptors, as well as integrins (Lapidot et al., 2002). The model by which mobilisation is achieved, however, is far more complex, as studies in mice lacking MMP-9 and neutrophil serine proteases still mobilised CD34+ cells normally in response to G-CSF, indicating that protease dependent and independent mechanisms exist (Levesque et al., 2004). The role of SCF and c-Kit also appears central to the mechanism of CD34+ cell mobilisation (Duarte et al., 2002). As already stated, c-Kit levels are reduced on G-CSF mobilised CD34+ cells, and one mechanism shown to be involved is proteolytic cleavage of the receptor (Levesque et al., 2003b).

In a recent study by To *et al* (To et al., 2003), a cohort of 44 patients who failed to adequately mobilise CD34 + stem cells on G-CSF or a combination of G-CSF and chemotherapy were subsequently remobilised with either a combination of G-CSF and SCF or a combination of G-CSF, chemotherapy and SCF. For both groups, mobilisation of CD34+ cells was improved, three and two fold respectively. Of note, this study revealed that the group of patients who did mobilise successfully on G-CSF

or a combination of G-CSF and chemotherapy downmodulated surface c-Kit levels on CD34 + cells. This observation confirmed those of several other studies (Roberts et al., 1999; Simmons et al., 1994c; To et al., 1994). Human SCF alone is incapable of mobilising CD34+ cells, yet is often a potent co-mobiliser with G-CSF or with a combination of G-CSF and chemotherapy (Basser et al., 1998; Moskowitz et al., 1997; Shpall et al., 1999; Stiff et al., 2000; To et al., 2003; Weaver et al., 1998). In the study of To and colleagues, approx 50% of the previously poor mobilising patients yielded sufficient CD34+ cells on subsequent mobilisations with SCF included (To et al., 2003).

It was of interest, therefore, to investigate if there was any difference in c-Kit isoform expression patterns between the various types of patients from the study of To and colleagues (To et al., 2003), given the findings already presented in Chapters 3 and 4 which show that the GNNK- isoform was more rapidly and completely downregulated in response to SCF stimulation. It was hypothesised that this isoform is predominant in the good mobilisers of CD34+ cells, given these patients demonstrate downmodulation of surface c-Kit. In addition, those patients that successfully mobilise with the addition of SCF on subsequent mobilisations may have a different expression profile to those who continue to fail to mobilise. These phenomena will be investigated in the sections to follow.

RESULTS

5.3. Analysis of GNNK+/- expression in Normal Bone Marrow Mononuclear Cells (MNCs)

In order to evaluate the relative expression of the GNNK+ and GNNK- isoforms of c-Kit in any given subpopulation of cells, a highly specific and sensitive methodology

was required. The difference between isoforms is subtle, and no known Mabs differentiate between these isoforms, eliminating the ability to use indirect immunofluorescence or immunoprecipitation and immunoblotting to evaluate the differential expression. These types of analyses also require large numbers of cells, leading to practical limitations of applying such techniques to small subpopulations of cells.

It was necessary, therefore, to utilise techniques to measure relative mRNA levels of the two species of c-Kit. Northern blotting, whilst quantitative, was unlikely to be sufficiently sensitive, particularly when required to use short probes to achieve specificity for the 12 bp difference between the isoforms. The approach chosen was Quantitative Real Time PCR (QPCR) analysis of reverse transcribed RNA isolated from FACS sorted haemopoietic cells.

5.3.1. *Design and validation of "minor groove binder" (MGB)-TaqMan probes*

To achieve specific identification of the two isoforms of c-Kit, one of two strategies could be used to satisfy the criteria. Firstly, specific primer sets that produce a productive reaction only on one of the two potential target sequences in conjunction with a common fluorescent probe can be used. Alternatively, a common set of primers can be used that flank the variable sequence, and isoform specific probes are employed. These strategies are shown diagrammatically in Figure 5.1.

Figure 5.1

Strategies to identify the GNNK+/- isoforms of human c-Kit

A. A common fluorescently tagged probe is used in conjunction with 2 sets of primers which produce similar size products. In the diagram, primer set 1 is only capable of producing a product when bound to the GNNK+ isoform. The primer is designed to reduce non-specific binding to GNNK- isoform due to its lack of the 12bp GGTAACAACAAA will lead to failure of this primer to anneal.

Primer set 2 anneals to flanking sequence of the 12bp insert, and can only bind in the absence of GGTAACAACAAA.

B. Unique fluorescent labelled probes that are specific for the insertion/deletion of GGTAACAACAAA are designed. Primer set 3 is used with either probe. Specificity of the probe is dictated by the inclusion/exclusion of GGTAACAACAAA.

The method chosen depends on the ability to meet the requirements of Tm values and differences as described in 5.3.1.

c-KIT

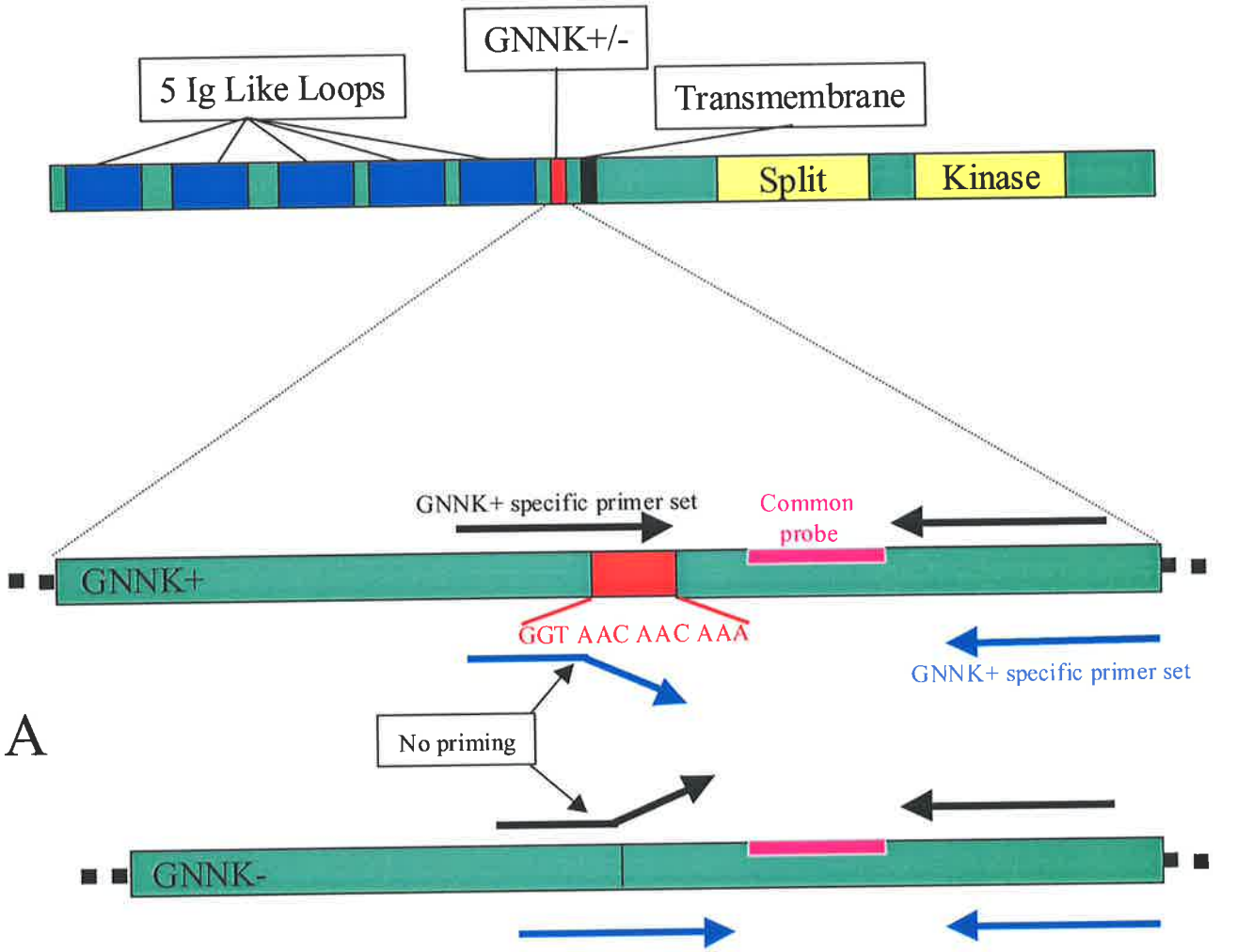
GNNK+/-
5 Ig Like Loops
Transmembrane
Split
Kinase
GNNK+ specific primer set
Common probe
GNNK+
GGT AAC AAC AAA
GNNK+ specific primer set
A
No priming
GNNK-

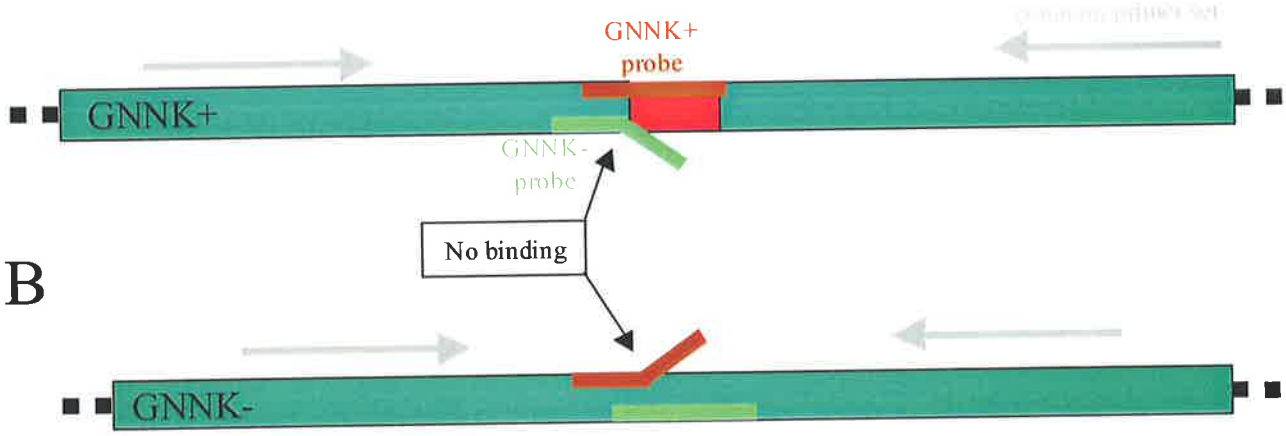
GNNK+ probe
GNNK+
GNNK- probe
No binding
B
GNNK-

The latter strategy was employed in this series of experiments. It was not feasible to design two sets of primers that met all criteria, however it was possible to generate common primers and 2 isoform specific probes that were suitable for QPCR. The key sequences and alignments are shown in Figure 5.2. It was also an advantage to use identical primers in 2 different reactions, as this removed any variability in the efficiency of different primer sets to initiate product formation. This is important when dealing with low yields of target sequence.

The QPCR system chosen for these analyses used MGB TaqMan probes produced by Applied Biosystems. The MGB at the 3' end of the probe increases the Tm of probes, allowing the use of shorter probes (Afonina et al., 1997; Kutyavin et al., 1997). This was critical to generate discrimination for the 12bp difference encoding GNNK in c-Kit. To ensure the technology was maximally sensitive and linear, and number of empirically derived criteria were stipulated by Applied Biosystems for the primers and probes to "guarantee" successful linear quantitation of target cDNA. These are summarised here:

Primer length 20-30bp with Tm 58-60°C, optimum 59°C

Probe Length 20-40bp with Tm 68-70°C, optimum 69°C

Probe Tm to be 10°C higher than primers

Product length to be <100bp

Probe preferably not to start with a G

To enable accurate quantitation of target cDNA sequences, it was necessary to generate standards for both isoforms of c-Kit cDNA. Fresh preparations of GNNK+S+ and GNNK-S+ human c-Kit in pRUFneo were prepared as described in

Figure 5.2

Specific primers and probes used for detection of GNNK+/- human c-Kit

Method B of figure 5.1 was chosen for these experiments. Two 6-FAM labelled MGB probes specific for the insertion/deletion of GGTAACAACAAA were designed, both with identical Tm values of 69°C. Both primers have a calculated Tm of 59°C, and the product length for both isoforms of c-Kit is less than 100bp.

GNNK+ c-Kit specific reaction probe and primers

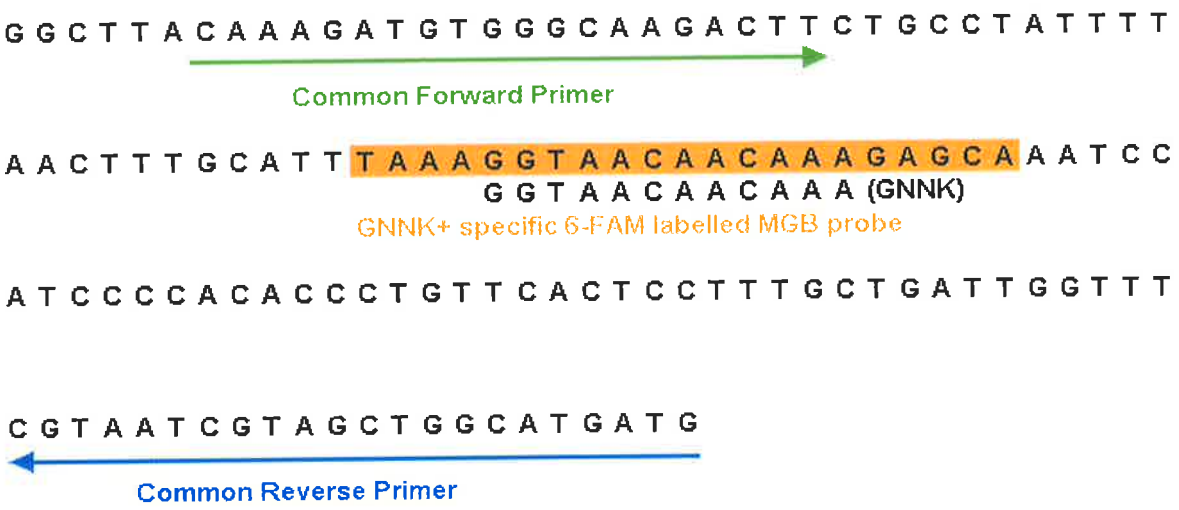

GNNK- c-Kit specific reaction probe and primers

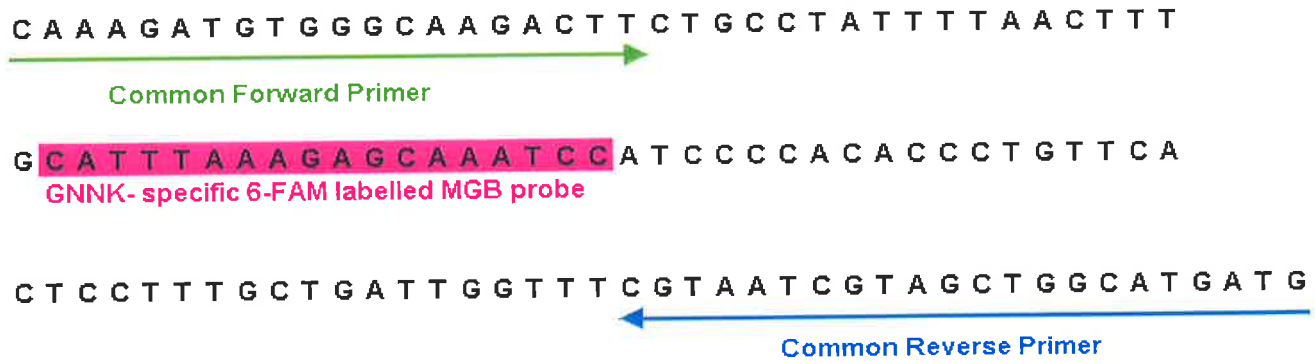

Section 2.7.9 and from these preparations, a set of standards were produced (Figure 5.3).

5.3.2. *Isolation of Normal Bone Marrow CD34+ subpopulations*

Direct immunofluorescence (see 2.3.2) was used to identify subsets of CD34 positive immature haemopoietic cells from normal bone marrow MNCs co-expressing or lacking CD7, CD19, CD33, CD38, CD61 and Glycophorin A.

Cell fractions were identified and isolated on a FACStar^{PLUS} fluorescence activated cell sorter. The cell yields for each normal bone marrow MNC fraction are shown in table 5.1. The relative percentages of each marker within the CD34 positive fraction of cells varied between donors, as did the percentage of CD34 positive cells, but all specimens fell within the expected ranges for normal donors (Civin et al., 1984; Fina et al., 1990; Lansdorp et al., 1990; Watt et al., 1987). Scatter plots from a representative sample are shown in Figure 5.4.

RNA was prepared from each subpopulation using TRIzol (as described in Materials and Methods - see 2.8.1) and cDNA generated using Superscript II^{TM} reverse transcription (as described in Materials and Methods - See 2.7.15). To maximise yields of cDNA for analysis in the QPCR, reverse transcription of RNA was performed using random hexamers rather than oligo dT primers. This, in theory, maximises the yield of cDNA containing the GNNK region of sequence, which is approximately 1.5 KB upstream of the polyA tail on c-Kit mRNA, making oligo dT priming less efficient for this purpose.

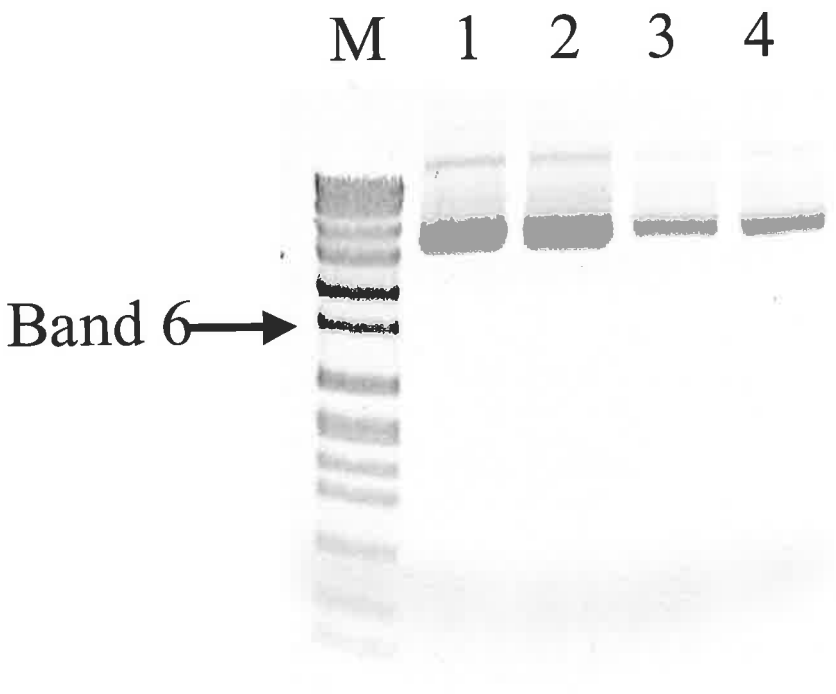

Figure 5.3

Establishment of GNNK+/- human c-Kit standards for use in QPCR

Fresh midi-preps of each isoform of c-Kit cDNA cloned in pRufNeo were prepared and diluted 1/10 in water for analysis on a 1% agarose gel stained with ethidium bromide and imaged for quantitation using a Typhoon fluorimager as described in 2.7.2 and 2.7.3.

Track M	1μl standard markers (SPP1 DNA digested with EcoR1) (band 6 will therefore contain 25.6ng DNA)
Track 1	5μl GNNK+ cDNA diluted 1/10
Track 2	5μl GNNK- cDNA diluted 1/10
Track 3	1μl GNNK+ cDNA diluted 1/10
Track 4	1μl GNNK- cDNA diluted 1/10

Band 6, tracks 1 and 2 were quantitated and the total DNA content of Track 1 (GNNK+ cDNA) was 95ng or 189ng/μl, and for Track 2 (GNNK- cDNA) was 101ng or 189ng/μl. Taking into account the molecular weight of c-Kit cDNA in pRufNeo (approx 6Kb, 3.96 x 10^6 Daltons), these cDNA preparations were both 0.05μM. This stock was used to generate standard preparations for QPCR.

CD34 Positive Cells (Mab HPCA-2 – BD 348053 and 348057)		Normal BM MNC 1		Normal BM MNC 2		Normal BM MNC 3	
Marker	Mab	% of MNCs	Sort Yield	% of MNCs	Sort Yield	% of MNCs	Sort Yield
CD61+	BD Cat 348093	2.00	15409	0.61	5500	1.33	25000
CD61-	BD Cat 348093	1.31	12417	2.68	39000	5.14	117000
CD33+	Leu-M9 BD Cat 347787	1.98	6491	1.00	11415	3.85	55700
CD33-	Leu-M9 BD Cat 347787	1.93	7250	1.32	18400	2.43	34250
CD7+	Leu 9 BD Cat 7483	0.27	2093	0.20	6200	0.41	10000
CD7-	Leu 9 BD Cat 7483	2.42	29516	2.15	55000	6.20	188000
CD38+	Leu 17 BD Cat 347687	2.46	21320	2.69	38400	4.65	136600
CD38-	Leu 17 BD Cat 347687	0.24	2300	0.12	2640	0.40	12500
Gly A+	Coulter Cat IM2212	0.22	2500	0.34	7000	0.44	10000
Gly A-	Coulter Cat IM2212	2.44	26500	2.71	45000	5.97	113000
CD19+	Coulter Cat IM1285	0.34	2500	0.19	4100	0.48	13600
CD19-	Coulter Cat IM1285	2.27	24500	1.80	23000	5.19	136000

Table 5.1

Statistics for sorting of CD34 positive cells in normal bone marrow MNCs by FACS

Cryopreserved normal bone marrow mononuclear cells were sorted after 2 colour direct immunofluorescence staining with antibodies to specific antigens as indicated using methodology described in section 2.3.2. Sorted cells were gated on Forward vs Side Scatter in addition to dual colour fluorescence gates as shown in a representative series in Figure 5.4. The percentage of total mononuclear cells for each subfraction is shown for the 3 independent bone marrow samples, as is the actual cell yield from the sorter for each subfraction. Sorted cells were subsequently processed for preparation of RNA.

Figure 5.4

Sorting parameters used for isolation of subsets of Normal BM MNCs expressing lineage associated markers

Normal bone marrow MNCs were labelled with directly conjugated anti-CD34 Mab in conjunction with Mabs against either CD33, CD38, Cd19, CD7, CD61 or Glycophorin A. CD34 positive cells were fractionated into positive and negative subsets and RNA prepared as described in Section 2.8.

A representative Normal BM scatter gate (A), and sort gates used for selection of CD34 positive CD61+/- (B), CD33 +/- (C), CD7 +/- (D), CD38 +/- (E), Glycophorin A +/- (F) and CD19 +/- (G) is shown.

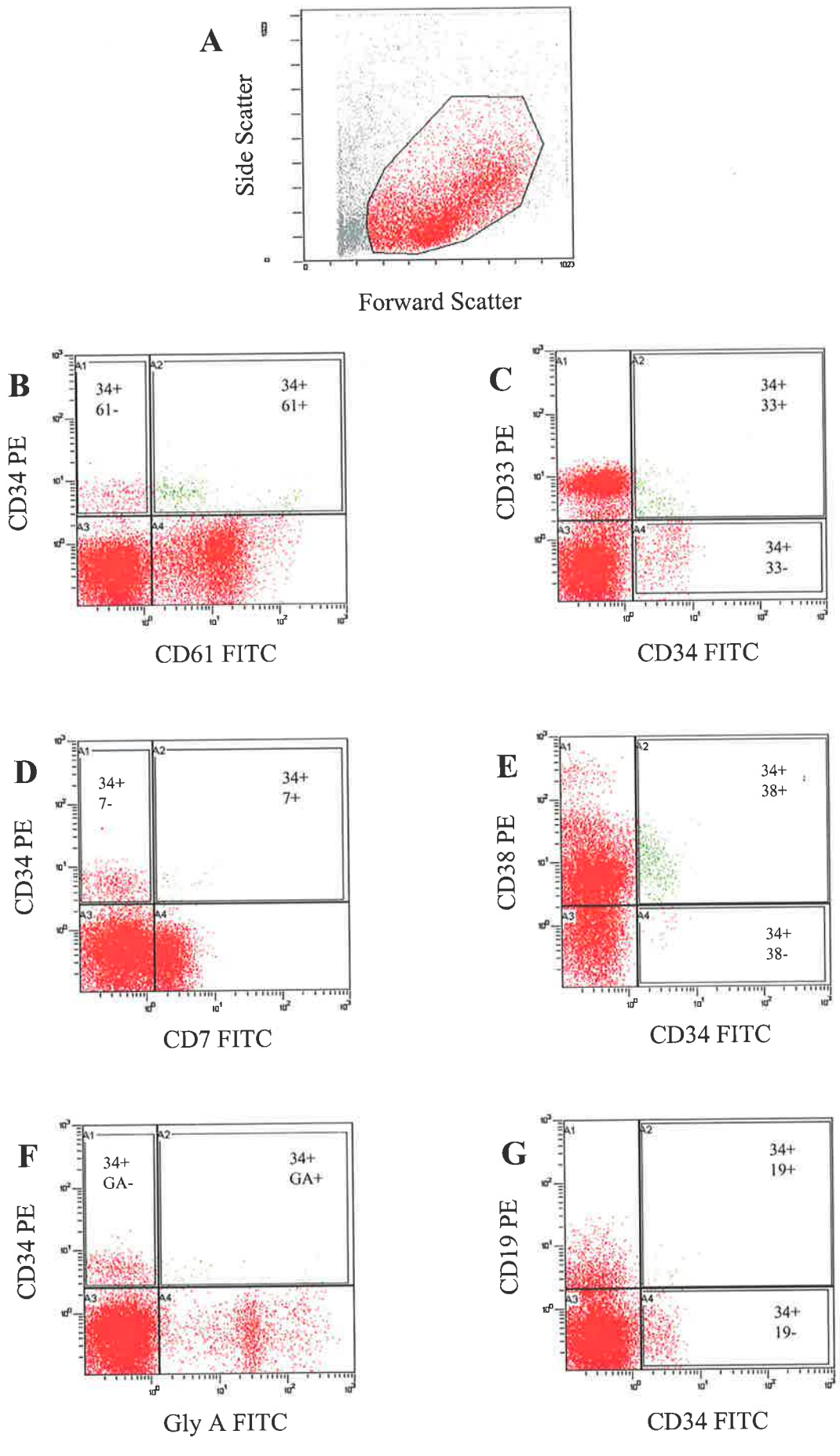
A
Side Scatter
Forward Scatter
B
CD34 PE
34+
61-
34+
61+
CD61 FITC
C
CD33 PE
34+
33+
34+
33-
CD34 FITC
D
CD34 PE
34+
7-
34+
7+
CD7 FITC
E
CD38 PE
34+
38+
34+
38-
CD34 FITC
F
CD34 PE
34+
GA-
34+
GA+
Gly A FITC
G
CD19 PE
34+
19+
34+
19-
CD34 FITC

5.3.3. QPCR analysis of Normal Bone Marrow subsets

cDNA samples from each sorted subpopulation of cells were subjected to QPCR analysis. Primers and probes used are shown in Figure 5.2 and the settings used for the analysis are given in section 2.7.15.

To validate the probes and primers against the standard reagents prepared as described in Figure 5.3, reactions were set up for the GNNK+ specific probe using no template or a range from 10 to 10^6 copies of GNNK+ human c-Kit cDNA standards. Likewise, reactions for GNNK- specific probe were set up using no template and a range from 10 to 10^6 copies of GNNK- c-Kit cDNA standards. As can be seen in Figure 5.5A and B, linearity across the range of 10^1 to 10^6 copies of cDNA (GNNK+ and GNNK- human c-Kit in pRUFneo) with the appropriate probe was achieved, with standard curve R^2 values always exceeding 0.999.

To confirm the specificity of each probe, GNNK+ probe was also included in reactions with GNNK- cDNA standards, and *vica versa*. As can be seen in Table 5.2, the GNNK+ probe displayed complete specificity for GNNK+ cDNA, producing no product when reacted in the presence of GNNK- cDNA at any level. However, the GNNK- probe was shown to weakly cross react with GNNK+ cDNA at levels of 10^4 copies or more of GNNK+ cDNA. At lower levels of the GNNK+ c-Kit cDNA, no product was detectable, and the level of "false" signal generated at high levels was approx 0.02-0.2% (average 0.1%).

Given the minute level of cross reactivity at high levels of GNNK+ cDNA, all GNNK- cDNA copy calculations were adjusted to take into account the value

Figure 5.5

Amplification Plots and Standard Curves for GNNK+ and GNNK- probes using GNNK+/- c-Kit cDNA standard reagents

Standard amounts (10 to 10^6 copies per reaction) of GNNK+/- cDNA were run against 6-FAM tagged MGB probes specific for GNNK +/- cDNA in every experiment. A representative set of standards is shown here for GNNK+ specific probe with GNNK+ c-Kit cDNA standards (A) and GNNK- specific probe with GNNK- c-Kit cDNA standards (B). In this and all reactions, the R^2 value for the standard curves derived using the Ct values (cycle number to reach threshold amplification* which is indicated by green line in amplification plot), was always greater than 0.999.

*The threshold is calculated from 10 times the standard deviation of the baseline fluorescence values.

Note: Rn is the reporter signal normalised to the Passive Reference for a given reaction. The Delta Rn value is the Rn value minus the Rn value for the No Template Control. This calculates the magnitude of the signal generated by the given set of PCR conditions.

A

GNNK + Standards

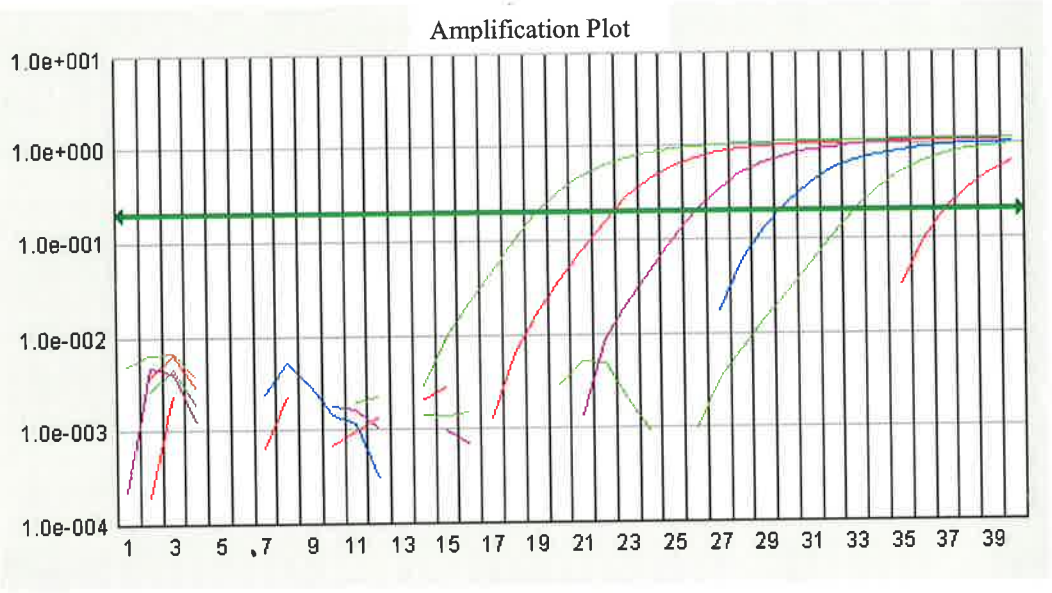

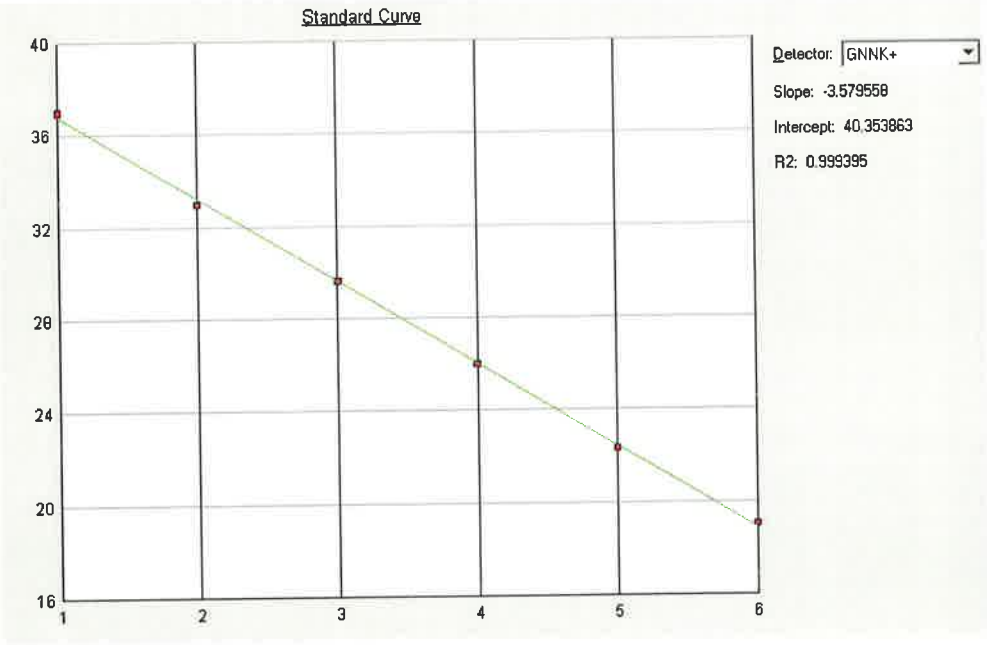

B

GNNK - Standards

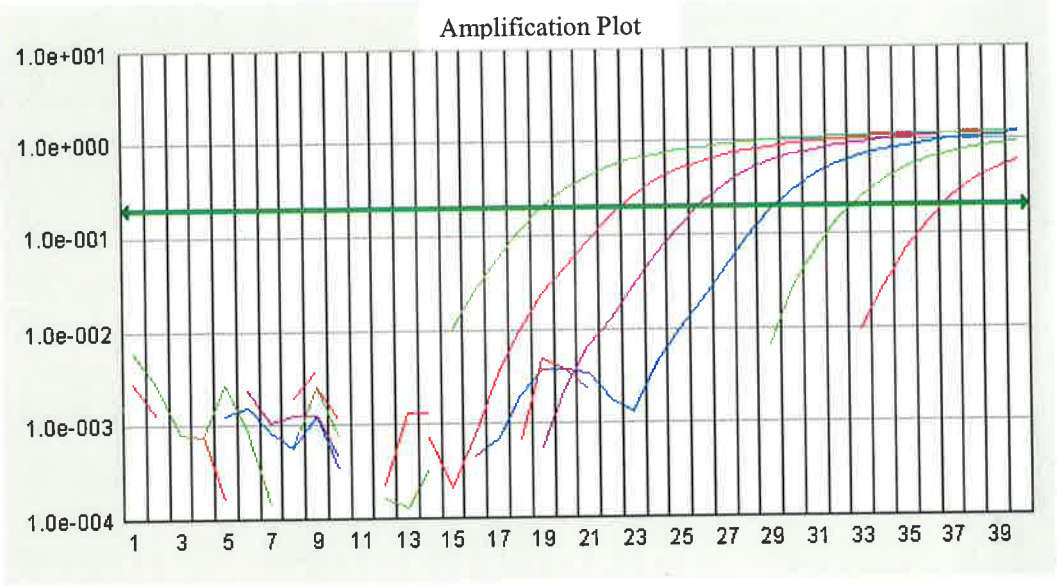

Delta Rn

Cycle No.

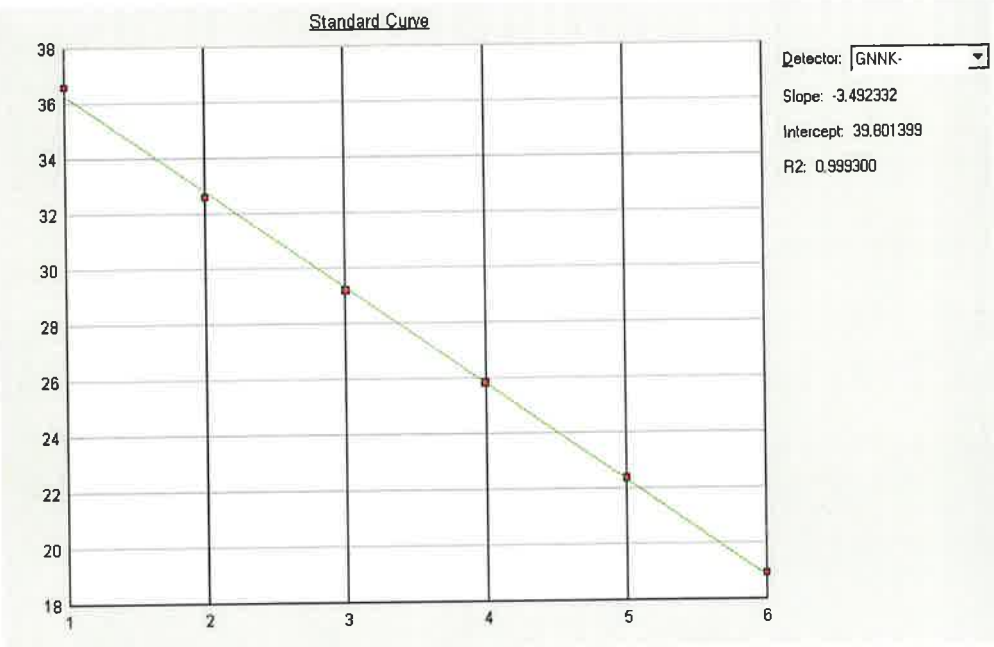

Ct

Log Copy No.

Target Sequence	No of copies	QPCR reaction 1 (BM1)			QPCR reaction 1 (BM2 & 3)		
		GNNK + Probe	GNNK- Probe	Cross reaction value *	GNNK + Probe	GNNK- Probe	Cross reaction value #
-	0	0	0	-	0	0	-
GNNK-	10^1	0	10^1	-	0	10^1	-
GNNK-	10^2	0	10^2	-	0	10^2	-
GNNK-	10^3	0	10^3	-	0	10^3	-
GNNK-	10^4	0	10^4	-	0	10^4	-
GNNK-	10^5	0	10^5	-	0	10^5	-
GNNK-	10^6	0	10^6	-	0	10^6	-
GNNK+	10^1	10^1	0	-	10^1	0	-
GNNK+	10^2	10^2	0	-	10^2	0	-
GNNK+	10^3	10^3	0	-	10^3	2	0.20%
GNNK+	10^4	10^4	4	0.04%	10^4	20	0.20%
GNNK+	10^5	10^5	20	0.02%	10^5	168	0.17%
GNNK+	10^6	10^6	104	0.01%	10^6	1297	0.13%

(*) mean correction value applied for GNNK- reactions in this QPCR run was 0.02% of GNNK+ result subtracted from GNNK- result

(#)mean correction value applied for GNNK- reactions in this QPCR run was 0.17% of GNNK+ result subtracted from GNNK- result

Table 5.2

Summary of standard curve data for QPCR runs used in analysis of fractionated CD34 positive cells from normal bone marrow MNCs.

In each analytical QPCR run, a set of common standards was incorporated to calibrate the reactions and enabled quantitation of target sequences in test samples. Known amounts of GNNK+/- c-Kit cDNA were tested in each run against their specific probe and a standard curve generated for quantitation of each species of cDNA in the samples as shown in Figure 5.6. In addition, known numbers of the incorrect target sequence were tested against the same probe to validate specificity of the probes. The GNNK+ c-Kit probe in all reactions (n= 5) exhibited complete fidelity with GNNK+ c-Kit cDNA. The GNNK- probe, however, consistently showed weak cross reaction with the GNNK+ c-Kit cDNA at levels above 1000 copies. The level of cross reaction in relevant representative QPCR runs is shown and the mean correction applied to all GNNK- c-Kit data as indicated for normal bone marrow MNC analysis.

attributable to cross reaction with the GNNK+ cDNA in each sample (ie. compensated). This was possible, as in all tests, identical quantities of test cDNA are loaded for each probe, and the values derived from the GNNK+ probe are unequivocal. The correction factor used in all data presented is shown in Table 5.2.

The results from 3 independent normal bone marrow specimens are shown in Figure 5.6A. It was clear that the dominant isoform in all subsets of CD34 cells was the GNNK- isoform, comprising approximately 90% of all transcripts detected and there was no significant difference in the expression pattern of c-Kit isoforms in any of the subpopulations tested. This was consistent with the findings of Crosier and colleagues who, using RNAse protection assays, also identified the GNNK- isoform as the dominant isoform of c-Kit in normal human bone marrow, normal melanocytes, several tumour cell lines, and the blasts patients with acute myeloid leukemia (Crosier et al., 1993).

It was also possible to relate the copy number for c-Kit RNA back to "copies/cell" using the assumption that all sorted populations were subjected to identical treatment and would have identical percentage yields of material at each step. These data are presented graphically in Figure 5.6B. It should be noted that the values calculated will not represent the true copy number per cell, as the high number of manipulations involved to produce the target cDNA for quantitation in the QPCR will all result in quantitative losses. However, these are assumed to be consistent, and the relative values are therefore meaningful. c-Kit expression was extremely low in subsets committed to lymphoid lineages (CD7+ and CD19+) as well as late erythroid progenitor subsets (Glycophorin A+). Megakaryocytic/early erythroid progenitor cells

Figure 5.6

QPCR analysis of fractionated CD34 positive cells in normal bone marrow MNCs

A. cDNAs synthesised by reverse transcription of RNA isolated from 3 independent normal bone marrow mononuclear cell subpopulations were analysed by QPCR to quantitate the levels of GNNK+/- c-Kit cDNA. All cell fractions were collected using a FACStar^{PLUS} cell sorter, selecting for CD34 positive cells expressing/lacking a lineage associated marker as indicated. Data are expressed as the percentage of total c-Kit cDNA that is GNNK- c-Kit cDNA (mean ±SEM, n=3).

B. The no. of copies determined in each QPCR reaction analysed in (A) has been used to determine of the relative abundance of c-Kit message in the various subpopulations of CD34 positive cells. It is assumed that this value will underestimate the true copy number per cell, as the extensive manipulation of the material to produce cDNA for analysis results in quantitative losses at each step of the target material.

A **Percentage of Total c-Kit cDNA detected as GNNK- isoform**

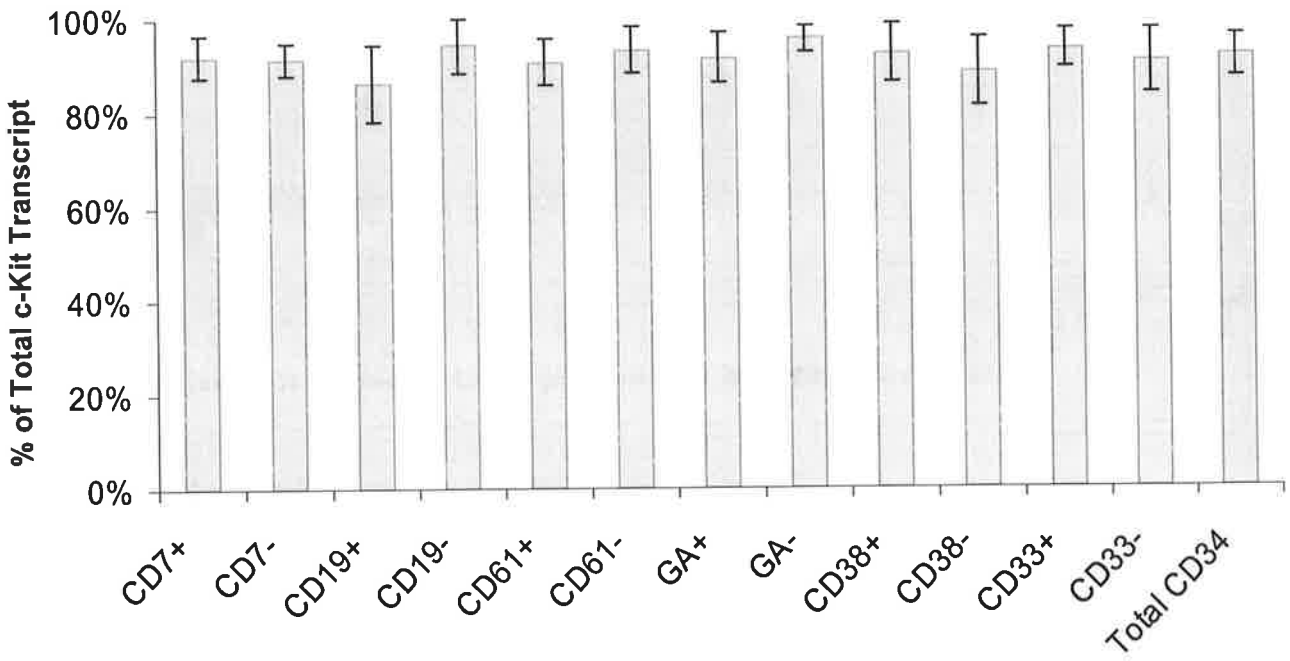

B **Total c-Kit cDNA detected per cell**

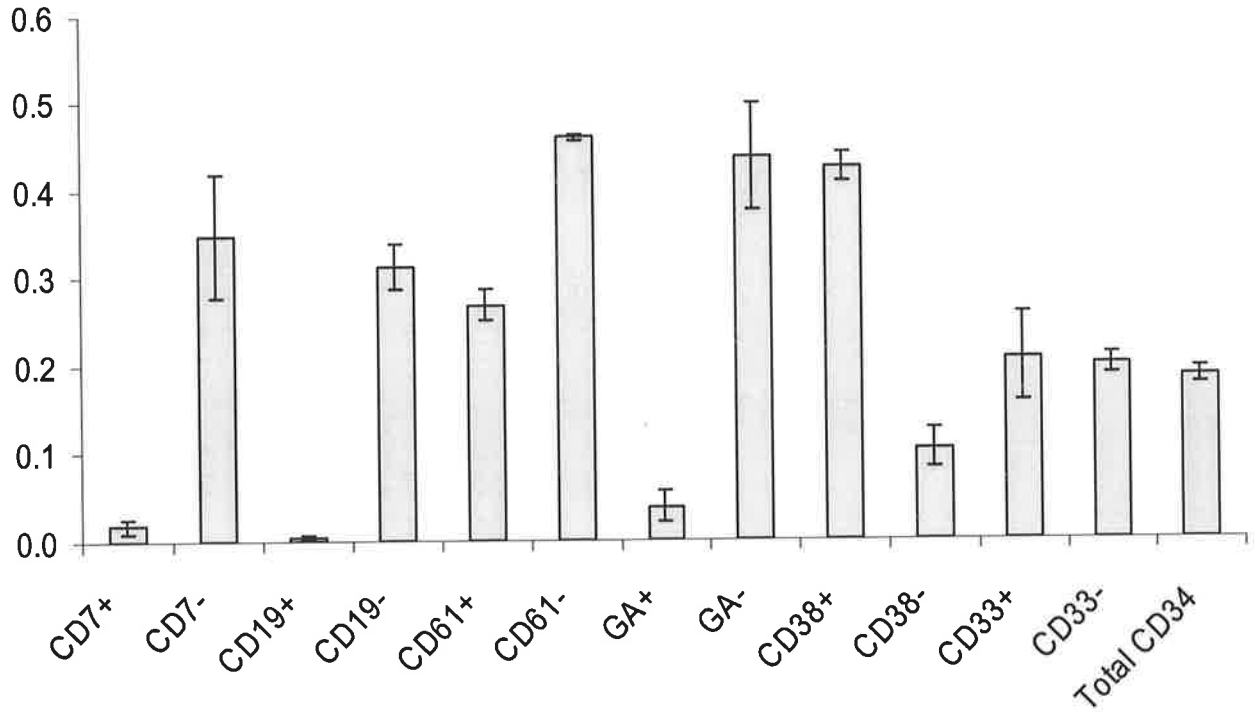

(CD61+), and myeloid committed progenitors (CD33+) expressed c-Kit RNA at similar levels. Of note, the most immature stem cells analysed (CD38-) appeared to express lower levels of c-Kit than the average level of total CD34 cells. This subset of cells has been reported to co-express other growth factor receptors such as Flt3, which was lost as c-Kit and CD38 levels rose (Xiao et al., 1999). This is consistent with observations that CD133+ CD34- c-Kit- CD38- cells appear to be the most immature subset known in the haemopoietic compartment (Buhring et al., 1999). It is plausible that c-Kit expression lags behind that of CD34, and increases with the acquisition of CD38.

5.4. Analysis of GNNK+/- expression in mobilised CD34+ cells

The objective of this series of experiments was to see if c-Kit isoform expression differences occurred on mobilisation, or were correlated with the variable responsiveness of individuals to mobilisation treatments.

5.4.1. Isolation of Peripheral Blood CD34 positive stem cells

Direct immunofluorescence (see section 2.3.2) was used to identify immature CD34+ haemopoietic cells from the mobilised peripheral blood. Total CD34 positive fractions were isolated on a FACStar^{PLUS} fluorescence activated cell sorter. Sort histograms are shown in Figure 5.7. RNA was prepared from each subpopulation using TRIzol (see section 2.8.1) and cDNA generated using Superscript II^{TM} reverse transcription (see section 2.7.15).

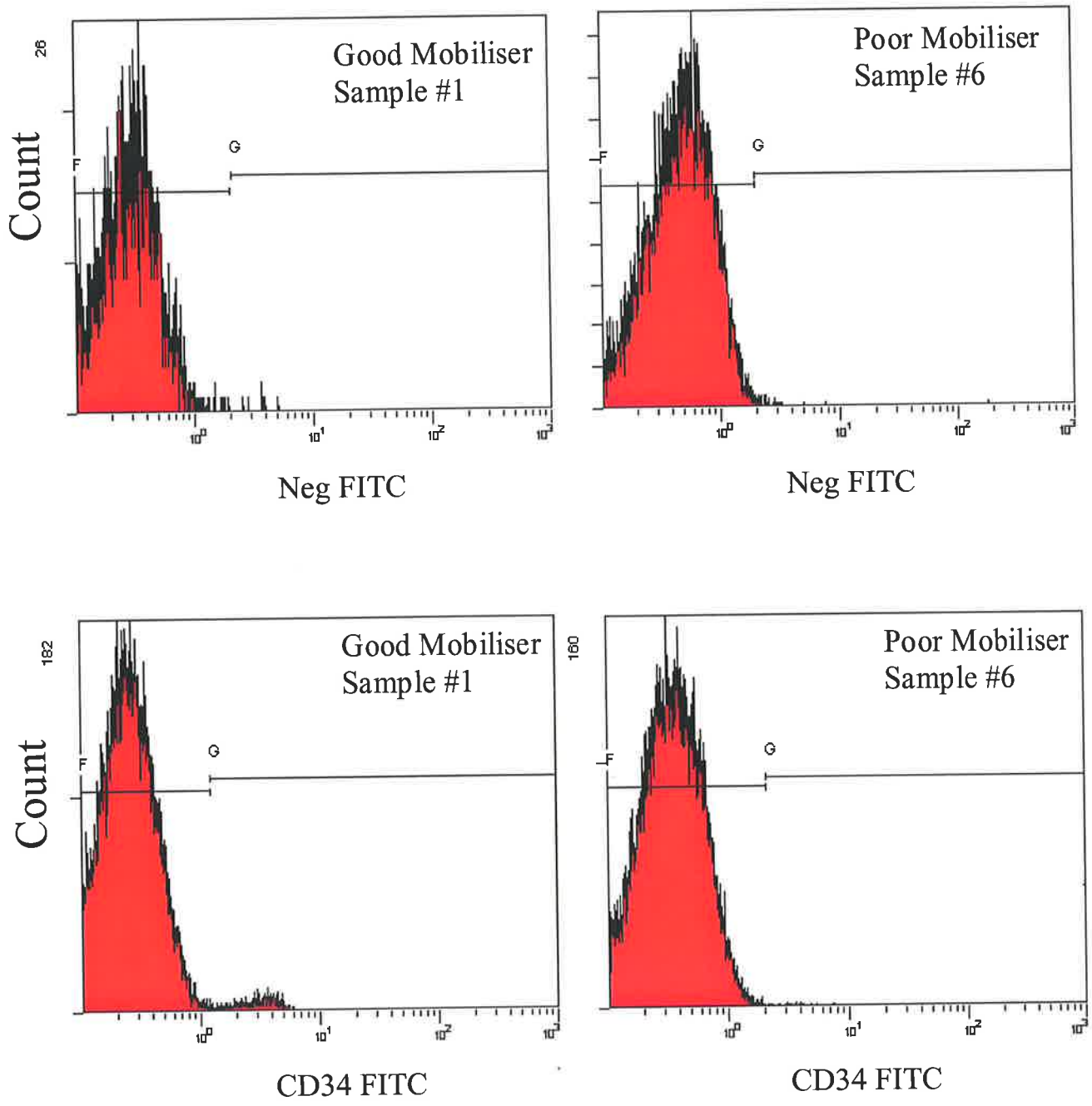

Figure 5.7

Sorting parameters for the isolation of CD34 positive mobilised PB MNCs

Mobilised peripheral blood MNCs were labelled with directly conjugated anti CD34 Mab. CD34 positive cells were sorted on a FACSTAR^{PLUS} cell sorter and RNA prepared as described in 2.8.1.

Representative histograms and sort gates (G) of samples from a good and poor mobiliser of CD34+ stem cells are shown. The sort gate (G) was set at the brightest 1% of cells stained with the IgG control Mab for collection of CD34+ cells.

5.4.2. *QPCR analysis of Peripheral Blood CD34 positive cells*

G-CSF or a combination of G-CSF and SCF mobilisation protocols have shown much variability in their efficacy to promote the release of CD34 positive stem cells from the marrow into the peripheral blood (To et al., 2003). The source of specimens for this series of experiments is detailed in Table 5.3. Four classes of mobilised peripheral blood apheresis specimens were analysed in these experiments –

1: G-CSF mobilised – "good" ($> 10^6$ CD34 cells/kg apheresed) (n=6)

2: G-CSF mobilised – "poor" ($<10^6$ CD34 cells/kg apheresed) (n=5)

3: G-CSF + SCF mobilised – "good" ($> 10^6$ CD34 cells/kg apheresed) (n=7)

4: G-CSF + SCF mobilised – "poor" ($< 10^6$ CD34 cells/kg apheresed) (n=4)

Specimens collected from patients of group 2 were all remobilised with a combination of G-CSF and SCF, and the resultant apheresis specimens fell into either class 3 or 4 as defined above. These matched specimens are colour coded in Table 5.3, together with the mobilisation protocols and resultant harvest data on each specimen. Additional specimens only ever treated with a combination of G-CSF and SCF were also analysed.

cDNA from these samples was subjected to QPCR analysis using primers and probes as shown in Figure 5.2 and settings given in section 2.7.15. The correction value used to determine true GNNK- cDNA quantitation was subtraction of 0.04% of GNNK+ cDNA value from the GNNK- cDNA value in these experiments.

Table 5.3

Analysis of apheresis products from mobilised patients.

4 classes of mobilisers are defined as:

1: G-CSF mobilised – "good" ($> 10^6$ CD34 cells/kg apheresed) (n=6)
2: G-CSF mobilised – "poor" ($<10^6$ CD34 cells/kg apheresed) (n=5)
3: G-CSF and SCF mobilised – "good" ($> 10^6$ CD34 cells/kg apheresed) (n=7)
4: G-CSF and SCF mobilised – "poor" ($< 10^6$ CD34 cells/kg apheresed) (n=4)

All patients in class 2 were all re-mobilised with a combination of G-CSF and SCF[$$] and these apheresis specimens were classified as either good or poor as indicated (class 3 or 4). These matched specimens are colour coded. CD34+ yields/kg were determined by the Transplant Unit, Division of Haematology at the time of apheresis using flow cytometry. The CD34+ percentage when cryopreserved material was sorted is also shown. In addition, the calculated percentage of total c-Kit cDNA that is GNNK- c-Kit from each CD34 sorted specimen and copy no. of total c-Kit is also shown.

Mobilisation protocols:

** G-CSF 10μg/kg/day – 7 days [Horsfall, 2000 #513; To, 2003 #359]
G-CSF 5-10μg/kg/day + SCF 10μg/kg/day – 7 days [Horsfall, 2000 #513]
$$ G-CSF 10μg/kg/day (days 3-10) + SCF 20μg/day – 10 days (for colour coded patients who failed on G-CSF alone mobilisations [To, 2003 #359]

Sample Code	Class of mobiliser	Specimen source	CD34+ yield at apheresis (10^6/kg)	CD34 + at SORT	% GNNK-cDNA	c-Kit cDNA copy No.
1	1**	Allogeneic Donor	11.5	2.56%	97.3%	0.07
2	1**	Allogeneic Donor	4.45	1.49%	92.8%	0.14
4	1**	Allogeneic Donor	4.65	0.41%	95.6%	0.10
10	1**	Allogeneic Donor	5.40	1.12%	96.0%	0.12
11	1**	Allogeneic Donor	2.24	0.44%	94.4%	0.08
19	1**	Allogeneic Donor	8.37	1.00%	91.8%	0.08
3	2**	Hodgkins Disease	0.34	0.18%	96.8%	0.06
5	2**	Not Known	0.28	1.36%	92.2%	0.10
9	2**	Non Hodgkins Lymphoma	0.10	0.43%	93.2%	0.20
15	2**	Non Hodgkins Lymphoma	0.47	0.14%	92.9%	0.11
22	2**	Multiple Myeloma	0.56	0.20%	93.4%	0.09
7	3##	Breast Cancer	3.70	0.70%	90.2%	0.13
8	3##	Breast Cancer	8.10	1.34%	90.1%	0.05
13	3##	Breast Cancer	8.67	1.90%	94.0%	0.10
14	3##	Breast Cancer	5.64	2.10%	92.7%	0.14
16	3##	Multiple Myeloma	1.17	0.50%	92.8%	0.07
20	3$$	Not Known	2.00	3.30%	93.2%	0.05
21	3$$	Multiple Myeloma	1.98	0.80%	89.4%	0.11
6	4$$	Multiple Myeloma	0.79	0.10%	91.6%	0.05
12	4$$	Non Hodgkins Lymphoma	0.80	0.29%	92.8%	0.06
17	4$$	Non Hodgkins Lymphoma	0.79	0.80%	95.2%	0.21
18	4$$	Hodgkins Disease	0.18	0.10%	86.9%	0.05

As can be seen in Table 5.3, there was a clear predominance in all specimens, of the GNNK- c-Kit isoform (range 86-96%). The different classes of mobilisers were clustered and analysed for both the percentages of GNNK- c-Kit cDNA and total c-Kit copy no. as previously described for normal BM MNC subsets. As can be seen from Figure 5.8, there was no significant difference between any of the groups in terms of either isoform expression or copy number.

These data clearly indicate that whilst many differences in signalling are attributable to the inclusion/exclusion of the GNNK motif in c-Kit (refer to Chapters 3 and 4), there was no evidence of differential expression of these isoforms in different cell subsets, nor was there any significant difference in expression of total c-Kit at the level mRNA as influenced by either transcription or mRNA stability.

5.4.3. *Cell surface c-Kit levels in mobilised CD34 stem cells*

A number of reports suggest that c-Kit surface expression is down-modulated during the process of mobilisation (Bellucci et al., 1999; To et al., 2003). Cell surface c-Kit expression was analysed by flow cytometry on CD34 positive mobilised stem cells using direct 2-colour immunofluorescence as described in section 2.3.2.

A sample of apheresis specimen was stained for CD34 and c-Kit. Analysis of c-Kit surface expression on CD34 positive cells revealed weak expression of c-Kit in all samples tested. Staining for c-Kit resulted in a subtle but complete peak shifts. This infers the majority of CD34 positive cells express c-Kit as expected. The same classes of apheresis specimens (defined by the mobilisation with G-CSF alone vs G-CSF + SCF, good v poor) were analysed and the increase in mean fluorescence

Figure 5.8

QPCR analysis of CD34 positive cells in apheresis products of mobilised patients

A. cDNAs isolated by reverse transcription of RNA isolated from 22 independent apheresis specimens were analysed by QPCR to quantitate the levels of GNNK+/- c-Kit cDNA. All CD34+ cell fractions were collected using a FACStar^{PLUS} cell sorter. Specimens were grouped according to the mobilisation treatment received by the patient (G-CSF alone (G) or G-CSF and SCF (G+S)) and also the efficiency of the mobilisation ("good" = apheresis yields of > 10^6 CD34+ cells/kg, "poor" = apheresis yields < 10^6 CD34+ cells/kg). Data are expressed as the percentage of total c-Kit cDNA that is GNNK- c-Kit cDNA (mean ± SEM, n=6 for "G Good", n=5 for "G Poor", n= 4 for "G and S Poor", and n = 7 for "G and S good".).

B. The no. of copies determined in each QPCR reaction analysed for (A) has been used to give an indication of the relative abundance of c-Kit message in the various samples of CD34 positive cells. It is assumed that this value will underestimate the true copy number per cell, as the extensive manipulation of the material to produce cDNA for analysis results in quantitative losses at each step of the target material.

A

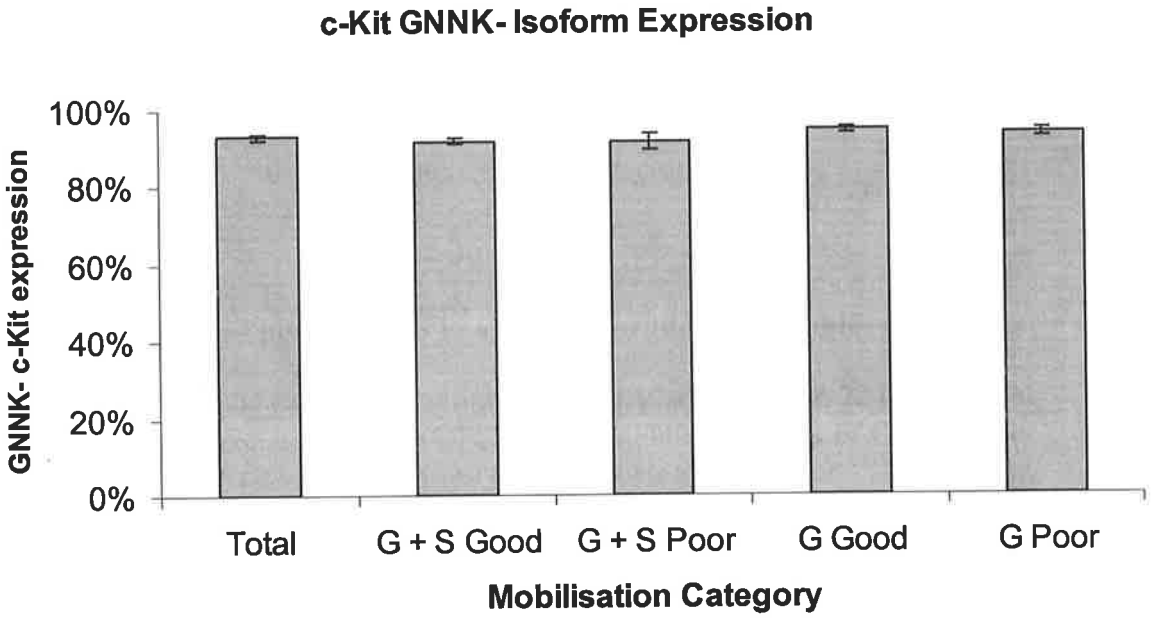
c-Kit GNNK- Isoform Expression
GNNK- c-Kit expression
100%
80%
60%
40%
20%
0%
Total
G + S Good
G + S Poor
G Good
G Poor
Mobilisation Category

B

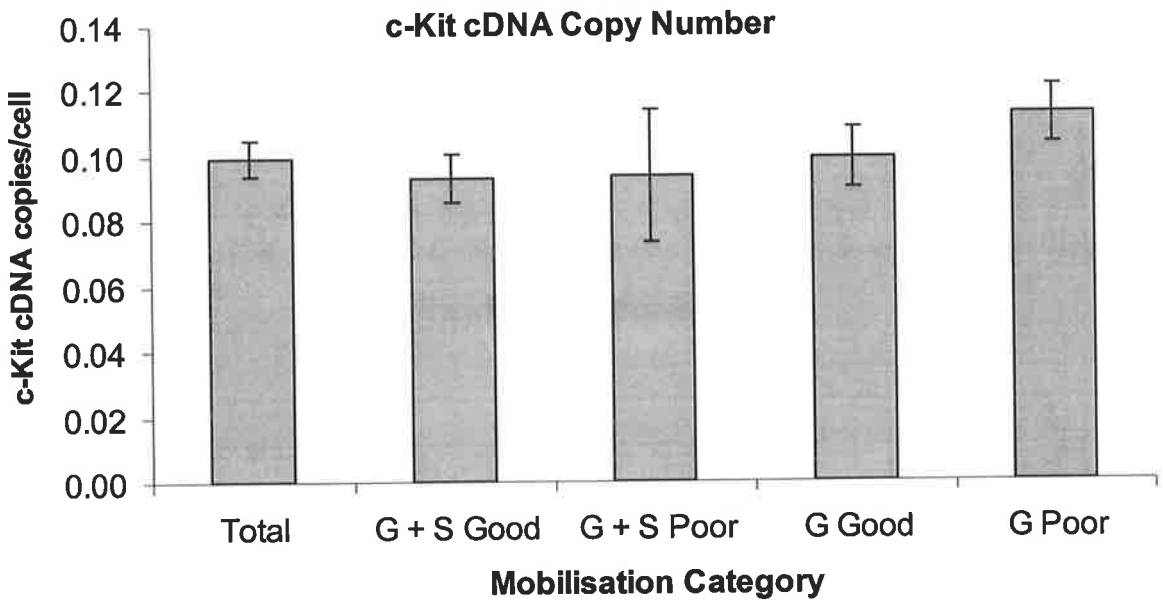
c-Kit cDNA Copy Number
c-Kit cDNA copies/cell
0.14
0.12
0.10
0.08
0.06
0.04
0.02
0.00
Total
G + S Good
G + S Poor
G Good
G Poor
Mobilisation Category

intensity recorded for c-Kit staining over an isotype matched negative control (mean +/- SEM) (Figure 5.9).

As previously demonstrated in the same samples investigated in the study of To *et al* (To et al., 2003), there was a clear and significant decrease in surface expression of c-Kit on successful mobilisers treated with G-CSF + SCF compared with good or poor responders to mobilisation with G-CSF alone ($p < 0.05$, 2 tailed student T test). The decrease in poor combination G-CSF + SCF treated mobilisers compared with samples from good or poor G-CSF alone mobilisations was not significant ($p = 0.22$ and 0.23 respectively, 2 tailed Student's T Test). There was no significant difference between good and poor mobilisers treated with G-CSF alone ($p = 0.7$, 2 tailed Student's T test) or between good and poor mobilisers treated with combination G-CSF and SCF ($p= 0.06$, 2 tailed Student's T Test).

It is clear that addition of SCF into the mobilisation regimen triggered a downmodulation of c-Kit from the surface of CD34+ cells, and the better mobilisers from this treatment downmodulate c-Kit no more extensively than specimens from people who respond poorly to this treatment. Quite clearly, addition of SCF to the mobilisation protocol has an effect in a subgroup of patients. This exogenous SCF appears to be responsible for the c-Kit down modulation, but other factors yet to be determined must also contribute to the total efficiency of CD34+ cell mobilisation. It would be informative to know what level of c-Kit is expressed on these CD34+ cells prior to mobilisation, but this presents technical difficulties as the cells are not readily accessible within the marrow environment.

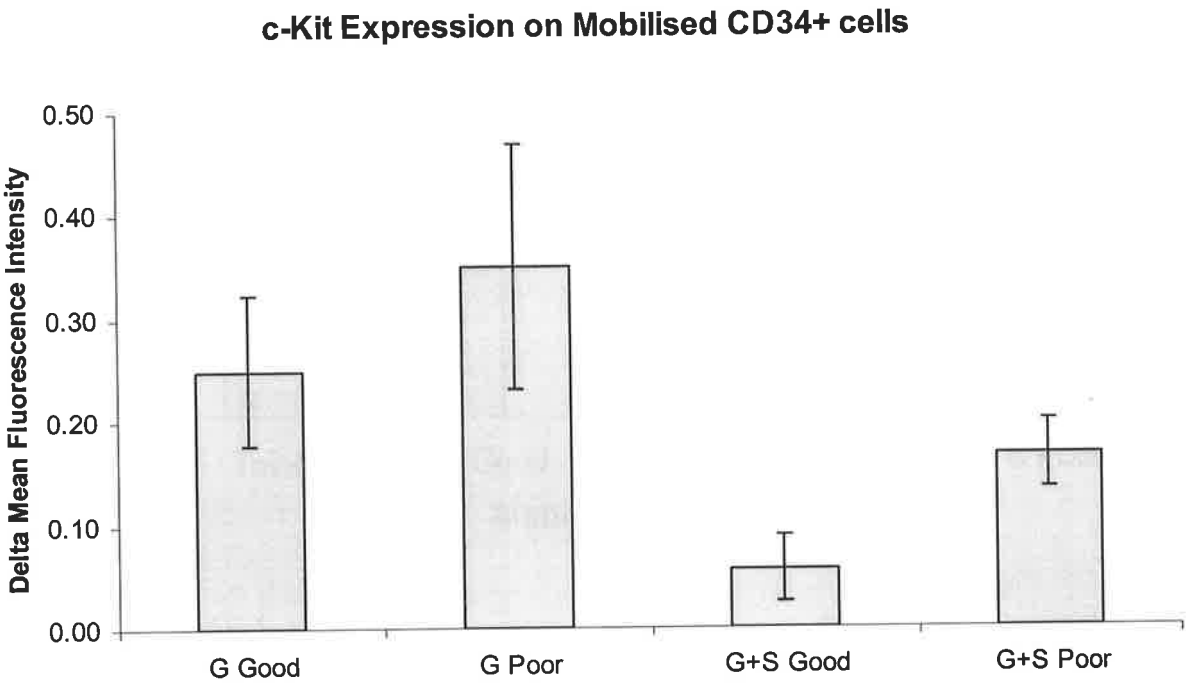

Figure 5.9

Analysis of cell surface c-Kit expression by CD34 + mobilised stem cells

Apheresis samples from patients 1-22 as detailed in Table 5.3 were stained with anti CD34-FITC (see Table 5.1) and anti CD117-PE (Coulter IM1360) as detailed in Section 2.3.2. CD34 positive cells were gated and analysed for their expression of c-Kit on a coulter EPICS-MCL flow cytometer. Data are presented as the mean +/- SEM of delta Mean Fluorescence Intensity (MFI) of the CD34 positive cells within each class of mobiliser (n=6 for G Good, n= 5 for G Poor, n= 7 for G+S Good and n = 4 for G+ S Poor).

5.5. Discussion

In this chapter, the hypothesis was that differential expression of the c-Kit isoforms in different cell subsets was a mechanism utilised by cells to elicit the observed broad range of cellular responses to SCF engagement of c-Kit. To investigate this, c-Kit isoform expression (GNNK+/-) was examined in a number of human haematopoietic subsets.

Methodology was developed for the sensitive detection of GNNK+/- c-Kit RNA using reverse transcription and QPCR analysis from rare subsets of cells from normal bone marrow MNCs and mobilised peripheral blood stem cells. The QPCR methodology demonstrated high sensitivity and specificity for the 12 bp variance between the 2 isoform sequences (Figure 5.5).

Normal bone marrow MNCs were sorted on the basis of CD34 expression to identify the immature stem cell/progenitor cell compartment. This compartment was further fractionated using Mabs to CD7 (to identify early T cell committed progenitors CD7+CD34+), CD19 (to identify early B cell committed progenitors CD19+CD34+), CD33 (to identify the majority of myeloid committed cells CD33+CD34+), CD38 (to identify the most immature compartment of CD34 cells CD38-CD34+), CD61 (to identify megakaryocyte/early erythroid committed progenitors CD61+CD34+) and Glycophorin A (to identify late erythroid committed progenitors GlyA+ CD34+). In all subsets analysed, there was no significant difference in expression patterns of the c-Kit isoforms, with all samples exhibiting approximately 90% of total c-Kit transcripts as the GNNK- isoform. It was clear that in the normal bone marrow, c-Kit

isoforms (GNNK+/-) are not differentially expressed in any of the subsets analysed in this study (Figure 5.7A).

A value for copy number was also determined for total c-Kit RNA in each sample and was presented in Figure 5.7B. This number was an underestimation, as there were quantitative losses of target material at each stage in the processes leading to QPCR (in particular at the stage of RNA production and cDNA synthesis). The data show that c-Kit expression was lowest in lymphoid committed subsets and also in the most immature CD34 subset (CD38-). This subset of cells is known to co-express other growth factor receptors such as Flt3 which was lost as c-Kit and CD38 levels rise (Xiao et al., 1999). Recent analysis of CD133+ primitive cells that are CD34-, c-Kit - , and CD38- (Buhring et al., 1999) lead to the suggestion that, if this cell was truly the most primitive haemopoietic stem cell, c-Kit expression is induced at or near the induction of CD34 expression. Other receptors such as Flt3 may play the role of promoting proliferation and survival in early, c-Kit- stem cells. c-Kit may take over from such receptors during the early stages of development and commitment before being downregulated on maturation in all cell lineages except mast cells.

It was also of value to assess the contribution, if any, of differential c-Kit isoform expression in mobilised peripheral blood CD34+ cells from patients who demonstrate different efficiencies for mobilisation of CD34+ cells. A series of patients were studied who failed to mobilise successfully when treated with G-CSF or G-CSF in combination with chemotherapy, and subsequently remobilised with a combination of G-CSF and SCF. A proportion of these patients now mobilised adequate cells for clinical application, whilst the remainder continued to mobilise poorly. Recent

studies suggest that c-Kit was significantly downmodulated on CD34+ cells when successfully mobilised with a combination of G-CSF and SCF, compared to CD34+ cells mobilised in the same patient with G-CSF alone or G-CSF in combination with chemotherapy (To et al., 2003). A number of these samples from the 2003 study (To et al., 2003) were obtained, together with additional samples of successful mobilisations in response to G-SCF alone or a combination of G-CSF and SCF. RNA was isolated from CD34+ cells isolated from these samples, and the resultant cDNA analysed by QPCR for their expression of the GNNK+ and GNNK- isoforms of c-Kit. As for normal bone marrow CD34 subsets, no differences in the expression patterns were observed in the classes of mobilised samples analysed, nor was there any significant variation in levels of transcript of c-Kit (Figure 5.8).

Cell surface c-Kit expression on mobilised CD34+ cells was also analysed by flow cytometry. The majority of CD34 positive cells within every sample expressed c-Kit. As previously demonstrated in the study of To *et al* (To et al., 2003), there was a clear and significant decrease in surface expression of c-Kit on specimens mobilising > 10^6 CD34+ cells/kg with a combination of G-CSF and SCF compared with any samples mobilised with G-CSF alone. However, the decrease in "poor" combination G-CSF and SCF treated mobilisers (<10^6/kg CD34+ cells) compared to any samples mobilised with G-CSF alone was not significant. It was clear that treatment of patients with SCF had triggered a down-modulation of c-Kit from the surface of CD34+ cells, but given this effect was not different between good and poor mobilisers in response to a combination of G-CSF and SCF, it was not a useful predictor of mobilisation efficiency.

This series of experiments indicated that, at the mRNA level, that there was no differential expression of c-Kit isoforms or total c-Kit expression levels in any subset of cells analysed. It has often been noted that c-Kit is down-modulated in mobilisation of CD34 cells, and it was clear from the above experiments that this was not influenced at the level of transcription or mRNA stability. The downmodulation of cell surface c-Kit, when it occurs, would appear to be controlled at the protein level, potentially in response to ligand, as demonstrated in previous chapters.

These data do not support the hypothesis that the haemopoietic system uses differential expression of c-Kit isoforms as a mechanism to generate signalling diversity from c-Kit, despite the potential of c-Kit isoforms to mediate signal diversity as has been clearly demonstrated in Chapters 3 and 4.

5.6. Appendix 1

5.6.1. CD34

Antibodies to CD34 allow identification of the immature compartment of stem cells within normal human bone marrow mononuclear cells and peripheral blood (mobilised) stem cells, as well as sub-populations of blast cells from various acute leukaemia specimens (Vaughan et al., 1988). The CD34 antigen is a monomeric cell surface glycoprotein of molecular weight 100-120 kDa (Watt et al., 1987). It belongs to the mucin-like family of adhesion molecules (He et al., 1992; Imai et al., 1993) now called sialomucins (Lanza et al., 2001). Most antibodies to CD34 are directed against glycan epitopes (Sutherland et al., 1988) and both the function and ligand for this molecule expressed on haemopoietic cells has yet to be fully elucidated (Lanza et al., 2001). The function of CD34 expressed on human endothelial venules is known, however, where it acts as a ligand for L-selectin (Baumheter et al., 1993; Lanza et al., 2001).

Positive selection for CD34 expressing cells is widely used in clinical autologous and allogeneic haemopoietic transplantation (Civin et al., 1995) and is regarded the best method for predicting engraftment success. CD34 is also extensively used in the diagnosis of leukaemias and myelodysplastic syndromes (Lanza et al., 2001).

CD34 is extensively used as a first marker in selection of primitive haemopoietic stem cells, and dual labelling of cells with Mabs to HLA-DR (to identify HLA-DR – subsets) (Lu et al., 1987) or Thy-1 (to identify Thy 1 + subsets) allows the

identification of the most immature CD34 cells in early studies (Baum et al., 1992; Craig et al., 1993; Murray et al., 1995; Murray et al., 1994; Peault et al., 1993).

In more recent studies, immature stem cells have been identified based on the phenotype CD34 positive, c-Kit positive, rhodamine 123 (dull) (Ratajczak et al., 1998). This subset constitutes 0.01-0.05% of the total mononuclear cells in normal bone marrow. These cells have also been shown to lack expression of CD33, CD38, CD20 and Glycophorin A. Functionally, this subset of cells have been shown to have high engraftment capacity in a SCID mouse model (Ratajczak et al., 1998).

More recently, studies suggest that CD34 positive cells that also express CD133 represent the most immature myeloid stem cell phenotype within the haemopoietic system (Goussetis et al., 2000). The CD133 antigen is a 120kDa 5-transmembrane glycoprotein (Miraglia et al., 1997; Yin et al., 1997). CD34+ CD133+ cells represent a potent subset of cells capable of long term engraftment in NOD/SCID mice. This subset has also been shown to contain dendritic cell precursors (de Wynter et al., 1998). CD34+, CD133+ cells are also CD164+, CD135+, c-Kit+, CD38 low, CD33+ and CD71 low. There was an additional subset of CD133+ cells that were CD34-, c-Kit-, CD71-, CD38 low, CD135+, CD45+ and HLA-DR+, but the lineage potentiality of these cells was not defined (Buhring et al., 1999). This subset has been demonstrated to have the ability to engraft in NOD/SCID mice (Kuci et al., 2003). CD34, c-Kit and CD133 antigens are co-expressed on most haemopoietic stem cells and progenitors, but CD133 is down-regulated earlier in the maturation pathways than CD34 and c-Kit (Majka et al., 2000).

CD34 was used as the marker for immature stem and progenitor cells in this study

5.6.2. CD33

The Mab My9 was first described by Griffin *et al* (Griffin et al., 1984) and shown to bind a 67kDa cell surface glycoprotein later identified as CD33 (Peiper et al., 1988). CD33 is a member of the Ig like superfamily and, in particular, the sialic acid dependent adhesion molecules of the sialoadhesin family (Freeman et al., 1995; Kelm et al., 1996) that is constitutively expressed on many myeloid progenitor cell lines (Simmons et al., 1988). The sialoadhesins are a family of I-type lectins that bind to sialic acids on the cell surface (Kelm et al., 1998). CD33 has long been used as a marker for myeloid differentiation (eg. (van der Schoot et al., 1987)), yet there was no clear function attributable to the glycoprotein. However, recent studies show that CD33 associates with the protein tyrosine phosphatases SHP-1 and SHP-2 via two immunoreceptor tyrosine-based inhibition motifs (ITIMs) present in its cytoplasmic domain. Phosphorylation of these ITIMs (necessary to recruit SHP-1 and SHP-2), is mediated by Src family tyrosine kinases and appears to modulate its ligand binding activity (Paul et al., 2000; Taylor et al., 1999). This also may regulate FcγR1 signal transduction (Ulyanova et al., 1999) and CD64 induced calcium mobilisation (Paul et al., 2000). More recently, CD33 has been implicated in the regulation of proliferation and survival of primitive myeloid cells induced by SCF and GM-CSF (Mingari et al., 2001). In addition to tyrosine phosphorylation targets on CD33, Protein Kinase C has been shown to phosphorylate 2 serine targets on the molecule, modulating lectin binding activity of CD33 (Grobe et al., 2002).

CD33 was used in this study to identify CD34 positive cells committed to myeloid differentiation pathways.

5.6.3. CD38

Whilst antibodies to CD34 allow positive selection of stem cells capable of reconstituting the haemopoietic system, utilisation of antibodies to the CD38 marker together with anti CD34 Mabs permits a further 10 – 100 fold enrichment of the most primitive stem cells. (Civin et al., 1995; Olweus et al., 1994). CD38 is a 45kDa Type II transmembrane glycoprotein whose expression is not restricted to the haemopoietic system (Funaro et al., 1999). Functions of CD38 identified include enzymic activity to synthesise and hydrolyse cyclic ADP-ribose (involved in Calcium mobilisation) (Mehta et al., 1996), and also activity on the substrate nicotinamide adenine dinucleotide (NAD) (Funaro et al., 1999). Ligation of CD38 on haemopoietic cells with agonistic antibodies can stimulate growth, block apoptosis, induce cytokine production and activate cellular kinase activity (Mehta et al., 1996). Finally, this unique protein also plays a role in adhesion, and is a counter-receptor to a variety of ligands including hyaluronan (Funaro et al., 1999).

Flt3 antigen (CD135), expressed on very primitive haemopoietic stem cells and required for growth and survival of primitive cells, is co-expressed on the subset of CD34 cells that do not express CD38. As these stem cells differentiate and acquire CD38 surface expression, Flt3 expression declines (Xiao et al., 1999).

In this study, CD38 negativity was used as criteria to identify one of the most immature stem cell subsets in normal bone marrow MNCs.

5.6.4. CD19

CD19 is a member of the Ig superfamily and is a 95kDa cell surface transmembrane glycoprotein (Stamenkovic et al., 1988; Tedder et al., 1989). CD19 is part of the B cell receptor complex and regulates mature B cell responses to ligation of the B cell antigen receptor (Fujimoto et al., 1998; Pesando et al., 1989; Sato et al., 1995) and is itself phosphorylated on tyrosine residues (Roifman et al., 1993). It transduces signals via activation of Src family kinases (Fujimoto et al., 1998) including Lyn (Roifman et al., 1993).

In normal haemopoietic cells, CD19 is expressed on most cell types within the B cell lineage (Pezzutto et al., 1987). Surface expression of CD19 commences when the primitive progenitor cell first commits to the B cell lineage, and remains expressed throughout the maturation process to the mature B cell, and is only downregulated at the stage of plasma cell development (Fluckiger et al., 1998; Scheuermann et al., 1995; Stapleton et al., 1995). Cells co-expressing CD34 and CD19 are believed to be B cell progenitors (Fritsch et al., 1995). Like CD7 (see 5.6.6), CD19 is also expressed on a subset of acute myeloid leukaemias (Scheuermann et al., 1995).

CD19 promotes the proliferation and survival of mature B cells, but also plays important roles in the maturation of early pre B cells (de Rie et al., 1989; Otero et al., 2003) and was used in this study to identify the subset of progenitor cells committed to the B cell lineage.

5.6.5. CD61

CD61 is a cell surface marker associated with the megakaryocytic lineage and cells co-expressing CD34 and CD61 are considered to be megakaryocyte progenitor cells (Bojko et al., 1998; Thoma et al., 1994). It is the platelet membrane glycoprotein GPIIb IIIa heterodimer that functions as a receptor for adhesive proteins on stimulated platelets (Duperray et al., 1989). In extremely immature but committed megakaryocyte progenitors, CD61 is only expressed intracellularly (Kafer et al., 1999). In addition, myeloid and erythroid progenitor cells are believed to be in this fraction of CD34 cells (Rasko et al., 1997). CD34 + CD61 + cells express the stromal cell-derived factor 1 (SDF-1) chemokine receptor CXCR4 and megakaryocyte progenitors expressing this receptor can be induced to migrate in response to SDF-1 (Wang et al., 1998). CD61 is co-expressed on CD34+ Mpl-Receptor+ progenitors (Mpl-receptor: haematopoietin receptor superfamily member restricted to megakaryocytes) (Debili et al., 1995). This subset of cells also co-expresses c-Kit. SCF, together with megakaryocyte growth and development factor (MGDF, thrombopoietin, mpl-ligand) represents a potent stimulus for both proliferation and survival of this subset of progenitor cells (Rasko et al., 1997). Studies by Lazzari and colleagues have demonstrated that IL-6 and IL-11 in addition to Mpl-Ligand and SCF play a role in the expansion of megakaryocyte precursors (Lazzari et al., 2000).

In this study CD61 was used as a marker for megakaryocyte progenitors, but it will also detect the less mature, bipotential erythroid/megakaryocytic progenitors.

5.6.6. CD7

CD7 is a 40 kDa single domain member of the Ig superfamily that is expressed by early stage T, B and myeloid cells and mature Natural Killer (NK) cells and T Cells (Palker et al., 1986; Sempowski et al., 1999; Ware et al., 1989). One of the first Mabs to identify this Ag, 4H9, was originally used to identify blasts in childhood T-ALL and T-NHL diseases (Link et al., 1983). A ligand for CD7 has not been identified, but studies examining CD7 deficient mice have shown a role for CD7 in regulation of mature T and NK cell cytokine production (Sempowski et al., 1999) and also intrathymic T cell development (Lee et al., 1998). CD7 is expressed on some acute myeloid leukaemic cells and CD34+ CD7+ cells have been identified in human foetal liver. These cells, when cultured with phorbol ester, rapidly lose CD7 expression and retain myeloid cell characteristics suggesting that the CD7 molecule is only transiently expressed in myeloid lineages (Tien et al., 1996).

There is also evidence for a more immature subset of cells expressing CD7 which are thought to represent a common lymphoid/myeloid progenitor (Tien et al., 1998). In support of this, CD7 is expressed on a higher proportion of CD34 positive cells from Philadelphia Chromosome positive Chronic Myeloid Leukaemia (CML) patients compared to normal CD34 positive cells (Normann et al., 2003). These CML cells, representing a clonal expansion of an immature phenotype progenitor, may serve as a useful prognostic indicator in the future (Normann et al., 2003).

CD7 is a useful marker for very early T cell lineage commitment, as CD7 expression precedes T cell receptor beta-chain gene rearrangements. Many lymphoblastic

neoplasms already have this rearrangement (Pittaluga et al., 1986), implying that CD7 is expressed very early in the commitment to T cell differentiation.

5.6.7. *Glycophorin A*

Glycophorin A is the major sialoglycoprotein of the erythrocyte membrane. It is organised into 3 domains (2 hydrophilic segments separated by a region of nonpolar amino acids) (Furthmayr, 1977) and exists predominantly as a dimer (Lemmon et al., 1992; Treutlein et al., 1992). Glycophorin A occurs in two allelic forms, M and N, and it forms the antigens of the MN blood group (DuPont et al., 1995). Glycophorin A has been shown to be the receptor for a variety of agents including Plasmodium falciparum (Breuer et al., 1983; Pasvol et al., 1982; Perkins, 1984), influenza virus (Baron et al., 1983), Escherichia coli alpha-hemolysin (Cortajarena et al., 2001), and sendai virus (Wybenga et al., 1996).

Glycophorin A has been shown to be surface expressed early in commitment to erythropoiesis and to increase with maturation (Daniels et al., 2000; Debili et al., 1996; Inada et al., 1997; Nakahata et al., 1994). Erythroid colony forming cells (ECFC) were shown to be dependent on SCF for survival, as they rapidly apoptose in the absence of SCF (Endo et al., 2001).

In this analysis, Glycophorin A was used to identify committed late erythroid progenitor cells.

6 General Discussion

The aim of this project was to investigate the signalling pathways initiated through the receptor tyrosine kinase c-Kit, and to correlate these results with the wide range of cellular responses (proliferation/ differentiation/ survival/ transformation) elicited by the ligand, SCF. Several naturally occurring isoforms of c-Kit had been identified (Crosier et al., 1993) and analysis of these isoforms by Caruana in a murine fibroblast model system demonstrated differences in their transformation potential in response to SCF (Caruana, 1996). Two of these isoforms (GNNK+S+ and GNNK-S+) were chosen for detailed analysis and both qualitative and quantitative differences between them were observed. To eliminate variations in biological responses attributable to receptor levels and therefore "strength of signal", care was taken at all times to control the level of c-Kit expressed in the model systems. The initial studies utilised murine cells in which full-length human c-Kit cDNA was expressed.

In addition to this, a second aim was to develop a more sophisticated murine haemopoietic cell model for the expression/analysis of c-Kit function. To more appropriately control c-Kit function, a chimaeric c-Kit was constructed containing the human extracellular domain and murine transmembrane and intracellular domains. It was hypothesised that the background (SCF independent) signalling observed in previous studies (shown in Chapter 3) using c-Kit in murine fibroblastoid cells, could be due to a loss of control of c-Kit by the host cell as a result of differences between the human and murine systems and/or an inappropriate host cell type. Use of this chimaeric receptor placed the correct species cytoplasmic domain in the host cell, and

allowed specific stimulation of the chimaeric c-Kit without interference from any endogenous murine c-Kit by use of human SCF, which is inactive on murine c-Kit.

In addition to generating chimaeric c-Kit, a murine factor dependent cell line model was developed to allow the introduction of the chimaeric receptor into a cell line that was representative of immature haemopoietic cells (an appropriate host cell type). This model was chosen to facilitate the investigation of several biological outcomes in the same cell (survival, proliferation and differentiation), and was postulated to enable exploitation of gene knockout technology, creating new lines missing specific components of the signalling cascade. In particular, the Src family kinase Lyn was investigated in this manner.

Having identified qualitative and quantitative differences between GNNK+ and GNNK- c-Kit isoforms in a number of model systems, the third aim of this work was to elucidate the expression patterns of two of these isoforms (GNNK+ and GNNK- c-Kit) in various subsets of normal human haemopoietic cells. Given the substantially different signalling properties of the isoforms, it was of value to investigate whether or not differential expression of these isoforms occurred at different stages of human haemopoietic cell differentiation, or influenced cytokine-induced mobilisation of stem/progenitor cells to the peripheral blood.

6.1. Murine c-Kit receptor levels

In Chapter 3, the analysis demonstrated that ectopic expression of the unaltered murine c-Kit receptor in NIH(mukit) pools of infectants induced transformed

characteristics in NIH3T3 cells (ie. morphological changes, growth in low levels of serum, focus formation, anchorage independent growth in soft agar, and tumourigenicity in nude mice) in a factor-dependent manner.

A threshold number of receptors ($2.5x10^4$ /cell) was needed to induce anchorage independent growth (colony formation) under these conditions. Intermediate levels of c-Kit expression resulted in enhanced colony growth and a positive correlation was identified between the level of c-Kit protein in these clones and colony number in the presence of muSCF. These levels were comparable to the average of $2x10^4$ copies/cell found on CD34+ human haemopoietic progenitor cells (Cole et al., 1996) suggesting that expression of c-Kit at levels only moderately higher than physiological was required to induce anchorage independent growth of the NIH(mukit) cells. Clones expressing the highest levels of c-Kit, however, produced few colonies even in the presence of muSCF. Similar results were observed when human c-Kit was expressed in NIH3T3 cell lines. In these, optimum colony formation occurred at $5x10^4$ receptors per cell, with inhibition at higher levels. These results indicate that there is an optimal level of c-Kit expression that was necessary for the production of anchorage-independent growth of NIH3T3 cells.

How receptor overexpression results in transformation of indicator cell lines is still not clearly understood, however this may be due to the activation of common signalling pathways. c-Kit activates the Ras/Raf/mitogen-activated protein kinase (MAPK) pathway, many components of which are known proto-oncogenes (Schlessinger et al., 1994). It is clear that the strength and duration of signal generated by RTKs as a consequence of the variation in receptor density on PC12

cells can alter the biological response (Dikic et al., 1994; Marshall, 1995; Traverse et al., 1994). Overexpression, most likely will trigger sustained high level signalling, leading to activation of pathways not normally stimulated to "activation thresholds" when normal physiological expression levels of the receptor are in place.

Inhibition of anchorage-independent growth was observed at high levels of receptor expression in two series of experiments (one series using murine c-Kit, one using human c-Kit). This too, may reflect strength of signal phenomena. Although NIH3T3 cells do not undergo differentiation, there was evidence that an optimal level of stimulation of the Ras/MAPK pathway is required for transformation. While moderate Raf kinase activity was associated with proliferation and transformation in these cells, high constitutive activity was shown to lead to p21Cip1 induction and cell cycle arrest (Woods et al., 1997). Similarly, there appeared to be an optimum level of signalling through c-Kit for transformation.

A significant level of factor-independent colony formation was observed with pools and clones of NIH3T3 cells expressing relatively high levels of c-Kit. Whilst this may have been due to autocrine SCF (Jozaki et al., 1991), studies using an antagonistic anti-c-Kit Mab, or a partially neutralising anti-muSCF antibody, failed to influence the 'factor-independent' colony yield. This was confirmed using a retroviral anti-sense SCF cDNA construct that blocked autocrine SCF production and also failed to inhibit factor-independent colony growth.

In conclusion, the data presented in Chapter 3 suggest that over-expression of normal c-Kit was capable of contributing to oncogenic transformation.

6.2. Hu-c-Kit isoforms

Alternative splicing of mRNA encoding human c-Kit occurs in several tissues (Crosier et al., 1993) and its significance was unknown. To investigate the function of the different isoforms, a retroviral vector was used to introduce different isoforms of human c-Kit into NIH3T3 fibroblasts, which do not express endogenous murine c-Kit. The resulting infectants were used to compare cellular responses elicited by human SCF through the different receptor isoforms and any differences were then explored biochemically to elucidate signalling pathways.

The GNNK- c-Kit was more strongly transforming than the GNNK+ isoform when expressed at similar levels (approximately 10^4 copies/cell). In addition, dissociation of the different indicators of transformation in the NIH3T3 model was observed. Whilst the GNNK+ isoform was at least as effective as GNNK- in inducing anchorage-independent growth (colony formation in soft agar), it was poor at overcoming contact inhibition (focus-formation assay), and was non-tumourigenic in nude mice.

6.2.1. Biochemical analysis

To gain some insight into the biochemical basis for these different cellular responses in NIH3T3 cells, receptor activation in response to SCF was examined. Given that saturation binding analysis (Chapter 3) indicated that both isoforms have similar affinity for SCF, subsequent experiments were performed with a single saturating level of SCF (100 ng/ml). The presence or absence of the GNNK tetrapeptide had a profound effect on the kinetics and extent of receptor phosphorylation, being

extremely rapid for GNNK- followed by downregulation which involved internalisation of the receptor. In contrast, the GNNK+ isoform displayed a later peak tyrosine phosphorylation and showed little dephosphorylation or down-regulation during the period of analysis. A marked difference was observed in the relative level of phosphorylation, with GNNK- c-Kit phosphorylated up to 7 fold higher than GNNK+ c-Kit. It remains unknown whether this is a reflection of lower efficiency of phosphorylation overall, or the lack of phosphorylation of specific sites. Support for specific tyrosine phosphorylation pattern differences between isoforms was shown in a recent study by Voytyuk *et al.* This study demonstrated that specific tyrosines of the GNNK+/- c-Kit were differentially phosphorylated (both kinetics and level of phosphorylation) when stimulated with SCF. Y568 (juxtamembrane region – Src family kinase association site) displayed rapid, transient phosphorylation in GNNK- c-Kit, whereas GNNK+ c-Kit was constantly phosphorylated at a low level, even in the absence of SCF. Y823 in the activation loop was identical to total tyrosine phosphorylation patterns (strong, rapid and transient phosphorylation for GNNK- c-Kit, and weak, slower phosphorylation for GNNK+ c-Kit). Y721 (PI3-K association site), was phosphorylated to the same level in either isoform, with kinetics for GNNK- c-Kit being faster than for GNNK+ c-Kit. Y936 (Grb2 and Grb7 association site) was strongly and rapidly phosphorylated in the GNNK- c-Kit, but even more strongly phosphorylated for longer in GNNK+ c-Kit (Voytyuk et al., 2003).

Despite the low level of phosphorylation of GNNK+ c-Kit, studies presented in Chapter 3 suggest that PI3-K was recruited similarly to both forms of the receptor and was similarly activated based on phosphorylation of its major down-stream effector,

c-Akt. In contrast, phosphorylation of MAPK paralleled that of c-Kit and was much stronger with the GNNK- isoform.

The relationship between hyperphosphorylation of GNNK- c-Kit and its more rapid endocytosis is unclear. Experiments with endocytosis-defective cells indicated that maximal phosphorylation of the EGF receptor requires internalisation. Furthermore, efficient MAPK phosphorylation and activation required receptor endocytosis while activation of phospholipase Cγ was more efficient in endocytosis-defective cells (Vieira et al., 1996). Thus the different rates of internalisation of the c-Kit isoforms may contribute to the variable signalling kinetics and cellular responses. Voytyuk *et al* demonstrated that Src family kinases were directly involved in the phosphorylation of c-Cbl (which leads to polyubiquitination of c-Kit) in response to SCF stimulation (Voytyuk et al., 2003). Given that Y568 (the recruitment site for Src family kinases on c-Kit) was more strongly phosphorylated on the GNNK- c-Kit (see above), this could be a mechanism contributing to the rapid SCF induced endocytosis and degradation of activated GNNK- c-Kit.

The results presented here differ from those of Reith *et al* (Reith et al., 1991) with murine GNNK+ and GNNK- isoforms transiently expressed in COS cells. These workers observed constitutive tyrosine phosphorylation of the GNNK- isoform, but not GNNK+, in the absence of ligand. In contrast, receptor phosphorylation in the absence of SCF was very low for both isoforms in this study. One possible explanation for these observations was that the levels of receptor expression, which were not determined by Reith *et al*, were probably somewhat higher than in this study due to the use of the transient expression system. However, a significant level of

factor-independent receptor activation can occur for both the GNNK+ and GNNK- isoforms of human c-Kit, as is evidenced from the results of the colony assays described here (Table 3.3) where relatively high frequencies of factor-independent colonies were observed.

Strong stimulation of certain signalling pathways may be inhibitory to NIH3T3 proliferation through induction of p21Cip1 (Sewing et al., 1997; Woods et al., 1997). In contrast to the findings of the colony assay, NIH3T3 infectants grown in plastic adherent conditions in the focus formation assay showed much less evidence of factor-independent c-Kit activation. The conditions in this assay were comparable to those under which the biochemical assays were performed. Furthermore, inhibition at higher receptor levels was not observed in this assay. These results suggest a complex interplay between signals via c-Kit and adhesion molecules.

The differences between the isoforms in their transforming ability could be correlated with differences in signalling. The GNNK- isoform, which induced anchorage-independence, loss of contact inhibition and tumorigenicity, displayed stronger receptor phosphorylation, more rapid internalisation, and stronger activation of the MAPK pathway following SCF stimulation than the GNNK+ isoform. In contrast, the GNNK+ isoform induced anchorage-independent growth with similar efficiency to GNNK- c-Kit, but was much less effective in inducing other attributes of transformation. The fact that SCF binding to the GNNK+ isoform efficiently recruited and activated PI3-K suggests that this pathway is particularly important in preventing death of cells deprived of contact with extracellular matrix (a process termed anoikis) (Ruoslahti et al., 1994).

There are strong parallels between GNNK+ c-Kit and R-Ras in both signalling and their ability to induce different attributes of transformation in vitro. Activated R-Ras was as effective as H-Ras in promoting growth of NIH3T3 cells in soft agar, but was much less effective in inducing focus formation (Cox et al., 1994). Furthermore, activated R-Ras stimulates the PI3-K pathway but, in contrast to other Ras proteins, has little effect on the MAPK pathway in fibroblasts (Marte et al., 1997, Berrier, 2000 #626). A further difference was observed in studies on bone marrow derived mast cells, where H-Ras and R-Ras potently stimulated adhesion and ligand binding activity of VLA-5 to fibronectin. H-Ras did this in a PI3-K dependent fashion, whereas R-Ras activity was independent of PI3-K (Kinashi et al., 2000; Oertli et al., 2000).

6.3. Development of a new model to test c-Kit cellular responses

6.3.1. Myb Immortalised Haemopoietic Cell (MIHC) development

The studies of Chapter 3 highlighted the need to develop an alternative model system to more closely examine cellular responses to c-Kit as the NIH3T3 model can only provide information on the transformation potential of the receptor. Furthermore, NIH3T3 cells are fibroblastoid, a cell type that does not normally express the receptor. This may lead to ligand-independent behaviour of c-Kit and erroneous signalling due to an inappropriate repertoire of downstream signalling proteins. The NIH3T3 model also failed to measure many of the normal cellular responses to SCF. In Chapter 4, an improved model was developed to redress some of these shortfalls.

This model was derived from cells of haemopoietic origin, and had the potential to measure proliferation, differentiation and survival in response to SCF stimulation of c-Kit.

The perceived strengths of this model included use of a physiologically relevant cell type, species matching of signalling components of the c-Kit molecule, consistent surface c-Kit expression, and careful elimination of clonal derived artefacts. This system was also used to biochemically analyse signalling of c-Kit isoforms in backgrounds differing only in the presence or absence of a single c-Kit downstream effector, Lyn.

The Myb Immortalised Haemopoietic Cell line model was successfully established for both WT (C57BL/6) and Lyn -/- genotypes. The system was factor dependent, requiring either murine GM-CSF or murine IL-3, and proved useful for evaluating proliferation and survival responses to SCF stimulated c-Kit upon withdrawal of murine factors. Disappointingly, it proved unsuitable for analysis of differentiation responses. In MIHC, the chimaeric c-Kit molecule successfully functioned in a tightly controlled, human ligand inducible manner. Subtle differences were noted between c-Kit isoforms in the presence/absence of Lyn, demonstrating the potential value of this approach in evaluating the role played by other downstream components in the c-Kit signalling cascades.

Whilst the generation of MIHC was in large part successful, a number of limitations were evident. The state of differentiation of the resultant immortalised cells was higher than desirable as shown in Figures 4.6, 4.7, 4.8 and 4.9. While the mouse

strain used could have been a contributing factor, this was most likely due to the use of Baculovirus derived murine growth factors. A yeast-derived mGM-CSF was subsequently demonstrated by Dr Ferrao to be a superior stimulant of growth without differentiation (personal communication). This was despite the fact that yeast and baculovirus derived factors were equivalent with respect to their potency in stimulating growth of the factor dependent cell line FDC-P1. The use of purified recombinant mGM-CSF could overcome this problem in future studies.

A more serious limitation of the MIHC model is whether or not it will ever be useful to evaluate differentiation due to the constitutive over-expression of activated c-Myb in these cells, which is known to have anti-differentiative effects. It is possible, with overexpression of receptors such as c-Kit, that a strong differentiation signal may over-ride the Myb effects (Ferrao et al., 1997), but the system may become too contrived to confidently interpret differentiation responses at all.

Another positive feature of the MIHC model was the ability to generate a series of different MIHC lines potentially only differing in the presence or absence of one protein, taking advantage of the many knockout mouse strains now available. The potential to do this was demonstrated clearly in this study using Lyn knockout mice, although refinements are necessary. Firstly, the C57 and Lyn -/- MIHC used in this study were not strictly identical except for the presence/absence of Lyn. The Lyn -/- mice were extensively backcrossed (six times) onto a C57BL/6 strain to bring them close possible to the C57BL/6 genotype. However, this would not have generated a pure C57 mouse strain lacking Lyn. In future, development of MIHC from identical strains (one with a targeted gene, the other "wild type") will eliminate this variability.

A second limitation in the approach of using knockout mouse cells as a source of cells for MIHC is the problem of redundancy encountered in knockout technology. Lyn -/- mice have relatively normal haemopoiesis and are viable despite lacking a downstream component of c-Kit signalling which would be presumed necessary for some aspects of haemopoietic development. This will limit the use of removal of a protein to assign functions to it, making it important to identify possible redundancies. It is feasible to cross knockout strains to generate double or triple knockouts to circumvent such redundancy. Even if progeny of such crosses are not viable, it is possible, if homozygous double knockout progeny can reach day 14 of gestation, to generate MIHC for analysis in this system.

6.3.2. *Cellular responses to exogenous Human SCF by chimaeric c-Kit in MIHC*

A number of cellular responses were analysed including surface receptor internalisation, survival, and proliferation (differentiation investigations were not performed for the reasons discussed previously).

Both isoforms of chimaeric-c-Kit were internalised in response to Human SCF to similar levels with subtle differences noted in the presence/absence of Lyn. GNNK-chi-c-Kit isoform internalised more rapidly and extensively than the GNNK+ isoform. The kinetics and extent of internalisation was dictated by the isoform, supporting the work done previously with murine fibroblasts and human c-Kit in Chapter 3. This was also supported by the biochemical analyses, where ubiquitination of the isoforms was shown to be slower for GNNK+ c-Kit than GNNK- c-Kit. The extent of

ubiquitination in the presence or absence of Lyn was also subtly different. The reduction observed was supported by the findings of Voytyuk *et al* (Voytyuk et al., 2003), where Src specific inhibitors affected c-Kit internalisation and degradation. Given the weak effects noted in Lyn -/- MIHC in Chapter 4, it is likely that redundancy between Src family kinases has masked the full effect of the Lyn deficiency in these MIHC.

The ability of all MIHCs (Lyn-/- and C57 expressing either isoform of c-Kit) to proliferate in response to Human SCF was potent and identical to that elicited by mGM-CSF/mIL-3. The responsiveness of Lyn -/- MIHC expressing either isoform of c-Kit suggests no role of Lyn in the proliferative response in these cells in contrast to the findings of O'Laughlin-Bunner in murine mast cells (O'Laughlin-Bunner et al., 2001). The data also demonstrated that the proliferation signal from GNNK+ and GNNK- c-Kit is identical, despite the large differences in kinetics of phosphorylation of c-Kit itself, MAPK and AKT (all of which are substantially higher in GNNK- compared to GNNK+ c-Kit).

Chimaeric GNNK- c-Kit was, however, superior to GNNK + in promoting survival in response to Human SCF over 3 days in the presence or absence of Lyn. In addition, these experiments showed that C57 MIHC had superior survival percentages to the Lyn-/- MIHC counterparts. The presence of Lyn may contribute to this survival response as roles for Lyn in anti-apoptotic responses have been demonstrated in a variety of cell types (Adachi et al., 1999; Pazdrak et al., 1998; Wei et al., 1996).

An alternative explanation for these phenomena may lie in the argument of strength of signal. Whilst every effort was made to match the surface expression of the chimaeric c-Kit isoforms on each MIHC type, the Lyn -/- MIHCs, on average, had 2-4 fold less c-Kit than C57 MIHCs in the signalling analyses. It is unclear as to where this consistent discrepancy arose, as the MIHC used were all passaged minimally from a common set of stocks after surface expression had been assessed. This may have been adequate to achieve a differential in the strength of signal arising from c-Kit to elicit the survival response. Irrespective of the presence/absence of Lyn, GNNK-c-Kit always induced a more rapid and extensive phosphorylation of c-Kit. Linked to the more extensive phosphorylation was increased recruitment of PI3K (p85 co-immunoprecipitation) and AKT phosphorylation. PI3-K plays a major role in survival responses (Benini et al., 2004; Scanga et al., 2000; Xu et al., 2003), and the level of recruitment (and subsequent activation) is dependent on phosphorylation levels and therefore is directly affected by the isoform of c-Kit. Given the lower levels of c-Kit retrievable from Lyn -/- MIHC, a lower gross level of c-Kit phosphorylation was reached in response to SCF, leading to a lower gross recruitment of PI3-K resulting in a reduced survival response. In addition, as shown in figure 4.14, Lyn -/- MIHC activation of AKT was not as sustained as the C57 MIHC counterparts. It is of interest to note that the chimaeric c-Kit isoforms differed with respect to PI3-K recruitment and activation compared to hu c-Kit in murine fibroblasts (Chapter 3 and Voytyuk et al (Voytyuk et al., 2003)). In NIH3T3 cells expressing human c-Kit isoforms, the receptor recruited and activated PI3-K equally well, suggesting that species mismatching of the receptor and host cell may have lead to altered kinetics and properties of this signalling pathway.

6.3.3. *Future directions for MIHC model*

It is important to re-visit this model system using optimal growth factor conditions. Where MIHC can be grown in yeast derived mGM-CSF alone (or an equivalent), and maintain a much more undifferentiated status, it may become possible to evaluate the usefulness of this model in assessment of differentiation responses to SCF stimulation. Also, MIHC generated from the original knockout and parental mice strains to eliminate genetic background variation introduced by backcrossing to C57BL/6 is required. The technical feasibility for this, however, is unknown.

Given the association of Tec kinase and Dok 1with Lyn, it would also be valuable to analyse the activation of these 2 molecules in the model used here. It is hypothesised that these molecules should remain unaltered in the Lyn -/- MIHC upon SCF stimulation. If, however, they are stimulated early (ie directly by SCF activation of c-Kit), it would be indicative of Src family kinase redundancy. The use of specific Src family kinase inhibitors (Blake et al., 2000) may be of value in resolving these questions.

6.4. Isoform expression

It is quite clear from the work of Chapters 3 and 4, that substantive differences in cellular responses are elicited by the GNNK+/- isoforms of c-Kit. Given the diverse range of cellular responses to c-Kit signalling, it was postulated that differential expression of the isoforms may be a mechanism used by cells to modulate the responses to SCF. To this end, c-Kit isoform expression (GNNK+/-) was investigated

in a number of human haemopoietic subsets. Methodology was developed for the sensitive detection of GNNK+/- c-Kit mRNA using reverse transcription and QPCR analysis from rare subsets of CD34+ cells from normal bone marrow MNCs and mobilised peripheral blood stem cells.

Normal bone marrow MNCs were sorted on the basis of CD34 expression to identify the immature stem cell/progenitor cell compartment. This compartment was further fractionated using Mabs to CD7 (to identify early T cell committed progenitors CD7+CD34+), CD19 (to identify early B cell committed progenitors CD19+CD34+), CD33 (to identify the majority of myeloid committed cells CD33+CD34+), CD38 (to identify the most immature compartment of CD34 cells CD38-CD34+), CD61 (to identify megakaryocyte/early erythroid committed progenitors CD61+CD34+) and Glycophorin A (to identify late erythroid committed progenitors GlyA+ CD34+). No significant difference in expression patterns of the c-Kit isoforms was observed in any subsets, with all samples expressing approximately 90% of total c-Kit transcripts as the GNNK- isoform.

It was also of value to assess the contribution, if any, of differential c-Kit isoform expression in mobilised CD34+ cells from patients who exhibit different efficiencies for mobilisation of CD34+ cells. A series of patients who failed to mobilise successfully when treated with G-CSF or G-CSF in combination with chemotherapy, then subsequently remobilised with a combination of G-CSF and SCF, were investigated. A proportion of this group then mobilised adequate CD34+ cells for clinical applications, whilst others in the group still failed to mobilise adequately.

A number of samples from a 2003 study of To *et al* (To et al., 2003) were obtained, together with additional samples that were successful mobilisations in response to G-SCF alone or combined G-CSF and SCF. In the analysis of isoform expression in these samples, no differences in the expression patterns were observed in any "class" of mobilised apheresis products, nor was there any significant variation in levels of transcript of c-Kit.

Cell surface c-Kit expression on mobilised CD34+ cells was also analysed by flow cytometry. As previously demonstrated in the study of To *et al* (To et al., 2003), there was a clear and significant decrease in surface expression of c-Kit on good mobilisers treated with combined G-CSF and SCF compared to good or poor responders to mobilisation with G-CSF alone. The decrease in surface c-Kit expression for poor combined G-CSF and SCF treated mobilisers compared to samples from good or poor G-CSF alone mobilisations was not significant. No significant difference was evident between good and poor mobilisers treated with G-CSF alone, or between good and poor mobilisers treated with combined G-CSF and SCF. From this analysis, it was clear that treatment of patients with SCF had triggered a downmodulation of c-Kit from the surface of CD34+ cells. However, given this effect was not different between good and poor mobilisers in response to combined G-CSF and SCF, it was not a useful predictor of mobilisation efficiency and provided no clues as to the mechanism involved in stem cell mobilisation.

It has often been noted that c-Kit is downmodulated in mobilisation of CD34 cells, and it was clear from the above experiments that this was not influenced at the level of transcription or mRNA stability. The downmodulation of c-Kit, when it occurs,

would appear to be controlled at the protein level, perhaps in response to ligand. It could also be indirectly downmodulated by proteases such as MMP-9 (Heissig et al., 2002; Lapidot et al., 2002).

These data disprove the hypothesis that differential expression of c-Kit isoforms plays a major role in the process of normal haemopoietic differentiation or stem cell mobilisation into the peripheral blood, despite the potential of c-Kit isoforms to mediate signal diversity as has been clearly demonstrated in Chapters 3 and 4.

6.5. Closing comments

At the initiation of this study, dissociation of several classical indicators of transformation in the NIH3T3 model were identified. The molecular mechanisms by which relatively minor sequence differences between the c-Kit isoforms lead to such remarkably different activation characteristics and biological behaviour were unknown. Clear differences in biochemical analysis of the c-Kit signalling pathways were identified in these cells. The signalling systems were then re-analysed in haemopoietic cells using a chimaeric receptor in order to remove ambiguities in analysis that arose using inappropriate cells for hu c-Kit (murine fibroblastoid cells). These studies have now been extended by Voytyuk *et al* (Voytyuk et al., 2003). It was unclear how the GNNK+/- variation in the juxtamembrane region of the extracellular domain influences the rate of receptor phosphorylation and internalisation, but it seems likely that it must modulate interactions with other membrane proteins, or alter the configuration of cytoplasmic domains to alter affinity or accessibility of different downstream effectors. Since the isoforms have similar

affinity for ligand, it seems improbable that the tetrapeptide has an appreciable effect on receptor homodimerisation.

Very few cellular responses were influenced by the presence/absence of Lyn in the MIHC model using chimaeric c-Kit (GNNK+ and GNNK- isoforms). The model did provide valuable information on differences in cellular responses between isoforms of c-Kit, and demonstrated the potential of this model, with refinements, to carefully analyse cellular responses to haemopoietic growth factors. Where major differences can be seen between parental and knockout MIHCs, verification of the need for the "knocked out" protein is possible by re-introduction of the protein (knock in) to demonstrate rescue of the phenotype.

Finally, whilst the c-Kit isoforms do demonstrate vastly different signalling kinetics and properties, differential expression of them was not evident in one of the major groups of cells expressing c-Kit – the haemopoietic stem cells and progenitor cells.

"Gain of function" mutations of c-Kit have demonstrated that the receptor plays a role in oncogenesis in many tissues and organs as discussed in Section 1.1.3. It is clear from the studies in Sections 3-5 that the GNNK- isoform of c-Kit elicits an increased range of cellular responses compared to the GNNK+ isoform, yet in haemopoietic progenitor cells, differential expression of the isoforms is unlikely to be involved in the diverse cellular responses elicited by c-Kit.

It would be of value, however, to extend this analysis to non-haemopoietic tissues and, in particular, compare normal and tumour derived samples looking for evidence of differential expression. In addition, analysis of gain of function mutations of c-Kit in both isoforms of c-Kit may demonstrate differences in the type or magnitude of cellular responses, and the information collectively may lead to development of novel targetted therapies.

At another level, the phenomenon observed of differential signalling by these two isoforms of c-Kit provide an opportunity to further study the basic biochemistry of the signalling process. How does the deletion of four amino acids in the extracellular domain elicit the changes in kinetics and magnitude of c-Kit signalling? Understanding the effects of conformation/orientation changes driven by the sequence change could provide information toward the development of novel treatments for altered receptors in disease states.

Amendments for incorrect citation format within text

- Replace "Austyn et al., 1981" with "Austyn and Gordon, 1981" p52, section 2.3.1
- Replace "Baluda et al., 1994" with "Baluda and Reddy, 1994" p119, section 4.1.1
- Replace "Bargmann et al., 1988" with "Bargmann and Weinberd, 1988" p19, section 1.5
- Replace "Baron et al., 1983" with "Baron and Blough, 1983" p181, section 5.6.7
- Replace "Bies et al., 1997" with "Bies and Wolf, 1997" p122, section 4.1.2
- Replace "Blume-Jensen et al., 2001" with "Blume-Jensen and Hunter, 2001" pp1-5, sections 1.1.1 to 1.1.2 and p18, section 1.5
- Replace "Carlberg et al., 1994" with "Carlberg and Rohrschneider, 1994" p19, section 1.5
- Replace "Civin et al., 1995" with "Civin and Small, 1995" p174, section 5.6.1 and p177, section 5.6.3
- Replace "Colucci et al., 2000" with "Colucci and Di Santo, 2000" p29-30, section 1.7.6
- Replace "Conlan et al., 1994" with "Conlan and North, 1994" p52, section 2.3.1
- Replace "Daniels et al., 2000" with "Daniels and Green, 1981" pp181, section 5.6.7
- Replace "Dasgupta et al., 1989" with "Dasgupta and Reddy, 1989" p121, section 4.1.2
- Replace "Duarte et al., 2002" with "Duarte and Franf, 2002" p159, section 5.2
- Replace "Dudek et al., 1989a" with "Dudek and Reddy, 1989a" p121, section 4.1.2
- Replace "Dudek et al., 1989b" with "Dudek and Reddy, 1989b" p121, section 4.1.2
- Replace "Eiseman et al., 1992" with "Eiseman and Bolen, 1992" p129, section 4.3.1
- Replace "Flanagan et al., 1990" with "Flanagan and Leder, 1990" p13, section 1.3
- Replace "Funaro et al., 1999" with "Funaro and Malavasi, 1999" p177, section 5.6.3
- Replace "Gadd et al., 1985" with "Gadd and Ashman, 1985" p9, section 1.2.1
- Replace "Garrington et al., 1999" with "Garrington and Johnson, 1999" p27, section 1.7.3
- Replace "Gewirtz et al., 1988" with "Gewirtz and Calabretta, 1988" p176, section 5.6.2
- Replace "Giebel et al., 1991" with "Giebel and Spritz, 1991" p13, section 1.2.2
- Replace "Gonda et al., 1984" with "Gonda and Metcalf, 2002" p124, section 4.1.4
- Replace "Grobe et al., 2002" with "Grobe and Powell, 1981" p52, section 2.3.1
- Replace "Hibbs et al., 1997" with "Hibbs and Dunn, 1997" p126, section 4.2
- Replace "Howe et al., 1991" with "Howe and Watson, 1991" p121, section 4.1.2
- Replace "Hubbard et al., 2000" with "Hubbard and Till, 2000" p4, section 1.1.2
- Replace "Huse et al., 2002" with "Huse and Kuriyan, 2002" p4, section 1.1.2
- Replace "Joaquin et al., 2003a" with "Joaquin and Watson, 2003a" p120, section 4.1.1
- Replace "Jove et al., 1987" with "Jove and Hanafusa, 1987" p125, section 4.2
- Replace "Kapeller et al., 1994" with "Kapeller and Cantley, 1994" p26, section 1.7.1
- Replace "Kinashi et al., 1994" with "Kinashi and Springer, 1994" p30, section 1.7.6 and p40, section 1.9.3
- Replace "Lapidot et al., 2002" with "Lapidot and Petit, 2002" p159, section 5.2 and p199, section 6.4
- Replace "Ledbetter et al., 1979" with "Ledbetter and Herzenberg, 1979" p52, section 2.3.1
- Replace "Lemmon et al., 1998" with "Lemmon and Ferguson, 1998" p22, section 1.6.3
- Replace "Lemmon et al., 1994" with "Lemmon and Schlessinger, 1994" p3, section 1.1.1; p18, section 1.5; p37-8, section 1.9.2
- Replace "Li et al., 1991" with "Li and Stanley, 1991" p18, section 1.5
- Replace "Manova et al., 1991" with "Manova and Bacharova, 1991" p11, section 1.2.2
- Replace "Melotti et al., 1994a" with "Melotti and Calabretta, 1994a" p123, section 4.1.3
- Replace "Nakahata et al., 1994" with "Nakahata and Okumura, 1994" p181, section 5.6.7
- Replace "Oh et al., 1997" with "Oh and Reddy, 1997" p122, section 4.1.3
- Replace "Oh et al., 1998" with "Oh and Reddy, 1998" p122, section 4.1.3
- Replace "Oh et al., 1999" with "Oh and Reddy, 1999" p119, section 4.1.1; p121, section 4.1.2; p124, section 4.1.4
- Replace "Pawson et al., 1993" with "Pawson and Schlessinger, 1993" p20-21, sections 1.6.1-2
- Replace "Rayner et al., 1994" with "Rayner and Gonda, 1994" p85, section 2.7.18 and p99, section 3.2.2
- Replace "Roifman et al., 1993" with "Roifman and Ke, 1993" p178, section 5.6.4
- Replace "Ruoslahti et al., 1994" with "Ruoslahti and Reed, 1994" p115, section 3.5.3 and p189, section 6.2.1
- Replace "Russel et al., 1968" with "Russel and Bernstein, 1968" p15, section 1.3
- Replace "Sarvella et al., 1956" with "Sarvella and Russell, 1956" p10, section 1.2.2 and p15, section 1.3
- Replace "Scheijen et al., 2002" with "Scheijen and Griffin, 2002" p25, section 1.7 and p128, section 4.3
- Replace "Scheuermann et al., 1995" with "Scheuermann and Racila, 1995" p52p178 section 5.6.4
- Replace "Schlessinger et al., 1994" with "Schlessinger and Bar-Sagi, 1994" p110, section 3.5.1 and p184, section 6.1
- Replace "Schlessinger et al., 1992" with "Schlessinger and Ullrich, 1992" p3, section 1.1.2
- Replace "Simmons et al., 1988" with "Simmons and Seep, 1988" p176, section 5.6.2
- Replace "Songyang et al., 2001" with "Songyang and Liu, 2001" p126, section 4.2.1
- Replace "Stamenkovic et al., 1988" with "Stamenkovic and Seed, 1988" p178, section 5.6.4
- Replace "Tatosyan et al., 2000" with "Tatosyan and Mizenina, 2000" p125-8, sections 4.2-4.2.1
- Replace "Tedder et al., 1989" with "Tedder and Isaacs, 1989" p178, section 5.6.4
- Replace "Thomas et al., 1997" with "Thomas and Brugge, 1997" p126, section 4.2.1
- Replace "Tien et al., 1998" with "Tien and Wang, 1998" p180, section 5.6.6
- Replace "Ullrich et al., 1990" with "Ullrich and Schlessinger, 1990" p1, section 1.1.1; p18, section 1.5; p24, section 1.6 and p96, section 3.1
- Replace "van der Geer et al., 1993" with "van der Geer and Hunter, 1993" p24, section 1.7
- Replace "Vanhaesebroeck et al., 2000" with "Vanhaesebroeck and Alessi, 2000" p22, section 1.6.3
- Replace "Vojtek et al., 1998" with "Vojtek and Der, 1998" p27, section 1.7.3
- Replace "Welham et al., 1991" with "Welham and Schrader, 1991" p34, section 1.8.5
- Replace "Welham et al., 1992" with "Welham and Schrader, 1992" p27, section 1.7.3
- Replace "Weston et al., 1989" with "Weston and Bishop, 1989" p121-2, section 4.1.2
- Replace "Yarden et al., 1988" with "Yarden and Ullrich, 1988" p1, section 1.1.1 and p96, section 3.1

7 Bibliography

Adachi, S., Tsujimura, T., Jippo, T., Morimoto, M., Isozaki, K., Kasugai, T., Nomura, S., and Kitamura, Y. (1995). Inhibition of attachment between cultured mast cells and fibroblasts by phorbol 12-myristate 13-acetate and stem cell factor. *Exp Hematol* **23**(1), 58-65.

Adachi, T., Stafford, S., Sur, S., and Alam, R. (1999). A novel Lyn-binding peptide inhibitor blocks eosinophil differentiation, survival, and airway eosinophilic inflammation. *J Immunol* **163**(2), 939-46.

Afonina, I., Zivarts, M., Kutyavin, I., Lukhtanov, E., Gamper, H., and Meyer, R. B. (1997). Efficient priming of PCR with short oligonucleotides conjugated to a minor groove binder. *Nucleic Acids Res* **25**(13), 2657-60.

Alai, M., Mui, A. L., Cutler, R. L., Bustelo, X. R., Barbacid, M., and Krystal, G. (1992). Steel factor stimulates the tyrosine phosphorylation of the proto- oncogene product, p95vav, in human hemopoietic cells. *J Biol Chem* **267**(25), 18021-5.

Anderson, D. M., Lyman, S. D., Baird, A., Wignall, J. M., Eisenman, J., Rauch, C., March, C. J., Boswell, H. S., Gimpel, S. D., Cosman, D., and et al. (1990). Molecular cloning of mast cell growth factor, a hematopoietin that is active in both membrane bound and soluble forms. *Cell* **63**(1), 235-43.

Asano, Y., Brach, M. A., Ahlers, A., de Vos, S., Butterfield, J. H., Ashman, L. K., Valent, P., Gruss, H. J., and Herrmann, F. (1993). Phorbol ester 12-O-tetradecanoylphorbol-13-acetate down-regulates expression of the c-kit proto-oncogene product. *J Immunol* **151**(5), 2345-54.

Ashley, D. M., Bol, S. J., Waugh, C., and Kannourakis, G. (1993). A novel approach to the measurement of different in vitro leukaemic cell growth parameters: the use of PKH GL fluorescent probes. *Leuk Res* **17**(10), 873-82.

Ashman, L. K. (1999a). The biology of stem cell factor and its receptor C-kit. *Int J Biochem Cell Biol* **31**, 1037-1051.

Ashman, L. K. (1999b). The biology of stem cell factor and its receptor C-kit. *Int J Biochem Cell Biol* **31**(10), 1037-51.

Ashman, L. K., Cambareri, A. C., To, L. B., Levinsky, R. J., and Juttner, C. A. (1991). Expression of the YB5.B8 antigen (c-kit proto-oncogene product) in normal human bone marrow. *Blood* **78**(1), 30-7.

Ashman, L. K., Ferrao, P., Cole, S. R., and Cambareri, A. C. (1999). Effects of mutant c-Kit in early myeloid cells. *Leuk Lymphoma* **34**(5-6), 451-61.

Ashman, L. K., Ferrao, P., Cole, S. R., and Cambareri, A. C. (2000). Effects of mutant c-kit in early myeloid cells. *Leuk Lymphoma* **37**(1-2), 233-43.

Ashman, L. K., Roberts, M. M., Gadd, S. J., Cooper, S. J., and Juttner, C. A. (1988). Expression of a 150-kD cell surface antigen identified by monoclonal antibody YB5.B8 is associated with poor prognosis in acute non- lymphoblastic leukaemia. *Leuk Res* **12**(11-12), 923-8.

Auguin, D., Barthe, P., Auge-Senegas, M. T., Stern, M. H., Noguchi, M., and Roumestand, C. (2004). Solution structure and backbone dynamics of the pleckstrin homology domain of the human protein kinase B (PKB/Akt). Interaction with inositol phosphates. *J Biomol NMR* **28**(2), 137-55.

Austyn, J. M., and Gordon, S. (1981). F4/80, a monoclonal antibody directed specifically against the mouse macrophage. *Eur J Immunol* **11**(10), 805-15.

Avanzi, G. C., Lista, P., Giovinazzo, B., Miniero, R., Saglio, G., Benetton, G., Coda, R., Cattoretti, G., and Pegoraro, L. (1988). Selective growth response to IL-3 of a human leukaemic cell line with megakaryoblastic features. *Br J Haematol* **69**(3), 359-66.

Avraham, S., Jiang, S., Ota, S., Fu, Y., Deng, B., Dowler, L. L., White, R. A., and Avraham, H. (1995). Structural and functional studies of the intracellular tyrosine kinase MATK gene and its translated product. *J Biol Chem* **270**(4), 1833-42.

Avruch, J., Zhang, X. F., and Kyriakis, J. M. (1994). Raf meets Ras: completing the framework of a signal transduction pathway. *Trends Biochem Sci* **19**(7), 279-83.

Aylett, G. W., Cole, S. R., Caruana, G., and Ashman, L. (1995). Specificity and functional effects of Mab to c-Kit protein (SCF receptor). *In* "Leucocyte Typing V - White Cell

Differentiation Antigens" (S. F. Schlossman, L. Boumsell, W. Gilks, J. M. Harlan, T. Kishimoto, C. Morimoto, J. Ritx, S. Shaw, R. Silverstein, T. Springer, T. F. Tedder, and R. F. Todd, Eds.), Vol. 2, pp. 1917. Oxford University Press, Oxford.

Aziz, N., Miglarese, M. R., Hendrickson, R. C., Shabanowitz, J., Sturgill, T. W., Hunt, D. F., and Bender, T. P. (1995). Modulation of c-Myb-induced transcription activation by a phosphorylation site near the negative regulatory domain. *Proc Natl Acad Sci U S A* **92**(14), 6429-33.

Baluda, M. A., and Reddy, E. P. (1994). Anatomy of an integrated avian myeloblastosis provirus: structure and function. *Oncogene* **9**(10), 2761-74.

Bargmann, C. I., and Weinberg, R. A. (1988). Increased tyrosine kinase activity associated with the protein encoded by the activated neu oncogene. *Proc Natl Acad Sci U S A* **85**(15), 5394-8.

Baron, C. B., and Blough, H. A. (1983). Binding of influenza virus to a reconstituted receptor complex containing glycophorin. *Intervirology* **19**(1), 33-43.

Basser, R. L., To, L. B., Begley, C. G., Maher, D., Juttner, C., Cebon, J., Mansfield, R., Olver, I., Duggan, G., Szer, J., Collins, J., Schwartz, B., Marty, J., Menchaca, D., Sheridan, W. P., Fox, R. M., and Green, M. D. (1998). Rapid hematopoietic recovery after multicycle high-dose chemotherapy: enhancement of filgrastim-induced progenitor-cell mobilization by recombinant human stem-cell factor. *J Clin Oncol* **16**(5), 1899-908.

Baum, C. M., Weissman, I. L., Tsukamoto, A. S., Buckle, A. M., and Peault, B. (1992). Isolation of a candidate human hematopoietic stem-cell population. *Proc Natl Acad Sci U S A* **89**(7), 2804-8.

Baumheter, S., Singer, M. S., Henzel, W., Hemmerich, S., Renz, M., Rosen, S. D., and Lasky, L. A. (1993). Binding of L-selectin to the vascular sialomucin CD34. *Science* **262**(5132), 436-8.

Bellucci, R., De Propris, M. S., Buccisano, F., Lisci, A., Leone, G., Tabilio, A., and de Fabritiis, P. (1999). Modulation of VLA-4 and L-selectin expression on normal CD34+ cells during mobilization with G-CSF. *Bone Marrow Transplant* **23**(1), 1-8.

Bendall, L. J., Makrynikola, V., Hutchinson, A., Bianchi, A. C., Bradstock, K. F., and Gottlieb, D. J. (1998). Stem cell factor enhances the adhesion of AML cells to fibronectin and augments fibronectin-mediated anti-apoptotic and proliferative signals. *Leukemia* **12**(9), 1375-82.

Benini, S., Manara, M. C., Cerisano, V., Perdichizzi, S., Strammiello, R., Serra, M., Picci, P., and Scotlandi, K. (2004). Contribution of MEK/MAPK and PI3-K signaling pathway to the malignant behavior of Ewing's sarcoma cells: therapeutic prospects. *Int J Cancer* **108**(3), 358-66.

Ben-Levy, R., Peles, E., Goldman-Michael, R., and Yarden, Y. (1992). An oncogenic point mutation confers high affinity ligand binding to the neu receptor. Implications for the generation of site heterogeneity. *J Biol Chem* **267**(24), 17304-13.

Bernstein, A., Forrester, L., Reith, A. D., Dubreuil, P., and Rottapel, R. (1991). The murine W/c-kit and Steel loci and the control of hematopoiesis. *Seminars Hematol* **28**(2), 138-142.

Besmer, P., Murphy, J. E., George, P. C., Qiu, F. H., Bergold, P. J., Lederman, L., Snyder, H. W., Jr., Brodeur, D., Zuckerman, E. E., and Hardy, W. D. (1986). A new acute transforming feline retrovirus and relationship of its oncogene v-kit with the protein kinase gene family. *Nature* **320**(6061), 415-21.

Betsholtz, C., Karlsson, L., and Lindahl, P. (2001). Developmental roles of platelet-derived growth factors. *Bioessays* **23**(6), 494-507.

Biedenkapp, H., Borgmeyer, U., Sippel, A. E., and Klempnauer, K. H. (1988). Viral myb oncogene encodes a sequence-specific DNA-binding activity. *Nature* **335**(6193), 835-7.

Bies, J., Mukhopadhyaya, R., Pierce, J., and Wolff, L. (1995). Only late, nonmitotic stages of granulocyte differentiation in 32Dcl3 cells are blocked by ectopic expression of murine c-myb and its truncated forms. *Cell Growth Differ* **6**(1), 59-68.

Bies, J., and Wolff, L. (1997). Oncogenic activation of c-Myb by carboxyl-terminal truncation leads to decreased proteolysis by the ubiquitin-26S proteasome pathway. *Oncogene* **14**(2), 203-12.

Bishayee, S., Majumdar, S., Khire, J., and Das, M. (1989). Ligand-induced dimerization of the platelet-derived growth factor receptor. Monomer-dimer interconversion occurs independent of receptor phosphorylation. *J Biol Chem* **264**(20), 11699-705.

Blake, R. A., Broome, M. A., Liu, X., Wu, J., Gishizky, M., Sun, L., and Courtneidge, S. A. (2000). SU6656, a selective src family kinase inhibitor, used to probe growth factor signaling. *Mol Cell Biol* **20**(23), 9018-27.

Blechman, J. M., Lev, S., Barg, J., Eisenstein, M., Vaks, B., Vogel, Z., Givol, D., and Yarden, Y. (1995). The fourth immunoglobulin domain of the stem cell factor receptor couples ligand binding to signal transduction. *Cell* **80**(1), 103-13.

Blechman, J. M., Lev, S., Brizzi, M. F., Leitner, O., Pegoraro, L., Givol, D., and Yarden, Y. (1993a). Soluble c-kit proteins and antireceptor monoclonal antibodies confine the binding site of the stem cell factor. *J Biol Chem* **268**(6), 4399-406.

Blechman, J. M., Lev, S., Givol, D., and Yarden, Y. (1993b). Structure-function analyses of the kit receptor for the steel factor. *Stem Cells* **11 Suppl 2**, 12-21.

Blume-Jensen, P., Claesson-Welsh, L., Siegbahn, A., Zsebo, K. M., Westermark, B., and Heldin, C. H. (1991). Activation of the human c-kit product by ligand-induced dimerization mediates circular actin reorganization and chemotaxis. *Embo J* **10**(13), 4121-8.

Blume-Jensen, P., and Hunter, T. (2001). Oncogenic kinase signalling. *Nature* **411**(6835), 355-65.

Blume-Jensen, P., Ronnstrand, L., Gout, I., Waterfield, M. D., and Heldin, C. H. (1994). Modulation of Kit/stem cell factor receptor-induced signaling by protein kinase C. *J Biol Chem* **269**(34), 21793-802.

Blume-Jensen, P., Siegbahn, A., Stabel, S., Heldin, C. H., and Ronnstrand, L. (1993). Increased Kit/SCF receptor induced mitogenicity but abolished cell motility after inhibition of protein kinase C. *Embo J* **12**(11), 4199-209.

Blume-Jensen, P., Wernstedt, C., Heldin, C. H., and Ronnstrand, L. (1995). Identification of the major phosphorylation sites for protein kinase C in kit/stem cell factor receptor in vitro and in intact cells. *J Biol Chem* **270**(23), 14192-200.

Bojko, P., Hester, J. P., Durett, A. G., Maadani, F., Korbling, M., and Champlin, R. E. (1998). Identification of megakaryocyte precursors in peripheral blood stem cell collections from normal donors. *J Clin Apheresis* **13**(1), 7-15.

Boldrini, L., Ursino, S., Gisfredi, S., Faviana, P., Donati, V., Camacci, T., Lucchi, M., Mussi, A., Basolo, F., Pingitore, R., and Fontanini, G. (2004). Expression and mutational status of c-kit in small-cell lung cancer: prognostic relevance. *Clin Cancer Res* **10**(12 Pt 1), 4101-8.

Boni-Schnetzler, M., and Pilch, P. F. (1987). Mechanism of epidermal growth factor receptor autophosphorylation and high-affinity binding. *Proc Natl Acad Sci U S A* **84**(22), 7832-6.

Breuer, W. V., Kahane, I., Baruch, D., Ginsburg, H., and Cabantchik, Z. I. (1983). Role of internal domains of glycophorin in Plasmodium falciparum invasion of human erythrocytes. *Infect Immun* **42**(1), 133-40.

Brizzi, M. F., Blechman, J. M., Cavalloni, G., Givol, D., Yarden, Y., and Pegoraro, L. (1994). Protein kinase C-dependent release of a functional whole extracellular domain of the mast cell growth factor (MGF) receptor by MGF-dependent human myeloid cells. *Oncogene* **9**(6), 1583-9.

Brizzi, M. F., Dentelli, P., Lanfrancone, L., Rosso, A., Pelicci, P. G., and Pegoraro, L. (1996). Discrete protein interactions with the Grb2/c-Cbl complex in SCF- and TPO-mediated myeloid cell proliferation. *Oncogene* **13**(10), 2067-76.

Broudy, V. C. (1997). Stem Cell Factor and haemopoiesis. *Blood* **90**(4), 1345-1364.

Broudy, V. C., Lin, N. L., Liles, W. C., Corey, S. J., O'Laughlin, B., Mou, S., and Linnekin, D. (1999). Signaling via Src family kinases is required for normal internalization of the receptor c-Kit. *Blood* **94**(6), 1979-86.

Buhring, H. J., Ashman, L. K., Gattei, V., Kniep, B., Larregina, A., Pinto, A., Valent, P., and van den Oord, J. J. (1995). *In* "Leucocyte Typing V", pp. 1882-8. Oxford University Press, Oxford.

Buhring, H. J., Seiffert, M., Bock, T. A., Scheding, S., Thiel, A., Scheffold, A., Kanz, L., and Brugger, W. (1999). Expression of novel surface antigens on early hematopoietic cells. *Ann N Y Acad Sci* **872,** 25-38; discussion 38-9.

Burkhardt, A. L., Brunswick, M., Bolen, J. B., and Mond, J. J. (1991). Anti-immunoglobulin stimulation of B lymphocytes activates src-related protein-tyrosine kinases. *Proc Natl Acad Sci U S A* **88**(16), 7410-4.

Carlberg, K., and Rohrschneider, L. (1994). The effect of activating mutations on dimerization, tyrosine phosphorylation and internalization of the macrophage colony stimulating factor receptor. *Mol Biol Cell* **5**(1), 81-95.

Carlberg, K., Tapley, P., Haystead, C., and Rohrschneider, L. (1991). The role of kinase activity and the kinase insert region in ligand- induced internalization and degradation of the c-fms protein. *Embo J* **10**(4), 877-83.

Carraway, K. L., 3rd, Soltoff, S. P., Diamonti, A. J., and Cantley, L. C. (1995). Heregulin stimulates mitogenesis and phosphatidylinositol 3-kinase in mouse fibroblasts transfected with erbB2/neu and erbB3. *J Biol Chem* **270**(13), 7111-6.

Caruana, G. (1996). The transforming potential and functional analysis of the c-Kit receptor tyrosine kinase and its naturally occurring isoforms. *University of Adelaide PhD Thesis.*

Caruana, G., Cambareri, A. C., and Ashman, L. K. (1999). Isoforms of c-KIT differ in activation of signalling pathways and transformation of NIH3T3 fibroblasts. *Oncogene* **18**(40), 5573-81.

Caruana, G., Cambareri, A. C., Gonda, T. J., and Ashman, L. K. (1998). Transformation of NIH3T3 fibroblasts by the c-Kit receptor tyrosine kinase: effect of receptor density and ligand-requirement. *Oncogene* **16**(2), 179-90.

Casteran, N., De Sepulveda, P., Beslu, N., Aoubala, M., Letard, S., Lecocq, E., Rottapel, R., and Dubreuil, P. (2003). Signal transduction by several KIT juxtamembrane domain mutations. *Oncogene* **22**(30), 4710-22.

Catron, K. M., Purkerson, J. M., Isakson, P. C., and Bender, T. P. (1992). Constitutive versus cell cycle regulation of c-myb mRNA expression correlates with developmental stages in murine B lymphoid tumors. *J Immunol* **148**(3), 934-42.

Chabot, B., Stephenson, D. A., Chapman, V. M., Besmer, P., and Bernstein, A. (1988). The proto-oncogene c-kit encoding a transmembrane tyrosine kinase receptor maps to the mouse W locus. *Nature* **335**(6185), 88-9.

Chan, P. M., Ilangumaran, S., La Rose, J., Chakrabartty, A., and Rottapel, R. (2003). Autoinhibition of the kit receptor tyrosine kinase by the cytosolic juxtamembrane region. *Mol Cell Biol* **23**(9), 3067-78.

Cho, M. J., Pestina, T. I., Steward, S. A., Lowell, C. A., Jackson, C. W., and Gartner, T. K. (2002). Role of the Src family kinase Lyn in TxA2 production, adenosine diphosphate secretion, Akt phosphorylation, and irreversible aggregation in platelets stimulated with gamma-thrombin. *Blood* **99**(7), 2442-7.

Cicchillitti, L., Jimenez, S. A., Sala, A., and Saitta, B. (2004). B-Myb acts as a repressor of human COL1A1 collagen gene expression by interacting with Sp1 and CBF factors in scleroderma fibroblasts. *Biochem J* **378**(Pt 2), 609-16.

Civin, C. I., and Small, D. (1995). Purification and expansion of human hematopoietic stem/progenitor cells. *Ann N Y Acad Sci* **770**, 91-8.

Civin, C. I., Strauss, L. C., Brovall, C., Fackler, M. J., Schwartz, J. F., and Shaper, J. H. (1984). Antigenic analysis of hematopoiesis. III. A hematopoietic progenitor cell surface antigen defined by a monoclonal antibody raised against KG-1a cells. *J Immunol* **133**(1), 157-65.

Claesson-Welsh, L. (1994). Platelet-derived growth factor receptor signals. *J Biol Chem* **269**(51), 32023-6.

Clarke, M. F., Kukowska-Latallo, J. F., Westin, E., Smith, M., and Prochownik, E. V. (1988). Constitutive expression of a c-myb cDNA blocks Friend murine erythroleukemia cell differentiation. *Mol Cell Biol* **8**(2), 884-92.

Cole, S. R., Aylett, G. W., Harvey, N. L., Cambareri, A. C., and Ashman, L. K. (1996). Increased expression of c-Kit or its ligand Steel Factor is not a common feature of adult acute myeloid leukaemia. *Leukemia* **10**(2), 288-96.

Colucci, F., and Di Santo, J. P. (2000). The receptor tyrosine kinase c-kit provides a critical signal for survival, expansion, and maturation of mouse natural killer cells. *Blood* **95**(3), 984-91.

Conlan, J. W., and North, R. J. (1994). Neutrophils are essential for early anti-Listeria defense in the liver, but not in the spleen or peritoneal cavity, as revealed by a granulocyte-depleting monoclonal antibody. *J Exp Med* **179**(1), 259-68.

Contreras, M. A., Bale, W. F., and Spar, I. L. (1983). Iodine monochloride (IC1) iodination techniques. *Methods Enzymol* **92**, 277-92.

Copeland, N. G., Gilbert, D. J., Cho, B. C., Donovan, P. J., Jenkins, N. A., Cosman, D., Anderson, D., Lyman, S. D., and Williams, D. E. (1990). Mast cell growth factor maps near the steel locus on mouse chromosome 10 and is deleted in a number of steel alleles. *Cell* **63**(1), 175-83.

Cordell, J. L., Falini, B., Erber, W. N., Ghosh, A. K., Abdulaziz, Z., MacDonald, S., Pulford, K. A., Stein, H., and Mason, D. Y. (1984). Immunoenzymatic labeling of monoclonal antibodies using immune complexes of alkaline phosphatase and monoclonal anti-alkaline phosphatase (APAAP complexes). *J Histochem Cytochem* **32**(2), 219-29.

Corey, S. J., Burkhardt, A. L., Bolen, J. B., Geahlen, R. L., Tkatch, L. S., and Tweardy, D. J. (1994). Granulocyte colony-stimulating factor receptor signaling involves the formation of a three-component complex with Lyn and Syk protein-tyrosine kinases. *Proc Natl Acad Sci U S A* **91**(11), 4683-7.

Cortajarena, A. L., Goni, F. M., and Ostolaza, H. (2001). Glycophorin as a receptor for Escherichia coli alpha-hemolysin in erythrocytes. *J Biol Chem* **276**(16), 12513-9.

Cottler-Fox, M. H., Lapidot, T., Petit, I., Kollet, O., DiPersio, J. F., Link, D., and Devine, S. (2003). Stem cell mobilization. *Hematology (Am Soc Hematol Educ Program)*, 419-37.

Cox, A. D., Brtva, T. R., Lowe, D. G., and Der, C. J. (1994). R-Ras induces malignant, but not morphologic, transformation of NIH3T3 cells. *Oncogene* **9**(11), 3281-8.

Craig, W., Kay, R., Cutler, R. L., and Lansdorp, P. M. (1993). Expression of Thy-1 on human hematopoietic progenitor cells. *J Exp Med* **177**(5), 1331-42.

Crosier, P. S., Ricciardi, S. T., Hall, L. R., Vitas, M. R., Clark, S. C., and Crosier, K. E. (1993). Expression of isoforms of the human receptor tyrosine kinase c-kit in leukemic cell lines and acute myeloid leukemia. *Blood* **82**(4), 1151-8.

Dahle, O., Bakke, O., and Gabrielsen, O. S. (2004). c-Myb associates with PML in nuclear bodies in hematopoietic cells. *Exp Cell Res* **297**(1), 118-26.

Daniels, G., and Green, C. (2000). Expression of red cell surface antigens during erythropoiesis. *Vox Sang* **78 Suppl 2,** 149-53.

Dasgupta, P., and Reddy, E. P. (1989). Identification of alternatively spliced transcripts for human c-myb: molecular cloning and sequence analysis of human c-myb exon 9A sequences. *Oncogene* **4**(12), 1419-23.

Davis, R. J. (1993). The mitogen-activated protein kinase signal transduction pathway. *J Biol Chem* **268**(20), 14553-6.

de Melker, A. A., van der Horst, G., Calafat, J., Jansen, H., and Borst, J. (2001). c-Cbl ubiquitinates the EGF receptor at the plasma membrane and remains receptor associated throughout the endocytic route. *J Cell Sci* **114**(Pt 11), 2167-78.

de Rie, M. A., Schumacher, T. N., van Schijndel, G. M., van Lier, R. A., and Miedema, F. (1989). Regulatory role of CD19 molecules in B-cell activation and differentiation. *Cell Immunol* **118**(2), 368-81.

de Wynter, E. A., Buck, D., Hart, C., Heywood, R., Coutinho, L. H., Clayton, A., Rafferty, J. A., Burt, D., Guenechea, G., Bueren, J. A., Gagen, D., Fairbairn, L. J., Lord, B. I., and Testa, N. G. (1998). CD34+AC133+ cells isolated from cord blood are highly enriched in long-term culture-initiating cells, NOD/SCID-repopulating cells and dendritic cell progenitors. *Stem Cells* **16**(6), 387-96.

Deberry, C., Mou, S., and Linnekin, D. (1997). Stat1 associates with c-kit and is activated in response to stem cell factor. *Biochem J* **327 (Pt 1),** 73-80.

Debili, N., Coulombel, L., Croisille, L., Katz, A., Guichard, J., Breton-Gorius, J., and Vainchenker, W. (1996). Characterization of a bipotent erythro-megakaryocytic progenitor in human bone marrow. *Blood* **88**(4), 1284-96.

Debili, N., Wendling, F., Cosman, D., Titeux, M., Florindo, C., Dusanter-Fourt, I., Schooley, K., Methia, N., Charon, M., Nador, R., and et al. (1995). The Mpl receptor is expressed in the megakaryocytic lineage from late progenitors to platelets. *Blood* **85**(2), 391-401.

Dent, P., Jarvis, W. D., Birrer, M. J., Fisher, P. B., Schmidt-Ullrich, R. K., and Grant, S. (1998). The roles of signaling by the p42/p44 mitogen-activated protein (MAP) kinase pathway; a potential route to radio- and chemo-sensitization of tumor cells resulting in the induction of apoptosis and loss of clonogenicity. *Leukemia* **12**(12), 1843-50.

Dexter, T. M., Garland, J., Scott, D., Scolnick, E., and Metcalf, D. (1980). Growth of factor-dependent hemopoietic precursor cell lines. *J Exp Med* **152**(4), 1036-47.

Di Fiore, P. P., Pierce, J. H., Fleming, T. P., Hazan, R., Ullrich, A., King, C. R., Schlessinger, J., and Aaronson, S. A. (1987). Overexpression of the human EGF receptor confers an EGF-dependent transformed phenotype to NIH 3T3 cells. *Cell* **51**(6), 1063-70.

Dikic, I., Schlessinger, J., and Lax, I. (1994). PC12 cells overexpressing the insulin receptor undergo insulin- dependent neuronal differentiation. *Curr Biol* **4**(8), 702-8.

Dorai, T., Levy, J. B., Kang, L., Brugge, J. S., and Wang, L. H. (1991). Analysis of cDNAs of the proto-oncogene c-src: heterogeneity in 5' exons and possible mechanism for the genesis of the 3' end of v-src. *Mol Cell Biol* **11**(8), 4165-76.

Dosil, M., Wang, S., and Lemischka, I. R. (1993). Mitogenic signalling and substrate specificity of the Flk2/Flt3 receptor tyrosine kinase in fibroblasts and interleukin 3-dependent hematopoietic cells. *Mol Cell Biol* **13**(10), 6572-85.

Downing, J. R., Margolis, B. L., Zilberstein, A., Ashmun, R. A., Ullrich, A., Sherr, C. J., and Schlessinger, J. (1989a). Phospholipase C-gamma, a substrate for PDGF receptor kinase, is

not phosphorylated on tyrosine during the mitogenic response to CSF-1. *Embo J* **8**(11), 3345-50.

Downing, J. R., Roussel, M. F., and Sherr, C. J. (1989b). Ligand and protein kinase C downmodulate the colony-stimulating factor 1 receptor by independent mechanisms. *Mol Cell Biol* **9**(7), 2890-6.

Duarte, R. F., and Franf, D. A. (2002). The synergy between stem cell factor (SCF) and granulocyte colony-stimulating factor (G-CSF): molecular basis and clinical relevance. *Leuk Lymphoma* **43**(6), 1179-87.

Dudek, H., and Reddy, E. P. (1989a). Identification of two translational products for c-myb. *Oncogene* **4**(9), 1061-6.

Dudek, H., and Reddy, E. P. (1989b). Murine myeloid leukemias with aberrant myb loci show heterogeneous expression of novel myb proteins. *Oncogene* **4**(12), 1489-95.

Duperray, A., Troesch, A., Berthier, R., Chagnon, E., Frachet, P., Uzan, G., and Marguerie, G. (1989). Biosynthesis and assembly of platelet GPIIb-IIIa in human megakaryocytes: evidence that assembly between pro-GPIIb and GPIIIa is a prerequisite for expression of the complex on the cell surface. *Blood* **74**(5), 1603-11.

DuPont, B. R., Grant, S. G., Oto, S. H., Bigbee, W. L., Jensen, R. H., and Langlois, R. G. (1995). Molecular characterization of glycophorin A transcripts in human erythroid cells using RT-PCR, allele-specific restriction, and sequencing. *Vox Sang* **68**(2), 121-9.

Duronio, V., Welham, M. J., Abraham, S., Dryden, P., and Schrader, J. W. (1992). p21ras activation via hemopoietin receptors and c-kit requires tyrosine kinase activity but not tyrosine phosphorylation of p21ras GTPase- activating protein. *Proc Natl Acad Sci U S A* **89**(5), 1587-91.

Eiseman, E., and Bolen, J. B. (1992). Engagement of the high-affinity IgE receptor activates src protein-related tyrosine kinases. *Nature* **355**(6355), 78-80.

Endo, T., Odb, A., Satoh, I., Haseyama, Y., Nishio, M., Koizumi, K., Takashima, H., Fujimoto, K., Amasaki, Y., Fujita, H., Koike, T., and Sawada, K. (2001). Stem cell factor protects c-kit+ human primary erythroid cells from apoptosis. *Exp Hematol* **29**(7), 833-41.

Escribano, L., Ocqueteau, M., Almeida, J., Orfao, A., and San Miguel, J. F. (1998). Expression of the c-kit (CD117) molecule in normal and malignant hematopoiesis. *Leuk Lymphoma* **30**(5-6), 459-66.

Ettenberg, S. A., Magnifico, A., Cuello, M., Nau, M. M., Rubinstein, Y. R., Yarden, Y., Weissman, A. M., and Lipkowitz, S. (2001). Cbl-b-dependent coordinated degradation of the epidermal growth factor receptor signaling complex. *J Biol Chem* **276**(29), 27677-84.

Evans, J. L., Moore, T. L., Kuehl, W. M., Bender, T., and Ting, J. P. (1990). Functional analysis of c-Myb protein in T-lymphocytic cell lines shows that it trans-activates the c-myc promoter. *Mol Cell Biol* **10**(11), 5747-52.

Ezoe, K., Holmes, S. A., Ho, L., Bennett, C. P., Bolognia, J. L., Brueton, L., Burn, J., Falabella, R., Gatto, E. M., Ishii, N., and et al. (1995). Novel mutations and deletions of the KIT (steel factor receptor) gene in human piebaldism. *Am J Hum Genet* **56**(1), 58-66.

Ferguson, K. M., Lemmon, M. A., Schlessinger, J., and Sigler, P. B. (1994). Crystal structure at 2.2 A resolution of the pleckstrin homology domain from human dynamin. *Cell* **79**(2), 199-209.

Ferrao, P., Gonda, T. J., and Ashman, L. K. (1997). Expression of constitutively activated human c-Kit in Myb transformed early myeloid cells leads to factor independence, histiocytic differentiation, and tumorigenicity. *Blood* **90**(11), 4539-52.

Fina, L., Molgaard, H. V., Robertson, D., Bradley, N. J., Monaghan, P., Delia, D., Sutherland, D. R., Baker, M. A., and Greaves, M. F. (1990). Expression of the CD34 gene in vascular endothelial cells. *Blood* **75**(12), 2417-26.

Flanagan, J. G., Chan, D. C., and Leder, P. (1991). Transmembrane form of the kit ligand growth factor is determined by alternative splicing and is missing in the Sld mutant. *Cell* **64**(5), 1025-35.

Flanagan, J. G., and Leder, P. (1990). The kit ligand: a cell surface molecule altered in steel mutant fibroblasts. *Cell* **63**(1), 185-94.

Fleischman, R. A., Saltman, D. L., Stastny, V., and Zneimer, S. (1991). Deletion of the c-kit protooncogene in the human developmental defect piebald trait. *Proc Natl Acad Sci U S A* **88**(23), 10885-9.

Fluckiger, A. C., Sanz, E., Garcia-Lloret, M., Su, T., Hao, Q. L., Kato, R., Quan, S., de la Hera, A., Crooks, G. M., Witte, O. N., and Rawlings, D. J. (1998). In vitro reconstitution of human B-cell ontogeny: from CD34(+) multipotent progenitors to Ig-secreting cells. *Blood* **92**(12), 4509-20.

Fox, E. A., Phillips, R. J., Byerly, M. S., Baronowsky, E. A., Chi, M. M., and Powley, T. L. (2002). Selective loss of vagal intramuscular mechanoreceptors in mice mutant for steel factor, the c-Kit receptor ligand. *Anat Embryol (Berl)* **205**(4), 325-42.

Freeman, S. D., Kelm, S., Barber, E. K., and Crocker, P. R. (1995). Characterization of CD33 as a new member of the sialoadhesin family of cellular interaction molecules. *Blood* **85**(8), 2005-12.

Fritsch, G., Stimpfl, M., Kurz, M., Leitner, A., Printz, D., Buchinger, P., Hoecker, P., and Gadner, H. (1995). Characterization of hematopoietic stem cells. *Ann N Y Acad Sci* **770**, 42-52.

Frost, M. J., Ferrao, P. T., Hughes, T. P., and Ashman, L. K. (2002). Juxtamembrane mutant V560GKit is more sensitive to Imatinib (STI571) compared with wild-type c-kit whereas the kinase domain mutant D816VKit is resistant. *Mol Cancer Ther* **1**(12), 1115-24.

Fujimoto, M., Poe, J. C., Inaoki, M., and Tedder, T. F. (1998). CD19 regulates B lymphocyte responses to transmembrane signals. *Semin Immunol* **10**(4), 267-77.

Fujita, J., Onoue, H., Ebi, Y., Nakayama, H., and Kanakura, Y. (1989). In vitro duplication and in vivo cure of mast-cell deficiency of Sl/Sld mutant mice by cloned 3T3 fibroblasts. *Proc Natl Acad Sci U S A* **86**(8), 2888-91.

Funaro, A., and Malavasi, F. (1999). Human CD38, a surface receptor, an enzyme, an adhesion molecule and not a simple marker. *J Biol Regul Homeost Agents* **13**(1), 54-61.

Funasaka, Y., Boulton, T., Cobb, M., Yarden, Y., Fan, B., Lyman, S. D., Williams, D. E., Anderson, D. M., Zakut, R., Mishima, Y., and et al. (1992). c-Kit-kinase induces a cascade of

protein tyrosine phosphorylation in normal human melanocytes in response to mast cell growth factor and stimulates mitogen-activated protein kinase but is down-regulated in melanomas. *Mol Biol Cell* **3**(2), 197-209.

Furitsu, T., Tsujimura, T., Tono, T., Ikeda, H., Kitayama, H., Koshimizu, U., Sugahara, H., Butterfield, J. H., Ashman, L. K., Kanayama, Y., and et al. (1993). Identification of mutations in the coding sequence of the proto-oncogene c-kit in a human mast cell leukemia cell line causing ligand-independent activation of c-kit product. *J Clin Invest* **92**(4), 1736-44.

Furthmayr, H. (1977). Structural analysis of a membrane glycoprotein: glycophorin A. *J Supramol Struct* **7**(1), 121-34.

Furukawa, Y., Piwnica-Worms, H., Ernst, T. J., Kanakura, Y., and Griffin, J. D. (1990). cdc2 gene expression at the G1 to S transition in human T lymphocytes. *Science* **250**(4982), 805-8.

Gadd, S. J., and Ashman, L. K. (1985). A murine monoclonal antibody specific for a cell-surface antigen expressed by a subgroup of human myeloid leukaemias. *Leuk Res* **9**(11), 1329-36.

Galli, S. J., Zsebo, K. M., and Geissler, E. N. (1994). The kit ligand, stem cell factor. *Adv Immunol* **55**, 1-96.

Garrington, T. P., and Johnson, G. L. (1999). Organization and regulation of mitogen-activated protein kinase signaling pathways. *Curr Opin Cell Biol* **11**(2), 211-8.

Geissler, E. N., Ryan, M. A., and Housman, D. E. (1988). The dominant-white spotting (W) locus of the mouse encodes the c-kit proto-oncogene. *Cell* **55**(1), 185-92.

Gewirtz, A. M., Anfossi, G., Venturelli, D., Valpreda, S., Sims, R., and Calabretta, B. (1989). G1/S transition in normal human T-lymphocytes requires the nuclear protein encoded by c-myb. *Science* **245**(4914), 180-3.

Gewirtz, A. M., and Calabretta, B. (1988). A c-myb antisense oligodeoxynucleotide inhibits normal human hematopoiesis in vitro. *Science* **242**(4883), 1303-6.

Giebel, L. B., and Spritz, R. A. (1991). Mutation of the KIT (mast/stem cell growth factor receptor) protooncogene in human piebaldism. *Proc Natl Acad Sci U S A* **88**(19), 8696-9.

Giebel, L. B., Strunk, K. M., Holmes, S. A., and Spritz, R. A. (1992). Organization and nucleotide sequence of the human KIT (mast/stem cell growth factor receptor) proto-oncogene. *Oncogene* **7**(11), 2207-17.

Golay, J., Loffarelli, L., Luppi, M., Castellano, M., and Introna, M. (1994). The human A-myb protein is a strong activator of transcription. *Oncogene* **9**(9), 2469-79.

Goldman, R., Levy, R. B., Peles, E., and Yarden, Y. (1990). Heterodimerization of the erbB-1 and erbB-2 receptors in human breast carcinoma cells: a mechanism for receptor transregulation. *Biochemistry* **29**(50), 11024-8.

Gonda, T. J. (1991). Targets for trans-activation by myb. *Cancer Cells* **3**(1), 22-3.

Gonda, T. J., Buckmaster, C., and Ramsay, R. G. (1989a). Activation of c-myb by carboxy-terminal truncation: relationship to transformation of murine haemopoietic cells in vitro. *Embo J* **8**(6), 1777-83.

Gonda, T. J., and Metcalf, D. (1984). Expression of myb, myc and fos proto-oncogenes during the differentiation of a murine myeloid leukaemia. *Nature* **310**(5974), 249-51.

Gonda, T. J., Ramsay, R. G., and Johnson, G. R. (1989b). Murine myeloid cell lines derived by in vitro infection with recombinant c-myb retroviruses express myb from rearranged vector proviruses. *Embo J* **8**(6), 1767-75.

Gonda, T. J., Sheiness, D. K., and Bishop, J. M. (1982). Transcripts from the cellular homologs of retroviral oncogenes: distribution among chicken tissues. *Mol Cell Biol* **2**(6), 617-24.

Goussetis, E., Theodosaki, M., Paterakis, G., Peristeri, J., Petropoulos, D., Kitra, V., Papassarandis, C., and Graphakos, S. (2000). A functional hierarchy among the CD34+ hematopoietic cells based on in vitro proliferative and differentiative potential of AC133+CD34(bright) and AC133(dim/)-CD34+ human cord blood cells. *J Hematother Stem Cell Res* **9**(6), 827-40.

Grasser, F. A., Graf, T., and Lipsick, J. S. (1991). Protein truncation is required for the activation of the c-myb proto-oncogene. *Mol Cell Biol* **11**(8), 3987-96.

Greenfield, C., Hiles, I., Waterfield, M. D., Federwisch, M., Wollmer, A., Blundell, T. L., and McDonald, N. (1989). Epidermal growth factor binding induces a conformational change in the external domain of its receptor. *Embo J* **8**(13), 4115-23.

Griffin, J. D., Linch, D., Sabbath, K., Larcom, P., and Schlossman, S. F. (1984). A monoclonal antibody reactive with normal and leukemic human myeloid progenitor cells. *Leuk Res* **8**(4), 521-34.

Grobe, K., and Powell, L. D. (2002). Role of protein kinase C in the phosphorylation of CD33 (Siglec-3) and its effect on lectin activity. *Blood* **99**(9), 3188-96.

Guerra, J., Withers, D. A., and Boxer, L. M. (1995). Myb binding sites mediate negative regulation of c-myb expression in T-cell lines. *Blood* **86**(5), 1873-80.

Gunther, N., Betzel, C., and Weber, W. (1990). The secreted form of the epidermal growth factor receptor. Characterization and crystallization of the receptor-ligand complex. *J Biol Chem* **265**(36), 22082-5.

Hall, W., Bean, C., and Pollard, M. (1941). *Am J Vet Res* **2**, 272-279.

Hallek, M., Druker, B., Lepisto, E. M., Wood, K. W., Ernst, T. J., and Griffin, J. D. (1992). Granulocyte-macrophage colony-stimulating factor and steel factor induce phosphorylation of both unique and overlapping signal transduction intermediates in a human factor-dependent hematopoietic cell line. *J Cell Physiol* **153**(1), 176-86.

Hanks, S. K., Quinn, A. M., and Hunter, T. (1988). The protein kinase family: conserved features and deduced phylogeny of the catalytic domains. *Science* **241**(4861), 42-52.

Harlan, J. E., Hajduk, P. J., Yoon, H. S., and Fesik, S. W. (1994). Pleckstrin homology domains bind to phosphatidylinositol-4,5-bisphosphate. *Nature* **371**(6493), 168-70.

Hayashi, S., Kunisada, T., Ogawa, M., Yamaguchi, K., and Nishikawa, S. (1991). Exon skipping by mutation of an authentic splice site of c-kit gene in W/W mouse. *Nucleic Acids Res* **19**(6), 1267-71.

Hazzalin, C. A., Cuenda, A., Cano, E., Cohen, P., and Mahadevan, L. C. (1997). Effects of the inhibition of p38/RK MAP kinase on induction of five fos and jun genes by diverse stimuli. *Oncogene* **15**(19), 2321-31.

He, X. Y., Antao, V. P., Basila, D., Marx, J. C., and Davis, B. R. (1992). Isolation and molecular characterization of the human CD34 gene. *Blood* **79**(9), 2296-302.

Heidaran, M. A., Pierce, J. H., Lombardi, D., Ruggiero, M., Gutkind, J. S., Matsui, T., and Aaronson, S. A. (1991). Deletion or substitution within the alpha platelet-derived growth factor receptor kinase insert domain: effects on functional coupling with intracellular signaling pathways. *Mol Cell Biol* **11**(1), 134-42.

Heidaran, M. A., Yu, J. C., Jensen, R. A., Pierce, J. H., and Aaronson, S. A. (1992). A deletion in the extracellular domain of the alpha platelet-derived growth factor (PDGF) receptor differentially impairs PDGF-AA and PDGF- BB binding affinities. *J Biol Chem* **267**(5), 2884-7.

Heinrich, M. C., Rubin, B. P., Longley, B. J., and Fletcher, J. A. (2002). Biology and genetic aspects of gastrointestinal stromal tumors: KIT activation and cytogenetic alterations. *Hum Pathol* **33**(5), 484-95.

Heissig, B., Hattori, K., Dias, S., Friedrich, M., Ferris, B., Hackett, N. R., Crystal, R. G., Besmer, P., Lyden, D., Moore, M. A., Werb, Z., and Rafii, S. (2002). Recruitment of stem and progenitor cells from the bone marrow niche requires MMP-9 mediated release of kit-ligand. *Cell* **109**(5), 625-37.

Heldin, C. H. (1995). Dimerization of cell surface receptors in signal transduction. *Cell* **80**(2), 213-23.

Heldin, C. H., Ernlund, A., Rorsman, C., and Ronnstrand, L. (1989). Dimerization of B-type platelet-derived growth factor receptors occurs after ligand binding and is closely associated with receptor kinase activation. *J Biol Chem* **264**(15), 8905-12.

Herbst, R., Lammers, R., Schlessinger, J., and Ullrich, A. (1991). Substrate phosphorylation specificity of the human c-kit receptor tyrosine kinase. *J Biol Chem* **266**(30), 19908-16.

Herbst, R., Munemitsu, S., and Ullrich, A. (1995a). Oncogenic activation of v-kit involves deletion of a putative tyrosine- substrate interaction site. *Oncogene* **10**(2), 369-79.

Herbst, R., Shearman, M. S., Jallal, B., Schlessinger, J., and Ullrich, A. (1995b). Formation of signal transfer complexes between stem cell and platelet- derived growth factor receptors and SH2 domain proteins in vitro. *Biochemistry* **34**(17), 5971-9.

Hernandez-Hansen, V., Mackay, G. A., Lowell, C. A., Wilson, B. S., and Oliver, J. M. (2004). The Src kinase Lyn is a negative regulator of mast cell proliferation. *J Leukoc Biol* **75**(1), 143-51.

Herskowitz, I. (1987). Functional inactivation of genes by dominant negative mutations. *Nature* **329**(6136), 219-22.

Hibbs, M. L., and Dunn, A. R. (1997). Lyn, a src-like tyrosine kinase. *Int J Biochem Cell Biol* **29**(3), 397-400.

Hibbs, M. L., Tarlinton, D. M., Armes, J., Grail, D., Hodgson, G., Maglitto, R., Stacker, S. A., and Dunn, A. R. (1995). Multiple defects in the immune system of Lyn-deficient mice, culminating in autoimmune disease. *Cell* **83**(2), 301-11.

Hicke, L. (1999). Gettin' down with ubiquitin: turning off cell-surface receptors, transporters and channels. *Trends Cell Biol* **9**(3), 107-12.

Hino, M., Nishizawa, Y., Tatsumi, N., Tojo, A., and Morii, H. (1995). Down-modulation of c-kit mRNA and protein expression by erythroid differentiation factor/activin A. *FEBS Lett* **374**(1), 69-71.

Hirota, S., Isozaki, K., Moriyama, Y., Hashimoto, K., Nishida, T., Ishiguro, S., Kawano, K., Hanada, M., Kurata, A., Takeda, M., Muhammad Tunio, G., Matsuzawa, Y., Kanakura, Y., Shinomura, Y., and Kitamura, Y. (1998). Gain-of-function mutations of c-kit in human gastrointestinal stromal tumors. *Science* **279**(5350), 577-80.

Hirota, S., Isozaki, K., Nishida, T., and Kitamura, Y. (2000). Effects of loss-of-function and gain-of-function mutations of c-kit on the gastrointestinal tract. *J Gastroenterol* **35 Suppl 12**, 75-9.

Hofmann, C. S., Sullivan, C. P., Jiang, H. Y., Stone, P. J., Toselli, P., Reis, E. D., Chereshnev, I., Schreiber, B. M., and Sonenshein, G. E. (2004). B-Myb represses vascular smooth muscle cell collagen gene expression and inhibits neointima formation after arterial injury. *Arterioscler Thromb Vasc Biol* **24**(9), 1608-13.

Honegger, A. M., Schmidt, A., Ullrich, A., and Schlessinger, J. (1990). Evidence for epidermal growth factor (EGF)-induced intermolecular autophosphorylation of the EGF receptors in living cells. *Mol Cell Biol* **10**(8), 4035-44.

Howe, K. M., and Watson, R. J. (1991). Nucleotide preferences in sequence-specific recognition of DNA by c-myb protein. *Nucleic Acids Res* **19**(14), 3913-9.

Hsu, Y. R., Wu, G. M., Mendiaz, E. A., Syed, R., Wypych, J., Toso, R., Mann, M. B., Boone, T. C., Narhi, L. O., Lu, H. S., and Langley, K. E. (1997). The majority of stem cell factor exists as monomer under physiological conditions. Implications for dimerization mediating biological activity. *J Biol Chem* **272**(10), 6406-15.

Hu, Y. L., Ramsay, R. G., Kanei-Ishii, C., Ishii, S., and Gonda, T. J. (1991). Transformation by carboxyl-deleted Myb reflects increased transactivating capacity and disruption of a negative regulatory domain. *Oncogene* **6**(9), 1549-53.

Huang, E., Nocka, K., Beier, D. R., Chu, T. Y., Buck, J., Lahm, H. W., Wellner, D., Leder, P., and Besmer, P. (1990). The hematopoietic growth factor KL is encoded by the Sl locus and is the ligand of the c-kit receptor, the gene product of the W locus. *Cell* **63**(1), 225-33.

Hubbard, S. R., and Till, J. H. (2000). Protein tyrosine kinase structure and function. *Annu Rev Biochem* **69**, 373-98.

Hudziak, R. M., Schlessinger, J., and Ullrich, A. (1987). Increased expression of the putative growth factor receptor p185HER2 causes transformation and tumorigenesis of NIH 3T3 cells. *Proc Natl Acad Sci U S A* **84**(20), 7159-63.

Hunter, T. (1995). Protein kinases and phosphatases: the yin and yang of protein phosphorylation and signaling. *Cell* **80**(2), 225-36.

Huse, M., and Kuriyan, J. (2002). The conformational plasticity of protein kinases. *Cell* **109**(3), 275-82.

Ikeda, H., Kanakura, Y., Furitsu, T., Kitayama, H., Sugahara, H., Nishiura, T., Karasuno, T., Tomiyama, Y., Yamatodani, A., Kanayama, Y., and et al. (1993). Changes in phenotype and proliferative potential of human acute myeloblastic leukemia cells in culture with stem cell factor. *Exp Hematol* **21**(13), 1686-94.

Imai, Y., Lasky, L. A., and Rosen, S. D. (1993). Sulphation requirement for GlyCAM-1, an endothelial ligand for L-selectin. *Nature* **361**(6412), 555-7.

Inada, T., Iwama, A., Sakano, S., Ohno, M., Sawada, K., and Suda, T. (1997). Selective expression of the receptor tyrosine kinase, HTK, on human erythroid progenitor cells. *Blood* **89**(8), 2757-65.

Irani, A. M., Nilsson, G., Miettinen, U., Craig, S. S., Ashman, L. K., Ishizaka, T., Zsebo, K. M., and Schwartz, L. B. (1992). Recombinant human stem cell factor stimulates differentiation of mast cells from dispersed human fetal liver cells. *Blood* **80**(12), 3009-21.

Jarvis, T. C., Alby, L. J., Beaudry, A. A., Wincott, F. E., Beigelman, L., McSwiggen, J. A., Usman, N., and Stinchcomb, D. T. (1996). Inhibition of vascular smooth muscle cell proliferation by ribozymes that cleave c-myb mRNA. *Rna* **2**(5), 419-28.

Jhun, B. H., Rivnay, B., Price, D., and Avraham, H. (1995). The MATK tyrosine kinase interacts in a specific and SH2-dependent manner with c-Kit. *J Biol Chem* **270**(16), 9661-6.

Jiang, X., Gurel, O., Mendiaz, E. A., Stearns, G. W., Clogston, C. L., Lu, H. S., Osslund, T. D., Syed, R. S., Langley, K. E., and Hendrickson, W. A. (2000). Structure of the active core of human stem cell factor and analysis of binding to its receptor kit. *Embo J* **19**(13), 3192-203.

Joaquin, M., and Watson, R. J. (2003a). Cell cycle regulation by the B-Myb transcription factor. *Cell Mol Life Sci* **60**(11), 2389-401.

Joaquin, M., and Watson, R. J. (2003b). The cell cycle-regulated B-Myb transcription factor overcomes cyclin-dependent kinase inhibitory activity of p57(KIP2) by interacting with its cyclin-binding domain. *J Biol Chem* **278**(45), 44255-64.

Jove, R., and Hanafusa, H. (1987). Cell transformation by the viral src oncogene. *Annu Rev Cell Biol* **3,** 31-56.

Jozaki, K., Kuriu, A., Hirota, S., Onoue, H., Ebi, Y., Adachi, S., Ma, J. Y., Tarui, S., and Kitamura, Y. (1991). Bone marrow-derived cultured mast cells and peritoneal mast cells as targets of a growth activity secreted by BALB/3T3 fibroblasts. *Exp Hematol* **19**(3), 185-90.

Juttner, C. A., To, L. B., Haylock, D. N., and Dyson, P. G. (1990). Peripheral blood stem cell selection, collection and auto-transplantation. *Prog Clin Biol Res* **333,** 447-59; discussion 460.

Kafer, G., Willer, A., Ludwig, W., Kramer, A., Hehlmann, R., and Hastka, J. (1999). Intracellular expression of CD61 precedes surface expression. *Ann Hematol* **78**(10), 472-4.

Kapeller, R., and Cantley, L. C. (1994). Phosphatidylinositol 3-kinase. *Bioessays* **16**(8), 565-76.

Kaplan, D. R., Morrison, D. K., Wong, G., McCormick, F., and Williams, L. T. (1990). PDGF beta-receptor stimulates tyrosine phosphorylation of GAP and association of GAP with a signaling complex. *Cell* **61**(1), 125-33.

Katz, M., Shtiegman, K., Tal-Or, P., Yakir, L., Mosesson, Y., Harari, D., Machluf, Y., Asao, H., Jovin, T., Sugamura, K., and Yarden, Y. (2002). Ligand-independent degradation of epidermal growth factor receptor involves receptor ubiquitylation and Hgs, an adaptor whose ubiquitin-interacting motif targets ubiquitylation by Nedd4. *Traffic* **3**(10), 740-51.

Katzen, A. L., Kornberg, T. B., and Bishop, J. M. (1985). Isolation of the proto-oncogene c-myb from D. melanogaster. *Cell* **41**(2), 449-56.

Kawamoto, T., Mendelsohn, J., Le, A., Sato, G. H., Lazar, C. S., and Gill, G. N. (1984). Relation of epidermal growth factor receptor concentration to growth of human epidermoid carcinoma A431 cells. *J Biol Chem* **259**(12), 7761-6.

Kawanishi, H., Medicus, R. G., and Palaszynski, E. W. (1986). Mast cells induced in vitro by interleukin 3 from native murine thymus cells. *Scand J Immunol* **24**(1), 29-38.

Kelm, S., Brossmer, R., Isecke, R., Gross, H. J., Strenge, K., and Schauer, R. (1998). Functional groups of sialic acids involved in binding to siglecs (sialoadhesins) deduced from interactions with synthetic analogues. *Eur J Biochem* **255**(3), 663-72.

Kelm, S., Schauer, R., and Crocker, P. R. (1996). The Sialoadhesins--a family of sialic acid-dependent cellular recognition molecules within the immunoglobulin superfamily. *Glycoconj J* **13**(6), 913-26.

Kennedy, S. G., Wagner, A. J., Conzen, S. D., Jordan, J., Bellacosa, A., Tsichlis, P. N., and Hay, N. (1997). The PI 3-kinase/Akt signaling pathway delivers an anti-apoptotic signal. *Genes Dev* **11**(6), 701-13.

Kern, J. A., Schwartz, D. A., Nordberg, J. E., Weiner, D. B., Greene, M. I., Torney, L., and Robinson, R. A. (1990). p185neu expression in human lung adenocarcinomas predicts shortened survival. *Cancer Res* **50**(16), 5184-7.

Keshet, E., Lyman, S. D., Williams, D. E., Anderson, D. M., Jenkins, N. A., Copeland, N. G., and Parada, L. F. (1991). Embryonic RNA expression patterns of the c-kit receptor and its cognate ligand suggest multiple functional roles in mouse development. *Embo J* **10**(9), 2425-35.

Khwaja, A., Rodriguez-Viciana, P., Wennstrom, S., Warne, P. H., and Downward, J. (1997). Matrix adhesion and Ras transformation both activate a phosphoinositide 3-OH kinase and protein kinase B/Akt cellular survival pathway. *Embo J* **16**(10), 2783-93.

Kinashi, T., Katagiri, K., Watanabe, S., Vanhaesebroeck, B., Downward, J., and Takatsu, K. (2000). Distinct mechanisms of alpha 5beta 1 integrin activation by Ha-Ras and R-Ras. *J Biol Chem* **275**(29), 22590-6.

Kinashi, T., and Springer, T. A. (1994). Steel factor and c-kit regulate cell-matrix adhesion. *Blood* **83**(4), 1033-8.

Kitamura, Y., Go, S., and Hatanaka, K. (1978). Decrease of mast cells in W/Wv mice and their increase by bone marrow transplantation. *Blood* **52**(2), 447-52.

Kitamura, Y., Hirota, S., and Nishida, T. (2001). A loss-of-function mutation of c-kit results in depletion of mast cells and interstitial cells of Cajal, while its gain-of-function mutation results in their oncogenesis. *Mutat Res* **477**(1-2), 165-71.

Kitayama, H., Kanakura, Y., Furitsu, T., Tsujimura, T., Oritani, K., Ikeda, H., Sugahara, H., Mitsui, H., Kanayama, Y., Kitamura, Y., and et al. (1995). Constitutively activating mutations of c-kit receptor tyrosine kinase confer factor-independent growth and tumorigenicity of factor-dependent hematopoietic cell lines. *Blood* **85**(3), 790-8.

Koike, T., Hirai, K., Morita, Y., and Nozawa, Y. (1993). Stem cell factor-induced signal transduction in rat mast cells. Activation of phospholipase D but not phosphoinositide-specific phospholipase C in c-kit receptor stimulation. *J Immunol* **151**(1), 359-66.

Kozlowski, M., Larose, L., Lee, F., Le, D. M., Rottapel, R., and Siminovitch, K. A. (1998). SHP-1 binds and negatively modulates the c-Kit receptor by interaction with tyrosine 569 in the c-Kit juxtamembrane domain. *Mol Cell Biol* **18**(4), 2089-99.

Kuci, S., Wessels, J. T., Buhring, H. J., Schilbach, K., Schumm, M., Seitz, G., Loffler, J., Bader, P., Schlegel, P. G., Niethammer, D., and Handgretinger, R. (2003). Identification of a novel class of human adherent CD34- stem cells that give rise to SCID-repopulating cells. *Blood* **101**(3), 869-76.

Kuehl, W. M., Bender, T. P., Stafford, J., McClinton, D., Segal, S., and Dmitrovsky, E. (1988). Expression and function of the c-myb oncogene during hematopoietic differentiation. *Curr Top Microbiol Immunol* **141**, 318-23.

Kumar, A., Lee, C. M., and Reddy, E. P. (2003). c-Myc is essential but not sufficient for c-Myb-mediated block of granulocytic differentiation. *J Biol Chem* **278**(13), 11480-8.

Kutyavin, I. V., Lukhtanov, E. A., Gamper, H. B., and Meyer, R. B. (1997). Oligonucleotides with conjugated dihydropyrroloindole tripeptides: base composition and backbone effects on hybridization. *Nucleic Acids Res* **25**(3718-23).

Lammie, A., Drobnjak, M., Gerald, W., Saad, A., Cote, R., and Cordon-Cardo, C. (1994). Expression of c-kit and kit ligand proteins in normal human tissues. *J Histochem Cytochem* **42**(11), 1417-25.

Lansdorp, P. M., Sutherland, H. J., and Eaves, C. J. (1990). Selective expression of CD45 isoforms on functional subpopulations of CD34+ hemopoietic cells from human bone marrow. *J Exp Med* **172**(1), 363-6.

Lanza, F., Healy, L., and Sutherland, D. R. (2001). Structural and functional features of the CD34 antigen: an update. *J Biol Regul Homeost Agents* **15**(1), 1-13.

Lapidot, T., and Petit, I. (2002). Current understanding of stem cell mobilization: the roles of chemokines, proteolytic enzymes, adhesion molecules, cytokines, and stromal cells. *Exp Hematol* **30**(9), 973-81.

Lasota, J., Dansonka-Mieszkowska, A., Stachura, T., Schneider-Stock, R., Kallajoki, M., Steigen, S. E., Sarlomo-Rikala, M., Boltze, C., Kordek, R., Roessner, A., Stachura, J., and Miettinen, M. (2003a). Gastrointestinal stromal tumors with internal tandem duplications in 3' end of KIT juxtamembrane domain occur predominantly in stomach and generally seem to have a favorable course. *Mod Pathol* **16**(12), 1257-64.

Lasota, J., Kopczynski, J., Sarlomo-Rikala, M., Schneider-Stock, R., Stachura, T., Kordek, R., Michal, M., Boltze, C., Roessner, A., Stachura, J., and Miettinen, M. (2003b). KIT 1530ins6 mutation defines a subset of predominantly malignant gastrointestinal stromal tumors of intestinal origin. *Hum Pathol* **34**(12), 1306-12.

Lazzari, L., Henschler, R., Lecchi, L., Rebulla, P., Mertelsmann, R., and Sirchia, G. (2000). Interleukin-6 and interleukin-11 act synergistically with thrombopoietin and stem cell factor to modulate ex vivo expansion of human CD41+ and CD61+ megakaryocytic cells. *Haematologica* **85**(1), 25-30.

Ledbetter, J. A., and Herzenberg, L. A. (1979). Xenogeneic monoclonal antibodies to mouse lymphoid differentiation antigens. *Immunol Rev* **47**, 63-90.

Lee, D. M., Staats, H. F., Sundy, J. S., Patel, D. D., Sempowski, G. D., Scearce, R. M., Jones, D. M., and Haynes, B. F. (1998). Immunologic characterization of CD7-deficient mice. *J Immunol* **160**(12), 5749-56.

Lemmon, M. A., and Ferguson, K. M. (1998). Pleckstrin homology domains. *In* "Protein modules in signal transduction" (A. J. Pawson, Ed.), Vol. 228, pp. 39-74. Springer -Verlag, Berlin Heidelberg.

Lemmon, M. A., Flanagan, J. M., Hunt, J. F., Adair, B. D., Bormann, B. J., Dempsey, C. E., and Engelman, D. M. (1992). Glycophorin A dimerization is driven by specific interactions between transmembrane alpha-helices. *J Biol Chem* **267**(11), 7683-9.

Lemmon, M. A., and Schlessinger, J. (1994). Regulation of signal transduction and signal diversity by receptor oligomerization. *Trends Biochem Sci* **19**(11), 459-63.

Lennartsson, J., Wernstedt, C., Engstrom, U., Hellman, U., and Ronnstrand, L. (2003). Identification of Tyr900 in the kinase domain of c-Kit as a Src-dependent phosphorylation site mediating interaction with c-Crk. *Exp Cell Res* **288**(1), 110-8.

Leprince, D., Gegonne, A., Coll, J., de Taisne, C., Schneeberger, A., Lagrou, C., and Stehelin, D. (1983a). A putative second cell-derived oncogene of the avian leukaemia retrovirus E26. *Nature* **306**(5941), 395-7.

Leprince, D., Saule, S., de Taisne, C., Gegonne, A., Begue, A., Righi, M., and Stehelin, D. (1983b). The human DNA locus related to the oncogene myb of avian myeloblastosis virus (AMV): molecular cloning and structural characterization. *Embo J* **2**(7), 1073-8.

Lerner, N. B., Nocka, K. H., Cole, S. R., Qiu, F. H., Strife, A., Ashman, L. K., and Besmer, P. (1991). Monoclonal antibody YB5.B8 identifies the human c-kit protein product. *Blood* **77**(9), 1876-83.

Lev, S., Blechman, J., Nishikawa, S., Givol, D., and Yarden, Y. (1993). Interspecies molecular chimeras of kit help define the binding site of the stem cell factor. *Mol Cell Biol* **13**(4), 2224-34.

Lev, S., Givol, D., and Yarden, Y. (1991). A specific combination of substrates is involved in signal transduction by the kit-encoded receptor. *Embo J* **10**(3), 647-54.

Lev, S., Givol, D., and Yarden, Y. (1992a). Interkinase domain of kit contains the binding site for phosphatidylinositol 3' kinase. *Proc Natl Acad Sci U S A* **89**(2), 678-82.

Lev, S., Yarden, Y., and Givol, D. (1992b). Dimerization and activation of the kit receptor by monovalent and bivalent binding of the stem cell factor. *J Biol Chem* **267**(22), 15970-7.

Lev, S., Yarden, Y., and Givol, D. (1992c). A recombinant ectodomain of the receptor for the stem cell factor (SCF) retains ligand-induced receptor dimerization and antagonizes SCF-stimulated cellular responses. *J Biol Chem* **267**(15), 10866-73.

Levesque, J. P., Hendy, J., Takamatsu, Y., Simmons, P. J., and Bendall, L. J. (2003a). Disruption of the CXCR4/CXCL12 chemotactic interaction during hematopoietic stem cell mobilization induced by GCSF or cyclophosphamide. *J Clin Invest* **111**(2), 187-96.

Levesque, J. P., Hendy, J., Winkler, I. G., Takamatsu, Y., and Simmons, P. J. (2003b). Granulocyte colony-stimulating factor induces the release in the bone marrow of proteases that cleave c-KIT receptor (CD117) from the surface of hematopoietic progenitor cells. *Exp Hematol* **31**(2), 109-17.

Levesque, J. P., Leavesley, D. I., Niutta, S., Vadas, M., and Simmons, P. J. (1995). Cytokines increase human hemopoietic cell adhesiveness by activation of very late antigen (VLA)-4 and VLA-5 integrins. *J Exp Med* **181**(5), 1805-15.

Levesque, J. P., Liu, F., Simmons, P. J., Betsuyaku, T., Senior, R. M., Pham, C., and Link, D. C. (2004). Characterization of hematopoietic progenitor mobilization in protease-deficient mice. *Blood* **104**(1), 65-72.

Li, W., and Stanley, E. R. (1991). Role of dimerization and modification of the CSF-1 receptor in its activation and internalization during the CSF-1 response. *Embo J* **10**(2), 277-88.

Lin, C. R., Chen, W. S., Lazar, C. S., Carpenter, C. D., Gill, G. N., Evans, R. M., and Rosenfeld, M. G. (1986). Protein kinase C phosphorylation at Thr 654 of the unoccupied EGF receptor and EGF binding regulate functional receptor loss by independent mechanisms. *Cell* **44**(6), 839-48.

Lin, H. H., Sternfeld, D. C., Shinpock, S. G., Popp, R. A., and Mucenski, M. L. (1996). Functional analysis of the c-myb proto-oncogene. *Curr Top Microbiol Immunol* **211**, 79-87.

Link, M., Warnke, R., Finlay, J., Amylon, M., Miller, R., Dilley, J., and Levy, R. (1983). A single monoclonal antibody identifies T-cell lineage of childhood lymphoid malignancies. *Blood* **62**(4), 722-8.

Linnekin, D. (1999). Early signaling pathways activated by c-Kit in hematopoietic cells. *Int J Biochem Cell Biol* **31**(10), 1053-74.

Linnekin, D., DeBerry, C. S., and Mou, S. (1997). Lyn associates with the juxtamembrane region of c-Kit and is activated by stem cell factor in hematopoietic cell lines and normal progenitor cells. *J Biol Chem* **272**(43), 27450-5.

Lipsick, J. S. (1996). One billion years of Myb. *Oncogene* **13**(2), 223-35.

Liu, E., Thor, A., He, M., Barcos, M., Ljung, B. M., and Benz, C. (1992). The HER2 (c-erbB-2) oncogene is frequently amplified in in situ carcinomas of the breast. *Oncogene* **7**(5), 1027-32.

Longley, B. J., Jr., Metcalfe, D. D., Tharp, M., Wang, X., Tyrrell, L., Lu, S. Z., Heitjan, D., and Ma, Y. (1999). Activating and dominant inactivating c-KIT catalytic domain mutations in distinct clinical forms of human mastocytosis. *Proc Natl Acad Sci U S A* **96**(4), 1609-14.

Longley, B. J., Tyrrell, L., Ma, Y., Williams, D. A., Halaban, R., Langley, K., Lu, H. S., and Schechter, N. M. (1997). Chymase cleavage of stem cell factor yields a bioactive, soluble product. *Proc Natl Acad Sci U S A* **94**(17), 9017-21.

Looijenga, L. H., de Leeuw, H., van Oorschot, M., van Gurp, R. J., Stoop, H., Gillis, A. J., de Gouveia Brazao, C. A., Weber, R. F., Kirkels, W. J., van Dijk, T., von Lindern, M., Valk, P., Lajos, G., Olah, E., Nesland, J. M., Fossa, S. D., and Oosterhuis, J. W. (2003). Stem cell factor receptor (c-KIT) codon 816 mutations predict development of bilateral testicular germ-cell tumors. *Cancer Res* **63**(22), 7674-8.

Lorenz, U., Bergemann, A. D., Steinberg, H. N., Flanagan, J. G., Li, X., Galli, S. J., and Neel, B. G. (1996). Genetic analysis reveals cell type-specific regulation of receptor tyrosine kinase c-Kit by the protein tyrosine phosphatase SHP1. *J Exp Med* **184**(3), 1111-26.

Lu, L., Walker, D., Broxmeyer, H. E., Hoffman, R., Hu, W., and Walker, E. (1987). Characterization of adult human marrow hematopoietic progenitors highly enriched by two-color cell sorting with My10 and major histocompatibility class II monoclonal antibodies. *J Immunol* **139**(6), 1823-9.

Luchetti, M. M., Paroncini, P., Majlingova, P., Frampton, J., Mucenski, M., Baroni, S. S., Sambo, P., Golay, J., Introna, M., and Gabrielli, A. (2003). Characterization of the c-Myb-responsive region and regulation of the human type I collagen alpha 2 chain gene by c-Myb. *J Biol Chem* **278**(3), 1533-41.

Lupu, R., Colomer, R., Zugmaier, G., Sarup, J., Shepard, M., Slamon, D., and Lippman, M. E. (1990). Direct interaction of a ligand for the erbB2 oncogene product with the EGF receptor and p185erbB2. *Science* **249**(4976), 1552-5.

Majka, M., Ratajczak, J., Machalinski, B., Carter, A., Pizzini, D., Wasik, M. A., Gewirtz, A. M., and Ratajczak, M. Z. (2000). Expression, regulation and function of AC133, a putative cell surface marker of primitive human haematopoietic cells. *Folia Histochem Cytobiol* **38**(2), 53-63.

Mann, R., Mulligan, R. C., and Baltimore, D. (1983). Construction of a retrovirus packaging mutant and its use to produce helper-free defective retrovirus. *Cell* **33**(1), 153-9.

Manova, K., and Bachvarova, R. F. (1991). Expression of c-kit encoded at the W locus of mice in developing embryonic germ cells and presumptive melanoblasts. *Dev Biol* **146**(2), 312-24.

Margolis, B., Rhee, S. G., Felder, S., Mervic, M., Lyall, R., Levitzki, A., Ullrich, A., Zilberstein, A., and Schlessinger, J. (1989). EGF induces tyrosine phosphorylation of phospholipase C-II: a potential mechanism for EGF receptor signaling. *Cell* **57**(7), 1101-7.

Marshall, C. J. (1995). Specificity of receptor tyrosine kinase signaling: transient versus sustained extracellular signal-regulated kinase activation. *Cell* **80**(2), 179-85.

Marte, B. M., Rodriguez-Viciana, P., Wennstrom, S., Warne, P. H., and Downward, J. (1997). R-Ras can activate the phosphoinositide 3-kinase but not the MAP kinase arm of the Ras effector pathways. *Curr Biol* **7**(1), 63-70.

Martin, F. H., Suggs, S. V., Langley, K. E., Lu, H. S., Ting, J., Okino, K. H., Morris, C. F., McNiece, I. K., Jacobsen, F. W., Mendiaz, E. A., and et al. (1990). Primary structure and functional expression of rat and human stem cell factor DNAs. *Cell* **63**(1), 203-11.

Martin, T. F. J. (1998). Phosphoinositide lipids as signaling molecules: Common themes for signal transduction, cytoskeletal regulation, and membrane trafficking. *Ann.Rev.Cell Dev.Biol.* **14,** 231-264.

Martinez, C., Urbano-Ispizua, A., Rozman, C., Marin, P., Mazzara, R., Carreras, E., Rovira, M., Sierra, J., Briones, J., Ordinas, A., and Montserrat, E. (1996). Effects of G-CSF administration and peripheral blood progenitor cell collection in 20 healthy donors. *Ann Hematol* **72**(4), 269-72.

Matous, J. V., Langley, K., and Kaushansky, K. (1996). Structure-function relationships of stem cell factor: an analysis based on a series of human-murine stem cell factor chimera and the mapping of a neutralizing monoclonal antibody. *Blood* **88**(2), 437-44.

Matsuguchi, T., Salgia, R., Hallek, M., Eder, M., Druker, B., Ernst, T. J., and Griffin, J. D. (1994). Shc phosphorylation in myeloid cells is regulated by granulocyte macrophage colony-stimulating factor, interleukin-3, and steel factor and is constitutively increased by p210BCR/ABL. *J Biol Chem* **269**(7), 5016-21.

Matthews, W., Jordan, C. T., Wiegand, G. W., Pardoll, D., and Lemischka, I. R. (1991). A receptor tyrosine kinase specific to hematopoietic stem and progenitor cell-enriched populations. *Cell* **65**(7), 1143-52.

Maxwell, M. J., Yuan, Y., Anderson, K. E., Hibbs, M. L., Salem, H. H., and Jackson, S. P. (2004). SHIP1 and Lyn Kinase Negatively Regulate Integrin alpha IIb beta 3 signaling in platelets. *J Biol Chem* **279**(31), 32196-204.

Mayrhofer, G., Gadd, S. J., Spargo, L. D., and Ashman, L. K. (1987). Specificity of a mouse monoclonal antibody raised against acute myeloid leukaemia cells for mast cells in human mucosal and connective tissues. *Immunol Cell Biol* **65 (Pt 3),** 241-50.

McCulloch, E. A., Siminovitch, L., and Till, J. E. (1964). Spleen colony formation in anemic mice of genotype W/Wv. *Science* **144,** 844.

McNeil, H. P., Frenkel, D. P., Austen, K. F., Friend, D. S., and Stevens, R. L. (1992). Translation and granule localization of mouse mast cell protease-5. Immunodetection with specific antipeptide Ig. *J Immunol* **149**(7), 2466-72.

Mehta, K., Shahid, U., and Malavasi, F. (1996). Human CD38, a cell-surface protein with multiple functions. *Faseb J* **10**(12), 1408-17.

Meininger, C. J., Yano, H., Rottapel, R., Bernstein, A., Zsebo, K. M., and Zetter, B. R. (1992). The c-kit receptor ligand functions as a mast cell chemoattractant. *Blood* **79**(4), 958-63.

Melotti, P., and Calabretta, B. (1994a). Ets-2 and c-Myb act independently in regulating expression of the hematopoietic stem cell antigen CD34. *J Biol Chem* **269**(41), 25303-9.

Melotti, P., Ku, D. H., and Calabretta, B. (1994b). Regulation of the expression of the hematopoietic stem cell antigen CD34: role of c-myb. *J Exp Med* **179**(3), 1023-8.

Mettus, R. V., Litvin, J., Wali, A., Toscani, A., Latham, K., Hatton, K., and Reddy, E. P. (1994). Murine A-myb: evidence for differential splicing and tissue-specific expression. *Oncogene* **9**(10), 3077-86.

Miettinen, M., Sarlomo-Rikala, M., and Lasota, J. (2000). KIT expression in angiosarcomas and fetal endothelial cells: lack of mutations of exon 11 and exon 17 of C-kit. *Mod Pathol* **13**(5), 536-41.

Milburn, C. C., Deak, M., Kelly, S. M., Price, N. C., Alessi, D. R., and Van Aalten, D. M. (2003). Binding of phosphatidylinositol 3,4,5-trisphosphate to the pleckstrin homology domain of protein kinase B induces a conformational change. *Biochem J* **375**(Pt 3), 531-8.

Mingari, M. C., Vitale, C., Romagnani, C., Falco, M., and Moretta, L. (2001). p75/AIRM1 and CD33, two sialoadhesin receptors that regulate the proliferation or the survival of normal and leukemic myeloid cells. *Immunol Rev* **181**, 260-8.

Miniero, R., Madon, E., Avanzi, G. C., Saitta, M., Forni, M., Ghisolfi, G., Coda, R., Lista, P., Cordero di Montezemolo, L., Cattoretti, G., and et al. (1987). Unusual cytogenetic, immunophenotypic and histochemical findings in a case of acute megakaryocytic leukemia. *Haematologica* **72**(6), 505-10.

Miraglia, S., Godfrey, W., Yin, A. H., Atkins, K., Warnke, R., Holden, J. T., Bray, R. A., Waller, E. K., and Buck, D. W. (1997). A novel five-transmembrane hematopoietic stem cell antigen: isolation, characterization, and molecular cloning. *Blood* **90**(12), 5013-21.

Miyazawa, K., Hendrie, P. C., Mantel, C., Wood, K., Ashman, L. K., and Broxmeyer, H. E. (1991). Comparative analysis of signaling pathways between mast cell growth factor (c-kit ligand) and granulocyte-macrophage colony-stimulating factor in a human factor-dependent myeloid cell line involves phosphorylation of Raf-1, GTPase-activating protein and mitogen-activated protein kinase. *Exp Hematol* **19**(11), 1110-23.

Miyazawa, K., Toyama, K., Gotoh, A., Hendrie, P. C., Mantel, C., and Broxmeyer, H. E. (1994). Ligand-dependent polyubiquitination of c-kit gene product: a possible mechanism of receptor down modulation in M07e cells. *Blood* **83**(1), 137-45.

Mohammadi, M., Froum, S., Hamby, J. M., Schroeder, M. C., Panek, R. L., Lu, G. H., Eliseenkova, A. V., Green, D., Schlessinger, J., and Hubbard, S. R. (1998). Crystal structure of an angiogenesis inhibitor bound to the FGF receptor tyrosine kinase domain. *Embo J* **17**(20), 5896-904.

Mol, C. D., Dougan, D. R., Schneider, T. R., Skene, R. J., Kraus, M. L., Scheibe, D. N., Snell, G. P., Zou, H., Sang, B. C., and Wilson, K. P. (2004). Structural basis for the autoinhibition and STI-571 inhibition of c-Kit tyrosine kinase. *J Biol Chem* **279**(30), 31655-63.

Mol, C. D., Lim, K. B., Sridhar, V., Zou, H., Chien, E. Y., Sang, B. C., Nowakowski, J., Kassel, D. B., Cronin, C. N., and McRee, D. E. (2003). Structure of a c-kit product complex reveals the basis for kinase transactivation. *J Biol Chem* **278**(34), 31461-4.

Moon, B. G., Takaki, S., Nishizumi, H., Yamamoto, T., and Takatsu, K. (2004). Abrogation of autoimmune disease in Lyn-deficient mice by the deletion of IL-5 receptor alpha chain gene. *Cell Immunol* **228**(2), 110-8.

Mori, S., Heldin, C. H., and Claesson-Welsh, L. (1992). Ligand-induced polyubiquitination of the platelet-derived growth factor beta-receptor. *J Biol Chem* **267**(9), 6429-34.

Mori, S., Heldin, C. H., and Claesson-Welsh, L. (1993). Ligand-induced ubiquitination of the platelet-derived growth factor beta-receptor plays a negative regulatory role in its mitogenic signaling. *J Biol Chem* **268**(1), 577-83.

Mosesson, Y., Shtiegman, K., Katz, M., Zwang, Y., Vereb, G., Szollosi, J., and Yarden, Y. (2003). Endocytosis of receptor tyrosine kinases is driven by monoubiquitylation, not polyubiquitylation. *J Biol Chem* **278**(24), 21323-6.

Moskowitz, C. H., Stiff, P., Gordon, M. S., McNiece, I., Ho, A. D., Costa, J. J., Broun, E. R., Bayer, R. A., Wyres, M., Hill, J., Jelaca-Maxwell, K., Nichols, C. R., Brown, S. L., Nimer, S. D., and Gabrilove, J. (1997). Recombinant methionyl human stem cell factor and filgrastim for peripheral blood progenitor cell mobilization and transplantation in non-Hodgkin's lymphoma patients--results of a phase I/II trial. *Blood* **89**(9), 3136-47.

Mucenski, M. L., McLain, K., Kier, A. B., Swerdlow, S. H., Schreiner, C. M., Miller, T. A., Pietryga, D. W., Scott, W. J., Jr., and Potter, S. S. (1991). A functional c-myb gene is required for normal murine fetal hepatic hematopoiesis. *Cell* **65**(4), 677-89.

Murray, L., Chen, B., Galy, A., Chen, S., Tushinski, R., Uchida, N., Negrin, R., Tricot, G., Jagannath, S., Vesole, D., and et al. (1995). Enrichment of human hematopoietic stem cell activity in the CD34+Thy-1+Lin- subpopulation from mobilized peripheral blood. *Blood* **85**(2), 368-78.

Murray, L., DiGiusto, D., Chen, B., Chen, S., Combs, J., Conti, A., Galy, A., Negrin, R., Tricot, G., and Tsukamoto, A. (1994). Analysis of human hematopoietic stem cell populations. *Blood Cells* **20**(2-3), 364-9; discussion 369-70.

Nakagoshi, H., Nagase, T., Kanei-Ishii, C., Ueno, Y., and Ishii, S. (1990). Binding of the c-myb proto-oncogene product to the simian virus 40 enhancer stimulates transcription. *J Biol Chem* **265**(6), 3479-83.

Nakahara, M., Isozaki, K., Hirota, S., Miyagawa, J., Hase-Sawada, N., Taniguchi, M., Nishida, T., Kanayama, S., Kitamura, Y., Shinomura, Y., and Matsuzawa, Y. (1998). A novel gain-of-function mutation of c-kit gene in gastrointestinal stromal tumors. *Gastroenterology* **115**(5), 1090-5.

Nakahata, T., and Okumura, N. (1994). Cell surface antigen expression in human erythroid progenitors: erythroid and megakaryocytic markers. *Leuk Lymphoma* **13**(5-6), 401-9.

Nakayama, K., Yamamoto, R., Ishii, S., and Nakauchi, H. (1993). Binding of c-Myb to the core sequence of the CD4 promoter. *Int Immunol* **5**(8), 817-24.

Ness, S. A. (2003). Myb protein specificity: evidence of a context-specific transcription factor code. *Blood Cells Mol Dis* **31**(2), 192-200.

Ness, S. A., Marknell, A., and Graf, T. (1989). The v-myb oncogene product binds to and activates the promyelocyte-specific mim-1 gene. *Cell* **59**(6), 1115-25.

Nicolaides, N. C., Gualdi, R., Casadevall, C., Manzella, L., and Calabretta, B. (1991). Positive autoregulation of c-myb expression via Myb binding sites in the 5' flanking region of the human c-myb gene. *Mol Cell Biol* **11**(12), 6166-76.

Nishida, T., Hirota, S., Taniguchi, M., Hashimoto, K., Isozaki, K., Nakamura, H., Kanakura, Y., Tanaka, T., Takabayashi, A., Matsuda, H., and Kitamura, Y. (1998). Familial gastrointestinal stromal tumours with germline mutation of the KIT gene. *Nat Genet* **19**(4), 323-4.

Niwa, H., Yamamura, K., and Miyazaki, J. (1991). Efficient selection for high-expression transfectants with a novel eukaryotic vector. *Gene* **108**(2), 193-9.

Nocka, K., Buck, J., Levi, E., and Besmer, P. (1990a). Candidate ligand for the c-kit transmembrane kinase receptor: KL, a fibroblast derived growth factor stimulates mast cells and erythroid progenitors. *Embo J* **9**(10), 3287-94.

Nocka, K., Majumder, S., Chabot, B., Ray, P., Cervone, M., Bernstein, A., and Besmer, P. (1989). Expression of c-kit gene products in known cellular targets of W mutations in normal and W mutant mice--evidence for an impaired c-kit kinase in mutant mice. *Genes Dev* **3**(6), 816-26.

Nocka, K., Tan, J. C., Chiu, E., Chu, T. Y., Ray, P., Traktman, P., and Besmer, P. (1990b). Molecular bases of dominant negative and loss of function mutations at the murine c-kit/white spotting locus: W37, Wv, W41 and W. *Embo J* **9**(6), 1805-13.

Normann, A. P., Egeland, T., Madshus, I. H., Heim, S., and Tjonnfjord, G. E. (2003). CD7 expression by CD34+ cells in CML patients, of prognostic significance? *Eur J Haematol* **71**(4), 266-75.

Nunn, M. F., Seeburg, P. H., Moscovici, C., and Duesberg, P. H. (1983). Tripartite structure of the avian erythroblastosis virus E26 transforming gene. *Nature* **306**(5941), 391-5.

Oertel, J., Oertel, B., Schleicher, J., and Huhn, D. (1996). Immunotyping of blasts in human bone marrow. *Ann Hematol* **72**(3), 125-9.

Oertli, B., Han, J., Marte, B. M., Sethi, T., Downward, J., Ginsberg, M., and Hughes, P. E. (2000). The effector loop and prenylation site of R-Ras are involved in the regulation of integrin function. *Oncogene* **19**(43), 4961-9.

Ogawa, K., Takeda, Y., Tashima, M., Sawai, H., Toi, T., Okazaki, T., Sawada, H., Maruyama, Y., and Okuma, M. (1995). High expression of c-kit in K562YO cells due to the prolonged half-life of its mRNA: the effects of modification with serine/threonine kinase signals. *Blood* **85**(6), 1496-503.

Ogawa, M., Matsuzaki, Y., Nishikawa, S., Hayashi, S., Kunisada, T., Sudo, T., Kina, T., and Nakauchi, H. (1991). Expression and function of c-kit in hemopoietic progenitor cells. *J Exp Med* **174**(1), 63-71.

Oh, I. H., and Reddy, E. P. (1997). Murine A-myb gene encodes a transcription factor, which cooperates with Ets-2 and exhibits distinctive biochemical and biological activities from c-myb. *J Biol Chem* **272**(34), 21432-43.

Oh, I. H., and Reddy, E. P. (1998). The C-terminal domain of B-Myb acts as a positive regulator of transcription and modulates its biological functions. *Mol Cell Biol* **18**(1), 499-511.

Oh, I. H., and Reddy, E. P. (1999). The myb gene family in cell growth, differentiation and apoptosis. *Oncogene* **18**(19), 3017-33.

Okada, M., Nada, S., Yamanashi, Y., Yamamoto, T., and Nakagawa, H. (1991). CSK: a protein-tyrosine kinase involved in regulation of src family kinases. *J Biol Chem* **266**(36), 24249-52.

O'Laughlin-Bunner, B., Radosevic, N., Taylor, M. L., Shivakrupa, DeBerry, C., Metcalfe, D. D., Zhou, M., Lowell, C., and Linnekin, D. (2001). Lyn is required for normal stem cell

factor-induced proliferation and chemotaxis of primary hematopoietic cells. *Blood* **98**(2), 343-50.

Olson, M. F., Paterson, H. F., and Marshall, C. J. (1998). Signals from Ras and Rho GTPases interact to regulate expression of p21Waf1/Cip1. *Nature* **394**(6690), 295-9.

Olweus, J., Lund-Johansen, F., and Terstappen, L. W. (1994). Expression of cell surface markers during differentiation of CD34+, CD38-/lo fetal and adult bone marrow cells. *Immunomethods* **5**(3), 179-88.

Otero, D. C., and Rickert, R. C. (2003). CD19 function in early and late B cell development. II. CD19 facilitates the pro-B/pre-B transition. *J Immunol* **171**(11), 5921-30.

Paik, S., Hazan, R., Fisher, E. R., Sass, R. E., Fisher, B., Redmond, C., Schlessinger, J., Lippman, M. E., and King, C. R. (1990). Pathologic findings from the National Surgical Adjuvant Breast and Bowel Project: prognostic significance of erbB-2 protein overexpression in primary breast cancer. *J Clin Oncol* **8**(1), 103-12.

Palker, T. J., Scearce, R. M., Hensley, L., Ho, W., and Haynes, B. F. (1986). Comparison of the CD7 (3A1) group of T cell workshop antibodies. *In* "Leukocyte Typing II: Human T Lymphocytes" (E. Reinherz, B. F. Haynes, L. Nadler, and I. Bernstein, Eds.), pp. 303-313. Springer-Verlag, New York.

Pardanani, A., Reeder, T. L., Kimlinger, T. K., Baek, J. Y., Li, C. Y., Butterfield, J. H., and Tefferi, A. (2003). Flt-3 and c-kit mutation studies in a spectrum of chronic myeloid disorders including systemic mast cell disease. *Leuk Res* **27**(8), 739-42.

Paronetto, M. P., Farini, D., Sammarco, I., Maturo, G., Vespasiani, G., Geremia, R., Rossi, P., and Sette, C. (2004). Expression of a truncated form of the c-Kit tyrosine kinase receptor and activation of Src kinase in human prostatic cancer. *Am J Pathol* **164**(4), 1243-51.

Pasvol, G., Jungery, M., Weatherall, D. J., Parsons, S. F., Anstee, D. J., and Tanner, M. J. (1982). Glycophorin as a possible receptor for Plasmodium falciparum. *Lancet* **2**(8305), 947-50.

Paul, S. P., Taylor, L. S., Stansbury, E. K., and McVicar, D. W. (2000). Myeloid specific human CD33 is an inhibitory receptor with differential ITIM function in recruiting the phosphatases SHP-1 and SHP-2. *Blood* **96**(2), 483-90.

Paulson, R. F., Vesely, S., Siminovitch, K. A., and Bernstein, A. (1996). Signalling by the W/Kit receptor tyrosine kinase is negatively regulated in vivo by the protein tyrosine phosphatase Shp1. *Nat Genet* **13**(3), 309-15.

Pawson, T. (1995). Protein modules and signalling networks. *Nature* **373,** 573-580.

Pawson, T. (2002). Regulation and targets of receptor tyrosine kinases. *Eur J Cancer* **38**(Suppl. 5), S3-S10.

Pawson, T., and Schlessinger, J. (1993). SH2 and SH3 domains. *Current Biology* **3,** 434.

Pazdrak, K., Olszewska-Pazdrak, B., Stafford, S., Garofalo, R. P., and Alam, R. (1998). Lyn, Jak2, and Raf-1 kinases are critical for the antiapoptotic effect of interleukin 5, whereas only Raf-1 kinase is essential for eosinophil activation and degranulation. *J Exp Med* **188**(3), 421-9.

Peault, B., Weissman, I. L., Buckle, A. M., Tsukamoto, A., and Baum, C. (1993). Thy-1-expressing CD34+ human cells express multiple hematopoietic potentialities in vitro and in SCID-hu mice. *Nouv Rev Fr Hematol* **35**(1), 91-3.

Pecora, A. L. (1999). Impact of stem cell dose on hematopoietic recovery in autologous blood stem cell recipients. *Bone Marrow Transplant* **23 Suppl 2,** S7-12.

Peiper, S. C., Ashmun, R. A., and Look, A. T. (1988). Molecular cloning, expression, and chromosomal localization of a human gene encoding the CD33 myeloid differentiation antigen. *Blood* **72**(1), 314-21.

Penengo, L., Rubin, C., Yarden, Y., and Gaudino, G. (2003). c-Cbl is a critical modulator of the Ron tyrosine kinase receptor. *Oncogene* **22**(24), 3669-79.

Pereira, S., and Lowell, C. (2003). The Lyn tyrosine kinase negatively regulates neutrophil integrin signaling. *J Immunol* **171**(3), 1319-27.

Perkins, M. E. (1984). Surface proteins of Plasmodium falciparum merozoites binding to the erythrocyte receptor, glycophorin. *J Exp Med* **160**(3), 788-98.

Pesando, J. M., Bouchard, L. S., and McMaster, B. E. (1989). CD19 is functionally and physically associated with surface immunoglobulin. *J Exp Med* **170**(6), 2159-64.

Pezzutto, A., Dorken, B., Rabinovitch, P. S., Ledbetter, J. A., Moldenhauer, G., and Clark, E. A. (1987). CD19 monoclonal antibody HD37 inhibits anti-immunoglobulin-induced B cell activation and proliferation. *J Immunol* **138**(9), 2793-9.

Piao, X., Curtis, J. E., Minkin, S., Minden, M. D., and Bernstein, A. (1994). Expression of the Kit and KitA receptor isoforms in human acute myelogenous leukemia. *Blood* **83**(2), 476-81.

Pittaluga, S., Raffeld, M., Lipford, E. H., and Cossman, J. (1986). 3A1 (CD7) expression precedes T beta gene rearrangements in precursor T (lymphoblastic) neoplasms. *Blood* **68**(1), 134-9.

Price, D. J., Rivnay, B., Fu, Y., Jiang, S., Avraham, S., and Avraham, H. (1997a). Direct association of Csk homologous kinase (CHK) with the diphosphorylated site Tyr568/570 of the activated c-KIT in megakaryocytes. *J Biol Chem* **272**(9), 5915-20.

Price, D. J., Rivnay, B., Fu, Y., Jiang, S., Avraham, S., and Avraham, H. (1997b). Direct association of Csk homologous kinase (CHK) with the diphosphorylated site Tyr568/570 of the activated c-KIT in megakaryocytes. *J Biol Chem* **272**(9), 5915-20.

Qian, X., Dougall, W. C., Fei, Z., and Greene, M. I. (1995). Intermolecular association and trans-phosphorylation of different neu- kinase forms permit SH2-dependent signaling and oncogenic transformation. *Oncogene* **10**(1), 211-9.

Qiu, F. H., Ray, P., Brown, K., Barker, P. E., Jhanwar, S., Ruddle, F. H., and Besmer, P. (1988). Primary structure of c-kit: relationship with the CSF-1/PDGF receptor kinase family--oncogenic activation of v-kit involves deletion of extracellular domain and C terminus. *Embo J* **7**(4), 1003-11.

Ramsay, R. G., Ikeda, K., Rifkind, R. A., and Marks, P. A. (1986). Changes in gene expression associated with induced differentiation of erythroleukemia: protooncogenes, globin genes, and cell division. *Proc Natl Acad Sci U S A* **83**(18), 6849-53.

Rankin, S., and Rozengurt, E. (1994). Platelet-derived growth factor modulation of focal adhesion kinase (p125FAK) and paxillin tyrosine phosphorylation in Swiss 3T3 cells. Bell-shaped dose response and cross-talk with bombesin. *J Biol Chem* **269**(1), 704-10.

Rasko, J. E., O'Flaherty, E., and Begley, C. G. (1997). Mpl ligand (MGDF) alone and in combination with stem cell factor (SCF) promotes proliferation and survival of human megakaryocyte, erythroid and granulocyte/macrophage progenitors. *Stem Cells* **15**(1), 33-42.

Ratajczak, M. Z., Luger, S. M., and Gewirtz, A. M. (1992). The c-kit proto-oncogene in normal and malignant human hematopoiesis. *Int J Cell Cloning* **10**(4), 205-14.

Ratajczak, M. Z., Pletcher, C. H., Marlicz, W., Machalinski, B., Moore, J., Wasik, M., Ratajczak, J., and Gewirtz, A. M. (1998). CD34+, kit+, rhodamine123(low) phenotype identifies a marrow cell population highly enriched for human hematopoietic stem cells. *Leukemia* **12**(6), 942-50.

Rayner, J. R., and Gonda, T. J. (1994). A simple and efficient procedure for generating stable expression libraries by cDNA cloning in a retroviral vector. *Mol Cell Biol* **14**(2), 880-7.

Reedijk, M., Liu, X., van der Geer, P., Letwin, K., Waterfield, M. D., Hunter, T., and Pawson, T. (1992). Tyr721 regulates specific binding of the CSF-1 receptor kinase insert to PI 3'-kinase SH2 domains: a model for SH2-mediated receptor-target interactions. *Embo J* **11**(4), 1365-72.

Reith, A. D., Ellis, C., Lyman, S. D., Anderson, D. M., Williams, D. E., Bernstein, A., and Pawson, T. (1991). Signal transduction by normal isoforms and W mutant variants of the Kit receptor tyrosine kinase. *Embo J* **10**(9), 2451-9.

Reith, A. D., Rottapel, R., Giddens, E., Brady, C., Forrester, L., and Bernstein, A. (1990). W mutant mice with mild or severe developmental defects contain distinct point mutations in the kinase domain of the c-kit receptor. *Genes Dev* **4**(3), 390-400.

Ren, C. L., Morio, T., Fu, S. M., and Geha, R. S. (1994). Signal transduction via CD40 involves activation of lyn kinase and phosphatidylinositol-3-kinase, and phosphorylation of phospholipase C gamma 2. *J Exp Med* **179**(2), 673-80.

Reynolds, A. B., Vila, J., Lansing, T. J., Potts, W. M., Weber, M. J., and Parsons, J. T. (1987). Activation of the oncogenic potential of the avian cellular src protein by specific structural alteration of the carboxy terminus. *Embo J* **6**(8), 2359-64.

Ricotti, E., Fagioli, F., Garelli, E., Linari, C., Crescenzio, N., Horenstein, A. L., Pistamiglio, P., Vai, S., Berger, M., di Montezemolo, L. C., Madon, E., and Basso, G. (1998). c-kit is expressed in soft tissue sarcoma of neuroectodermic origin and its ligand prevents apoptosis of neoplastic cells. *Blood* **91**(7), 2397-405.

Riedel, H., Schlessinger, J., and Ullrich, A. (1987). A chimeric, ligand-binding v-erbB/EGF receptor retains transforming potential. *Science* **236**(4798), 197-200.

Roberts, M. M., Swart, B. W., Simmons, P. J., Basser, R. L., Begley, C. G., and To, L. B. (1999). Prolonged release and c-kit expression of haemopoietic precursor cells mobilized by stem cell factor and granulocyte colony stimulating factor. *Br J Haematol* **104**(4), 778-84.

Rohr, U. P., Rehfeld, N., Pflugfelder, L., Geddert, H., Muller, W., Steidl, U., Fenk, R., Graf, T., Schott, M., Thiele, K. P., Gabbert, H. E., Germing, U., Kronenwett, R., and Haas, R. (2004). Expression of the tyrosine kinase c-kit is an independent prognostic factor in patients with small cell lung cancer. *Int J Cancer* **111**(2), 259-63.

Roifman, C. M., and Ke, S. (1993). CD19 is a substrate of the antigen receptor-associated protein tyrosine kinase in human B cells. *Biochem Biophys Res Commun* **194**(1), 222-5.

Rosnet, O., Marchetto, S., deLapeyriere, O., and Birnbaum, D. (1991). Murine Flt3, a gene encoding a novel tyrosine kinase receptor of the PDGFR/CSF1R family. *Oncogene* **6**(9), 1641-50.

Rottapel, R., Reedijk, M., Williams, D. E., Lyman, S. D., Anderson, D. M., Pawson, T., and Bernstein, A. (1991). The Steel/W transduction pathway: kit autophosphorylation and its association with a unique subset of cytoplasmic signaling proteins is induced by the Steel factor. *Mol Cell Biol* **11**(6), 3043-51.

Ruoslahti, E., and Reed, J. C. (1994). Anchorage dependence, integrins, and apoptosis. *Cell* **77**(4), 477-8.

Russell, E. S. (1979). Hereditary anemias of the mouse: a review for geneticists. *Adv Genet* **20,** 357-459.

Russell, E. S., and Bernstein, S. E. (1968). Proof of whole-cell implant in therapy of W-series anemia. *Arch Biochem Biophys* **125**(2), 594-7.

Saikumar, P., Murali, R., and Reddy, E. P. (1990). Role of tryptophan repeats and flanking amino acids in Myb-DNA interactions. *Proc Natl Acad Sci U S A* **87**(21), 8452-6.

Sakuma, Y., Sakurai, S., Oguni, S., Hironaka, M., and Saito, K. (2003). Alterations of the c-kit gene in testicular germ cell tumors. *Cancer Sci* **94**(6), 486-91.

Sakura, H., Kanei-Ishii, C., Nagase, T., Nakagoshi, H., Gonda, T. J., and Ishii, S. (1989). Delineation of three functional domains of the transcriptional activator encoded by the c-myb protooncogene. *Proc Natl Acad Sci U S A* **86**(15), 5758-62.

Sanchez, I., Hughes, R. T., Mayer, B. J., Yee, K., Woodgett, J. R., Avruch, J., Kyriakis, J. M., and Zon, L. I. (1994). Role of SAPK/ERK kinase-1 in the stress-activated pathway regulating transcription factor c-Jun. *Nature* **372**(6508), 794-8.

Sanjay, A., Horne, W. C., and Baron, R. (2001). The Cbl family: ubiquitin ligases regulating signaling by tyrosine kinases. *Sci STKE* **2001**(110), E40.

Sansilvestri, P., Cardoso, A. A., Batard, P., Panterne, B., Hatzfeld, A., Lim, B., Levesque, J. P., Monier, M. N., and Hatzfeld, J. (1995). Early CD34high cells can be separated into KIThigh cells in which transforming growth factor-beta (TGF-beta) downmodulates c-kit and KITlow cells in which anti-TGF-beta upmodulates c-kit. *Blood* **86**(5), 1729-35.

Sarvella, P., and Russell, L. (1956). Steel, a new dominant gene in the house mouse. *J Hered* **47,** 123-128.

Sato, S., Steeber, D. A., and Tedder, T. F. (1995). The CD19 signal transduction molecule is a response regulator of B-lymphocyte differentiation. *Proc Natl Acad Sci U S A* **92**(25), 11558-62.

Scanga, S. E., Ruel, L., Binari, R. C., Snow, B., Stambolic, V., Bouchard, D., Peters, M., Calvieri, B., Mak, T. W., Woodgett, J. R., and Manoukian, A. S. (2000). The conserved

PI3'K/PTEN/Akt signaling pathway regulates both cell size and survival in Drosophila. *Oncogene* **19**(35), 3971-7.

Scheijen, B., and Griffin, J. D. (2002). Tyrosine kinase oncogenes in normal hematopoiesis and hematological disease. *Oncogene* **21**(21), 3314-33.

Scheuermann, R. H., and Racila, E. (1995). CD19 antigen in leukemia and lymphoma diagnosis and immunotherapy. *Leuk Lymphoma* **18**(5-6), 385-97.

Schlessinger, J. (1995). Cellular signaling by receptor tyrosine kinases. *The Harvey Lectures* **89**, 105-123.

Schlessinger, J. (2000). Cell signaling by receptor tyrosine kinases. *Cell* **103**(2), 211-25.

Schlessinger, J., and Bar-Sagi, D. (1994). Activation of Ras and other signaling pathways by receptor tyrosine kinases. *Cold Spring Harb Symp Quant Biol* **59**, 173-9.

Schlessinger, J., Lax, I., and Lemmon, M. (1995). Regulation of growth factor activation by proteoglycans: what is the role of the low affinity receptors? *Cell* **83**(3), 357-60.

Schlessinger, J., Plotnikov, A. N., Ibrahimi, O. A., Eliseenkova, A. V., Yeh, B. K., Yayon, A., Linhardt, R. J., and Mohammadi, M. (2000). Crystal structure of a ternary FGF-FGFR-heparin complex reveals a dual role for heparin in FGFR binding and dimerization. *Mol Cell* **6**(3), 743-50.

Schlessinger, J., and Ullrich, A. (1992). Growth factor signaling by receptor tyrosine kinases. *Neuron* **9**(3), 383-91.

Schubert, S., Horstmann, S., Bartusel, T., and Klempnauer, K. H. (2004). The cooperation of B-Myb with the coactivator p300 is orchestrated by cyclins A and D1. *Oncogene* **23**(7), 1392-404.

Schumacher, R., Mosthaf, L., Schlessinger, J., Brandenburg, D., and Ullrich, A. (1991). Insulin and insulin-like growth factor-1 binding specificity is determined by distinct regions of their cognate receptors. *J Biol Chem* **266**(29), 19288-95.

Sempowski, G. D., Lee, D. M., Kaufman, R. E., and Haynes, B. F. (1999). Structure and function of the CD7 molecule. *Crit Rev Immunol* **19**(4), 331-48.

Serve, H., Hsu, Y. C., and Besmer, P. (1994). Tyrosine residue 719 of the c-kit receptor is essential for binding of the P85 subunit of phosphatidylinositol (PI) 3-kinase and for c-kit-associated PI 3-kinase activity in COS-1 cells. *J Biol Chem* **269**(8), 6026-30.

Serve, H., Yee, N. S., Stella, G., Sepp-Lorenzino, L., Tan, J. C., and Besmer, P. (1995). Differential roles of PI3-kinase and Kit tyrosine 821 in Kit receptor- mediated proliferation, survival and cell adhesion in mast cells. *Embo J* **14**(3), 473-83.

Sewing, A., Wiseman, B., Lloyd, A. C., and Land, H. (1997). High-intensity Raf signal causes cell cycle arrest mediated by p21Cip1. *Mol Cell Biol* **17**(9), 5588-97.

Shangary, S., Lerner, E. C., Zhan, Q., Corey, S. J., Smithgall, T. E., and Baskaran, R. (2003). Lyn regulates the cell death response to ultraviolet radiation through c-Jun N terminal kinase-dependent Fas ligand activation. *Exp Cell Res* **289**(1), 67-76.

Shearman, M. S., Herbst, R., Schlessinger, J., and Ullrich, A. (1993). Phosphatidylinositol 3'-kinase associates with p145c-kit as part of a cell type characteristic multimeric signalling complex. *Embo J* **12**(10), 3817-26.

Sheridan, W. P., Begley, C. G., Juttner, C. A., Szer, J., To, L. B., Maher, D., McGrath, K. M., Morstyn, G., and Fox, R. M. (1992). Effect of peripheral-blood progenitor cells mobilised by filgrastim (G-CSF) on platelet recovery after high-dose chemotherapy. *Lancet* **339**(8794), 640-4.

Shinjo, K., Takeshita, A., Ohnishi, K., and Ohno, R. (1997). Granulocyte colony-stimulating factor receptor at various differentiation stages of normal and leukemic hematopoietic cells. *Leuk Lymphoma* **25**(1-2), 37-46.

Shpall, E. J., Wheeler, C. A., Turner, S. A., Yanovich, S., Brown, R. A., Pecora, A. L., Shea, T. C., Mangan, K. F., Williams, S. F., LeMaistre, C. F., Long, G. D., Jones, R., Davis, M. W., Murphy-Filkins, R., Parker, W. R., and Glaspy, J. A. (1999). A randomized phase 3 study of peripheral blood progenitor cell mobilization with stem cell factor and filgrastim in high-risk breast cancer patients. *Blood* **93**(8), 2491-501.

Siena, S., Schiavo, R., Pedrazzoli, P., and Carlo-Stella, C. (2000). Therapeutic relevance of CD34 cell dose in blood cell transplantation for cancer therapy. *J Clin Oncol* **18**(6), 1360-77.

Sillaber, C., Strobl, H., Bevec, D., Ashman, L. K., Butterfield, J. H., Lechner, K., Maurer, D., Bettelheim, P., and Valent, P. (1991). IL-4 regulates c-kit proto-oncogene product expression in human mast and myeloid progenitor cells. *J Immunol* **147**(12), 4224-8.

Simmons, D., and Seed, B. (1988). Isolation of a cDNA encoding CD33, a differentiation antigen of myeloid progenitor cells. *J Immunol* **141**(8), 2797-800.

Simmons, P. J., Aylett, G. W., Niutta, S., To, L. B., Juttner, C. A., and Ashman, L. K. (1994a). c-kit is expressed by primitive human hematopoietic cells that give rise to colony-forming cells in stroma-dependent or cytokine-supplemented culture. *Exp Hematol* **22**(2), 157-65.

Simmons, P. J., Leavesley, D. I., Levesque, J. P., Swart, B. W., Haylock, D. N., To, L. B., Ashman, L. K., and Juttner, C. A. (1994b). The mobilization of primitive hemopoietic progenitors into the peripheral blood. *Stem Cells* **12**(Suppl 1), 187-201; discussion 201-2.

Simmons, P. J., Leavesley, D. I., Levesque, J. P., Swart, B. W., Haylock, D. N., To, L. B., Ashman, L. K., and Juttner, C. A. (1994c). The mobilization of primitive hemopoietic progenitors into the peripheral blood. *Stem Cells* **12 Suppl 1**, 187-201; discussion 201-2.

Siu, G., Wurster, A. L., Lipsick, J. S., and Hedrick, S. M. (1992). Expression of the CD4 gene requires a Myb transcription factor. *Mol Cell Biol* **12**(4), 1592-604.

Slamon, D. J., Clark, G. M., Wong, S. G., Levin, W. J., Ullrich, A., and McGuire, W. L. (1987). Human breast cancer: correlation of relapse and survival with amplification of the HER-2/neu oncogene. *Science* **235**(4785), 177-82.

Slamon, D. J., Godolphin, W., Jones, L. A., Holt, J. A., Wong, S. G., Keith, D. E., Levin, W. J., Stuart, S. G., Udove, J., Ullrich, A., and et al. (1989). Studies of the HER-2/neu proto-oncogene in human breast and ovarian cancer. *Science* **244**(4905), 707-12.

Sleeman, J. P. (1993). Xenopus A-myb is expressed during early spermatogenesis. *Oncogene* **8**(7), 1931-41.

Smarda, J., Sugarman, J., Glass, C., and Lipsick, J. (1995). Retinoic acid receptor alpha suppresses transformation by v-myb. *Mol Cell Biol* **15**(5), 2474-81.

Smithgall, T. E. (1995). SH2 and SH3 domains: Potential targets for anti-cancer drug design. *Journal of Pharmacological and Toxicological Methods* **34,** 125-132.

Songyang, Z., and Liu, D. (2001). Peptide library screening for determination of SH2 or phosphotyrosine-binding domain sequences. *Methods Enzymol* **332,** 183-95.

Spivak-Kroizman, T., Rotin, D., Pinchasi, D., Ullrich, A., Schlessinger, J., and Lax, I. (1992). Heterodimerization of c-erbB2 with different epidermal growth factor receptor mutants elicits stimulatory or inhibitory responses. *J Biol Chem* **267**(12), 8056-63.

Springer, T., Galfre, G., Secher, D. S., and Milstein, C. (1979). Mac-1: a macrophage differentiation antigen identified by monoclonal antibody. *Eur J Immunol* **9**(4), 301-6.

Stamenkovic, I., and Seed, B. (1988). CD19, the earliest differentiation antigen of the B cell lineage, bears three extracellular immunoglobulin-like domains and an Epstein-Barr virus-related cytoplasmic tail. *J Exp Med* **168**(3), 1205-10.

Stapleton, P., Kozmik, Z., Weith, A., and Busslinger, M. (1995). The gene coding for the B cell surface protein CD19 is localized on human chromosome 16p11. *Hum Genet* **95**(2), 223-5.

Stefanova, I., Corcoran, M. L., Horak, E. M., Wahl, L. M., Bolen, J. B., and Horak, I. D. (1993). Lipopolysaccharide induces activation of CD14-associated protein tyrosine kinase p53/56lyn. *J Biol Chem* **268**(28), 20725-8.

Stiff, P., Gingrich, R., Luger, S., Wyres, M. R., Brown, R. A., LeMaistre, C. F., Perry, J., Schenkein, D. P., List, A., Mason, J. R., Bensinger, W., Wheeler, C., Freter, C., Parker, W. R. L., and Emmanouilides, C. (2000). A randomized phase 2 study of PBPC mobilization by stem cell factor and filgrastim in heavily pretreated patients with Hodgkin's disease or non-Hodgkin's lymphoma. *Bone Marrow Transplant* **26**(5), 471-81.

Sutherland, D. R., Watt, S. M., Dowden, G., Karhi, K., Baker, M. A., Greaves, M. F., and Smart, J. E. (1988). Structural and partial amino acid sequence analysis of the human hemopoietic progenitor cell antigen CD34. *Leukemia* **2**(12), 793-803.

Tajima, Y., Huang, E. J., Vosseller, K., Ono, M., Moore, M. A., and Besmer, P. (1998). Role of dimerization of the membrane-associated growth factor kit ligand in juxtacrine signaling: the Sl17H mutation affects dimerization and stability-phenotypes in hematopoiesis. *J Exp Med* **187**(9), 1451-61.

Takahashi, T., Nakagoshi, H., Sarai, A., Nomura, N., Yamamoto, T., and Ishii, S. (1995). Human A-myb gene encodes a transcriptional activator containing the negative regulatory domains. *FEBS Lett* **358**(1), 89-96.

Tang, B., Mano, H., Yi, T., and Ihle, J. N. (1994). Tec kinase associates with c-kit and is tyrosine phosphorylated and activated following stem cell factor binding. *Mol Cell Biol* **14**(12), 8432-7.

Tanikawa, J., Yasukawa, T., Enari, M., Ogata, K., Nishimura, Y., Ishii, S., and Sarai, A. (1993). Recognition of specific DNA sequences by the c-myb protooncogene product: role of three repeat units in the DNA-binding domain. *Proc Natl Acad Sci U S A* **90**(20), 9320-4.

Tashiro, S., Sumi, T., Uozimi, N., and Nakamura, T. (2004). B-Myb dependent regulation of c-Myc expression by cytosolic phopholipase A2. *J Biol Chem* **279**(17), 17715-22.

Tatosyan, A. G., and Mizenina, O. A. (2000). Kinases of the Src family: structure and functions. *Biochemistry (Mosc)* **65**(1), 49-58.

Tatton, L., Morley, G. M., Chopra, R., and Khwaja, A. (2003). The Src-selective kinase inhibitor PP1 also inhibits Kit and Bcr-Abl tyrosine kinases. *J Biol Chem* **278**(7), 4847-53.

Tauchi, T., Feng, G. S., Marshall, M. S., Shen, R., Mantel, C., Pawson, T., and Broxmeyer, H. E. (1994). The ubiquitously expressed Syp phosphatase interacts with c-kit and Grb2 in hematopoietic cells. *J Biol Chem* **269**(40), 25206-11.

Taylor, D., Badiani, P., and Weston, K. (1996). A dominant interfering Myb mutant causes apoptosis in T cells. *Genes Dev* **10**(21), 2732-44.

Taylor, G. R., Reedijk, M., Rothwell, V., Rohrschneider, L., and Pawson, T. (1989). The unique insert of cellular and viral fms protein tyrosine kinase domains is dispensable for enzymatic and transforming activities. *Embo J* **8**(7), 2029-37.

Taylor, V. C., Buckley, C. D., Douglas, M., Cody, A. J., Simmons, D. L., and Freeman, S. D. (1999). The myeloid-specific sialic acid-binding receptor, CD33, associates with the protein-tyrosine phosphatases, SHP-1 and SHP-2. *J Biol Chem* **274**(17), 11505-12.

Tedder, T. F., and Isaacs, C. M. (1989). Isolation of cDNAs encoding the CD19 antigen of human and mouse B lymphocytes. A new member of the immunoglobulin superfamily. *J Immunol* **143**(2), 712-7.

Thoma, S. J., Lamping, C. P., and Ziegler, B. L. (1994). Phenotype analysis of hematopoietic CD34+ cell populations derived from human umbilical cord blood using flow cytometry and cDNA-polymerase chain reaction. *Blood* **83**(8), 2103-14.

Thomas, S. M., and Brugge, J. S. (1997). Cellular functions regulated by Src family kinases. *Annu Rev Cell Dev Biol* **13**, 513-609.

Thommes, K., Lennartsson, J., Carlberg, M., and Ronnstrand, L. (1999). Identification of Tyr-703 and Tyr-936 as the primary association sites for Grb2 and Grb7 in the c-Kit/stem cell factor receptor. *Biochem J* **341**(Pt 1), 211-6.

Thompson, C. B., Challoner, P. B., Neiman, P. E., and Groudine, M. (1986). Expression of the c-myb proto-oncogene during cellular proliferation. *Nature* **319**(6052), 374-80.

Tien, H. F., Chou, C. C., Wang, C. H., Chang, C. H., and Hsing, C. C. (1996). Putative normal counterparts of leukaemic cells from CD7-positive acute myeloid leukaemia can be demonstrated in human haemopoietic tissues. *Br J Haematol* **94**(3), 501-6.

Tien, H. F., and Wang, C. H. (1998). CD7 positive hematopoietic progenitors and acute myeloid leukemia and other minimally differentiated leukemia. *Leuk Lymphoma* **31**(1-2), 93-8.

Tilbrook, P. A., Ingley, E., Williams, J. H., Hibbs, M. L., and Klinken, S. P. (1997). Lyn tyrosine kinase is essential for erythropoietin-induced differentiation of J2E erythroid cells. *Embo J* **16**(7), 1610-9.

Timm, D., Salim, K., Gout, I., Guruprasad, L., Waterfield, M., and Blundell, T. (1994). Crystal structure of the pleckstrin homology domain from dynamin. *Nat Struct Biol* **1**(11), 782-8.

Timokhina, I., Kissel, H., Stella, G., and Besmer, P. (1998). Kit signaling through PI 3-kinase and Src kinase pathways: an essential role for Rac1 and JNK activation in mast cell proliferation. *Embo J* **17**(21), 6250-62.

To, L. B., Bashford, J., Durrant, S., MacMillan, J., Schwarer, A. P., Prince, H. M., Gibson, J., Lewis, I., Swart, B., Marty, J., Rawling, T., Ashman, L., Charles, S., and Cohen, B. (2003). Successful mobilization of peripheral blood stem cells after addition of ancestim (stem cell factor) in patients who had failed a prior mobilization with filgrastim (granulocyte colony-stimulating factor) alone or with chemotherapy plus filgrastim. *Bone Marrow Transplantation* **31,** 371-378.

To, L. B., Haylock, D. N., Dowse, T., Simmons, P. J., Trimboli, S., Ashman, L. K., and Juttner, C. A. (1994). A comparative study of the phenotype and proliferative capacity of peripheral blood (PB) CD34+ cells mobilized by four different protocols and those of steady-phase PB and bone marrow CD34+ cells. *Blood* **84**(9), 2930-9.

To, L. B., Haylock, D. N., Simmons, P. J., and Juttner, C. A. (1997). The biology and clinical uses of blood stem cells. *Blood* **89**(7), 2233-58.

To, L. B., Shepperd, K. M., Haylock, D. N., Dyson, P. G., Charles, P., Thorp, D. L., Dale, B. M., Dart, G. W., Roberts, M. M., Sage, R. E., and et al. (1990). Single high doses of cyclophosphamide enable the collection of high numbers of hemopoietic stem cells from the peripheral blood. *Exp Hematol* **18**(5), 442-7.

Todokoro, K., Watson, R. J., Higo, H., Amanuma, H., Kuramochi, S., Yanagisawa, H., and Ikawa, Y. (1988). Down-regulation of c-myb gene expression is a prerequisite for erythropoietin-induced erythroid differentiation. *Proc Natl Acad Sci U S A* **85**(23), 8900-4.

Tomita, A., Watanabe, T., Kosugi, H., Ohashi, H., Uchida, T., Kinoshita, T., Mizutani, S., Hotta, T., Murate, T., Seto, M., and Saito, H. (1998). Truncated c-Myb expression in the human leukemia cell line TK-6. *Leukemia* **12**(9), 1422-9.

Toscani, A., Mettus, R. V., Coupland, R., Simpkins, H., Litvin, J., Orth, J., Hatton, K. S., and Reddy, E. P. (1997). Arrest of spermatogenesis and defective breast development in mice lacking A-myb. *Nature* **386**(6626), 713-7.

Traverse, S., Gomez, N., Paterson, H., Marshall, C., and Cohen, P. (1992). Sustained activation of the mitogen-activated protein (MAP) kinase cascade may be required for differentiation of PC12 cells. Comparison of the effects of nerve growth factor and epidermal growth factor. *Biochem J* **288 (Pt 2),** 351-5.

Traverse, S., Seedorf, K., Paterson, H., Marshall, C. J., Cohen, P., and Ullrich, A. (1994). EGF triggers neuronal differentiation of PC12 cells that overexpress the EGF receptor. *Curr Biol* **4**(8), 694-701.

Treutlein, H. R., Lemmon, M. A., Engelman, D. M., and Brunger, A. T. (1992). The glycophorin A transmembrane domain dimer: sequence-specific propensity for a right-handed supercoil of helices. *Biochemistry* **31**(51), 12726-32.

Tsai, M., Shih, L. S., Newlands, G. F., Takeishi, T., Langley, K. E., Zsebo, K. M., Miller, H. R., Geissler, E. N., and Galli, S. J. (1991a). The rat c-kit ligand, stem cell factor, induces the development of connective tissue-type and mucosal mast cells in vivo. Analysis by anatomical distribution, histochemistry, and protease phenotype. *J Exp Med* **174**(1), 125-31.

Tsai, M., Takeishi, T., Thompson, H., Langley, K. E., Zsebo, K. M., Metcalfe, D. D., Geissler, E. N., and Galli, S. J. (1991b). Induction of mast cell proliferation, maturation, and heparin synthesis by the rat c-kit ligand, stem cell factor. *Proc Natl Acad Sci U S A* **88**(14), 6382-6.

Ueda, S., Mizuki, M., Ikeda, H., Tsujimura, T., Matsumura, I., Nakano, K., Daino, H., Honda Zi, Z., Sonoyama, J., Shibayama, H., Sugahara, H., Machii, T., and Kanakura, Y. (2002). Critical roles of c-Kit tyrosine residues 567 and 719 in stem cell factor-induced chemotaxis: contribution of src family kinase and PI3-kinase on calcium mobilization and cell migration. *Blood* **99**(9), 3342-9.

Ullrich, A., and Schlessinger, J. (1990). Signal transduction by receptors with tyrosine kinase activity. *Cell* **61**(2), 203-12.

Ulyanova, T., Blasioli, J., Woodford-Thomas, T. A., and Thomas, M. L. (1999). The sialoadhesin CD33 is a myeloid-specific inhibitory receptor. *Eur J Immunol* **29**(11), 3440-9.

van Daalen Wetters, T., Hawkins, S. A., Roussel, M. F., and Sherr, C. J. (1992). Random mutagenesis of CSF-1 receptor (FMS) reveals multiple sites for activating mutations within the extracellular domain. *Embo J* **11**(2), 551-7.

van der Geer, P., and Hunter, T. (1993). Mutation of Tyr697, a GRB2-binding site, and Tyr721, a PI 3-kinase binding site, abrogates signal transduction by the murine CSF-1 receptor expressed in Rat-2 fibroblasts. *Embo J* **12**(13), 5161-72.

van der Schoot, C. E., von dem Borne, A. E., and Tetteroo, P. A. (1987). Characterization of myeloid leukemia by monoclonal antibodies, with an emphasis on antibodies against myeloperoxidase. *Acta Haematol* **78 Suppl 1**, 32-40.

van Dijk, T. B., van Den Akker, E., Amelsvoort, M. P., Mano, H., Lowenberg, B., and von Lindern, M. (2000). Stem cell factor induces phosphatidylinositol 3'-kinase-dependent Lyn/Tec/Dok-1 complex formation in hematopoietic cells. *Blood* **96**(10), 3406-13.

van Hoek, M. L., Allen, C. S., and Parsons, S. J. (1997). Phosphotyrosine phosphatase activity associated with c-Src in large multimeric complexes isolated from adrenal medullary chromaffin cells. *Biochem J* **326 (Pt 1)**, 271-7.

Vandenbark, G. R., deCastro, C. M., Taylor, H., Dew-Knight, S., and Kaufman, R. E. (1992). Cloning and structural analysis of the human c-kit gene. *Oncogene* **7**(7), 1259-66.

Vanhaesebroeck, B., and Alessi, D. R. (2000). The PI3K-PDK1 connection: more than just a road to PKB. *Biochem J* **346 Pt 3**, 561-76.

Vassbotn, F. S., Andersson, M., Westermark, B., Heldin, C. H., and Ostman, A. (1993). Reversion of autocrine transformation by a dominant negative platelet- derived growth factor mutant. *Mol Cell Biol* **13**(7), 4066-76.

Vaughan, W. P., Civin, C. I., Weisenburger, D. D., Karp, J. E., Graham, M. L., Sanger, W. G., Grierson, H. L., Joshi, S. S., and Burke, P. J. (1988). Acute leukemia expressing the normal human hematopoietic stem cell membrane glycoprotein CD34 (MY10). *Leukemia* **2**(10), 661-6.

Velu, T. J., Beguinot, L., Vass, W. C., Willingham, M. C., Merlino, G. T., Pastan, I., and Lowy, D. R. (1987). Epidermal-growth-factor-dependent transformation by a human EGF receptor proto-oncogene. *Science* **238**(4832), 1408-10.

Venturelli, D., Mariano, M. T., Szczylik, C., Valtieri, M., Lange, B., Crist, W., Link, M., and Calabretta, B. (1990a). Down-regulated c-myb expression inhibits DNA synthesis of T-leukemia cells in most patients. *Cancer Res* **50**(22), 7371-5.

Venturelli, D., Travali, S., and Calabretta, B. (1990b). Inhibition of T-cell proliferation by a MYB antisense oligomer is accompanied by selective down-regulation of DNA polymerase alpha expression. *Proc Natl Acad Sci U S A* **87**(15), 5963-7.

Vieira, A. V., Lamaze, C., and Schmid, S. L. (1996). Control of EGF receptor signaling by clathrin-mediated endocytosis. *Science* **274**(5295), 2086-9.

Vojtek, A. B., and Der, C. J. (1998). Increasing complexity of the Ras signaling pathway. *J Biol Chem* **273**(32), 19925-8.

Voytyuk, O., Lennartsson, J., Mogi, A., Caruana, G., Courtneidge, S., Ashman, L. K., and Ronnstrand, L. (2003). Src family kinases are involved in the differential signaling from two splice forms of c-Kit. *J Biol Chem* **278**(11), 9159-66.

Wada, T., Qian, X. L., and Greene, M. I. (1990). Intermolecular association of the p185neu protein and EGF receptor modulates EGF receptor function. *Cell* **61**(7), 1339-47.

Wahl, M. I., Daniel, T. O., and Carpenter, G. (1988). Antiphosphotyrosine recovery of phospholipase C activity after EGF treatment of A-431 cells. *Science* **241**(4868), 968-70.

Wandzioch, E., Edling, C. E., Palmer, R. H., Carlsson, L., and Hallberg, B. (2004). Activation of the MAP kinase pathway by c-Kit is PI-3 kinase dependent in hematopoietic progenitor/stem cell lines. *Blood* **104**(1), 51-7.

Wang, J. F., Liu, Z. Y., and Groopman, J. E. (1998). The alpha-chemokine receptor CXCR4 is expressed on the megakaryocytic lineage from progenitor to platelets and modulates migration and adhesion. *Blood* **92**(3), 756-64.

Ward, K. A., Moss, C., and Sanders, D. S. (1995). Human piebaldism: relationship between phenotype and site of kit gene mutation. *Br J Dermatol* **132**(6), 929-35.

Ware, R. E., Scearce, R. M., Dietz, M. A., Starmer, C. F., Palker, T. J., and Haynes, B. F. (1989). Characterization of the surface topography and putative tertiary structure of the human CD7 molecule. *J Immunol* **143**(11), 3632-40.

Waterman, H., Katz, M., Rubin, C., Shtiegman, K., Lavi, S., Elson, A., Jovin, T., and Yarden, Y. (2002). A mutant EGF-receptor defective in ubiquitylation and endocytosis unveils a role for Grb2 in negative signaling. *Embo J* **21**(3), 303-13.

Watson, R. J., Robinson, C., and Lam, E. W. (1993). Transcription regulation by murine B-myb is distinct from that by c-myb. *Nucleic Acids Res* **21**(2), 267-72.

Watt, S. M., Karhi, K., Gatter, K., Furley, A. J., Katz, F. E., Healy, L. E., Altass, L. J., Bradley, N. J., Sutherland, D. R., Levinsky, R., and et al. (1987). Distribution and epitope analysis of the cell membrane glycoprotein (HPCA-1) associated with human hemopoietic progenitor cells. *Leukemia* **1**(5), 417-26.

Weaver, A., Chang, J., Wrigley, E., de Wynter, E., Woll, P. J., Lind, M., Jenkins, B., Gill, C., Wilkinson, P. M., Pettengell, R., Radford, J. A., Collins, C. D., Dexter, T. M., Testa, N. G., and Crowther, D. (1998). Randomized comparison of progenitor-cell mobilization using chemotherapy, stem-cell factor, and filgrastim or chemotherapy plus filgrastim alone in patients with ovarian cancer. *J Clin Oncol* **16**(8), 2601-12.

Wei, S., Liu, J. H., Epling-Burnette, P. K., Gamero, A. M., Ussery, D., Pearson, E. W., Elkabani, M. E., Diaz, J. I., and Djeu, J. Y. (1996). Critical role of Lyn kinase in inhibition of neutrophil apoptosis by granulocyte-macrophage colony-stimulating factor. *J Immunol* **157**(11), 5155-62.

Weiner, D. B., Liu, J., Cohen, J. A., Williams, W. V., and Greene, M. I. (1989). A point mutation in the neu oncogene mimics ligand induction of receptor aggregation. *Nature* **339**(6221), 230-1.

Welham, M. J., and Schrader, J. W. (1991). Modulation of c-kit mRNA and protein by hemopoietic growth factors. *Mol Cell Biol* **11**(5), 2901-4.

Welham, M. J., and Schrader, J. W. (1992). Steel factor-induced tyrosine phosphorylation in murine mast cells. Common elements with IL-3-induced signal transduction pathways. *J Immunol* **149**(8), 2772-83.

Wen, D., Suggs, S. V., Karunagaran, D., Liu, N., Cupples, R. L., Luo, Y., Janssen, A. M., Ben-Baruch, N., Trollinger, D. B., Jacobsen, V. L., and et al. (1994). Structural and functional aspects of the multiplicity of Neu differentiation factors. *Mol Cell Biol* **14**(3), 1909-19.

Westin, E. H., Gallo, R. C., Arya, S. K., Eva, A., Souza, L. M., Baluda, M. A., Aaronson, S. A., and Wong-Staal, F. (1982). Differential expression of the amv gene in human hematopoietic cells. *Proc Natl Acad Sci U S A* **79**(7), 2194-8.

Weston, K., and Bishop, J. M. (1989). Transcriptional activation by the v-myb oncogene and its cellular progenitor, c-myb. *Cell* **58**(1), 85-93.

Williams, D. E., de Vries, P., Namen, A. E., Widmer, M. B., and Lyman, S. D. (1992). The Steel factor. *Dev Biol* **151**(2), 368-76.

Williams, D. E., Eisenman, J., Baird, A., Rauch, C., Van Ness, K., March, C. J., Park, L. S., Martin, U., Mochizuki, D. Y., Boswell, H. S., and et al. (1990). Identification of a ligand for the c-kit proto-oncogene. *Cell* **63**(1), 167-74.

Williams, L. T. (1989). Signal transduction by the platelet-derived growth factor receptor. *Science* **243**(4898), 1564-70.

Wisniewski, D., Strife, A., and Clarkson, B. (1996). c-kit ligand stimulates tyrosine phosphorylation of the c-Cbl protein in human hematopoietic cells. *Leukemia* **10**(9), 1436-42.

Wollberg, P., Lennartsson, J., Gottfridsson, E., Yoshimura, A., and Ronnstrand, L. (2003). The adapter protein APS associates with the multifunctional docking sites Tyr-568 and Tyr-936 in c-Kit. *Biochem J* **370**(Pt 3), 1033-8.

Woo, C. H., Sopchak, L., and Lipsick, J. S. (1998). Overexpression of an alternatively spliced form of c-Myb results in increases in transactivation and transforms avian myelomonoblasts. *J Virol* **72**(8), 6813-21.

Woods, D., Parry, D., Cherwinski, H., Bosch, E., Lees, E., and McMahon, M. (1997). Raf-induced proliferation or cell cycle arrest is determined by the level of Raf activity with arrest mediated by p21Cip1. *Mol Cell Biol* **17**(9), 5598-611.

Wybenga, L. E., Epand, R. F., Nir, S., Chu, J. W., Sharom, F. J., Flanagan, T. D., and Epand, R. M. (1996). Glycophorin as a receptor for Sendai virus. *Biochemistry* **35**(29), 9513-8.

Wybenga-Groot, L. E., Baskin, B., Ong, S. H., Tong, J., Pawson, T., and Sicheri, F. (2001). Structural basis for autoinhibition of the Ephb2 receptor tyrosine kinase by the unphosphorylated juxtamembrane region. *Cell* **106**(6), 745-57.

Xiao, M., Oppenlander, B. K., Plunkett, J. M., and Dooley, D. C. (1999). Expression of Flt3 and c-kit during growth and maturation of human CD34+CD38- cells. *Exp Hematol* **27**(5), 916-27.

Xu, Q., Simpson, S. E., Scialla, T. J., Bagg, A., and Carroll, M. (2003). Survival of acute myeloid leukemia cells requires PI3 kinase activation. *Blood* **102**(3), 972-80.

Xu, W., Doshi, A., Lei, M., Eck, M. J., and Harrison, S. C. (1999). Crystal structures of c-Src reveal features of its autoinhibitory mechanism. *Mol Cell* **3**(5), 629-38.

Yaciuk, P., and Shalloway, D. (1986). Features of the pp60v-src carboxyl terminus that are required for transformation. *Mol Cell Biol* **6**(8), 2807-19.

Yam, L. T., Li, C. Y., and Crosby, W. H. (1971). Cytochemical identification of monocytes and granulocytes. *Am J Clin Pathol* **55**(3), 283-90.

Yamanashi, Y., Fukushige, S., Semba, K., Sukegawa, J., Miyajima, N., Matsubara, K., Yamamoto, T., and Toyoshima, K. (1987). The yes-related cellular gene lyn encodes a possible tyrosine kinase similar to p56lck. *Mol Cell Biol* **7**(1), 237-43.

Yamanashi, Y., Kakiuchi, T., Mizuguchi, J., Yamamoto, T., and Toyoshima, K. (1991a). Association of B cell antigen receptor with protein tyrosine kinase Lyn. *Science* **251**(4990), 192-4.

Yamanashi, Y., Miyasaka, M., Takeuchi, M., Ilic, D., Mizuguchi, J., and Yamamoto, T. (1991b). Differential responses of p56lyn and p53lyn, products of alternatively spliced lyn mRNA, on stimulation of B-cell antigen receptor. *Cell Regul* **2**(12), 979-87.

Yan, K. S., Kuti, M., and Zhou, M. (2002). PTB or not PTB - that is the question. *FEBS Lett* **513**, 67-70.

Yarden, Y., Kuang, W. J., Yang-Feng, T., Coussens, L., Munemitsu, S., Dull, T. J., Chen, E., Schlessinger, J., Francke, U., and Ullrich, A. (1987a). Human proto-oncogene c-kit: a new cell surface receptor tyrosine kinase for an unidentified ligand. *Embo J* **6**(11), 3341-51.

Yarden, Y., and Schlessinger, J. (1987b). Epidermal growth factor induces rapid, reversible aggregation of the purified epidermal growth factor receptor. *Biochemistry* **26**(5), 1443-51.

Yarden, Y., and Ullrich, A. (1988). Growth factor receptor tyrosine kinases. *Annu Rev Biochem* **57**, 443-78.

Yasuoka, R., Sakakura, C., Shimomura, K., Fujita, Y., Nakanishi, M., Aragane, H., Hagiwara, A., Bamba, M., Abe, T., and Yamagishi, H. (2003). Mutations in exon 11 of the c-kit gene in a myogenic tumor and a neurogenic tumor as well as in gastrointestinal stromal tumors. Utility of c-kit mutation as a prognostic biomarker for gastrointestinal mesenchymal tumor. *Dig Surg* **20**(3), 183-91.

Yee, N. S., Hsiau, C. W., Serve, H., Vosseller, K., and Besmer, P. (1994a). Mechanism of down-regulation of c-kit receptor. Roles of receptor tyrosine kinase, phosphatidylinositol 3'-kinase, and protein kinase C. *J Biol Chem* **269**(50), 31991-8.

Yee, N. S., Langen, H., and Besmer, P. (1993). Mechanism of kit ligand, phorbol ester, and calcium-induced down- regulation of c-kit receptors in mast cells. *J Biol Chem* **268**(19), 14189-201.

Yee, N. S., Paek, I., and Besmer, P. (1994b). Role of kit-ligand in proliferation and suppression of apoptosis in mast cells: basis for radiosensitivity of white spotting and steel mutant mice. *J Exp Med* **179**(6), 1777-87.

Yi, T., and Ihle, J. N. (1993). Association of hematopoietic cell phosphatase with c-Kit after stimulation with c-Kit ligand. *Mol Cell Biol* **13**(6), 3350-8.

Yin, A. H., Miraglia, S., Zanjani, E. D., Almeida-Porada, G., Ogawa, M., Leary, A. G., Olweus, J., Kearney, J., and Buck, D. W. (1997). AC133, a novel marker for human hematopoietic stem and progenitor cells. *Blood* **90**(12), 5002-12.

Yuan, Q., Austen, K. F., Friend, D. S., Heidtman, M., and Boyce, J. A. (1997). Human peripheral blood eosinophils express a functional c-kit receptor for stem cell factor that stimulates very late antigen 4 (VLA-4)- mediated cell adhesion to fibronectin and vascular cell adhesion molecule 1 (VCAM-1). *J Exp Med* **186**(2), 313-23.

Zhang, Z., Zhang, R., Joachimiak, A., Schlessinger, J., and Kong, X. P. (2000). Crystal structure of human stem cell factor: implication for stem cell factor receptor dimerization and activation. *Proc Natl Acad Sci U S A* **97**(14), 7732-7.

Zhu, W. M., Dong, W. F., and Minden, M. (1994). Alternate splicing creates two forms of the human kit protein. *Leuk Lymphoma* **12**(5-6), 441-7.

Zsebo, K. M., Williams, D. A., Geissler, E. N., Broudy, V. C., Martin, F. H., Atkins, H. L., Hsu, R. Y., Birkett, N. C., Okino, K. H., Murdock, D. C., and et al. (1990). Stem cell factor is encoded at the Sl locus of the mouse and is the ligand for the c-kit tyrosine kinase receptor. *Cell* **63**(1), 213-24.

Caruana, G., Cambareri, A.C. and Ashman, L.K. (1999) Isoforms of c-KIT differ in activation of signalling pathways and transformation of NIH3T3 fibroblasts. *Oncogene, v. 18 (40), pp. 5573-5581, September 1999*